X-69 CARGOSAT SPACE-PLANE FOR LEO DELIVERIES

Rushikesh Badgujar

May 2020
AE 295A & B
Dr. Nikos Mourtos

Abstract

In the era of rapidly developing CubeSats, the payload sizes have been drastically reduced, making the traditional rocket launch and delivery system quite expensive and time-consuming in terms of scheduled delays and long waiting. This project is an attempt to use a spaceplane with a sophisticated and reliable mission profile, high performance, and the ability to efficiently deliver CubeSats to at least 110 km of altitude. Specifically, the research project considers the preliminary design of an X-69 CargoSat Spaceplane, using an airplane design concept to deliver CubeSats to Low Earth Orbit (LEO). This could be one of the least polluting, highly efficient approaches with less launch vehicle schedule delays in comparison with traditional rockets. The preliminary aircraft design approach uses computer programs and simulations to analyze the proposed components – such as fuselage, wing, vertical and horizontal tail and landing gear – assessing the parameters that play a vital role during all operational phases of flight. This has allowed for conceptual design of the spaceplane using core methodologies and relevant software to increase accuracy and reduce the design process time. Since this spaceplane has a mid-air launch system using a mothership, it requires relatively less fuel to climb from 45,000 ft of altitude where the air resistance is very low, increasing the aerodynamic efficiency of the climb phase with less drag. Furthermore, efforts are made to verify the re-entry and adverse deceleration during descent, making it an unpowered glider. The maximum payload capacity of 1,500 kg is considered, which allows 24 large sized CubeSats (27U).

Acknowledgements

I would like to express my gratitude to several individuals and organizations for supporting me throughout this master's project and the graduate studies. First, I would like to sincerely thank my advisor and supervisor, Dr. Nikos J. Mourtos, for his enthusiasm, patience, insightful recommendations, practical advice, helpful information and unceasing ideas that have always helped me prodigiously in my research. His immense knowledge , profound experience and professional expertise in airplane design, aerodynamics, flight mechanics and several other core fields in aerospace engineering has enabled me to complete this research successfully. One of his recommendations to use the airplane design software Advanced Aircraft Analysis (AAA) published by Darcorporation has vastly assisted me to ease the preliminary design process for X-69 CargoSat with equal understanding of the concepts affiliated to it. Without his support and guidance, this research would be unfinished.

I would also like to thank Mrs. Heidi L. Eisips, one of my advisors to recommend and support me throughout the report so that the project is comprehensive to every reader. She has helped me word to word, grammar to grammar maintaining the professionalism of the report without affecting the technical insights of the project. She made herself available to assist me apart from her office hours that completed the report to the professional level. While working with Mrs. Heidi, I have exceled my skills in technical writing that includes equations and mathematical expressions vastly with considerable pace.

I would like to thank people from Darcorporation to assist me with the software, providing me useful guidelines from time to time and many relevant example files for AAA to better understand the working of the AAA software. It accelerated the pace of my research itself assuaging the efforts required for calculations and verification of the same. Since this software relies on Roskam's Airplane Design series from vol 1 to vol 8, it helped to understand conceptually what goes into preliminarily designing the airplane.

Last but not the least, I would like to thank my parents to stand by my side financially, understandably throughout this project. They didn't think a bit before helping financially when I asked them that I'd require to purchase a software to complete this project successfully. Even though they don't understand much of aerospace engineering, they are very good listeners and advisors in their own way that encouraged me to continue the work with equal enthusiasm. They didn't let me work alone where they kept asking me questions, doubts that made me a better presenter for this project so that I can explain about it to someone with less knowledge about aerospace.

I cannot express the gratitude more than anything when Dr. Mourtos and my parents assisted during my specifically worst times where I almost lost all the hopes to achieve what I am striving for. Their immense and endless support is just out of the world.

Contents

Figures

Tables

Abbreviations & Symbols

Abbreviations

AR	Aspect Ratio
AAA	Advanced Aircraft Analysis
Vol	Volume (books)
tent	Tentative
TO	Take-off
PL	Payload
psf	Pounds. Square feet
kts	Knots
max	Maximum
min	Minimum
CSD	Canisterized Satellite Dispenser
CAD	Computer Aided Drawing
HTPB	Hydroxylterpolybutadiene
N_2O	Nitrous Oxide
MAC	Mean Aerodynamic Chord
MGC	Mean Geometric Chord
C.G	Center of Gravity
H.T	Horizontal Tail
V.T	Vertical Tail
N.C	Closed Circuit
N.O	Open Circuit
fus	Fuselage
F.S	Fuselage Station
W.L	Water Lines
B.L	Buttock Lines

Symbols

A	Aspect Ratio
S	Area
b	Span
W	Weight
A	Regression Coefficient
B	Regression Coefficient
C	Regression Coefficient
D	Regression Coefficient
M_{ff}	Mission Fuel Fraction
F	Fuel
R	Range
V	Velocity
c_j	Specific fuel consumption
L/D	Lift-to-drag ratio
E	Endurance
W/S	Wing loading
ρ	Density of air
$C_{L_{max}}$	Maximum lift coefficient Clean
$C_{L_{max_L}}$	Maximum lift coefficient for Landing
$C_{L_{max_{TO}}}$	Maximum Lift Coefficient for Take-off
δ	Pressure ratio
θ	Temperature ratio

T/W	Thrust-to-Weight ratio
S_{wet}	Wetted area
c_f	Skin friction
C_{D_0}	Coefficient of drag at zero lift
γ	Flight path angle
M	Mach Number
M_{Cr}	Critical Mach Number
e	Oswald's Efficiency
$\bar{q}$	Dynamic pressure
λ	Taper ratio
Λ	Sweep Angle
Γ	Dihedral Angle
ε	Twist angle
c_r	Root chord
c_t	Tip chord
i_w	Incidence angle
x_{ac}	X-Location of aerodynamic center
$\bar{C}$	MAC length
t/c	Thickness ratio
Re	Reynolds Number
LE	Leading Edge
TE	Trailing Edge
c/4	Quarter chord
Struct	Structure
feq	Fixed Equipment
plt	Powerplant
GW	Gross Weight
FWD	Forward Direction

Subscripts

E	Empty
TO	Take-off
L	Landing
TOFL	Take-off and Landing
ff	Fuel Fraction
TFO	trapped fuel and oil
res	Residual
crew	Pilots
Cr	Critical
t	Tip
r	Root
W	Wing
h	Horizontal tail
v	Vertical tail

1. Chapter 1 – Introduction

1.1 Motivation

It is quite often to use cryogenic rockets to deliver various satellites into space. Due to the size constraints of rockets, their payload, propulsive efficiencies, rocket companies house all the satellites together with a strategy to launch them at once which keeps customers waiting till all the tickets are booked even if some of them happen to be small sized satellites. This project is an attempt to use the X-69 CargoSat spaceplane concept instead of rockets to deliver those small satellites to desired orbit individually or all together if accommodated without long waiting and required efficiencies.

1.2 Literature Review

There are various spaceplanes that have been designed, tested and even implemented for further development such as X-15A-2, Dyna Soar, Virgin Galactic's Spaceship One, Spaceship Two, etc. Table 1 shows a comparison from various literature sources highlighting why in today's world spaceplane are more advantageous than rockets:

Table 1.1: Advantages of Spaceplanes over Rockets

Parameter/ Phase	Rockets	Spaceplanes
Design & Assembly	• Design and assembly of rockets over-cautious, since every investment is sitting right on the tons of high octane. • Even if the rockets are designed module by module, their assembly must be done vertically which requires a tall building (or structure), which may in turn cause unusual errors or challenges. .	• Spaceplanes are less risky since most of them require solid propellant rockets and have mid-air launch feature. • Spaceplanes are quite easy to design and assemble the components together. Payload compartment can be modified as desired or based on the type, size, shape of payload.
Launch	• Rocket launches are still not 100% accurate and have at least 35% risk that it might be blow up right at the first stage. • It requires comparatively more fuel for lift off from the ground excluding the climb. • Since the launch is from the ground, the complete rocket has to deal with heavy aerodynamic drag which makes a big drawback during the climb phase.	• Spaceplane launches usually work on a mid-air launch concept, requiring a mothership to take it to 45,000ft of altitude, drop it and then climb higher using a rocket motor. • This gives comparatively less aerodynamic drag to them complete vessel due to thinner atmosphere at higher altitudes; to achieve higher rate of climb requiring comparatively less fuel.
Coasting, Deploying, Docking and Undocking	• The usual upper stages are only designed to coast in space using RCS thrusters but not designed to glide in the atmosphere as they have to splash down into the water while coming back.	• Coasting is quite easy and reliable due to integrated design and retained avionics. • Docking and undocking gets easier if mission requires any damaged satellite to return to earth.

Parameter/ Phase	Rockets	Spaceplanes
Landing	• Reusability features for rockets are emerging as technology advances-- which would allow rockets to re-land and re-launch in the future. However, the reusability concept is still at an early stage of development and has not reach a reliable stage for common use. • Rockets also requires a separate landing pad, isolated from any city—either in the sea or in the desert—so that rockets can crash land if necessary and not pose a threat to civilians. .	• Spaceplanes are just like any other airplane that can land at any airport. • With the help of RCS thrusters, spaceplanes can coast to targeted ground locations so that they can dive in, glide and land with less effort other than hypersonic speeds. • There is no need of separate landing pad like rockets to for landing and no avionics has to be lost during the complete mission.

These points if considered, can help with cost optimization of the mission. We are dealing with advanced technologies where every necessary component for engineering is shrinking to smaller sizes ultimately giving rise to CubeSats. In future, other than heavy payload deliveries, rockets are quite extra-investments.

1.3 Project Proposal

The objective of this project is to design spaceplane capable of delivering CubeSats to at Low Earth Orbits (LEOs). The project also helps to understand aerodynamics of delta wings of X-69 that will face high temperatures and pressures due to hypersonic speeds during re-entry, their optimal angle-of-attack to achieve perfect gliding as the returning is completely unpowered. The project will overlook the coasting parameters and capabilities of X-69.

1.4 Methodology

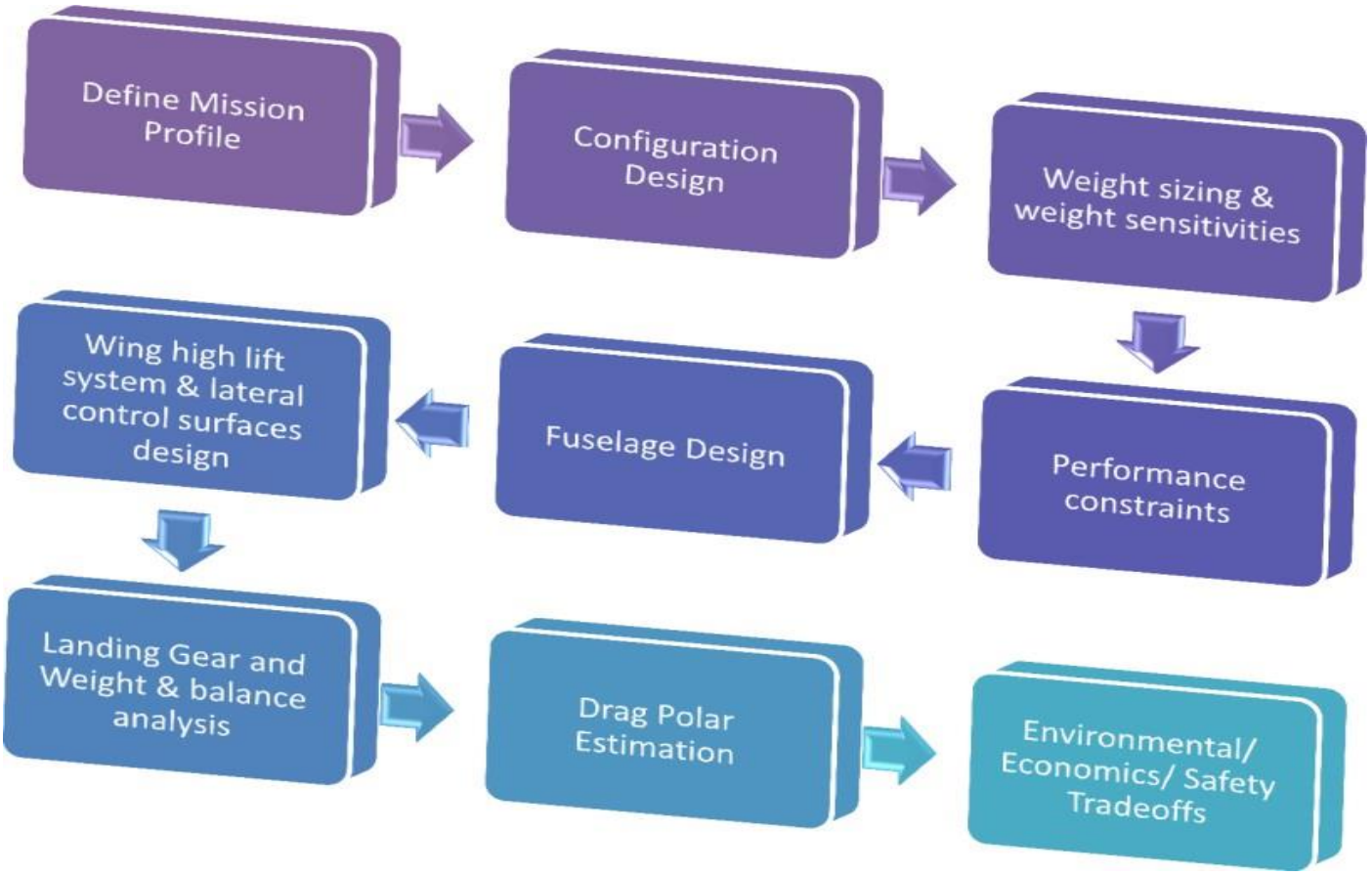

Figure 1.1: Methodology

2. Chapter 2 – Mission Specification

2.1 Mission Specifications

Table 2.1: Anticipated specifications

General Characteristics	
Crew	2
Maximum Payload	1,500 kg (3,310 lbs.)
Loaded weight	10,000 kg (22046.23 lbs. .)
Powerplant	1x RocketmotorTwo liquid/solid hybrid rocket engine or similar
Performance	
Maximum speed	4,000 km/hr. (2,500 mph)
Orbit	Low Earth Orbit
Mach	3.5 – 4.0
Launch and Landing Characteristics	
Launch Vehicles	B-52 Stratofortress, White Knight Two
Launch Speed	Approx. 0.7 – 0.8
Launch Altitude/Service Ceiling	45,000 ft to 50,000 ft

2.2 Mission Profile

Mission profile for X-69 will look similar to that of X-15 as shown in Fig. 1. There will be modifications after X-69 dives into the space, although its in-atmosphere is similar to that of X-15. Any mothership will help to air launch X-69. After detachment, it will burnout and climb towards LEO using RocketMotorTwo engine or similar ones.

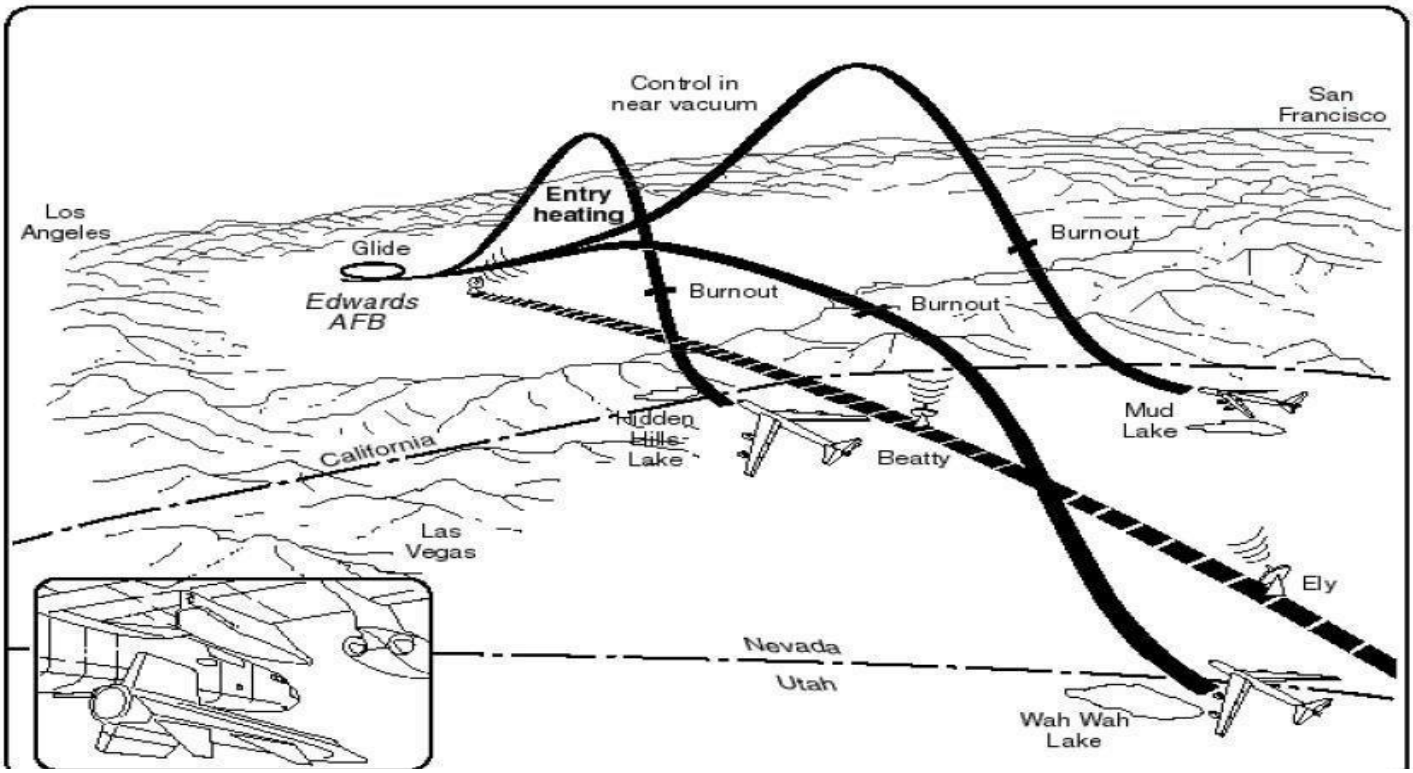

Figure 2.1: Mission profile of X-15

Fig 2.2 shows anticipated mission profile of X-69 CargoSat. Depending on mission it may spend variable amount of time in space either to just deploy and or wait for docking back another satellite. Re-entry will be initiated as it drops into the atmosphere and will glide and land on airport.

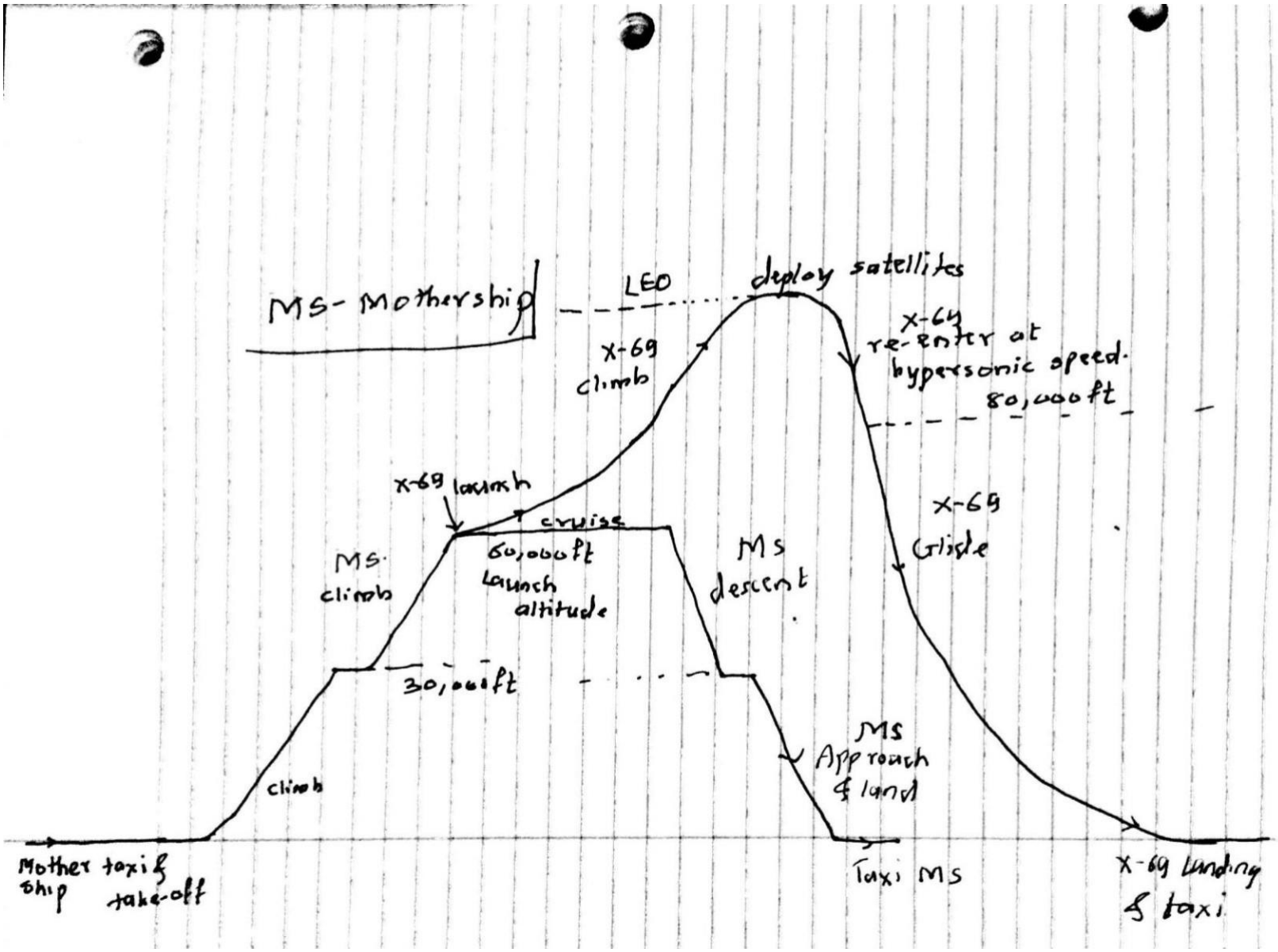

Figure 2.2: Estimated mission profile of X-69

2.3 Market Analysis

Since a decade, concept of CubeSats and other small satellites has been trending with a rising market. They deliver crucial advantages like compactness, multifunctional characteristics due to advanced technologies and highly efficient features. To date, rockets have been used to deliver these satellites into the space or orbits. Rockets are good to transport heavy and large instruments into the space. Although if a company or a customer wants to put their small-sized satellites to space, they have to wait or pay more price

if they seek to launch through rockets. Moreover, it keeps them waiting till all other satellite companies collaborate for launch.

Reusable spaceplanes have capabilities to reach up to LEO and further. Small satellites can be delivered into space by spaceplanes with reusable capabilities. X-planes like Virgin Galactic's Spaceship Two, X-15, X-37B can make return trips with crew inside.

2.4 Technical and Economic Feasibility

Spaceplanes carrying human to space have been under research and even been flown quite many times. From technical perspective, it would be feasible to re-design the spaceplanes for satellite transport with reusability which essentially gives the benefit for aborted missions. These planes can also be used to bring back damaged or reparable satellites with efficient re-entry. Following points can be considered to propose the design of X-69 CargoSat:

- Based on payload and other avionics features, the design of X-69 will be similar to that been trending for spaceplanes for human space flight.
- Air-launch will be same, using either B-52 Stratofortress or White Knight Two aircrafts.
- Will have to re-consider the aerodynamics for re-entry and landing aspects.
- Propulsion system will change based on payload, carrying satellites back and forth.

Reusability is always an advantage for space transportation. Moreover, many attempts have been made and some of them are even successful to bring back rockets from space like SpaceX and Blue Origin. Although, this takes lot of fuel to fight with re-entry speeds and again to manage a perfect landing. It is quite easy for an airplane-like structure to land with less maintenance and accuracy. Again, spaceplanes would not need specific launch/landing pad. If X-69 brings reparable satellites from space, it can be delivered wherever it is necessary with less earth-transportation issues. It can land on any airport, deliver the satellite.

For instance, let's say a Chinese Space agency collaborates and asks American space agency who makes X-69 to bring back their damaged satellite, it will be easy and feasible to rendezvous X-69 to that satellite, dock it in, re-enter and land on any airport in China delivering the payload and flying back to home country. This will reduce ground transport cost, will not have to bother about damaged satellites and many other advantages.

2.5 Critical Mission Requirements

Following are the critical mission requirements that should be considered for design:

- Delta-wing design for re-entry and efficient landing.
- Efficient propulsion system for X-69 while air launching.
- Outer body material to deal with re-entry heat and high temperatures.

Delta-wing pattern is quite traditional for supersonic aircrafts. Its design depends on requirements of aircraft and other technical specifications like altitude, speed, take-off and landing distance etc. Due to hypersonic speeds at re-entry, the surround atmospheric air heats up which is unfavorable for aircrafts with normal body material. Using carbon-composite makes it light-weight, resistant to high temperature and pressure and many other structural advantages.

2.6 Comparative study of Similar Airplanes

Table 2.2: Comparative study

Parameters	X-69 CargoSat	Virgin Galactic's Spaceship Two	Virgin Galactic's Spaceship One	Boeing's X-37	Boeing's X-20 Dyna-Soar	X-15
Crew	2	2 crew and 6 passengers	1 pilot	none	1 pilot	1 pilot
Takeoff/Launch weight	22,000 lbs.	21,428 lbs. (9,740 kg)	21,428 lbs. (9,740 kg)	11,000 lbs. (4,990 kg)	11,387 lbs. (5,165 kg)	34,000 lbs. (15,420 kg)
Empty weight	15,000 lbs. (6,804 kg)	15,000 lbs. (6,804 kg)	2,640 lbs. (1,200 kg)	NA (electric powered)	10,395 lbs. (4,715 kg)	14,600 lbs. (6,620 kg)
Thrust	60,000 lbf to 75,000 lbf	60,000 lbf (270 kN)	20,000 lbf (88 kN)	157.4 lbf 700kN)	72,000 lbf (323 kN)	70,400 lbf (313 kN)
Critical Speed, V_{cr}	2,500 mph	2,500 mph (4,000 km/hr.)	2,170 mph (3,518 km/hr.)	(Orbital) 17,426 mph (28,440 km/hr.)	17,500 mph (28,165 km/hr.)	4,520 mph (7,274 km/hr.)
Range, R	300 mi and apogee of up to LEO of 160 – 250 km	Planned apogee of 110 km	40 mi (65 km)	270 days (design)	Earth orbit 22,000 nm (40,700 km)	280 mi (450 km)
Wing Area, S	450 ft^2 (estimated)	273.34 ft^2 (25.4 m^2) (estimated)	161.4 ft^2 (15 m^2)		345 ft^2 (32m^2)	200 ft^2 (18.6m^2)
Wing span, b	27ft (estimated)	27 ft (8.3 m)	16 ft. 5 in (8.05 m)	14 ft 11 in (4.5 m)	20 ft 10 in (6.34 m)	22 ft 4 in (6.8 m)
Aspect Ratio, AR	1.62 (estimated)	2.667 (estimated)	1.6		1.256	2.486
Type of Payload	Crew and satellite	Crew	Pilot	Satellites	Crew	Crew
Powerplant	1x Rocket Motor Two liquid/solid hybrid rocket engine (proposed)	1x Rocket Motor Two liquid/solid hybrid rocket engine	1x N_2O/HTPB SpaceDev Hybrid rocket,	Gallium Arsenide Solar Cells with Li-Ion batteries	1x Transtage rocket engine	1xReaction Motors XLR99-RM-2 liquid propellant rocket engine

2.7 Discussion:

Various design the design of X-69 will be challenging from various aerospace aspects. There is quite a lot of versatility in comparing X-69 with other Spaceplanes considering their performance, general characteristics, applications, etc. As discussed, its launch weight will be similar to that of SpaceShipTwo of about 22,000 lbs. From the comparison table, optimal thrust will be considered in the range of 60,000 to 75,000 lbs. f based on payload. X-15 using XLR99-RM-2 liquid propellant rocket engine manages to produce around 70,000 lbs. f of thrust which is enough to approach Mach 3 – 4. Anticipated body design of X-69 will be like that of X-15 and SpaceShipTwo with additional concentration on its body material and its efficiency for re-entry. RocketMotorTwo is an advanced powerplant that uses liquid/solid hybrid propellant which can reduce weight unlike X-15's XLR99. Again, mission requirements can vary after

entering to the space based on altitude from earth, position of damaged satellite or position of undocking on-board satellites.

An efficient re-entry system will allow X-69 simply glide and land back to base. This considers advanced aerodynamics characteristics and wing, tail and body parts along with its material, preferably a carbon composite.

2.8 Conclusion and Recommendation

2.8.1 Conclusion:

X-69 will make satellite deliveries a lot easier and cost effective as compared to existing methods. Advanced technologies in electronics and computer have shrunk all the devices and have made them compact. This gives rise to high market for small-sized satellites or CubeSats. Using a spaceplane like X-69 or an existing SpaceShipTwo makes the system efficient. Also, we don't have to pollute space by disposing fairly working satellites. They can be brought back to earth, rework on it, modify the design and send it back to space using X-69. X-69 will be an efficient glider that will use its aerodynamics to reach the destination and safe landing.

2.8.2 Recommendations:

Air launch has many developments since X-15 launched from B-52 Stratofortress and other missile launches from fighter jets. Motherships should have efficient performance to maintain launch altitude and launch speed. Motherships are expected to be sophisticated from structural point of view. Air launches are quite delicate while cruising with high speeds which might be vulnerable to structural integrity. Virgin Galactic uses central air launch mechanism for SpaceShipTwo.

3. Chapter 3 - Weight Sizing & Weight Sensitivities of X-69 CargoSat

3.1 Introduction

The mission profile of X-69 divides its flight into two phases. X-69 makes an air launch and climbs at supersonic speed in Phase I. This phase will last for about 90 seconds in which X-69 will reach to altitude of about 360,000 ft (110 km) at Mach 3.0 – 3.5. Deploying the payload (satellites) into space and docking back returning satellites if required by mission, it will descend and land using its gliding characteristics decelerating itself to subsonic speeds in Phase II. X-69 will have reaction control system such as RV-105 RCS Thruster block or Vernor Engine to control transcend between phase I and II. These thrusters use very less fuel to maintain the required thrust in x, y and z direction for maneuvering and attitude control. In phase I for weight analysis, we consider supersonic cruise fuel-fraction for initial calculations. In phase II for weight analysis, we consider sail plane fuel-fraction which eventually is like small home-built airplanes.

3.2 Mission Weight Estimates

3.2.1 Database for Takeoff Weights and Empty Weights of Similar Airplanes:

Table 3.1 provides a database for takeoff and empty weights of similar airplanes. Boeing X-37B is an exception since this ROT vehicle is electric powered which has same empty weight as takeoff.

Table 3.1: Database for takeoff weights and empty weights of similar airplanes

Airplane	Type	Takeoff Weight	Empty Weight
Lockheed CL-1200 Lancer	Supersonic	35,000 lbs. (15,900 kg)	17,885 lbs. (8,112 kg)
Martin Marietta X-24B	Supersonic	13,800 lbs. (6,260 kg)	8,500 lbs. (3,855 kg)
Virgin Galactic Spaceship One	Supersonic	7,900 lbs. (3,600 kg)	2,640 lbs. (1,200 kg)
Virgin Galactic Spaceship Two	Supersonic	21,428 lbs. (9,740 kg)	10,423 lbs. (4,272.8 kg)
Boeing X-20 Dyna Soar	Supersonic	11,387 lbs. (5,165 kg)	10,395 lbs. (4,715 kg)
North American X-15	Supersonic	34,000 lbs. (15,420 kg)	14,600 lbs. (6,620 kg)
Lockheed Martin X-33	suborbital spaceplane	285,000 lbs. (129,000 kg)	75,000 lbs. (34,019.43 kg)
NASA X-38	CRV re-entry vehicle	54,500 lbs. (24,721 kg)	23,500 lbs. (10,660 kg)
Douglas X-3 Stiletto	Supersonic	23,840 lbs. (10,810 kg)	16,120 lbs. (7,310 kg)
Ryan X-13 Vertijet	VTOL jet aircraft	7,200 lbs. (3,272 kg)	5,334 lbs. (2,424 kg)
Boeing X-37B	Reusable Orbital Test vehicle	11,000 lbs. (4,990 kg)	11,000 lbs. (4,990 kg)
North American X-10	cruise missile	42,300 lbs. (19,187 kg)	25,800 lbs. (11,703 kg)
Boeing X-40	Reusable launch vehicle	3,700 lbs. (1,640 kg)	2,500 lbs. (1,100 kg)

3.2.2 Determination of Regression Coefficients A and B:

Before initiating the calculation for determination of mission weights and empty weight, it is necessary to make an initial guess for takeoff weight based on similar airplanes take-off weight data. Fig. 3.1 is the plot of empty weight v/s takeoff weight of similar airplanes as tabulated in table 3.1. Initial takeoff weight can be guessed close to trend line. For X-69 the payload weight will be 1,500 kg (3,310 lbs.). considering maximum capacity of 24 number of 27U size CubeSats.

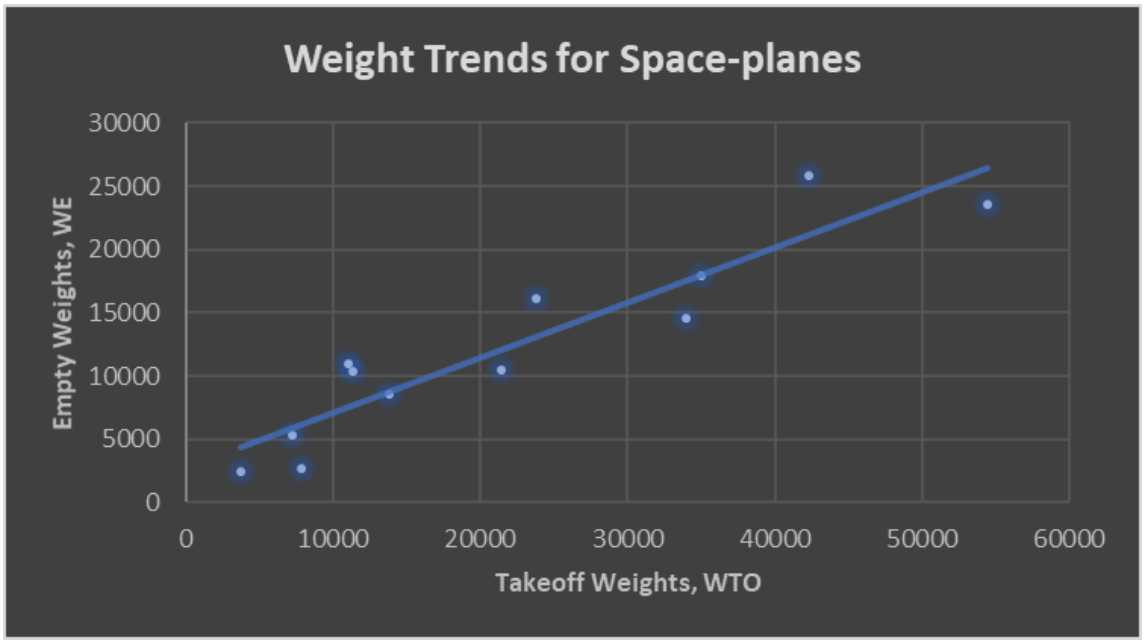

Figure 3.1: Weight trends for spaceplanes

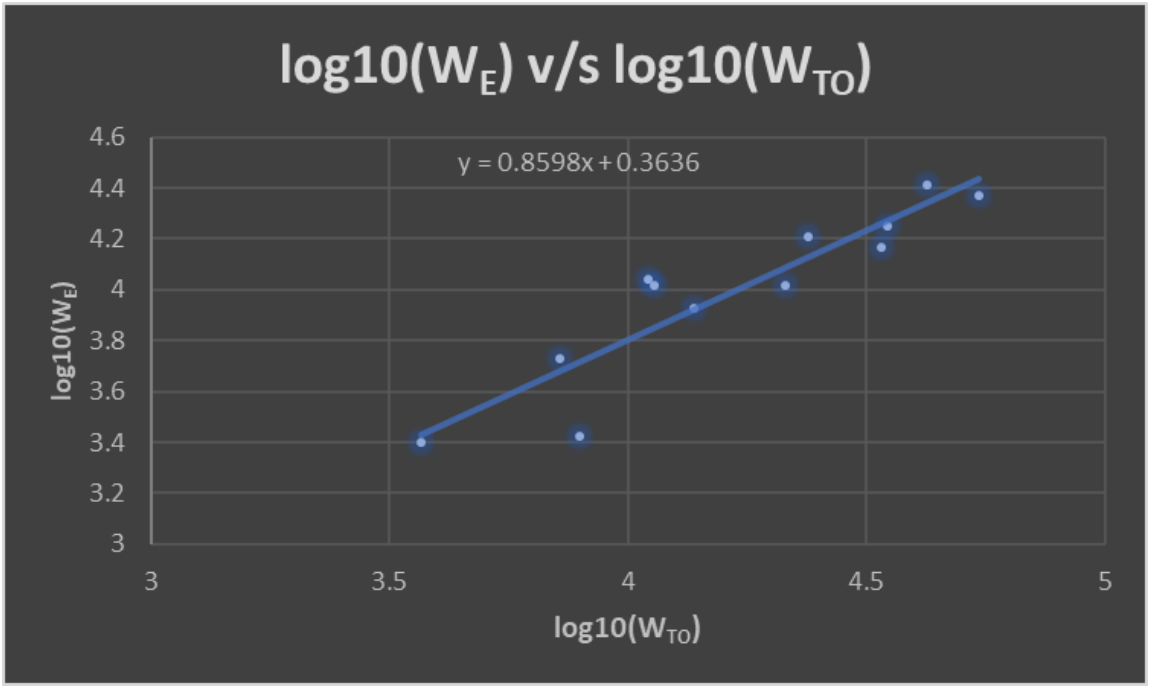

Figure 3.2: log-log plot of weight data

It is necessary to determine regression coefficients A and B for X-69. Fig.3.2 is a log-log plot of weight data of similar airplanes that are considered. Equation of trend line will give regression coefficients A and B as follows:

Equation of trend line is:

$$y = 0.8598 \times x + 0.3636 \quad (3.1)$$

In this case,

$$y = \log_{10}(W_E) \quad (3.2a)$$
$$x = \log_{10}(W_{TO}) \quad (3.2) \quad (3.2b)$$

from equation 2.16 in *Roskam vol I,*

$$W_E = 10^{\left[\frac{log_{(10)}W_{(TO)} - A}{B}\right]} \quad (3.3)$$

Simplifying above equation (3.3), we get

$$log_{10}(W_E) = \frac{1}{B} log_{10} W_{TO} - \frac{A}{B} \quad (3.4)$$

Therefore,

$$\frac{1}{B} = 0.8598$$

$$B = 1.163$$

And,

$$-\frac{A}{B} = 0.3636$$

$$A = -0.423$$

Hence, we find the regression coefficients as *A = -0.423* and *B = 1.163.*

3.2.3 Determination of Mission Weights:

There are two methods such as manual calculation and using AAA program to determine mission weights. Both methods begin by guessing a takeoff weight followed by sequential phases of flight like engine start and warmup, taxi, takeoff, climb, loiter if necessary, descent and approach and landing. The methods are described as follows:

$$W_{takeoff} = 32{,}000\ lbs\ (Guess)$$

As discussed, X-69 flight consists of two phases in its complete flight. It will make an air launch from mothership with a clean release and climb at supersonic speed. Although while descending and landing X-69 will glide decelerating to subsonic speed using aerodynamics and efficient wing configuration. Hence fuel-fractions will be considered according to the mission phase of the flight. Subsonic glide fuel fractions are average of fuel-fractions of light weight aircrafts like Homebuilt, Single Engine, Twin Engine and Agricultural airplanes. Highlighted section of table 3.2 are the fuel-fractions considered for two phases of X-69 flight and hence to calculate its takeoff weight.

Referring to table 2.1. *Suggested Fuel-fractions for Several Mission Phases* in *Roskam vol I,*

Table 3.2: Suggested fuel-fractions for several mission phases

Mission Phase	Engine start	Takeoff/Air launch	Climb	Descent	Landing, Taxi and Shutdown
Supersonic Cruise	0.990	0.995	0.92-0.87	0.985	0.992
Subsonic Glide	0.995	0.997	0.994	0.993	0.995

Referring to Table 2.15. *Regression Line Constants A and B* in *Roskam vol I,* regression coefficients A and B are 0.4221 and 0.9876 respectively since X-69 will be in supersonic flight.

3.2.4 Manual Calculation of Mission Weights:

The fuel-fraction, m_{ff} for each phase is defined as the ratio of end weight to begin weight.

The next step is to assign a numerical value to the fuel-fraction corresponding to each mission phase. This is done as follows referring to Table 3.2:

Phase 1. Engine Start and warm up:

This phase can be considered when X-69 is attached to the mothership, preparing for drop at 45,000 ft (mid-air launch). Hence to avoid rocket firing delays, or mission abort, it would be necessary to start the rocket motor by igniting the solid propellant but keeping the LOX or oxidizer pressure at minimum to achieve to idle state of the engine. Therefore, the Begin weight becomes W_{TO} with end weight W_1. The fuel fraction for this phase is given by: W_1/W_{TO}.

Therefore,

$$fuel - fraction = \frac{W_1}{W_{TO}}$$

$$0.990 = \frac{W_1}{32{,}000 \text{ lbs}}$$

$$W_1 = 31{,}680 lbs$$

Phase 2. Clean Release (mid-air launch) followed by firing up of rocket motor:

Begin weight is W_1. End weight is W_2. The fuel fraction for this phase is W_2/W_1.

Therefore,

$$fuel - fraction = \frac{W_2}{W_1}$$

$$0.995 = \frac{W_2}{31{,}680 \text{ lbs}}$$

$$W_2 = 31{,}521.6 lbs$$

Phase 3. Climb at Supersonic speed:

Begin weight is W_2. End weight is W_3. The fuel fraction W_3/W_2 for this phase is 0.9 according to the fig 3.3 referred from *Roskam vol I,* as the cruising speed of X-69 will be around Mach 3.0 at the end of climb phase. It will be assumed that the climb is performed at an average climb-rate of 82,000 fpm referring to similar airplanes to 365,000 ft (110,000 km) which takes around 90 seconds. Hence the range covered is $\frac{90}{3600} \times 810\ kts = \ 20.25 nm$. This range is simply a powered range as the later phases are unpowered glide and landing.

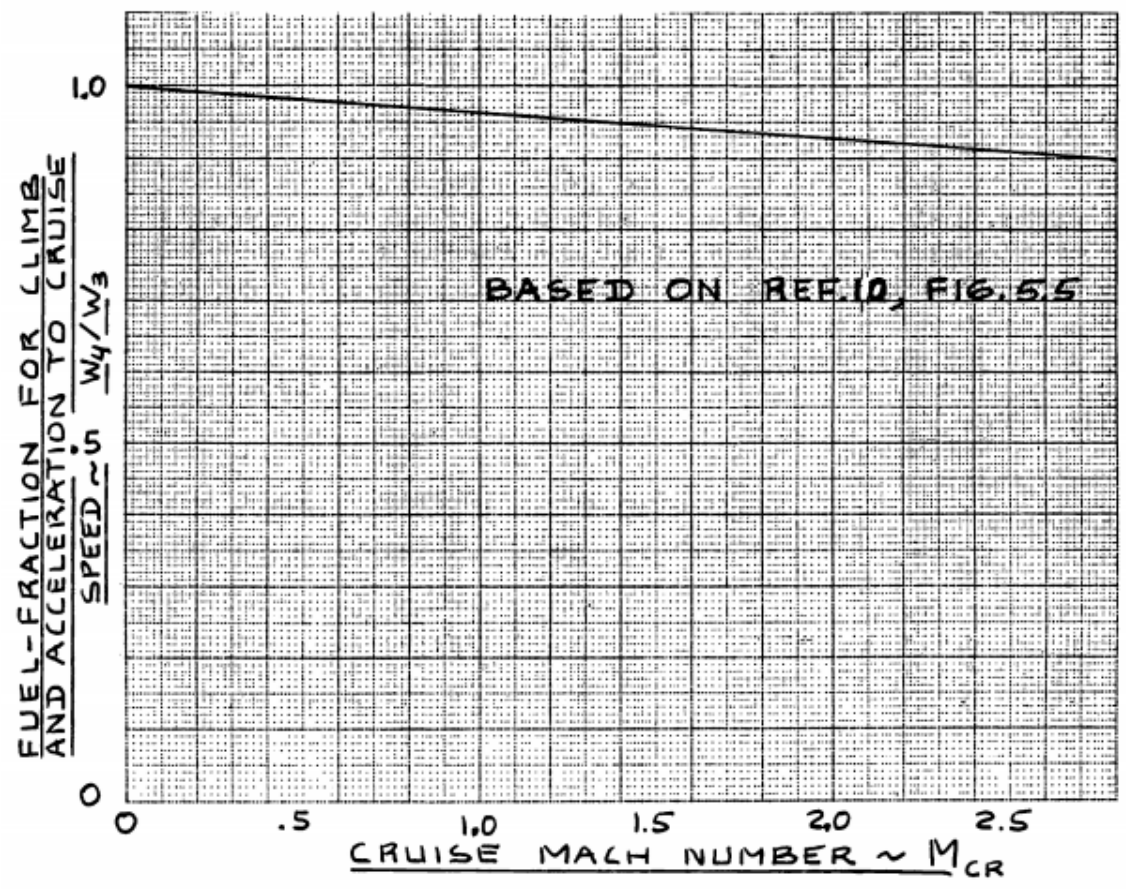

Figure 3.3: Fuel fraction for phase 5 of mission profile

Therefore,

$$fuel - fraction = \frac{W_3}{W_2}$$

$$0.9 = \frac{W_3}{31{,}521.6\ lbs}$$

$$W_3 = 28{,}369.44 lbs$$

Phase 4. Drop from the space and descent towards earth from 80,000 ft:

Begin weight is W_4. End weight is W_3. The fuel fraction for this phase is W_4/W_3.

Therefore,

$$fuel - fraction = \frac{W_4}{W_3}$$

$$0.993 = \frac{W_4}{28{,}369.44 lbs}$$

$$W_4 = 28{,}170.85 lbs$$

Phase 5. Glide, Approach, Landing, Taxi and shutdown:

Begin weight is W_5. End weight is W_4. The fuel fraction for this phase is W_5/W_4.

Therefore,

$$fuel - fraction = \frac{W_5}{W_4}$$

$$0.995 = \frac{W_5}{28{,}170.85lbs}$$

$$W_5 = 28{,}030lbs$$

Therefore, the mission fuel-fraction, M_{ff} is given as:

$$M_{ff} = \left(\frac{W_1}{W_{TO}}\right) * \prod_{i=1}^{i=5} \left(\frac{W_{i+1}}{W_i}\right) \tag{3.4a}$$

$$M_{ff} = \left(\frac{W_1}{W_{TO}}\right)\left(\frac{W_2}{W_1}\right)\left(\frac{W_3}{W_2}\right)\left(\frac{W_4}{W_3}\right)\left(\frac{W_5}{W_4}\right) \tag{3.4b}$$

$$M_{ff} = \left(\frac{W_5}{W_{TO}}\right)$$

$$M_{ff} = \left(\frac{28{,}030}{32{,}000}\right)$$

$$M_{ff} = 0.876$$

Weight of fuel used, $W_{F_{used}}$

$$W_{F_{used}} = (1 - M_{ff})W_{TO} \tag{3.5}$$

$$W_{F_{used}} = (1 - 0.876) \times 32{,}000$$
$$W_{F_{used}} = 3{,}968\ lbs$$

$$A = -0.423, B = 1.163$$

$$W_E = 10^{\left(\frac{log_{10}32{,}000 + 0.423}{1.163}\right)}$$

$$W_E = 17{,}276lbs$$

A tentative value for W_{OE} is found from equation below:

$$W_{OE_{tent}} = W_{TO} - W_{F_{used}} - W_{PL} \tag{3.6}$$

Payload weight, W_{PL} is 3,310 lbs.

$$W_{OE_{tent}} = 32{,}000 - 3{,}968 - 3310$$

$$W_{OE_{tent}} = 24{,}722lbs$$

A tentative value for W_E is found from equation below:

$$W_{E_{tent}} = W_{OE_{tent}} - W_{TFO} - W_{crew} \quad (3.7)$$

$$W_{TFO} = 0.005 \times W_{TO} = 0.005 \times 32{,}000$$

$$W_{TFO} = 160lbs$$

$$W_{E_{tent}} = 24{,}722 - 160 - 350$$

$$W_{E_{tent}} = 24{,}212lbs$$

Comparing $W_{E\text{-}tent}$ and $W_{E\text{-}allowable}$/ W_E,

$$\frac{|W_E - W_{E_{tent}}|}{\frac{W_E + W_{E_{tent}}}{2}} = \frac{|17{,}276 - 24{,}722|}{\frac{17{,}276 + 24{,}722}{2}} \times 100 = 35.5\%$$

Using MATLAB, W_{TO} can be iterated to obtain required comparison less than 0.5%. The code can be referred from Appendix C.

After iterating, W_{TO} = 13,870 lbs. give comparison percentage of about 0.0111% which is less than 0.5% with empty weight, W_E = 8418.81 lbs.

Table 3.3: Mission weights with respect to selected takeoff weight = 13,870 lbs.

Engine start and warmup, w1	13,731.3 lbs.
Air launch/ takeoff, w2	13,662.6 lbs.
Climb, w3	12,296.4 lbs.
Descent, w4	12,210.3 lbs.
Land and taxi, w5	12,149.2 lbs.
Weight of fuel used, W_f	1,720.75 lbs.

3.2.5 Calculation of Mission weights using AAA program:

Before starting the calculation for take-off weight, it is necessary to set up the configuration of X- 69 in the software. Appendix D shows initial steps to set the parameters and configuration of aircraft:

In AAA program, after configuring X-69, we start with weight analysis by defining mission profile and respective fuel-fractions. Fig. 3.4 shows sequentially arranged segment-wise mission profile with required fuel-fractions:

Mission Profile	M_{ff}
Warmup	0.9900
Take-off	0.9950
Climb	0.9192
Descent	0.9930
Loiter	0.9998
Land/Taxi	0.9950

Figure 3.4 Mission profile of X-69 with fuel-fraction.

After mission profile is defined, we obtain regression coefficients based of empty and takeoff weights of similar airplanes that are accounted in table.1. Clicking on *"Weight Sizing"* opens following window as shown in Fig. 3.5 where user needs to feed in similar airplanes data as I did it for X-69.

It is necessary to maintain the airplane data less scattered. The more the airplanes, more will be the accuracy for regression coefficients. For X-69, I found up to 11 similar airplanes that were considered to compute regression coefficients and will be used to compute takeoff weight in next step. Fig. 3.6 shows the trend line for empty weight v/s takeoff weight from which regression coefficients were obtained.

After obtaining regression coefficients A and B, it is safe to proceed for takeoff weight. We input required parameters in "*Take-off weight: Flight condition 1*" window as shown in Fig. 3.7 We input same regression coefficients A and B that we obtained in previous step. Any near-takeoff weight can be guessed under W_{TOest}. There are no passengers in X-69 but 2 pilots weighing approximately 350 lbs. each. Rest of the payload of satellites have been considered under W_{cargo} = 1,500 lbs. Fuel fraction of trapped fuel (slivers in the empty rocket motor) and oil is assumed to be 0.005% as referred from *Roskam*. X-69 won't need any reserve fuel, so $M_{res}=0$.

After hitting calculate, it gives following output parameters with slightly different value of takeoff weight than that obtained from manual calculation.

Fig. 3.8 shows the design point for takeoff weight using the same equations that were used to perform manual calculations. AAA program gives W_{TO} as design point equal to 12,683.3 lbs. which is lower number than that obtained from manual calculation with W_{TO} = 13,870 lbs.

W_{TO}	12683.3	lb	W_E	7684.0	lb	Number	12

Empty Weight - Take-off Weight Table

#	Manufacturer	Airplane Name	W_{TO} lb	W_E lb	Reference
1	NASA	Martin Marietta X-24B	13800.0	7800.0	
2	Virgin Galactic	Virgin Galactic Spaceship One	7900.0	2640.0	
3	Virgin Galactic	Virgin Galactic Spaceship Two	21428.0	10423.0	
4	Boeing	Boeing X-20 Dyna Soar	11387.0	10395.0	
5	NASA	North American X-15	34000.0	14600.0	
6	Lockheed	Lockheed Martin X-33	285000.0	75000.0	
7	NASA	NASA X-38	25000.0	23500.0	
8	NASA	Douglas X-3 Stiletto	22400.0	14345.0	
9	NASA	Ryan X-13 Vertijet	7200.0	5334.0	
10	Boeing	Boeing X-37B	11000.0	11000.0	

Output Parameters

A	-0.0888	B	1.0789

Figure 3.6 Regression coefficients A and B

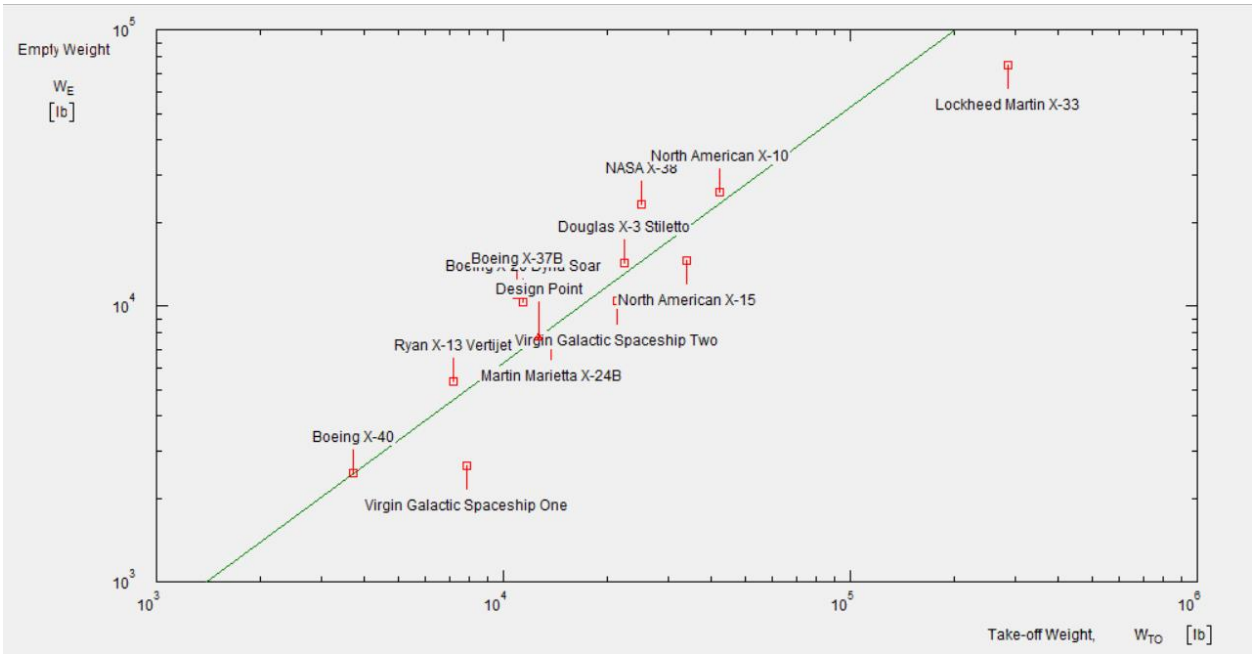

Figure 3.5 Regression plot and trend line.

Input Parameters

A	-0.0888	$W_{TO_{est}}$	14000.0	lb	$W_{\Sigma crew}$	350.0	lb	M_{tfo}	0.500	%	$W_{TO_{min}}$	10000.0	lb
B	1.0789	$W_{\Sigma pax}$	0	lb	$W_{\Sigma cargo}$	3310.0	lb	$M_{F_{res}}$	0.000	%	$W_{TO_{max}}$	15000.0	lb

Output Parameters

M_{ff}	0.8945	W_F	1358.9	lb	$W_{F_{res}}$	0.0	lb	W_{PL}	3310.0	lb	W_E	7791.4	lb
$W_{F_{used}}$	1358.9	lb	$W_{F_{max}}$	1358.9	lb	W_{tfo}	64.4	lb	W_{useful}	5018.9	lb	W_{TO}	12874.6	lb

Mission Profile Table: Output

	Mission Profile	W_{begin} lb	$\Delta W_{F_{used}}$ lb	$W_{F_{begin}}$ lb
1	Warmup	12874.6	128.7	1358.9
2	Take-off	12745.9	63.7	1230.1
3	Climb	12682.1	1024.2	1166.4
4	Descent	11658.0	81.6	142.2
5	Loiter	11576.4	2.8	60.6
6	Land/Taxi	11573.6	57.9	57.9

Figure 3.8 Takeoff weight: Flight condition 1.

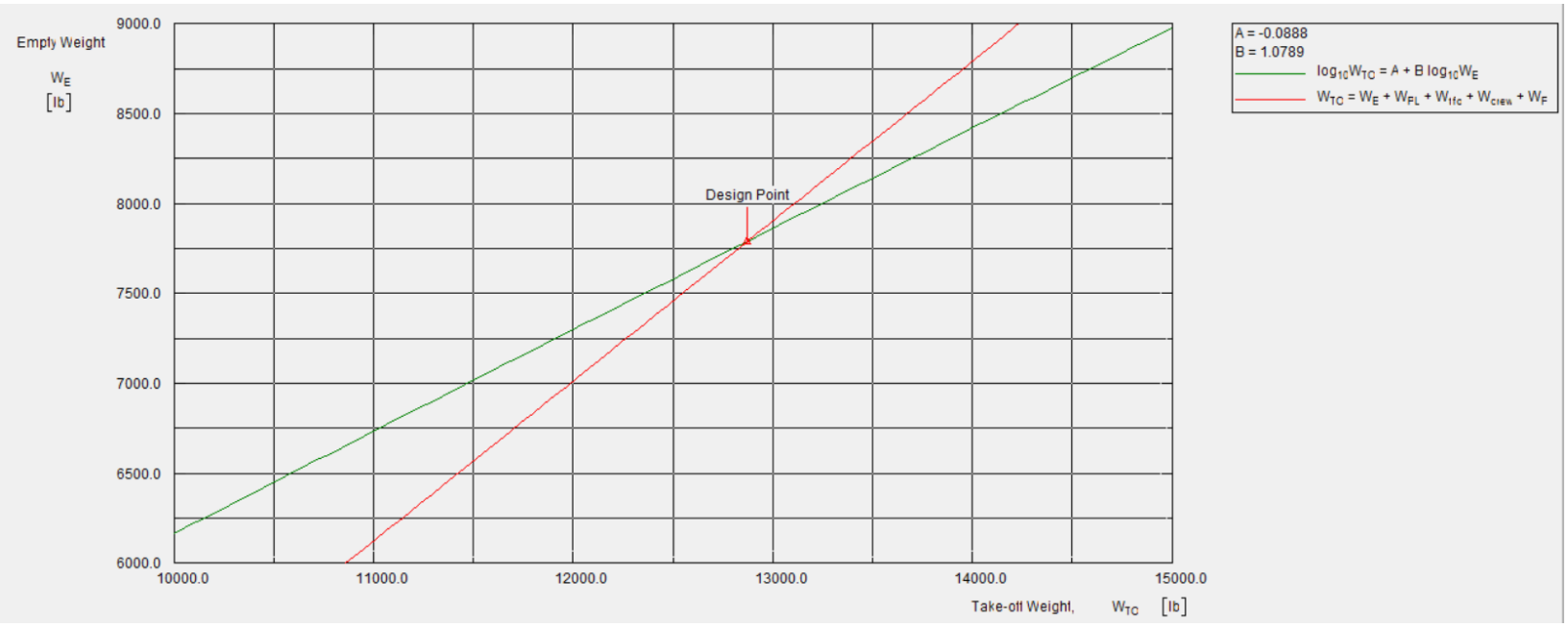

Figure 3.7 Design point on trend line @ 12,874.6 lbs.

3.3 Takeoff Weight Sensitivities:

3.3.1 Manual Calculation of Takeoff Weight Sensitivities:

Before starting sensitivity calculations, it should be checked if equation 2.24 from *Roskam* yields approximately same takeoff weight, W_{TO} as we obtained from iterative method in section 3.2.5. To do that we can substitute values of regression coefficients A, B, C and D in equation 2.24 as stated below:

$$\log_{10} W_{TO} = A + B \log_{10}(C.W_{TO} - D)$$

Substituting *A=-0.423, B=1.163, C=0.872* and *D=3,660 lbs.* and using small MATLAB solver from Appendix 3.1, we get

$$\log_{10} W_{TO} = -0.423 + 1.163 \times \log_{10}(0.872 \times W_{TO} - 3{,}660)$$

$$W_{TO} = 13{,}825.2\ lbs$$

W_{TO} that we just obtained is quite close to that we got from iterative method, hence we can move ahead with this takeoff weight for sensitivity calculations.

X-69 will not be cruising at any time throughout its flight since it will climb at supersonic speed as it drops from mothership. Hence there is no cruise consideration while calculating sensitivities either in AAA program.

After preliminary sizing, it is mandatory to conduct sensitivity studies on parameters such as

Payload, W_{PL}:

Sensitivity of Take-off weight to Payload Weight:

From section 2.7.2 *Sensitivity of Take-off weight to Payload weight* of *Roskam vol I*, sensitivity of take-off weight to payload weight is given by:

$$\frac{\partial W_{TO}}{\partial W_{PL}} = \frac{B.W_{TO}}{(D - C(1-B).W_{TO})}$$

$$A = -0.423, B = 1.163$$

$$C = \left[1 - (1 + M_{res})\left(1 - M_{ff}\right) - M_{tfo}\right]$$

$$W_{F_{res}} = M_{res}.\left(1 - M_{ff}\right).W_{TO}$$

$$M_{res} = \left(\frac{W_{F_{res}}}{\left(\left(1 - M_{ff}\right).W_{TO}\right)}\right)$$

No reserves, therefore

$$M_{res} = 0$$

$$C = \{1 - (1 + M_{res})\,(1 - M_{ff}) - M_{tfo}\}$$
$$C = \{1 - (1 + 0)\,(1 - 0.867) - 0.005\}$$
$$C = 0.872$$

$$D = W_{PL} + W_{crew}$$
$$D = 3{,}310 + 350$$
$$D = 3{,}660\ lbs$$

$$\frac{\partial W_{TO}}{\partial W_{PL}} = \frac{B.W_{TO}}{(D - C(1-B).W_{TO})}$$

$$\frac{\partial W_{TO}}{\partial W_{PL}} = \frac{1.163 \times 13{,}870}{3{,}360 - 0.872(1 - 1.163) \times 13{,}870}$$

$$\frac{\partial W_{TO}}{\partial W_{PL}} = 3.0256$$

This means that for each pound of payload added, the airplane take-off gross weight will have to be increased by 3.0256 lbs. and is called growth factor due to payload for X-69.

Empty weight, W_E

Sensitivity of Take-off weight to Payload Weight:

From section 2.7.3, *Sensitivity of Take-off weight to Empty weight* of *Roskam*, sensitivity of take-off weight to payload weight is given by:

$$\frac{\partial W_{TO}}{\partial W_E} = \frac{B.W_{TO}}{[10^{(log_{10}W_{TO} - A)/B}]}$$

$$\frac{\partial W_{TO}}{\partial W_E} = \frac{1.163 \times 13{,}870}{[10^{(log_{10}13{,}870.4 + 0.423)/1.163}]}$$

$$\frac{\partial W_{TO}}{\partial W_E} = 4.43$$

For each lb of increase in empty weight, the take-off weight will increase by 4.43 lbs. and is a growth factor due to empty weight for X-69.

- **Range, R**

Sensitivity of Take-off weight to Range:

Estimated range of X-69 is 120nm (110 km) return trip including re-entry and landing. X- 69 will climb at supersonic speed and hence the characteristics for calculating sensitivities of take- off weight and range will be like that of fighter airplanes. From It is necessary to calculate a factor F using equation 2.44 in *Roskam* as given below:

$$F = \frac{-B.W_{TO}^2}{C.W_{TO}.(1-B) - D} \times (1 + M_{res})M_{ff}$$

Substituting values of B, C, D in above equation.

$$F = \frac{-1.163 \times 13{,}870^2}{0.872 \times 13{,}870 \times (1 - 1.163) - 3{,}660} \times 0.867$$

$$F = 34{,}446$$

$$\frac{\partial W_{TO}}{\partial R} = \frac{F \times c_j}{\frac{VL}{D}}$$

As X-69 is powered by a hybrid rocket motor, average specific fuel consumption, c_j ranges between 8-14, hence considering c_j around 10

$c_j = 10$, $V = 1984\ kts$ ($supersonic$, 3186 $\frac{km}{hr}$ = Mach 3.0), $\frac{L}{D} = 7{:}\,1$

Therefore,

$$\frac{\partial W_{TO}}{\partial R} = \frac{34{,}446 \times 10}{3{,}186\ \text{km/hr} \times 7}$$

$$\frac{\partial W_{TO}}{\partial R} = 15.445\ lbs/km$$

Hence for every increase of kilometer, gross take-off weight will increase by 15.445 lbs.

Endurance, E

Sensitivity of Take-off weight to Endurance:

Same as Range, sensitivity of takeoff weight to endurance is given by

$$\frac{\partial W_{TO}}{\partial \mathrm{E}} = \frac{F_{c_j}}{\frac{L}{D}}$$

$$\frac{\partial W_{TO}}{\partial \mathrm{E}} = \frac{34{,}446 \times 10}{7}$$

$$\frac{\partial W_{TO}}{\partial \mathrm{E}} = 637.14\ lbs/hr$$

Lift-to-drag ratio, L/D

Sensitivity of Take-off weight to Lift-to-drag ratio with respect to range requirement:

$$\frac{\partial W_{TO}}{\partial \left(\frac{L}{D}\right)} = -\frac{F.R_{c_j}}{V \times \left(\frac{\mathrm{L}}{\mathrm{D}}\right)^2}$$

$$\frac{\partial W_{TO}}{\partial \left(\frac{L}{D}\right)} = -\frac{34{,}446 \times 110\ km \times 10}{3{,}186 km/hr \times 7^2}$$

X-69 will use fuel only while climbing. As said earlier, it will just glide while descending without any use of fuel. Hence range, R in above equation is taken only when it is climbing from 50,000 ft to 360,000 ft which gives around 110 km of climb.

Hence,

$$\frac{\partial W_{TO}}{\partial \left(\frac{L}{D}\right)} = -242.7 lbs$$

If the lift-to-drag ratio of the airplane were 16 instead of the assumed 14, the design take- off gross weight would decrease by *16-14=2*×242.7*=485.4 lbs.*

Specific fuel consumption, c_j

Sensitivity of Take-off weight to specific fuel consumption, cj with respect to range requirement:

$$\frac{\partial W_{TO}}{\partial c_j} = \frac{F.R}{V.\frac{L}{D}}$$

$$\frac{\partial W_{TO}}{\partial c_j} = \frac{34{,}446 \times 110km}{3{,}186km/hr \times 7}$$

$$\frac{\partial W_{TO}}{\partial c_j} = 170\,\frac{lbs}{hr}$$

3.3.2 Calculation of Takeoff Weight Sensitivities using the AAA program:

AAA program provides sensitivity computation if required parameters have been inserted. If sequential procedure is followed, i.e. starting with mission profile, obtaining regression coefficients and hence takeoff weight, then sensitivity automatically considers those basic parameters. Hitting calculate button gives sensitivities of takeoff weight with payload, empty weight, range, specific fuel consumption, L/D ratio and endurance.

Since X-69 will never cruise neither loiter, there is no takeoff sensitivity with respect to range. As stated earlier, after completing its mission in space it will be dropped towards earth with accurate attitude using reaction control system. As it reaches 80,000 – 85,000 ft, it will use its wing and aerodynamics to slow down and glide to destination. Although its total range will be 120 nm considering return trip excluding cruising, loitering phase of flight.

There is significant percentage difference between manually calculated and AAA computed sensitivities. Regression coefficients A and B are the major cause responsible for this difference. It is unclear that what method does AAA program use to calculate regression coefficients A and B using same similar airplane database and hence trend line that is been used for manual calculation. Although from the linear characteristics and using method described in *Roskam Book,* we obtain different A and B for manual calculations than from AAA program. Table. 5 describes the percentage difference which on an average is up to 30%.

Input Parameters

B	1.0789		W_{PL}	3310.0	lb	M_{tfo}	0.500	%	W_{TO}	12874.6	lb
M_{ff}	0.8945		$W_{\Sigma crew}$	350.0	lb	$M_{F_{res}}$	0.000	%	W_E	7791.4	lb

Output Parameters

$\partial W_{TO}/\partial W_{PL}$	3.00		$\partial W_{TO}/\partial W_{crew}$	3.00		$\partial W_{TO}/\partial W_E$	1.78

Mission Sensitivity Table: Output

	Mission Profile	$\partial W_{TO}/\partial W_{FL_{exp}}$	$\partial W_{TO}/\partial W_{FL_{reload}}$	$\partial W_{TO}/\partial W_{F_{refuel}}$	$\partial W_{TO}/\partial c_j$ lb-hr	$\partial W_{TO}/\partial R$ $\frac{lb}{nm}$	$\partial W_{TO}/\partial L/D$ lb	$\partial W_{TO}/\partial E$ $\frac{lb}{hr}$
1	Warmup							
2	Take-off							
3	Climb				287.0		-410.0	48689.9
4	Descent							
5	Loiter				1623.0		-1.2	24.3
6	Land/Taxi							

Figure 3.8. Sensitivity calculation and growth factors

3.4 Trade Studies:

The trade studies for sensitivity of take-off weight with respect to specific fuel consumption for rate of climb is done with reference to the sensitivity output from AAA. However, the analysis requires more of it from propulsion viewpoint which will be carried out in propulsion system analysis since the climb of X-69 is completely governed by the rocket executed after the mid-air launch. For the weight analysis however, it is feasible to trade some payload either for rate of climb or loiter time. As we discussed earlier in section 3.2, the loitering should not last for more than 20 minutes which is more likely a waiting time for confirmation for landing approach.

In case of aborted missions where the climb is simply aborted to cruise followed by loiter and landing, extending the loitering time is vital. Moreover, the complete cruise and loiter is unpowered making it a gliding flight. Therefore, sensitivity of take-off weight with respect to specific fuel consumption is neglected. Hence, the trade studies will be carried out for loiter for take-off weight with respect to L/D and endurance, understanding how much payload we have to shed in pursuit of more L/D.

At this point we need to understand the size and weight of payload based on their types. Maximum payload considered for X-69 is 3,310 lbs. which is about 1,500 kg. The CubeSats are accommodated in special type of dispensers called Canisterized Satellite Dispenser (CSD) that are discussed in detail in Fuselage section. The total number of each type CubeSats are indeed rounded off to lower value to account for all CSDs weight which is about 5lbs. Moreover, These CSDs are operated based on either launch sequence using ejection system or by using small solid rocket boosters. The dispensing mechanism depends up on the payload owner considering the sensitivity of the instruments onboard the CubeSat. The calculation is as follows:

Table 3.4. Types of payload

Type of Payload	Size per unit, in cm	Weight per unit, lbs./kg	Total number of payloads to reach 3,310 lbs. (maximum limit)
6U CubeSats	12 cm x 24 cm x 36 cm	26.45 lbs./ 12 kg	125 no. of 6U CubeSats
12U CubeSats	23 cm x 24 cm x 36 cm	52.91 lbs./ 24 kg	62 no. of 12U CubeSats
27U CubeSats	34 cm x 35 cm x 36 cm	119.05 lbs./ 54 kg	27 no. of 27U CubeSats

Now that we have understood the payloads, trade studies are as follows:

Table 3.5. Trade study for payload

Type of CubeSat	Total number as payload	$\partial W_{TO}/\partial c_j$, lb-hr.	$\partial W_{TO}/\partial(L/D)$, lb	$\partial W_{TO}/\partial E$, lb/hr.	$\partial W_{TO}/\partial c_j$, lb-hr.	$\partial W_{TO}/\partial(L/D)$, lb	$\partial W_{TO}/\partial E$, lb/hr.
		Climb			Loiter		
6U	6U						
	125	295.2	-421.7	50076.5	1669.2	-1.2	25
	120	304	-434.3	51571.2	1719	-1.2	25.8
	115	313.3	-447.6	53157.8	1771.9	-1.3	26.6
	110	323.3	-461.8	54848.2	1828.2	-1.3	27.4
	105	333.9	-477	56643.2	1888.1	-1.3	28.3
	100	345.2	-493.1	58563	1952	-1.4	29.3
	95	357.3	-510.4	60617.6	2020.6	-1.4	30.3
	90	370.3	-529	62821.6	2094.1	-1.5	31.4
12U	12U						
	62	295.2	-421.7	50076.5	1669.2	-1.2	25
	60	302.2	-431.7	51265.4	1708.8	-1.2	25.6
	58	309.5	-442.2	52512.1	1750.4	-1.3	26.3
	56	317.2	-453.2	53820.9	1794	-1.3	26.9
	54	325.3	-464.8	55196.6	1839.9	-1.3	27.6
	52	333.9	-477	56644.6	1888.2	-1.3	28.3
	50	342.9	-489.8	58170.5	1939	-1.4	29.1
	48	352.4	-503.4	59780.9	1990.7	-1.4	29.9
	46	362.4	-517.7	61483	2049.4	-1.5	30.7
	44	373	-532.9	63284.9	2109.5	-1.5	31.6
27U	27U						
	27	295.2	-421.7	50076.5	1669.2	-1.2	25
	25	311.4	-444.9	52833.3	1761.1	-1.3	26.4
	23	329.6	-470.8	55911.4	1863.7	-1.3	28
	21	349.9	-499.9	59370.2	1979	-1.4	29.7
	19	373	-532.9	63285.3	2109.5	-1.5	31.6

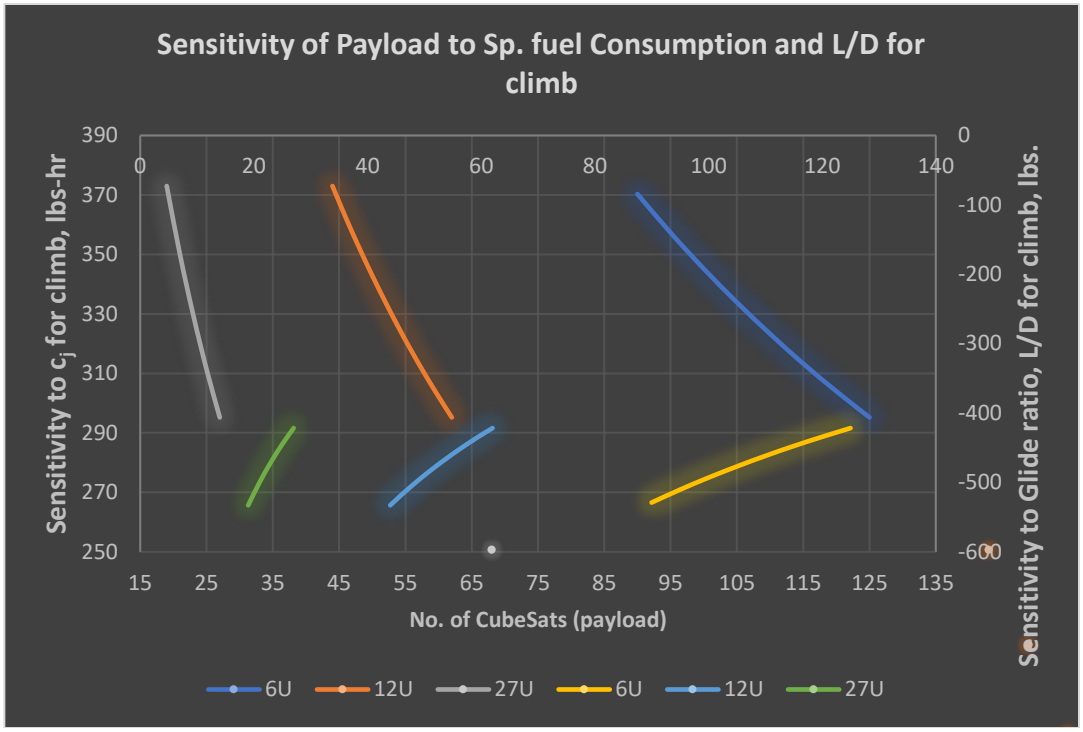

Figure 3.9. Sensitivity of payload to specific fuel consumption and L/D for climb

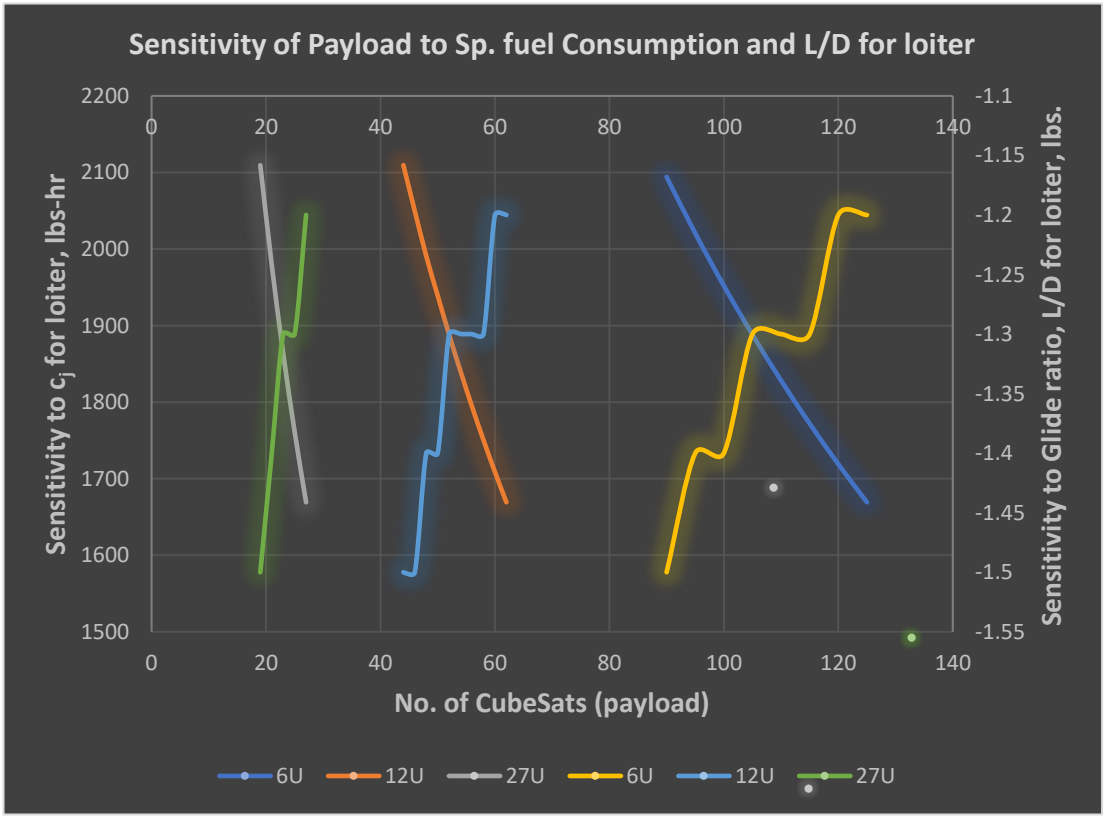

Figure 3.10. Sensitivity of payload to specific fuel consumption and L/D for Loiter

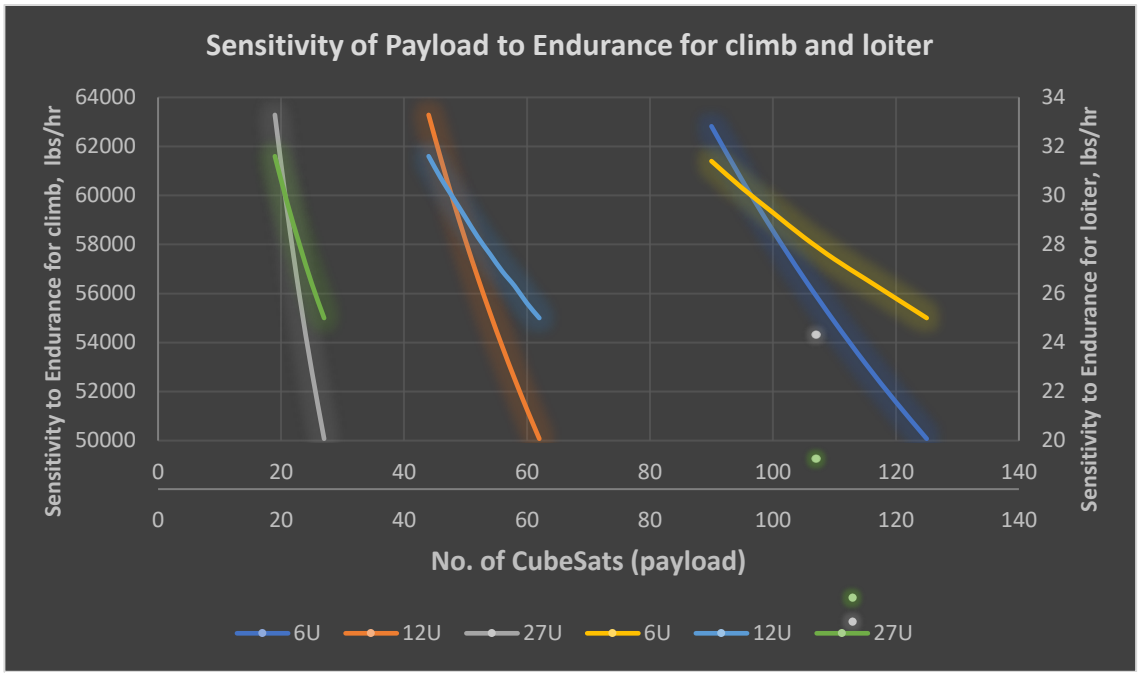

Figure 3.11. Sensitivity of payload to endurance for climb and loiter

From fig 3.9, we can see that take-off weight per unit glide ratio is increases with increase in payload. This in turn affects the glide performance. Furthermore, this plot is applicable only in aborted mission condition where X-69 will execute unpowered glide back to base instead of landing which changes with respect to the payload. Reader should understand that this glide ratio is different to that of loiter. Effect of payload on sensitivity with respect specific fuel consumption is inversely proportional. Also, this verifies the fact that X-69 will require more fuel per payload. Fig 3.10 and 3.11 give more idea about similar conditions in loitering and Endurance respectively. The detailed version of table 3.5 can be referred in appendix 3.

3.5 Discussion:

AAA software refers the theory of *Roskam book* up to some extent. Although, it is unclear that how diverse airplanes data it can handle that should give close values to that obtained from manual calculation. As we can observe that there is slight difference in final parameters in AAA program than we obtained using manual calculations. Following is Table. 3.4 showing percentage difference between manually calculated and AAA program computed parameters:

Table 3.6. Percentage difference for mission weights in lbs.

Parameters	Manually Calculated	AAA program computed	% difference
Takeoff weight, W_{TO}	13,870	12,874.6	7.177%
Empty Weight, W_E	8,418.81	7,791.4	7.45%
Fuel weight, W_F	1,720.75	1,358.9	21.03%

Assuming that AAA program estimation has higher accuracy than manual calculation, it is beneficial to proceed with AAA computed takeoff weight for trade studies. Also, the fuel-fractions considered for each phase in both manual calculation and AAA program are close. Takeoff weight and hence other dependent parameters also depend on regression coefficients A and B. And as we can see those coefficients

are slightly different giving rise to difference in takeoff weight and other parameters.

Same as mission weight calculation, we have considerable difference in parameters obtained from manual calculation and using AAA program. Table. 3.7 gives the percentage difference between significant parameters:

Table 3.7. Percentage difference for sensitivities

Parameters	Manually calculated	AAA computed	% difference
$\partial W_{TO}/\partial W_{PL}$	3.026	3.00	0.8%
$\partial W_{TO}/\partial W_{E}$	4.43	3.00	32.3%
$\partial W_{TO}/\partial E$	49,208.6	48,689.9	1.05%
$\partial W_{TO}/\partial(L/D)$	-242.71	-410.0	40.8%
$\partial W_{TO}/\partial c_j$	170	287	40.76%

Takeoff weight is very significant and primary parameter for aircraft design. Hence it is necessary and mandatory to analyze accurately takeoff weight sensitivities with respect to payload weight, empty weight, endurance, range, life-to-drag L/D ratio and specific fuel consumption (sfc) if practical data is available.

Considering the accuracy of AAA program, it is preferable to consider the computed values for design. Hence for each pound of payload added, the airplane take-off gross weight will have to be increased by 3.00 lbs. and is called growth factor due to payload for X-69. Similarly, for each lbs. of increase in empty weight, the take-off weight will increase by 3.00 lbs. and is a growth factor due to empty weight for X-69. If the lift-to-drag ratio of the airplane were 16 instead of the assumed 14, the design take-off gross weight would decrease by *16-14=2*× 410*=820 lbs.* If specific fuel consumption was incorrectly assumed to be 0.5 and, turns out to be 0.9, the design take-off gross weight will increase by *0.9-0.5=0.4*× 287*=114.8 lbs.*

Observing takeoff weight sensitivity for specific fuel consumption, c_j and trade study plot fig. 9, we can see that if X-69 owner desires to have more payload, specific fuel consumption has to be sacrificed making the engine less efficient per pounds of thrust. Although keeping the takeoff weight constant and varying payload has less impact on specific fuel consumption as compared that with takeoff weight. Referring the table. 6, we can see that for slight reduction in specific fuel consumption, c_j gross takeoff weight increases drastically.

3.6 Conclusion and Recommendations:

3.6.1 Conclusions:

X-69 is desired to have the payload weight of *3,310 lbs.* that will accommodate satellites, racks to place and hold satellites and instruments together unharmed from high speed climb of X-69. Having mentioned the consistency of payload weight, takeoff weight of X-69 has been calculated using manual calculation as well as AAA program. After considering all parametric aspects, *13,870 lbs.* will be a design point for takeoff weight of X-69. X-69 will be manufactured using composites hence regression coefficients A and B must be calculated separately for manual calculation as mentioned in *Roskam*. X-69 will be using hybrid rocket motor with either nylon or HTPB as solid fuel and liquid nitrous oxide as liquid oxidizer.

3.6.2 Recommendations:

The weight analysis has been done very diverse data obtained from various resources. The compared similar airplanes have very diverse configurations with respect to their missions. Hence unlike conventional airplanes, there is no reference on previously done analysis on these type of airplanes in *Roskam* or any other resources. Altitude limit can be extended to low earth orbit to about 160 km. Also, if reaction control thrusters are efficient enough, besides maneuvering for satellites they can be used to orbit X-69 over certain location before it drops to earth gravity. From initial research, HS 130 airfoil will be used for wing, elevons and stabs since it has high gliding efficiency at high altitude and speeds.

4. Chapter 4 - Performance Sizing/ Constraints for X-69 CargoSat

4.1 Introduction:

This report investigates the performance constraints of X-69 based weight analysis and previous flight data of similar airplanes. Performance of X-69 signifies parameters like stall speed, take-off field length, landing field length, cruise speed, climb rate. This will help to estimate major airplane design parameters as mentioned below:

1) Wing Area, S
2) Take-off Thrust, T_{TO}
3) Maximum required takeoff lift coefficient: clean
4) Maximum takeoff lift coefficient
5) Maximum landing lift coefficient and many parameters.

As discussed in previous reports, X-69 flight profile is divided into several stages as also shown in figure below:

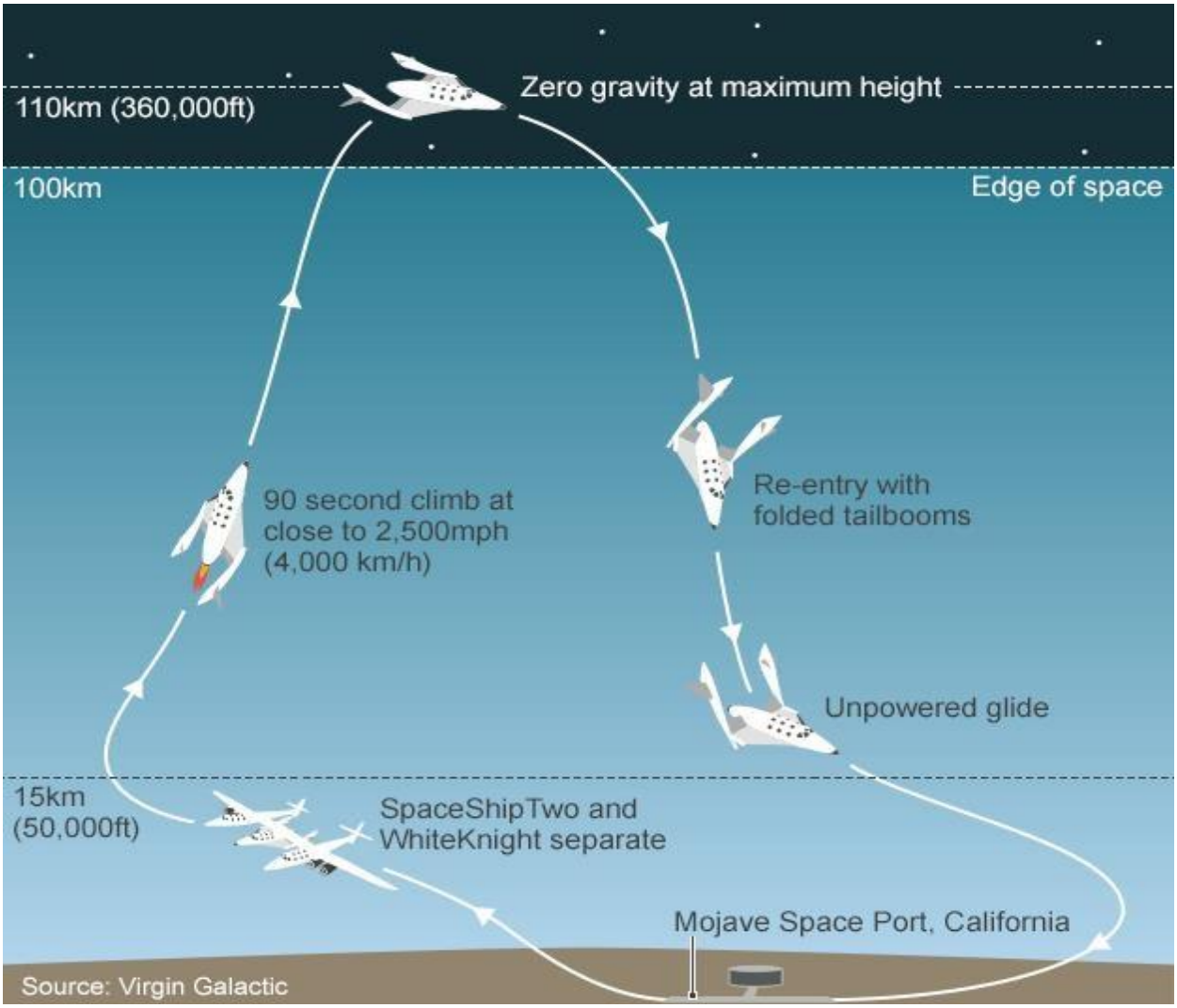

Figure 4.1. Mission profile of V.G's SpaceShipTwo

a) Air launch and clean release: The mothership such as WhiteKnightTwo (WK2) makes a clean release with pullup angle of 65°.

b) Boost/Climb: Rocket engine fires up climbing X-69 to high altitudes. The total burn time is expected to be approximately 90 seconds at which X-69 will attain 360,000 ft.

Rocket engine is the primary engine to boost X-69 to climb to 360,000 ft altitude at supersonic speed. The boost phase of X-69 relies on Newton's Second Law of Motion.

$$\sum F = ma$$

$\sum F$ is the summation of all external forces applied to the rocket, m is the mass of the X-69 accelerating with "a" ft/sec^2. The forces acting on X-69 during thrusting phase (climbing) of flight are its weight (W), Thrust (T) and aerodynamic drag (D). The effectiveness of thrust varies as the vertical component propels the vehicle to the target altitude and depends on flight path (pullup) angle with weight continuously changing due to the burning of rocket fuel.

c) Coast: After 90 seconds of boost and reaching apogee, X-69 performs the desired mission to deploy satellites using precise maneuverability with RCS thrusters.

d) Re-entry: Using RCS thrusters to orient its attitude for re-entry. The reentry phase is up to 80,000 ft – 85,000 ft. Reentry is accompanied by changing wing configuration to feathered state where wing feather gets locked to 60° using pneumatic system.

e) Descend and Glide: X-69 decelerates using aerodynamic drag with efficient gliding performance. The wing is designed to generate more and stable drag to kill the reentry speeds.

f) Approach and Landing: X-69 makes an approach for landing at subsonic speed. Further landing performance is studied in performance constraints section. For this analysis, Mojave Airspace and Spaceport is considered to simplify and compare the analysis with spaceship two since flights of spaceship two were performed on this airport.

4.2 Sizing to stall speed requirements:

According to *Aircraft Design – Vol I, section 3.1,* we can determine power-off stall speed of X-69 using following equation:

$$V_S = \sqrt{\frac{2 \times \frac{W}{S}}{\rho C_{L_{max}}}} \tag{4.1}$$

We can consider similar power-off condition for X-69 since it will be an unpowered glide and landing. Referring both flaps full down and flaps up stall speeds of 50 kts (93 km/hr. or 84.4 ft/sec) and 60 kts (110 km/hr. or 101.3 ft/sec) respectively in power-off situation from *section 3.1.1 example* and maximum coefficient of lift values from *Table 3.1* within the 'state-of-the-art'

$$C_{L_{max}} = 1.60 \;\; and \;\; C_{L_{max_L}} = 2.00$$

To meet the flaps down requirement, we take $C_{L_{max_L}} = 2.00$ & $V_S = 50kts = 84.4ft/s$

$$\left(\frac{W}{S}\right)_{TO} = \frac{V_S^2 \times \rho \times C_{L_{max_L}}}{2}$$

$$\left(\frac{W}{S}\right)_{TO} = \frac{(84.4ft/s)^2 \times 0.07647lbm/ft^3 \times 2.00}{2 \times 32.174lbm - ft/s^2}$$

$$\left(\frac{W}{S}\right)_{TO} < 17.0psf$$

To meet the flaps up requirements, we take $C_{L_{max}} = 1.60$ & $V_S = 60kts = 101.3\ ft/s$

$$\left(\frac{W}{S}\right)_{TO} = \frac{V_S^2 \times \rho \times C_{L_{max}}}{2}$$

$$\left(\frac{W}{S}\right)_{TO} = \frac{(101.3ft/s)^2 \times 0.07647lbm/ft^3 \times 1.60}{2 \times 32.174lbm - ft/s^2}$$

$$\left(\frac{W}{S}\right)_{TO} < 19.5\ psf$$

4.3 Sizing to Take-off distance requirements:

For X-69, sizing to FAR 25 take-off distance requirements from *Roskam's section 3.2.3* is referred. There are several assumptions made to achieve relation between $(W/S)_{TO}$ and $(T/W)_{TO}$ which we require to select optimum performance for X-69.

4.3.1 Assumptions for take-off distance sizing:

1) In the mission profile, X-69 gets dropped at around 45,000 ft of altitude to which we call a mid-air launch. Before the drop, X-69 is completely idle like any airplane preparing for take-off.
2) Airspeed of X-69 drop will be equal to the airspeed of the mothership of around Mach 0.8 since mothership is flying at cruising speed at an average of Mach 0.8.
3) After the detachment from mothership and during the drop, X-69 stabilizes itself and then fires up the rocket motor for the next climb phase. This phase can be considered analogous to airplane running up for the take-off and climb.
4) After the rocket motor firing, X-69 will fly straight for 2-3 seconds followed by climb (or lift-off) gradually increasing its flight path angle and hence the speed to higher Mach.
5) Atmospheric conditions at 40,000 ft (since considering a dropping altitude limit) are:

   Pressure ratio at 40,000 ft, δ = 0.1844
   Temperature ratio at 40,000 ft, θ = 1.07
   Hence, $\sigma = \delta/\theta = 0.1844/1.07 = 0.1724$
   Considering the field length, S_{TOFL} = 5,000 ft
   TOP_{25} = 5,000/37.5 = 133.3 lbs./ft^2.

   Therefore, from *equation (3.8) of section 3.2.3,* we can relate:

$$S_{TOFL} = \frac{37.5(W/S)_{TO}}{\left[\sigma . C_{L_{max_{TO}}} . (T/W)_{TO}\right]} = 37.5\ TOP_{25} \quad (4.2)$$

Therefore,

$$(T/W)_{TO} = \frac{0.00544(W/S)_{TO}}{C_{L_{max_{TO}}}}$$

The following tabulation can be made for the required values of $(T/W)_{TO}$.

Table 4.1: Required values of $(T/W)_{TO}$

$(W/S)_{TO}\ psf$	$C_{L_{max_{TO}}} =$	1.6	2.0	2.4
15	$(T/W)_{TO} =$	0.051	0.0408	0.037091
20		0.068	0.0544	0.049455
25		0.085	0.068	0.061818
30		0.102	0.0816	0.074182

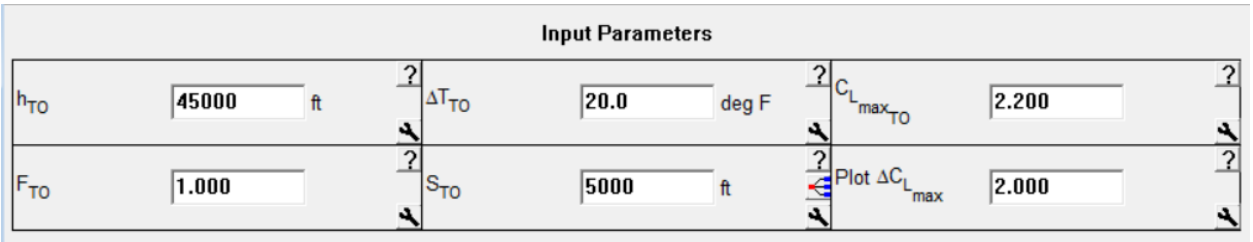

Figure 4.2. Input parameters for take-off distance from AAA

4.4 Sizing to Landing Distance requirements:

It is assumed that X-69 achieves adverse deceleration to about 60 kts to 70 kts using its aerodynamic features explained further which conforms with FAR23 landing distance requirements. Hence, we follow the same method as that in *section 3.3.1 of Aircraft Design vol I.*

Therefore,

$$V_A = 1.3V_{S_L} \tag{4.3}$$

$$S_{LG} = 0.265V_{SL}^2 \tag{4.4}$$

$$S_L = 1.938S_{LG} \tag{4.5}$$

$$S_L = 0.5136V_{S_L}^2 \tag{4.6}$$

Now we can essentially size X-69 to landing field length of 2,500 ft at 5,000 ft altitude. The design landing weight as specified in *table 3.3 of Aircraft Design vol I, of* $W_L = 0.77W_{TO}$ like that fighters considering the payload and empty rocket motor (propulsion system),

$$V_{S_L} = \sqrt{\frac{2{,}500}{0.5136}} = 69.8kts$$

From equation (4.1),

$$\frac{2 \times \left(\frac{W}{S}\right)_L}{0.002049 \times C_{L_{max_L}}} = (69.8 \times 1.688)^2 = 13{,}869ft^2/s^2$$

From this it follows that:

$$\left(\frac{W}{S}\right)_L = 14.2C_{L_{max_L}},$$

$$with \;\; W_L = 0.77W_{TO}, \;\; this \;\; yields:$$

$$\left(\frac{W}{S}\right)_{TO} = 10.934C_{L_{max_L}}$$

Hence from following fig, 4.1 we can verify the range of $(W/S)_{TO}$ and $C_{L_{max_L}}$ which meet the landing requirement. From *table 3.1 from Roskam's,* the typical values for $C_{L_{max_L}}$ for X-69 operating under similar conditions are: 1.6 – 2.5.

In this case, a range of values of 1.7, 2.0, 2.3 are considered to obtain maximum allowable wing loadings of 18.5878, 21.868 and 25.1482 psf respectively adding the same to $(T/W)_{TO}$ v/s $(W/S)_{TO}$ plot.

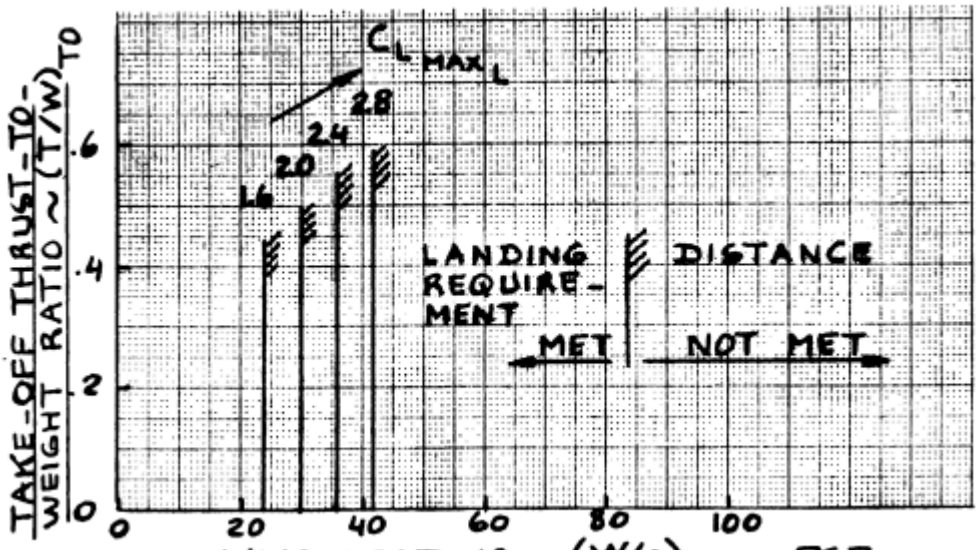

Figure 4.3 Allowable wing loading to meet a landing distance requirement

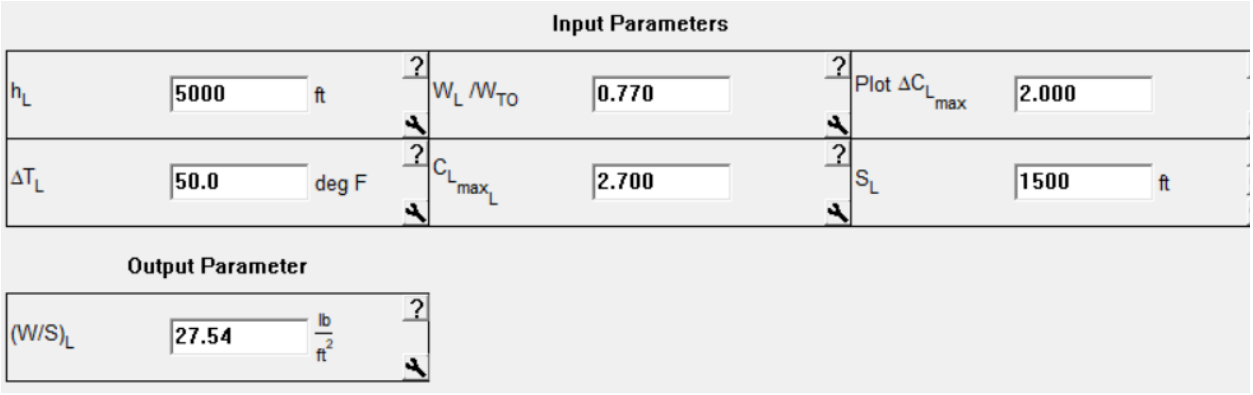

Figure 4.4. Parameters for landing distance from AAA

4.5 Drag Polar estimation:

We need to obtain clean, take-off and landing drag polars for X-69 with W_{TO} = 13,870 lbs.
Using the *equation (3.2.2) from Roskam,* we get wetted area as follows:

$$log_{10}S_{wet} = c + d.log_{10}W_{TO}$$

Referring to the regression coefficients c and d of jet airplane as $c = 0.2263$ and $d = 0.6977$

$$S_{wet} = 10^{0.2263+0.6977\times log_{10}13{,}870}$$
$$S_{wet} = 1{,}306.85ft^2$$

From *fig. 3.21,* it is apparent that a c_f value of 0.003 is reasonable. Hence, coefficients a and b for $cf = 0.003$ is $a = -2.523$ and $b = 1$

$$f = 10^{-2.523+1.log_{10}.S_{wet}}$$
$$f = 10^{-2.523+log_{10}.1{,}306.85}$$

$$f = 3.919ft^2$$

For X-69, the wing loading is observed to be ranging from 15 psf to 35 psf. Hence taking the average wing loading of 27.5 psf and W_{TO} = 13,870 lbs. the following data are obtained:

$$S = \frac{W_{TO}}{(W/S)_{TO}} = \frac{13{,}870}{21.03} = 659.65ft^2$$

Therefore,

$$C_{D_0} = f/S = 3.919/659.65 = 0.00594$$

To calculate drag polars, we have e = 0.85 and will consider the range of aspect ratio, A from 1.9 to 2.25. Table. 4.2 shows drag polars for 3 conditions that X-69 will face considering various aspect ratios for further analysis.

Table 4.2: Drag polars at various conditions and aspect ratios

Aspect ratio, A	Clean drag polar	Take-off drag polar, gear up	Landing drag polar, gear down
1.9	$0.00594+0.1971C_L^2$	$0.02094+0.1855C_L^2$	$0.08294+0.1855C_L^2$
2.0	$0.00594+0.0.1872C_L^2$	$0.02094+0.1762C_L^2$	$0.08294+0.1762C_L^2$

Aspect ratio, A	Clean drag polar	Take-off drag polar, gear up	Landing drag polar, gear down
2.1	$0.00594+0.1783C_L^2$	$0.02094+0.1678C_L^2$	$0.08294+0.1678C_L^2$
2.15	$0.00594+0.0.1742C_L^2$	$0.02094+0.1639C_L^2$	$0.08294+0.1639C_L^2$
2.18	$0.00594+0.0.172C_L^2$	$0.02094+0.0.162C_L^2$	$0.08294+0.0.162C_L^2$
2.20	$0.00594+0.17C_L^2$	$0.02094+0.16C_L^2$	$0.08294+0.16C_L^2$
2.25	$0.00594+0.166C_L^2$	$0.02094+0.1566C_L^2$	$0.08294+0.1566C_L^2$

4.6 Sizing for Climb Requirements:

The climb rate of X-69 is quite higher due to supersonic flight and higher flight path angles, $\gamma > 15°$. Hence according to *Roskam*, we can find the relation between thrust-to-weight ratio during climb and flight path angles from following equations that apply for high speed airplanes such as fighter.

$$sin\gamma = \frac{T}{W}\left[P_{dl} - \sqrt{P_{dl}^2 - P_{dl} + \left(1+\left(\frac{L}{D}\right)^2\right)^{-1} \times \left(\frac{T}{W}\right)^{-2}}\right] \tag{4.6}$$

$$where, P_{dl} = \frac{\left(\frac{L}{D}\right)^2}{1+\left(\frac{L}{D}\right)^2} \tag{4.7}$$

For the best climb performance, the value of L/D in equation (4.7) can be taken to be $(L/D)_{max}$ which is 7:1 for X-69, as of other spaceplanes

Table.4.3 and graph in figure. 4.5 shows T/W changes with respect to flight path angle.

Table 4.3: Thrust-to-Weight ratio v/s flight path angles

Flight path angle, in degree	T/W
10	0.318311
15	0.404375
20	0.488453
25	0.569905
30	0.64811
35	0.722472
40	0.792424
45	0.857434
50	0.917006
55	0.970684
60	1.018061
65	1.058775
70	1.092515

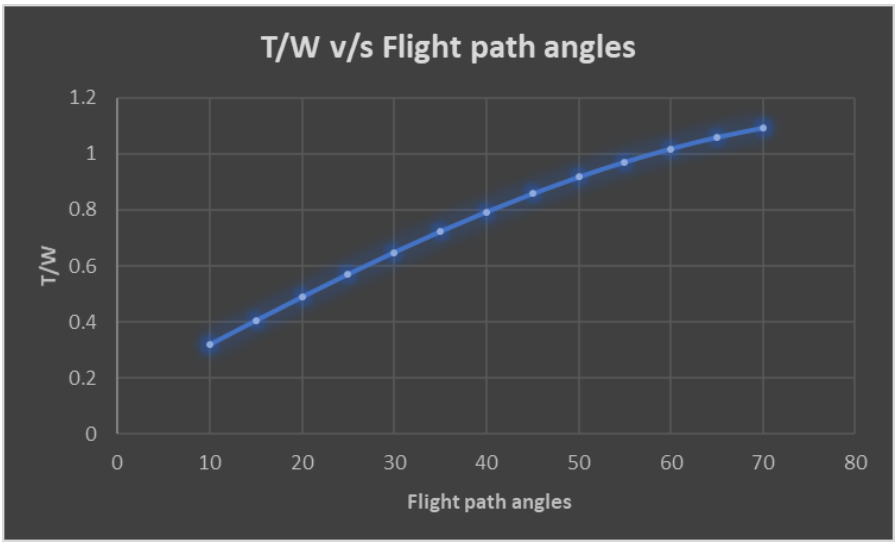

Figure 4.5. Thrust-to-Weight ratio v/s flight path angles

4.7 Cruise speed sizing of X-69:

Cruise phase for X-69 is an exceptional phase which would occur only if the mission is aborted. For example, after mid-air launch (drop) if the mission requires to be aborted for some reason, X-69 will cruise back to the spaceport maintaining the cruising altitude before descent. Hence in this condition, since no rocket motor is fired and X-69 is dropped at an average Mach of 0.8, it is desired to maintain the speed which is maximum at sea level.

Therefore, we consider maximum airspeed of M=0.8 and C_{D0} = 0.00594
Assuming compressibility drag increment to be 0.003, giving C_{D0}=0.00594+0.003 = 0.00894 and an average aspect ratio of 2.18 with e=0.8 and dynamic pressure at 50,000 ft altitude, $\bar{q} =$ 1,070.2 psf *equation (3.60) from Roskam* can be written as:

$$\frac{T}{W} = C_{D_0}\bar{q}S/W + \frac{W}{\bar{q}S\pi Ae} \tag{4.8}$$

Therefore,

$$\frac{T}{W} = \frac{9.567}{(W/S)} + \frac{(W/S)}{5{,}863.6}$$

Therefore, the following table can be made:

Table 4.4 Cruise speed sizing

$(W/S)_{TO}$	T/W @ M=0.8
15	0.06613878
20	0.05192504
25	0.0439273
30	0.03903756

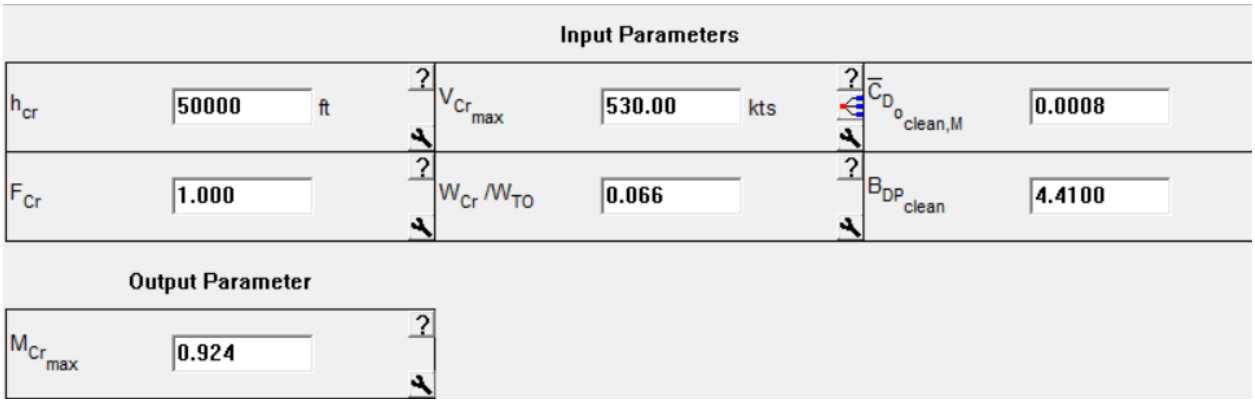

Figure 4.6. Parameters for maximum cruise speed from AAA

4.8 Matching of all sizing requirements:

After establishing some relations between thrust-to-weight ratio, take-off wing loading, it is possible to determine the best combination of these quantities for the design. As for X-69, all the parameters calculated can plotted in one graph as follows:

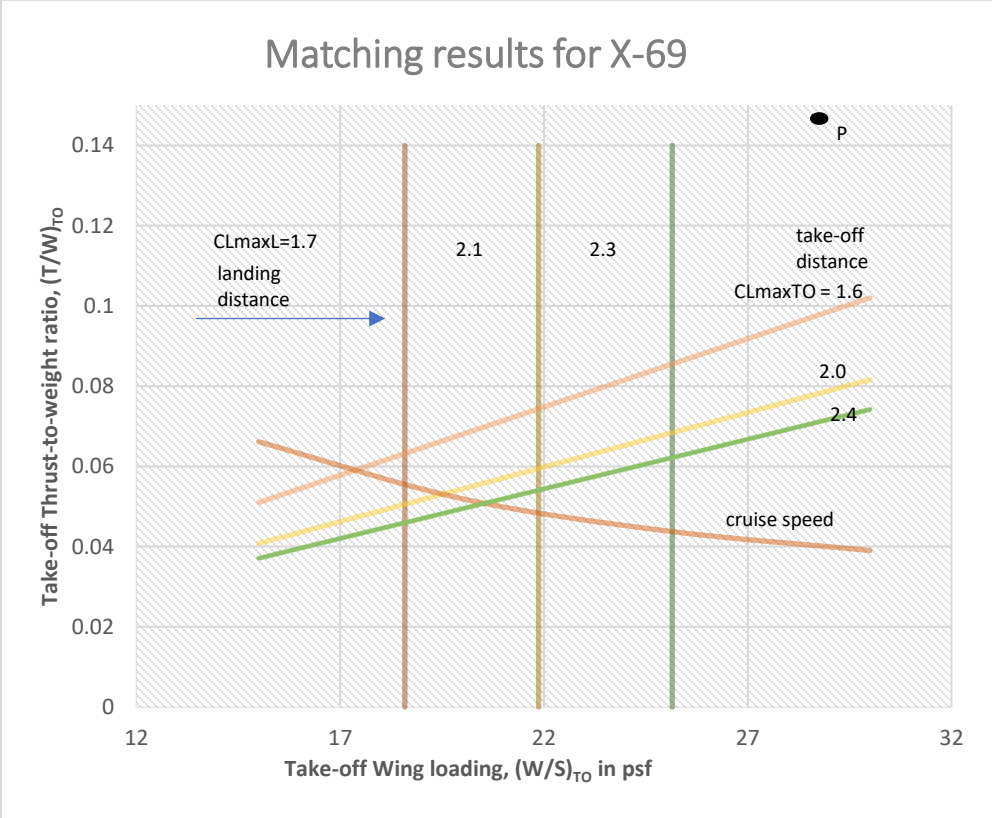

Figure 4.7 Matching results for X-69

Therefore, in this section we can relate and determine landing distance and some other parameters as follows:

If point P is accepted as a satisfactory match point, the airplane characteristics can be summarized as follows:

Take-off weight: $W_{TO} =$ 13,870 lbs.

Empty weight, W_E =	8,418.8 lbs.
Fuel weight, W_F =	1,720.75 lbs.
Maximum lift coefficients:	
Clean: $C_{L_{max}}$ =	1.6
Take-off: $C_{L_{max_{TO}}}$ =	1.4
Landing: $C_{L_{max_L}}$ =	2.5
Aspect ratio, A =	1.65
Take-off Wing loading: $(W/S)_{TO}$ =	28 psf (point P)
Wing area: S =	13,870/28 = 495.65 ft^2
Take-off thrust-to-weight ratio: $(T/W)_{TO}$ =	0.15 (point P)
Take-off thrust: T_{TO} =	2,080.5 lbs.

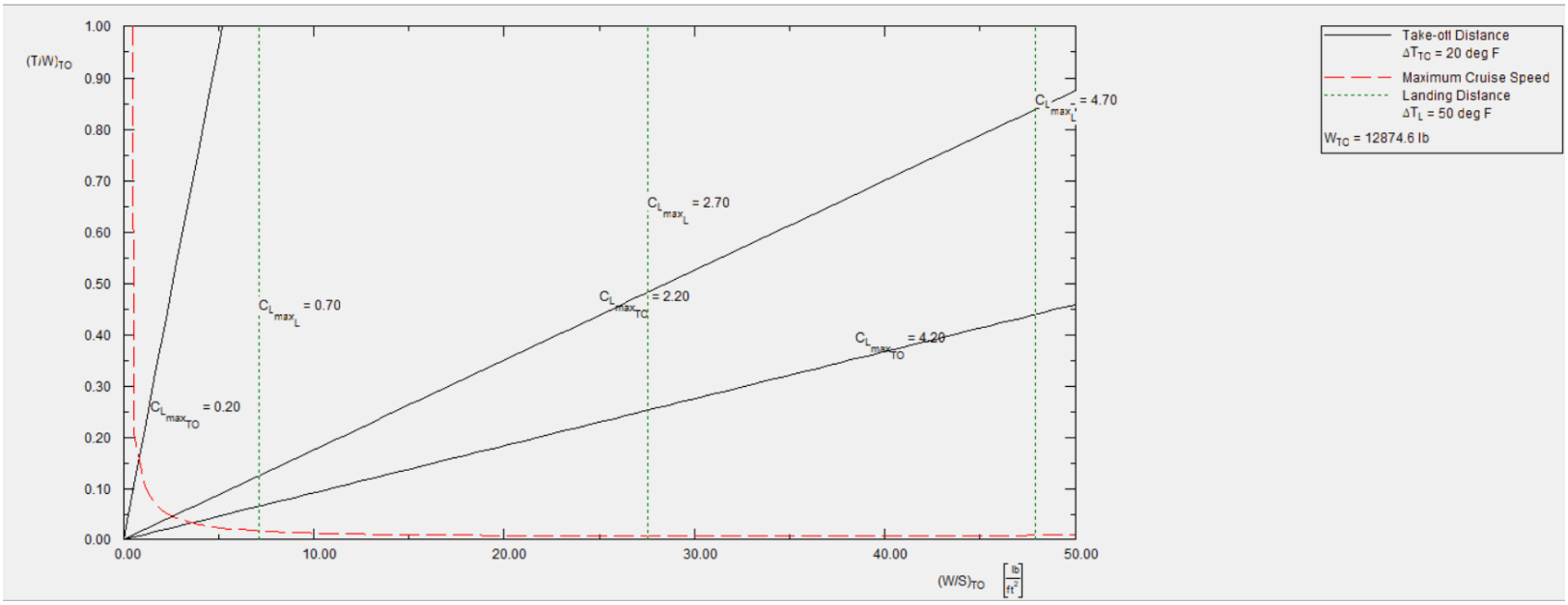

Figure 4.8. Matching plot from AAA @ 12,874.6 lbs. of W_{TO}

4.9 Discussion:

X-69 is designed to climb at supersonic speed to high altitudes and coast near LEO to deploy CubeSats. In report 3 we estimated takeoff weight of X-69 of 13,870 lbs. To estimate precise climb, glide and landing, calculations for performance constraints have been performed manually. From fig. 4.3, we can see that thrust to weight ratio varies in similar pattern with respect to wing loading at various possible pullup angles. In previous flights spaceship one and spaceship two, standard pullup angle at clean release from mothership and thereon boost is 65^o to 75^o. Further efforts will be made analyze and optimize the glide performance of X-69 which happens to be another significant parameter for X-69. The return is solely governed by unpowered glide after hypersonic re-entry.

Rate of climb is one of the significant parameters that has major impact on design and hence the performance. Consequently, it is also important to have optimal primary propulsion system that can provide continuous thrust to complete the boost phase of about 90 seconds. Advantage of using hybrid rocket propulsion is that thrust can be controlled by pilot maintaining the oxidizer flow during combustion unlike solid propellant rockets. In this analysis it is assumed that the secondary propulsion system that is required

for orbital maneuvering is optimal and will only come into play at coasting and re-entry initiating phase.

4.10 Conclusion and Recommendations:

This chapter solely discusses the possibility of optimal performance with given resources. Further efforts will be made to improve the cruise phase of the flight to enhance the smooth landing approach performance. Moreover, the configuration will be built in such a way that the energy from re-entry can be utilized for the gliding phase.

5. Chapter 5 – Configuration Design

5.1 Introduction:

This report describes the configuration design for X-69. Based on mission requirements, it is necessary to propose a preliminary design which considers several aspects of aircraft like its general characteristics, overall configuration, wing configuration, propulsion system and its disposition, landing gear disposition, etc. With the help of performance sizing we have some basic parameters such as wing area, aspect ratio and maximum coefficient of lift for various conditions. While studying overall configuration in this report, we will understand the basic layout of X-69 and how should its appearance be.

5.2 Comparative Study:

Table 1 includes a comparison of the parameters for Boeing's X-37B, X-20, and Dyna-Soar, along with NASA's X-15, and Virgin Galactic's Spaceships One and Two.

Table 5.1. Comparative study

Parameters	Boeing's X-37B	Virgin Galactic's Spaceship One	Virgin Galactic's Spaceship Two	Boeing's X-37	Boeing's X-20 Dyna-Soar	X-15
Crew	None	1 pilot	2 crew and 6 passengers	none	1 pilot	1 pilot
Takeoff/ Launch weight	11,000 lb (4,990 kg)	21,428 lb (9,740 kg)	21,428 lbs. (9,740 kg)	11,000 lbs. (4,990 kg)	11,387 lbs. (5,165 kg)	34,000 lbs. (15,420 kg)
Empty weight	N/A (electric powered)	2,640 lb (1,200 kg)	15,000 lbs. (6,804 kg)	NA (electric powered)	10,395 lbs. (4,715 kg)	14,600 lbs. (6,620 kg)
Thrust	157.4 lbf (700 kN)	16,534.67 lbf (74 kN)	60,000 lbf (270 kN)	157.4 lbf 700kN)	72,000 lbf (323 kN)	70,400 lbf (313 kN)
Critical Speed, V_{cr}	(Orbital) 17,426 mph (28,440 km/h)	2,170 mph (3,518 km/hr.)	2,500 mph (4,000 km/hr.)	(Orbital) 17,426 mph (28,440 km/hr.)	17,500 mph (28,165 km/hr.)	4,520 mph (7,274 km/hr.)
Range, R	675 days (longest flight)	40 mi (65 km)	Planned apogee of 110 km	270 days (design)	Earth orbit 22,000 nm (40,700 km)	280 mi (450 km)
Wing Area, S		161.4 ft^2 (15 m^2)	273.34 ft^2 (25.4 m^2) (estimated)		345 ft^2 (32m^2)	200 ft^2 (18.6m^2)
Wing span, b	14 ft 11 in (4.5 m)	16 ft. 5 in (8.05 m)	27 ft (8.3 m)	14 ft 11 in (4.5 m)	20 ft 10 in (6.34 m)	22 ft 4 in (6.8 m)
Aspect Ratio, AR		1.6	2.667 (estimated)		1.256	2.486
Type of Payload	Satellites	Pilot	Crew	Satellites	Crew	Crew

Parameters	Boeing's X-37B	Virgin Galactic's Spaceship One	Virgin Galactic's Spaceship Two	Boeing's X-37	Boeing's X-20 Dyna-Soar	X-15
Powerplant	Gallium Arsenide Solar Cells with Li-Ion batteries	1x N_2O/HTPB SpaceDev Hybrid rocket	1x Rocket Motor Two liquid/solid hybrid rocket engine	Gallium Arsenide Solar Cells with Li-Ion batteries	1x Transtage rocket engine	1xReaction Motors XLR99-RM-2 liquid propellant rocket engine

5.2.1 Configuration Comparison of Similar Airplanes:

a) Boeing's X-37B

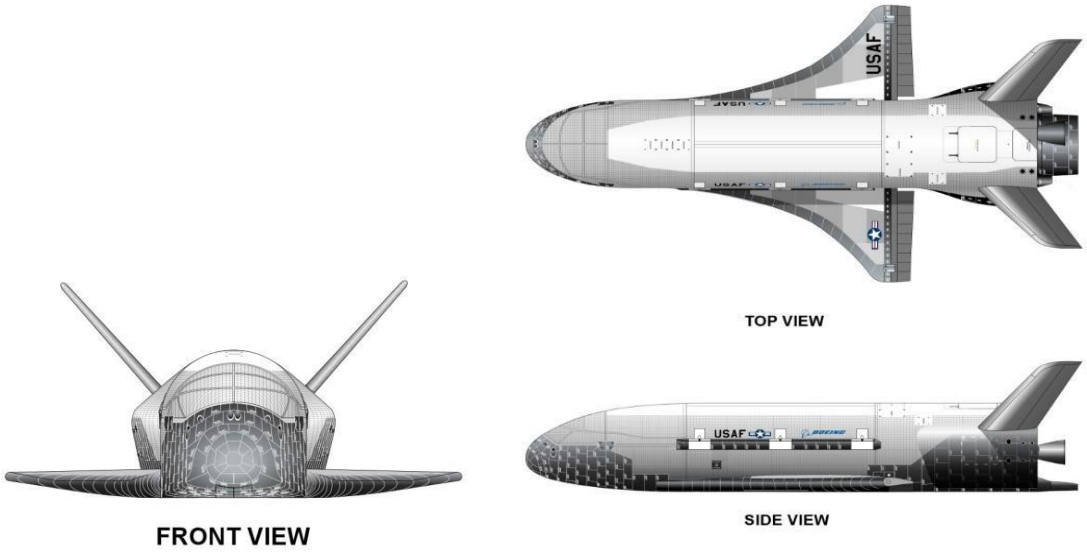

b) Virgin Galactic's SpaceShipOne

Figure 5.1. All views of Boeing's X-37B

Figure 5.2. All views of V.G's SpaceShipOne

c) Virgin Galactic's SpaceShipTwo

Figure 5.3 All views of V.G's SpaceShipTwo

Figure 5.4 Front view with trimmed up configuration

d) Boeing's X-20 Dyna Soar

Figure 5.5 All views of X-20 Dyna Soar

e) X-15A-2

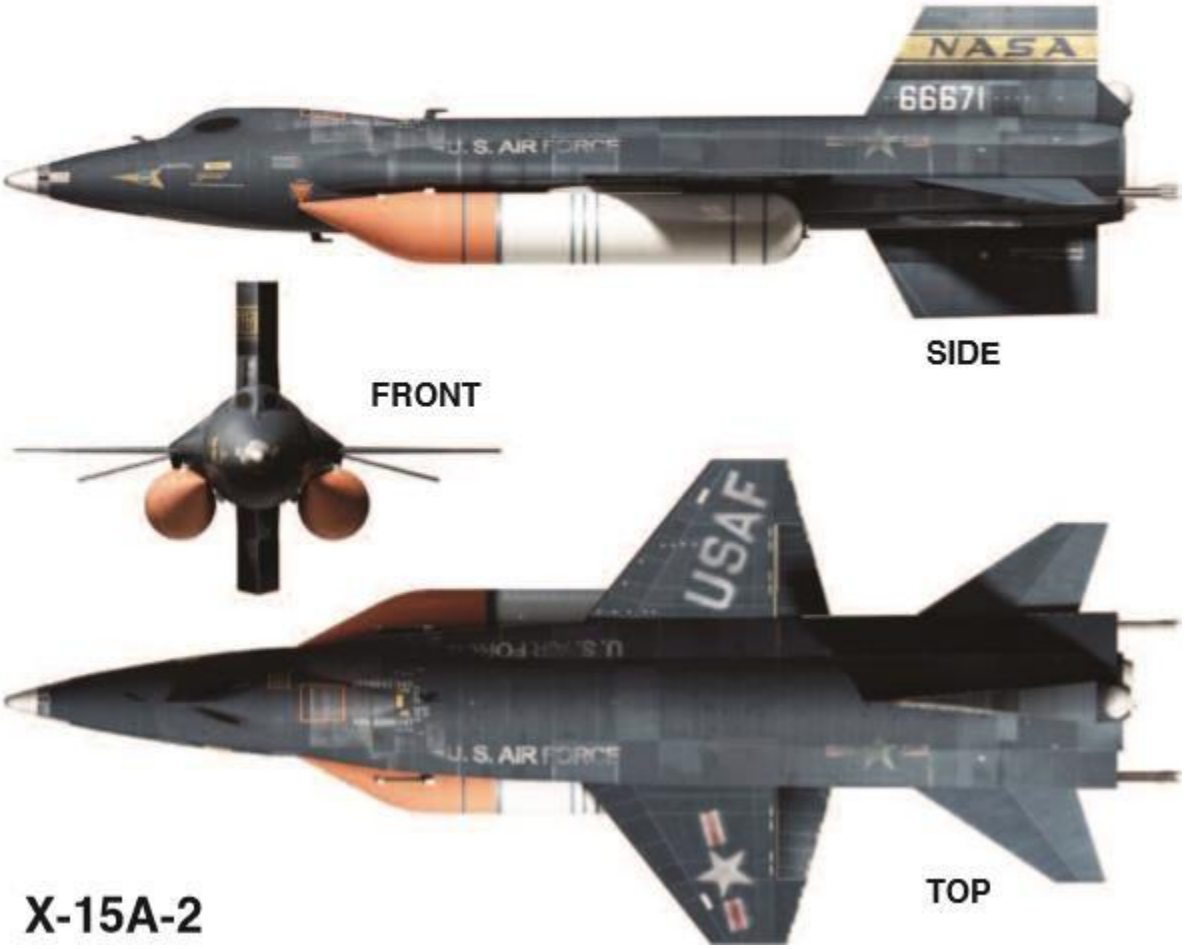

Figure 5.6. All views of X-15A-2 with externally assembled rocket engine

5.2.2 Discussion:

Following are the parameters that can have major impact on the design of X-69 as briefly discussed in report 1:

As we can notice many facts are common in these aircrafts. Almost all the airplanes are designed to land back dealing with hypersonic speeds and gliding. Also, they use motherships to air launch except X-37B which was launched using traditional rockets. Basically, a delta-wing pattern has been implemented on almost all the above designs with certain variations. Delta-wings give efficient performance at hypersonic speeds with better gliding as they descend.

Low wing: X-37B, Spaceship Two, X-20 Dyna Soar Advantages:

1. Over-wing exits.
2. While in space, it is quite easy to deploy small satellites from upper fuselage where wing does not come in the way.
3. Easier to stick the main gear on.
4. Low wing doesn't block any of the cabin.
5. Easy to access for maintenance and refueling.

Med Wing: X-15A-2. (also, its predecessor, X-15A) Advantages:

1. Med Wing provide best maneuverability.
2. Wing can be continuous through the fuselage.
3. Maintains structural integrity with the fuselage.

High Wing: Spaceship One Advantages:

1. Quick loading and unloading.
2. Higher clearance from the ground providing less ground effect.

A certain disadvantage of high wing has been documented especially for Spaceship One. The design was susceptible to roll excursions. It has been noticed that wind shear causes a large roll immediately after ignition progressing into multiple rapid rolls. Although as it gains high speed upon climb, this anomaly mitigates making the flight stable.

5.3 Overall Configuration:

Following the guidelines as per *Roskam's vol II,* X-69

a) Will be a land-based spaceplane.
b) Will be a conventional type meaning tail aft.

5.3.1 Fuselage Configuration:

Design of X-69 fuselage will be conventional that seeks to accommodate satellites with sophisticated mechanisms to deploy or undock satellites into LEO or dock back returning satellites without any damage to either X-69 or satellite. Deployment systems like NanoRacks CubeSat Deployer (NRCSD) or XPOD Separation System can be used based on the layout of racks and fuselage design. Direction of deployment can be from sideways or rear since wing can be moved up or down with relatively less effect on X-69 maneuvering.

Fuselage of X-69:

a) Will be a twin boom with center fuselage type.
b) Will have a regular cockpit with 2 pilots.
c) Engine buried in the fuselage.

5.3.2 Engine Type:

- *Engine type*: Rocket Motor engine
- *Engine Integration:* Engine inside the fuselage from behind.

This is a X-type of plane that uses rocket motors for propulsion. For X-69, we seek to use solid/liquid hybrid propellant rocket that can deliver thrust in the range of 60,000 lbf to 75,000 lbf. X-15 uses XLR99- RM-2 liquid propellant rocket engine. Although this system makes it quite bulky to handle liquid propellants and sloshing issues. On the other hand, Virgin Galactic and Scaled Composites used hybrid rocket motor with benign fuel and oxidizer. The advantage of hybrid rocket motor is that it is controllable and can be shut down at any time during boost phase of flight. It has less issues with sloshing.

As a new requirement, it seems necessary to use Reaction Control System (RCS) thrusters on small scale for in-space maneuverability, attitude control to efficiently undock/dock satellites from X-69.

5.3.3 Wing Configuration:

These types of planes have relatively different wing patterns unlike traditional airplanes. Wing design of both Spaceship One and Two are standard and similar consisting Elevons and Stabilator. From structural viewpoint,

a) A braced (or strutted wing) wing will be preferred over cantilever wing due to structural advantage that will be discussed later.
b) Have a low wing arrangement on fuselage has major advantage when combined with braced wings.
c) An aft sweep (positive sweep) will be incorporated due to delta configuration of the wing.
d) This design will not necessarily require winglets due to presence of elevons and stabilators.
e) Other parameters of wing such as airfoil, thickness ratio taper ratio, twist angle, incidence angle, dihedral angle. High lift and control surface requirements, winglets will be discussed later.

5.3.4 Empennage Configuration:

The empennage of X-69 will consist of:

a) Horizontal tail/stabilizers mounted on twin booms running backwards from the wing to maintain the longitudinal stability. These components are also called as stabilators or stabs since they are movable in angular manner as the tail boom tilts at different angles up to 65^{o} while re-entry.
b) Like traditional airplanes, elevons are aircraft control surfaces that combine the functions of elevator that controls pitch and aileron that controls roll. For above aircrafts, elevons are located behind the stabilator (also called as stab) directly connected to the stick in the cockpit using cables.
c) Vertical stabilizers are also mounted of twin booms to maintain the lateral stability.
d) There are spoilers attached to the wing that play key role in deceleration of X-69 from hypersonic speeds during re-entry which will be discussed later in detail.

As discussed earlier, the stabs and elevons will be controlled using electromechanical system. Although, it is very important to pick the efficient configuration for better performance specially to glide, loiter if necessary and safe landing. From the research so far, there are three options such as tail plane mounted, Twin tail boom or Wing mounted as shown in Fig. 11. For initial guess and referring to previous designs, wing mounted configuration can be picked.

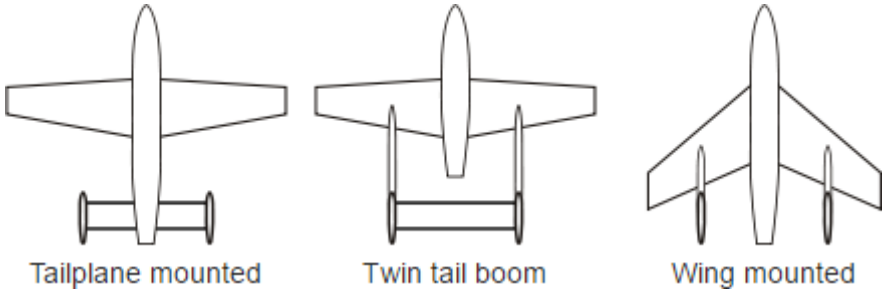

Figure 5.7: Empennage configurations

5.3.5 Landing Gear type and Disposition:

X-69 will have combination of retractable landing gear and nose skid. The rear landing gear will be mounted under the wing retracting inwards towards the fuselage.

Due to space constraints at the nose, instead of nose gear a nose skid is preferred.

- *Landing Gear:* Retractable gear
- Nose-wheel landing gear
- *Landing gear integration:* In the fuselage
- Rear gears attached to wings retracting inwards.

Airfoils used for Wings:

X-69 like other X-planes does not need much of aerodynamics while climbing from around 45,000 ft to 50,000 ft. The climb is solely governed by rocket motor which takes barely 10-15 minutes to reach LEO. Ion Thrusters can be installed for efficient maneuver while in space.

Efficient airfoil selection will play vital role in returning phase and re-entry. X-69 will glide as it descends after re-entry with required loitering to decelerate followed by landing approach. In the first test flight of Spaceship One, landing procedure used modified version of a standard engine out approach that is generally used by the military. HS 130 airfoil popular for dynamic soaring can be used for wing to obtain efficient glide. From the research it is found that HS 130 delivers very less drag and has characteristics of slope soaring. This airfoil is also used for elevons with 25% chord.

5.4 Proposed Configuration:

Basic design of X-69 is almost like that of Spaceship Two. Although, based on requirements such as, ground effects, type of propulsion system, docking/undocking mechanisms, design of fuselage will be slightly different. As proposed earlier, fuselage will have sideway doors to deploy satellites from upwards which is why low wing has been chosen. Placement of RCS thrusters has not decided yet which is required for maneuver in space to conveniently operate docking/undocking.

Using SolidWorks, following is the preliminary design of X-69 as shown in figures, 12,13,14,15,16 from various orientation and angles. Due to time constraints, the design is missing complete tail which is of on-wing mounted type, proportionate size of fuselage, landing gears pockets for retraction, etc. HS 130 airfoil has been used for wing and tail modelling

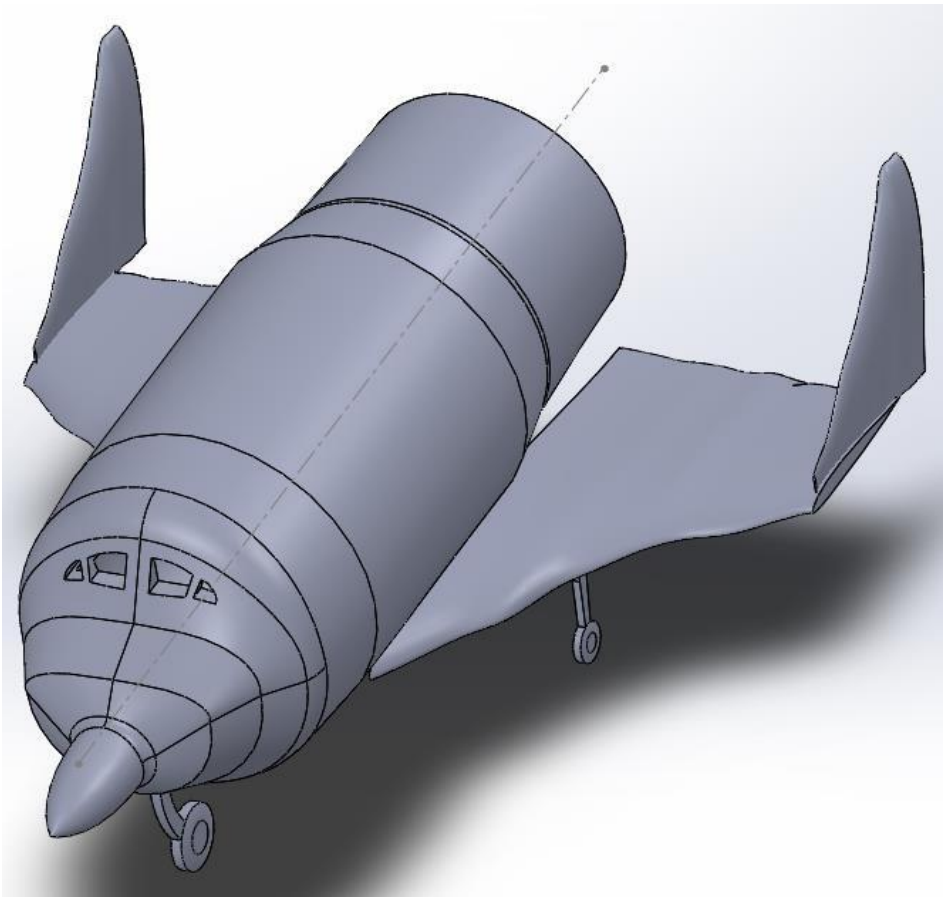

Figure 5.8 Isometric 3-D view of X-69

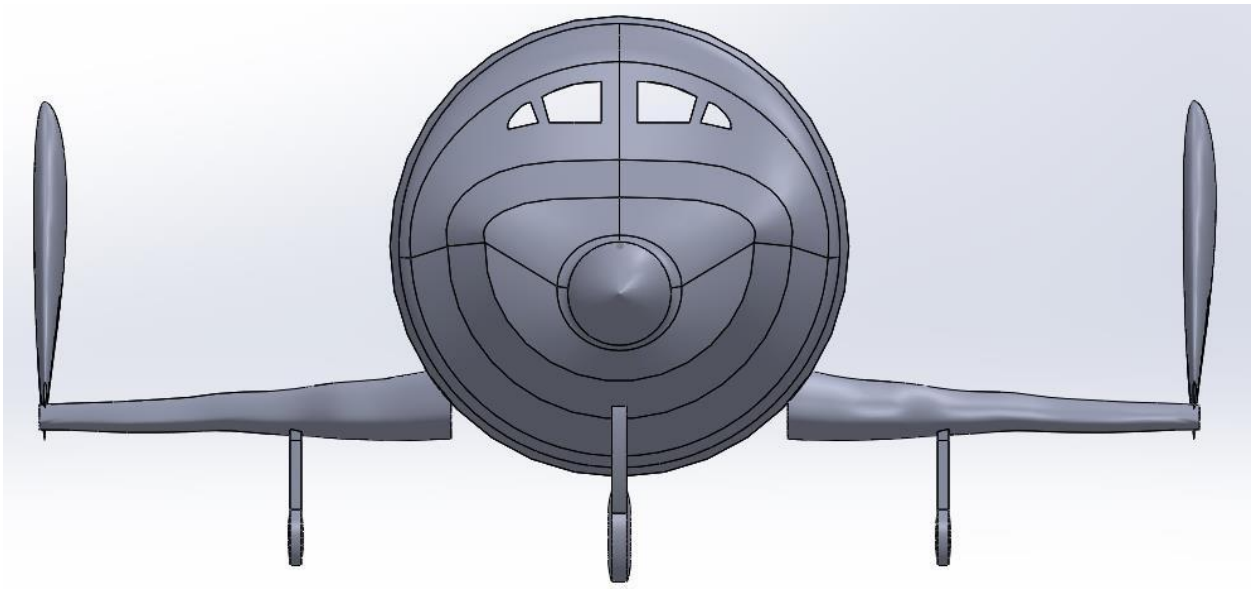

Figure 5.9 Front view of X-69

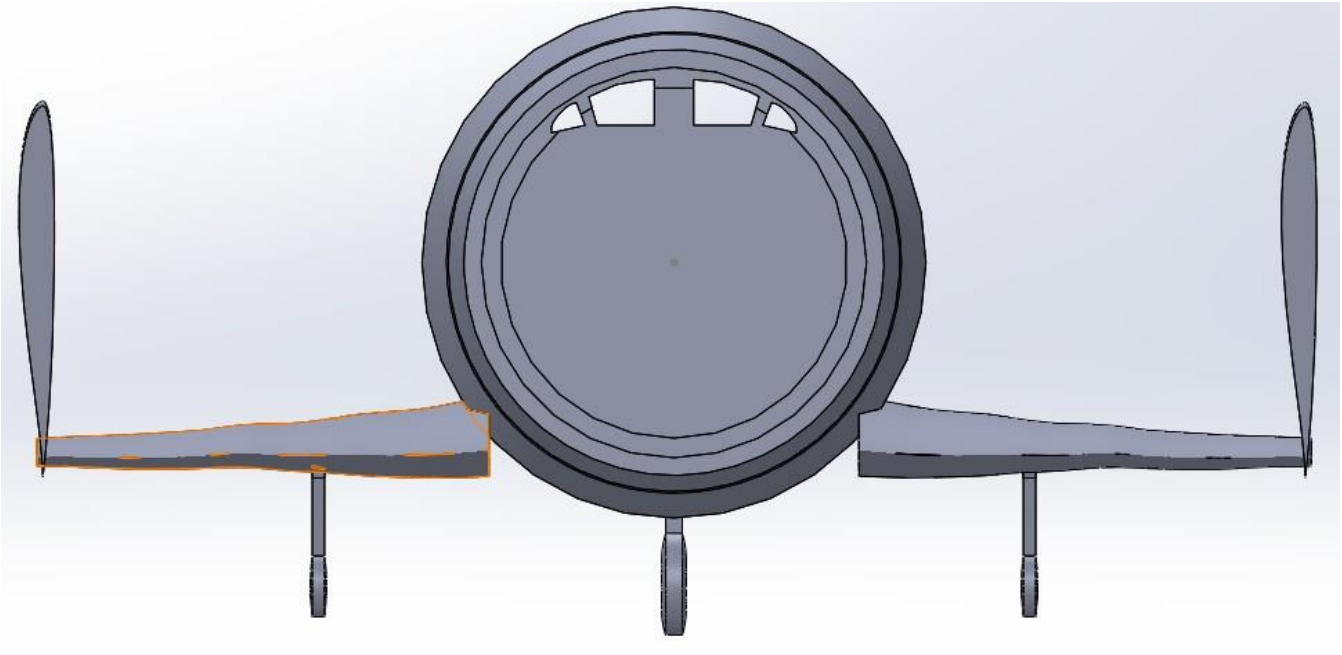

Figure 5.10 Rear view of X-69

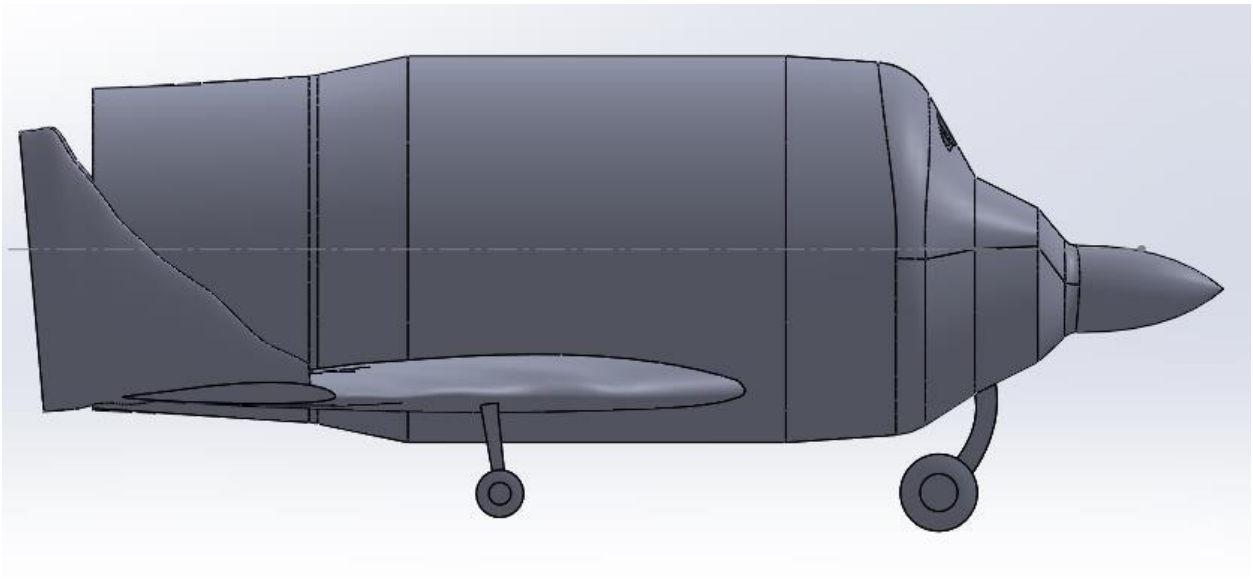

Figure 5.11 Side view of X-69

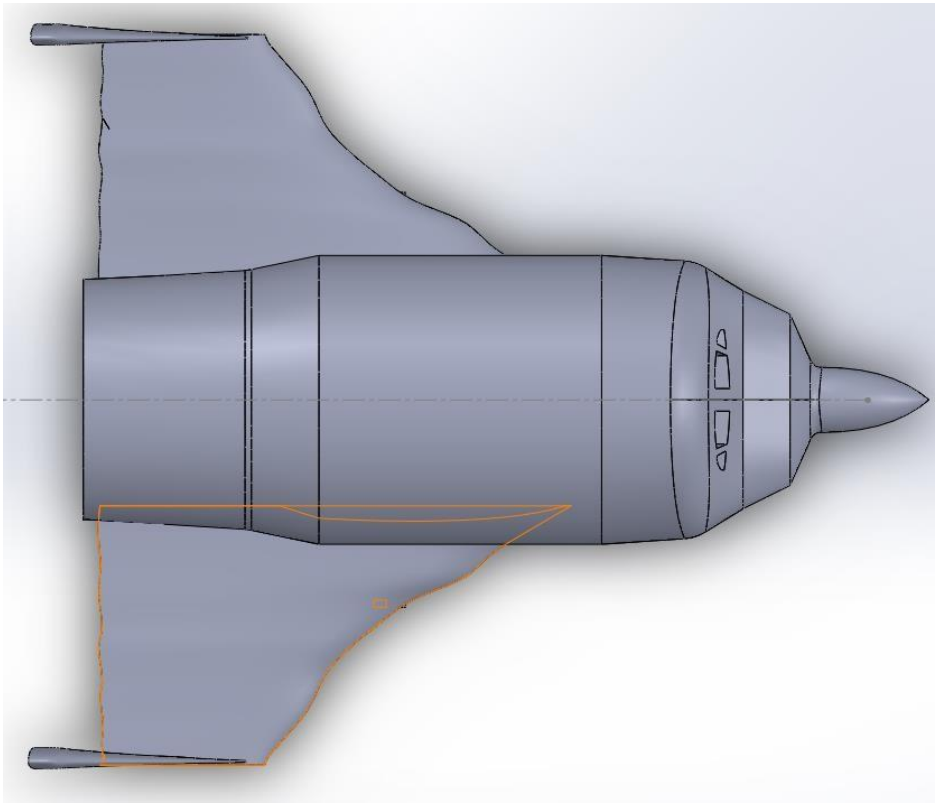

Figure 5.12 Top view of X-69

6. Chapter 6 – Fuselage Design of X-69 CargoSat

6.1 Introduction:

Before starting layout design of cockpit and fuselage, it is important to revise the mission specification based on which a comprehensive overall configuration can be interpreted.

Table 6.1. Mission specification

Crew	2 pilots
Weight of crew	350 lbs. (175 lbs. each)
Payload	CubeSats or small-sized satellites
Maximum Payload weight	3,310 lbs. (1,500 kg.)
Deployment altitude	360,000 ft to 400,000 ft
Wing configuration	Low wing
Deployment direction from fuselage	Upwards with retractable door mechanism
In-fuselage major components	NanoRack Canister mechanism to swiftly deploy satellites
Cockpit and fuselage avionics	

The strategy of low wing is for convenient deployment of satellites from above. Wing and nose of X-69 have RCS thrusters to control roll and pitch & yaw respectively during coasting. Considering this project as a prototype, at this time X-69 can contain 24 CubeSats with various categories. Before studying cockpit and fuselage layout, it is important to understand type of payload and their mission requirements. Upon research it is found that some CubeSats require spacecraft assist deployment whereas some have self-deployment mechanisms using either rails or small solid propellant rockets.

Development of CubeSats started with 1U and 3U sizes build by various resources. After successful services delivered by this concept, demand for bigger sized CubeSats increased due to which sizes of CubeSats now ranges from 1U (10cm x 10cm x 10cm) to 27U (34cm x 35cm x 36cm). There are many types of CubeSats dispensers that are used from time to time such as Canisterized Satellite Dispenser (CSD), small rocket boosters, etc. Due to ease and convenience in Canisterized Satellite Dispenser design, this type of dispenser has been considered for preliminary deployment system. Moreover, CSDs are dimensionally accurate and gives better idea to design interior of the fuselage. Section 6.1.1 discusses about CSDs in more detail:

6.1.1 Canisterized Satellite Dispenser(CSD)

These dispensers come with in-built ejection system controlled by deployment switches followed by door opening and ejection of the CubeSats as shown in fig.6.1. CSD uses either rail or tabs mechanisms to achieve proper attitude deployment. Rails or tabs also help to stabilize the CubeSats during launch or harsh conditions. Canisters reduce risk to the payload and also provide easy restrictions on payload materials and components. The tabs or rails are along the ejection axis directed upwards. Fig. 6.2 shows the dimensions of 27U CubeSat and canister. As mentioned earlier, canisters can either installed rails or tabs for satellite dispensing is up to the satellite owner and depending up on the delicacy of satellite. Fig. 6.2 is example of each payload that will house in the fuselage of X-69

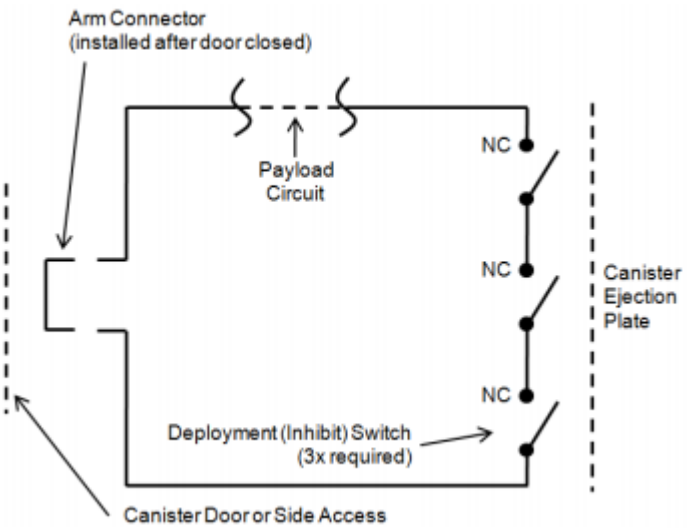

Figure 6.1. Payload inhibit and safe/arm circuit

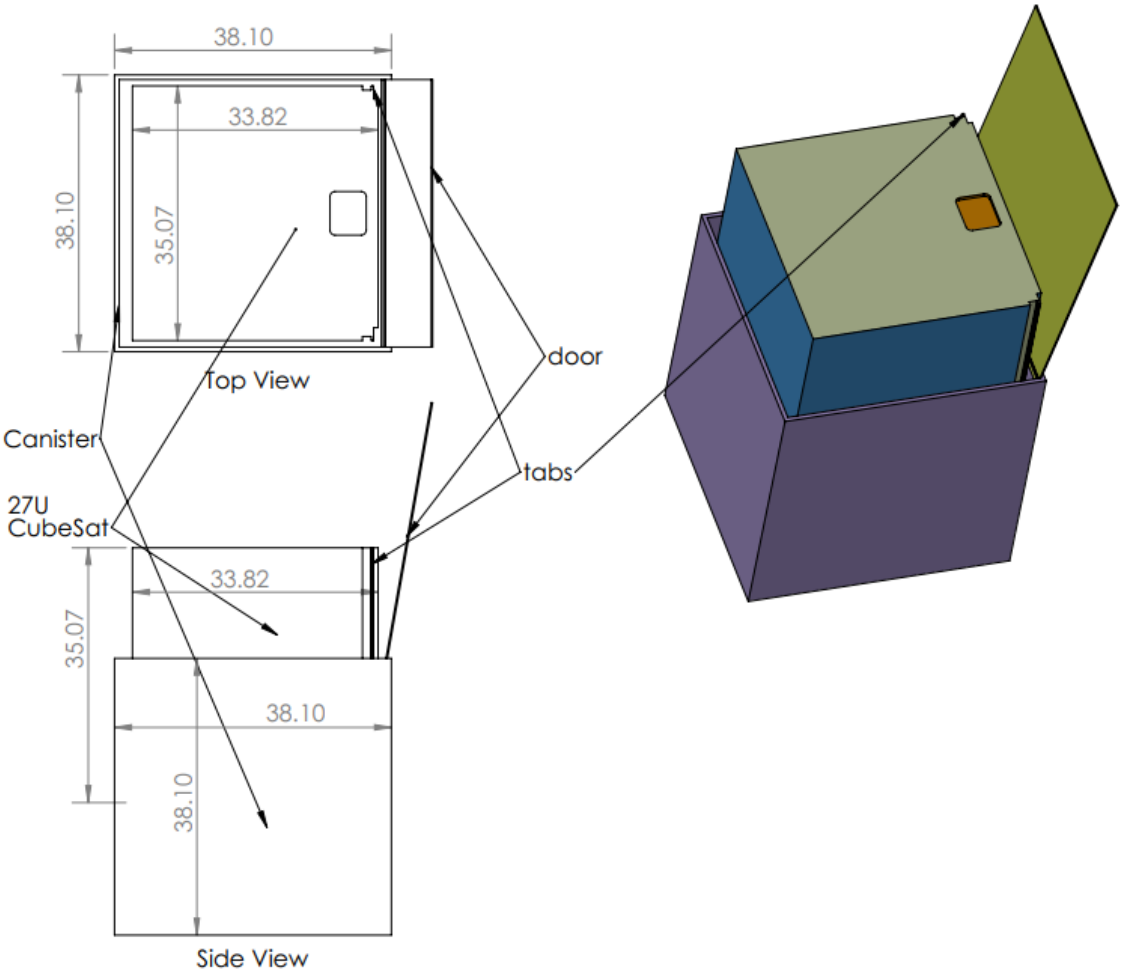

Figure 6.2. 27U CubeSat with canister (All dimensions are in cm)

6.1.2 Defining Fuselage geometry using AAA:

The fuselage geometry is design with its basic parameters using AAA software. The nozzle extension at the rear end has been excluded in the design of fuselage giving us the overall length of fuselage to about 74 ft considering 90 number of fuselage stations. Fig 6.3 shows the plot of the fuselage from cockpit cone to the nozzle inlet. The co-ordinates of the fuselage can be referred from the appendix 6.1.

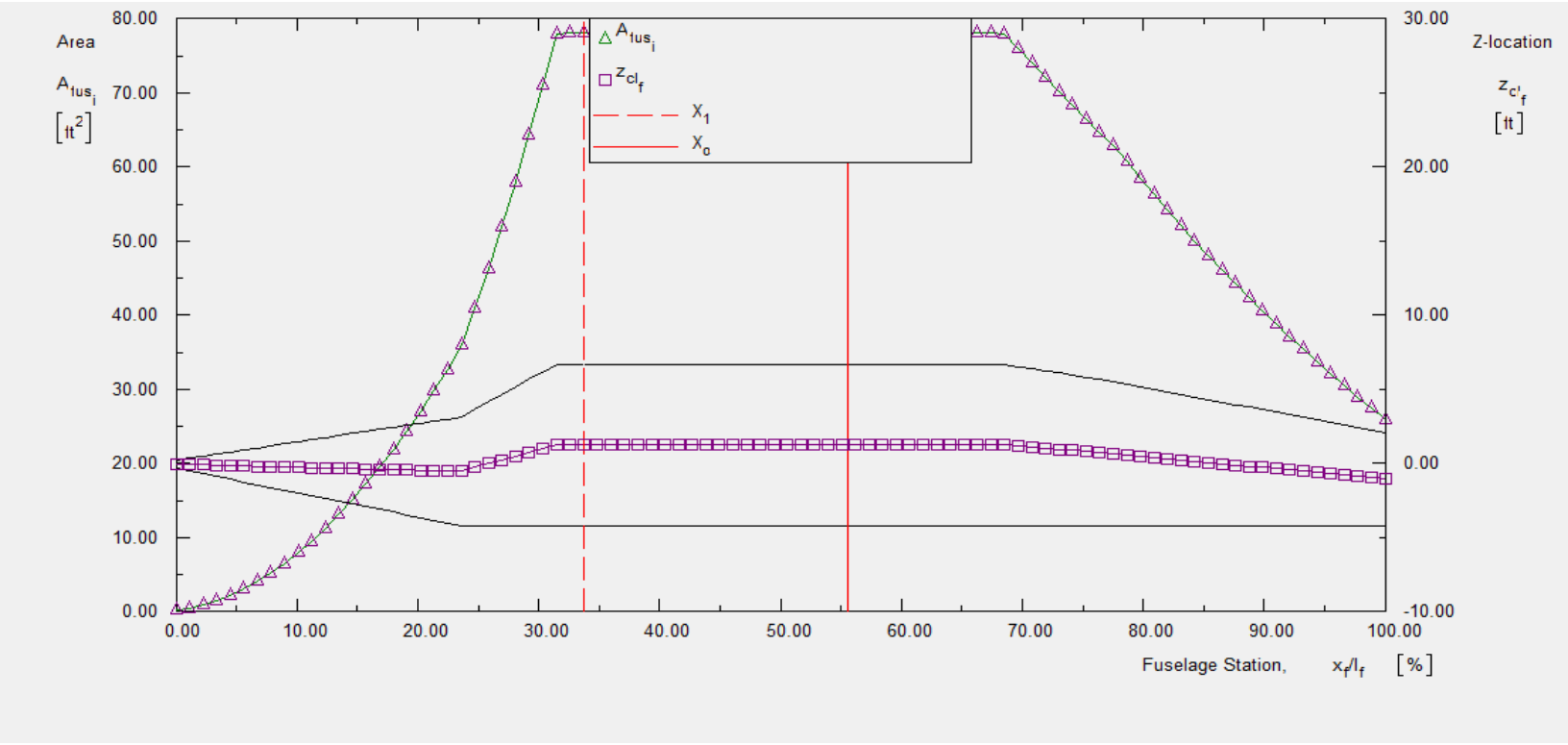

Figure 6.4. Fuselage plot and area ruling

Output Parameters

l_f	67.50	ft	S_{B_s}	565.57	ft^2	S_o	78.06	ft^2	Z_{fc_w}	6.25	ft
$h_{f_{max}}$	10.83	ft	S_{plf_f}	478.89	ft^2	V_f	3535.49	ft^3	h_{f_w}	10.83	ft
$w_{f_{max}}$	9.17	ft	S_{wet_f}	1667.35	ft^2	X_{c_f}	38.98	ft	$D_{f_{max_w}}$	9.97	ft
S_{b_f}	26.01	ft^2	X_1	24.01	ft	$h_{f_{0.25}}$	7.21	ft	h_{f_h}	0.00	ft
$S_{f_{max}}$	78.06	ft^2	X_o	38.76	ft	$h_{f_{0.75}}$	10.26	ft	D_{f_h}	0.00	ft

Figure 6.3. Output parameters of fuselage using AAA

Following table. 6.2 explains the output parameters,

Table 6.2. Output parameters of fuselage

Parameter	Explanation	Quantity
l_f	Fuselage length, excluding rocket nozzle	67.50 ft
S_{B_S}	Fuselage side projected area	565.57 ft^2
S_0	Cross-sectional area of fuselage at station X_0 where flow ceases to be potential	78.06 ft^2
$h_{f_{max}}$	Maximum height of the fuselage	10.833 ft
S_{plf_f}	Fuselage Planform Area	478.9 ft^2
V_f	Fuselage Volume	3535.5 ft^3
$w_{f_{max}}$	Maximum Fuselage Width	9.1667 ft^2
S_{wet_f}	Fuselage Wetted Area. It is the area of the fuselage that is exposed to the air	1,667.34 ft^2
$D_{f_{max_w}}$	Maximum Fuselage Diameter at Wing-Fuselage Intersection	9.97 ft^2
S_{b_f}	Fuselage Base Area	26 ft^2
$h_{f_{0.25}}$	Fuselage Height at Quarter Length of the Fuselage	7.213 ft^2
$S_{f_{max}}$	Fuselage Maximum Frontal Area	78.06 ft^2

6.1.3 CAD model of Fuselage:

It is necessary to understand the basic layout of the interior of fuselage to provide the background for selection of exterior fuselage layout that is obtained from AAA in fig. 6.5. The complete fuselage is divided into 3 compartments i.e. cockpit, payload compartment (main fuselage) and rear rocket housing.

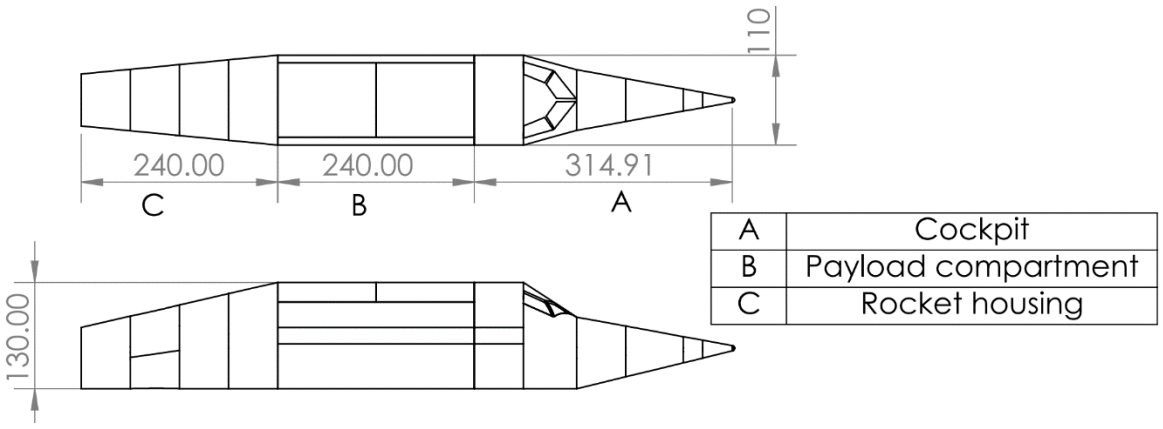

Figure 6.5. Fuselage dimensions (inches)

- **Cockpit:** A conventional cockpit will contain main flight avionics, crew, nose skid and pitching & yawing thrusters at the nose end for coasting while in space.

- **Payload compartment:** The payload compartment is sub-divided into two compartments to accommodate the hybrid rocket motor at the bottom and payload (CubeSats) at the top. Fig 6.6 shows only in-service fuselage overview with sliding door to allow the payload to be deployed.

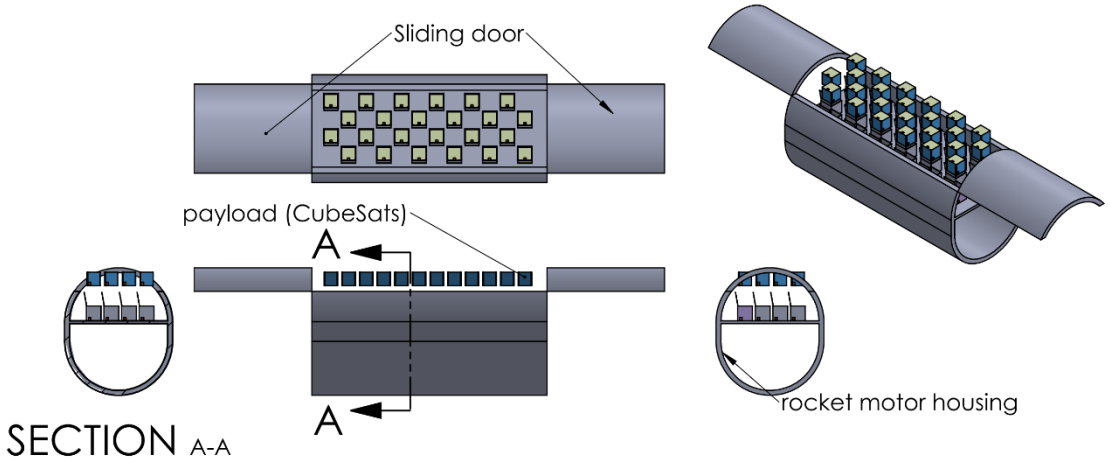

Figure 6.6. Fuselage overview

Sliding door method would be an efficient method as it has easy mechanism and can rest on cockpit and rocket motor housing during deployment. Moreover, the depressurization and sliding door mechanism is quite traditional and allows depressurize the vessel gradually not causing harm to the structural integrity of the vessel.

- **Rocket motor housing:** The rearmost component of the fuselage allows space for the rocket motor which extends to the payload compartment as discussed earlier. The length of the rocket motor is referred from that used for Virgin Galactic's SpaceShipOne. SpaceShipOne uses N_2O-HTPB hybrid rocket propulsion system as shown in fig 6.7. The oxidizer tank containing N_2O will be at the front end of the rocket motor either under the cockpit or payload compartment. The rear part of the complete does not show the nozzle that will be left out in the open to limit the heat and high temperatures of the exhaust gas.

  The grain configuration can be seen the fig 6.7 that burns from center to the periphery. The oxidizer regulates thrust requirement that happens to be that advantage of the hybrid rockets to get the thrust up on demand unlike solid propellant system. The solid propellant is contained in the steel case of 72-inch diameter. The steel case is referred to design the lower part of the payload compartment and the rearmost part.

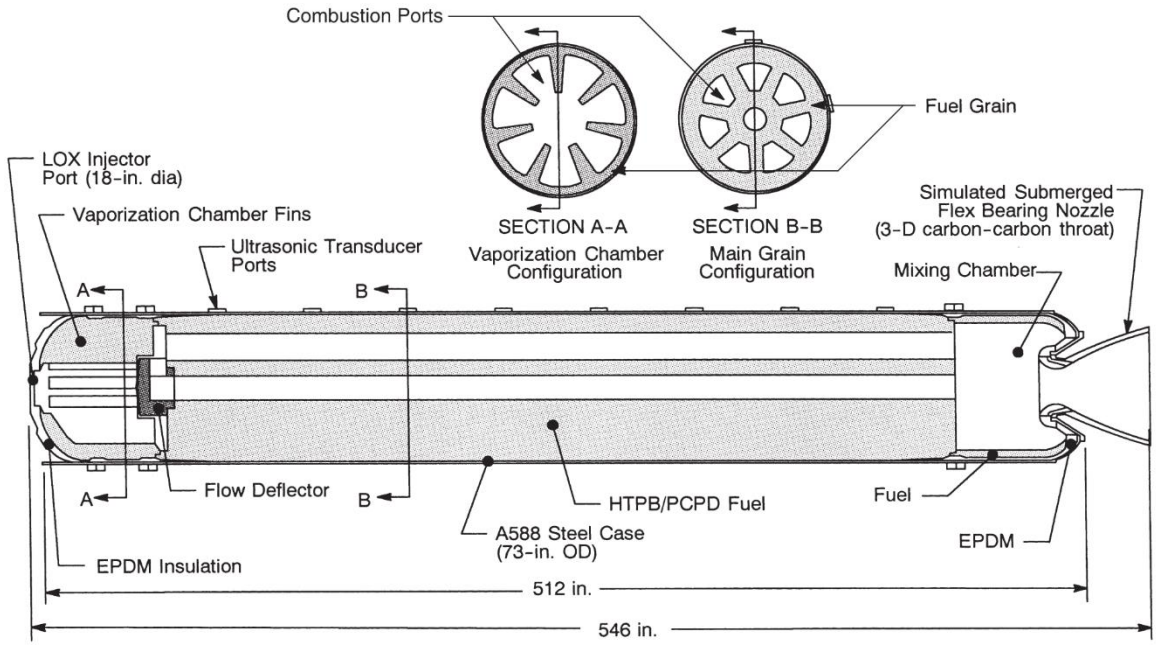

Figure 6.7. The hybrid rocket motor of SpaceShipOne

6.2 Layout design of the cockpit:

Initial proposed X-69 will have cockpit with conventional layout. As shown in fig.6.8 pilot seats approximately aligned at 15 inches from the center line running through the nose. Nose is essentially long to house RCS thrusters for pitch and yaw control while coasting in space. Fuel management system for RCS thrusters for both at nose and wing is provided through the layer under dashboard. Blank space behind the crew in cockpit is to accommodate accessories such as washrooms, facility to store beverages, etc. The crew (pilot) loading and unloading is preferred to be carried through hatch-door mechanism as shown in fig.6.10. This configuration is feasible for both while in space and on the ground. The doors on left and right will open in upward direction without interfering with payload compartment door. Hence the pilots can have easy support of the wing for feet and can be easily tethered to the X-69 for secure spacewalk if necessary, whereas on the ground the system can use ladder connecting to the wing for pilots to come out of the cockpit.

6.2.1 Convenience for pilots:

For a successful cockpit, it is vital to consider the pilot's ease of access to every flight factor such as visibility, flight avionics, quick reaction accessibility, etc. At least the basic functions done by pilots must have to occur with least efforts. Hence considering these points following points have been proposed:

A general factor of the pilot about visibility is shown in fig. 6.8. In reference to *Roskam's Aircraft Design vol III,* basic visibility aspects have been considered with some tradeoffs due to design restraints. As indicated in the fig. 6.8, a small ball-like structure is nothing but a theoretical position of eye when an average male sits at resting position that accounts to about 4.5 ft from the floor including the chair base. The cockpit nose contains nose-skid at the bottom extending towards the flight desk and pitching and yawing thrusters. Therefore, the cockpit cone in the side view remains restrained giving the down visibility of about 10.22^{o}. However, the side visibility is quite satisfying as both the pilots have to take efforts to see at least 135^{o} around his eye position.

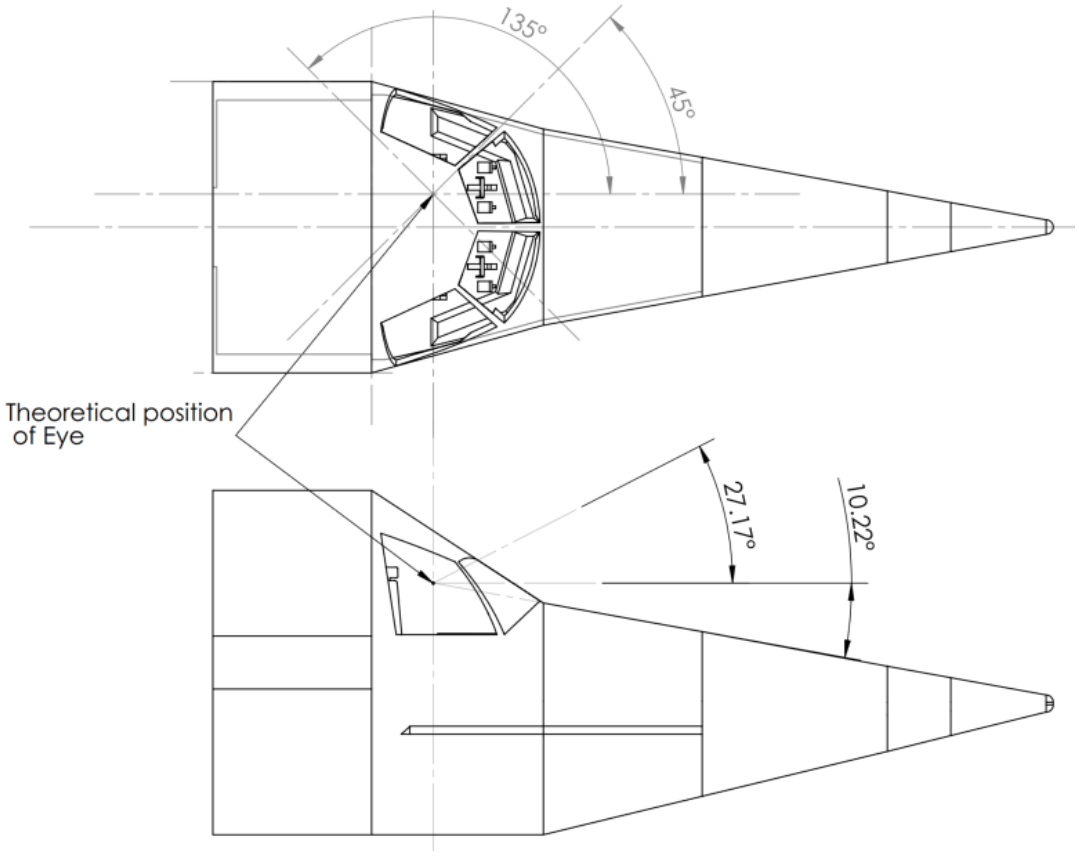

Figure 6.8. Cockpit visibility factor

6.2.2 Pilot's ease of access to major avionics:

Fig. 6.9 shows the basic sitting arrangement for pilots including flight deck and basic controls such pitch, roll and yaw along handle and pedals respectively. The dimensions for the position of these components are also referred and averaged from *Roskam's Aircraft Design vol III*. In fig 6.9, various section views are shown to better understand the cockpit layout. Section A-A shows the bisected side view with clear vision flight controls and pilot seat along with the dimension. The line running through all the section is an eye position line for the reference. The blacked outer edge is the border that signifies the solid part and rest as hollow.

Similarly, section B-B signifies the cross-section of the cockpit that exteriorly run with dimension through the payload compartment. A window is considered at the rear end of the cockpit to spectate the deployment of the CubeSats.

Section C-C shows the top-bisected view with handle to hand distance of 12 inch that ease access for pitch and roll. The flight deck remains close the pilot's controls including the avionics.

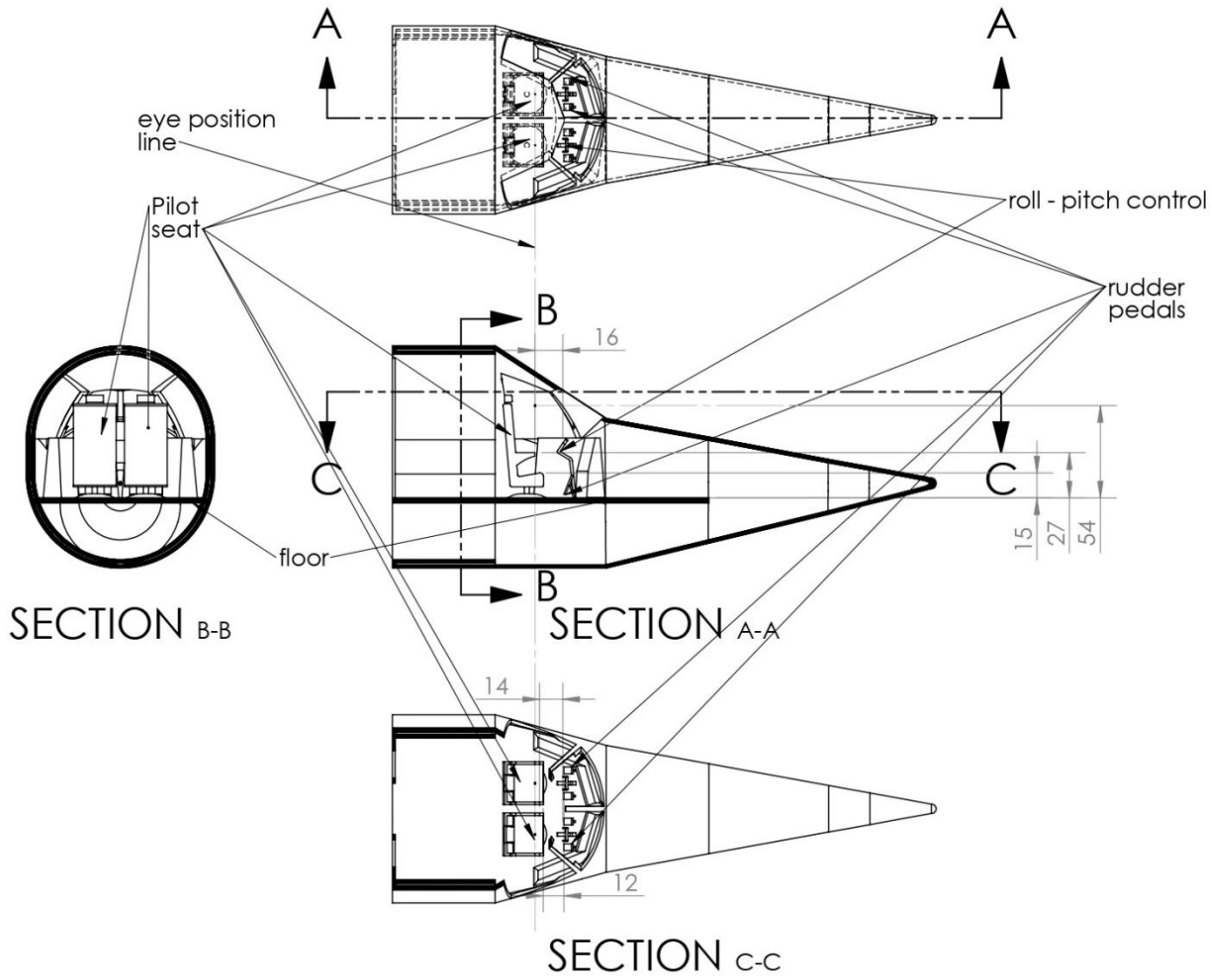

Figure 6.9. Pilot seating arrangement of the cockpit (all dimensions in inches)

6.2.3 Access to the outer environment:

This part of cockpit is bit tricky and includes many tradeoffs in design, aesthetics, manufacturing cost that will be discussed later. However, basic layout is considered as follows:

A) While in Space during Coasting:

It will be a rare part of any mission for pilots to come out of the cockpit as most of the phase is coasting. However, it is important to consider and involve basic feature of any space-vehicle to X-69. Since pilots, who officially become astronauts at 360,000 ft for newcomers, want to commit the spacewalks or manage any avionics from outside in case emergencies such blockage thrusters or payload itself while deployment. A tethered mechanism is preferred that attaches to the spacesuit of astronaut to restrict the major dive of an astronaut. Also, the wing comes right the door of the cockpit and gives better support for the pilots' feet resting on the wing.

B) After Landing:

Many small-sized planes such as fighters, or even rocket-planes have elevator type of pilot entrance coming from the bottom near the nose gear. However, considering a different alternative, it is quite

convenient to use a simple external ladder mechanism to unload the pilots. The ladder can be directed supported to the wing to descend to the ground. Moreover, the ground clearance of X-69 is very low which gives another advantage for pilot unloading.

Fig 6.10 shows the basic illustration of access to the outer environment factor:

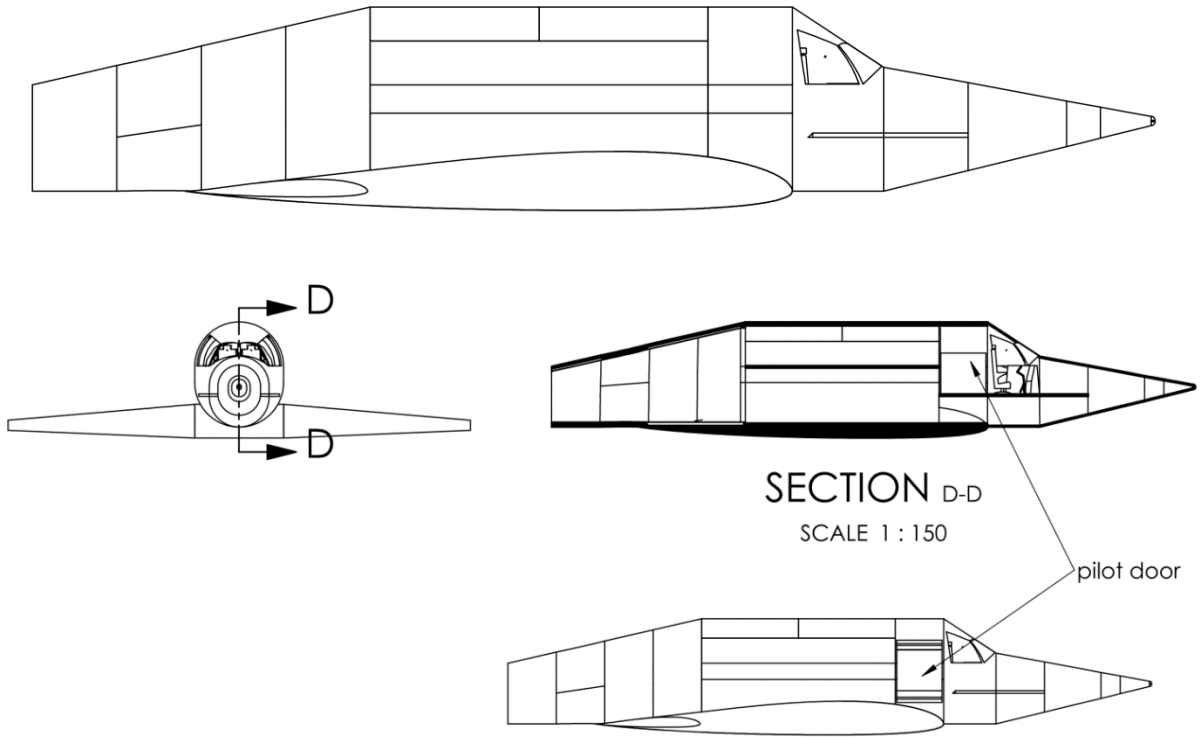

Figure 6.10. Access to the outer environment

6.2.4 2D CAD models:

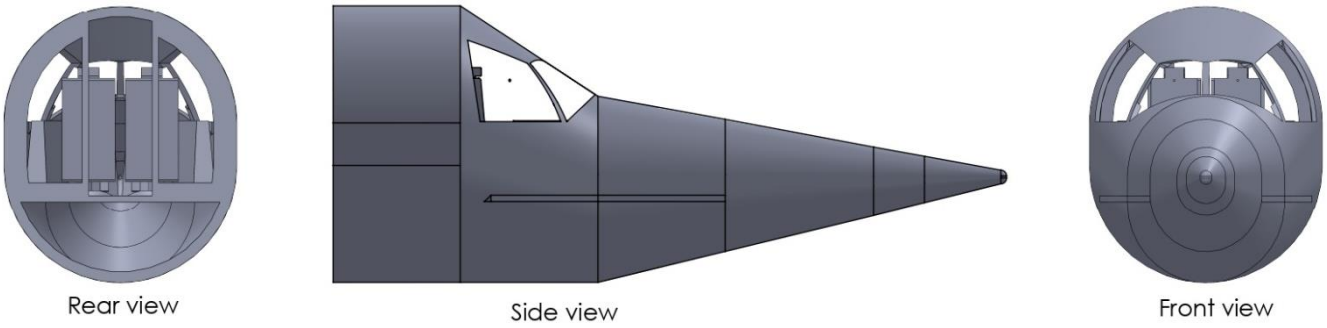

Figure 6.11. Front, rear and side view of cockpit

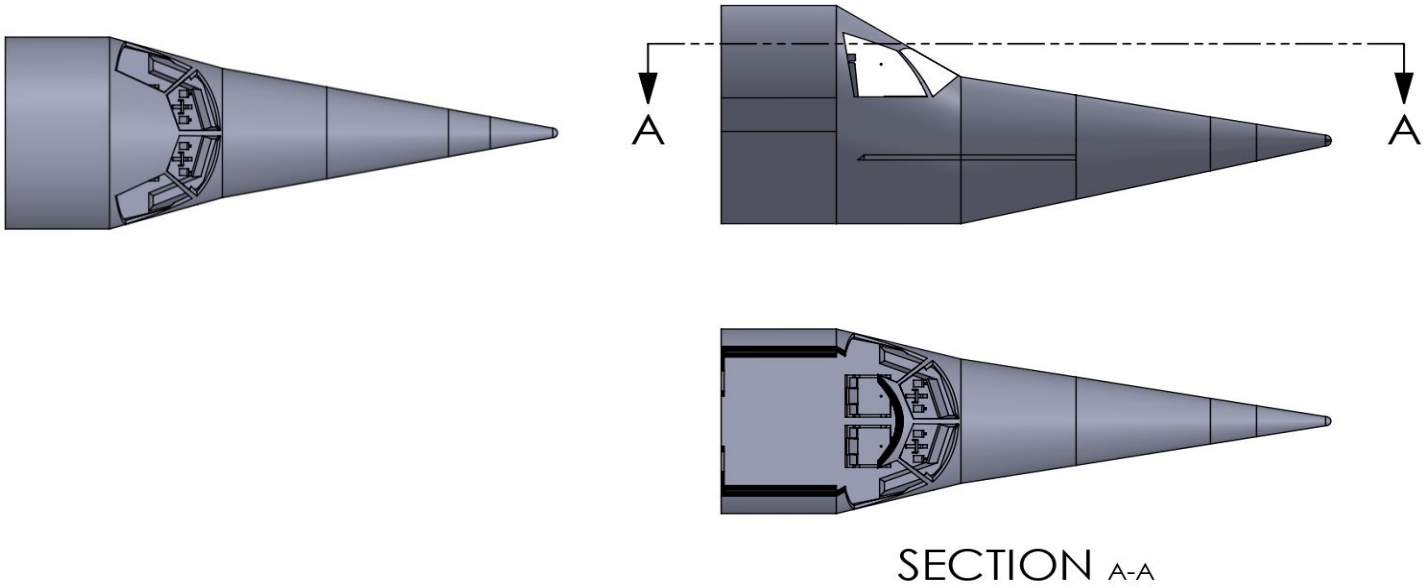

Figure 6.12. Top and top-section view of cockpit

6.2.5 3D CAD Models:

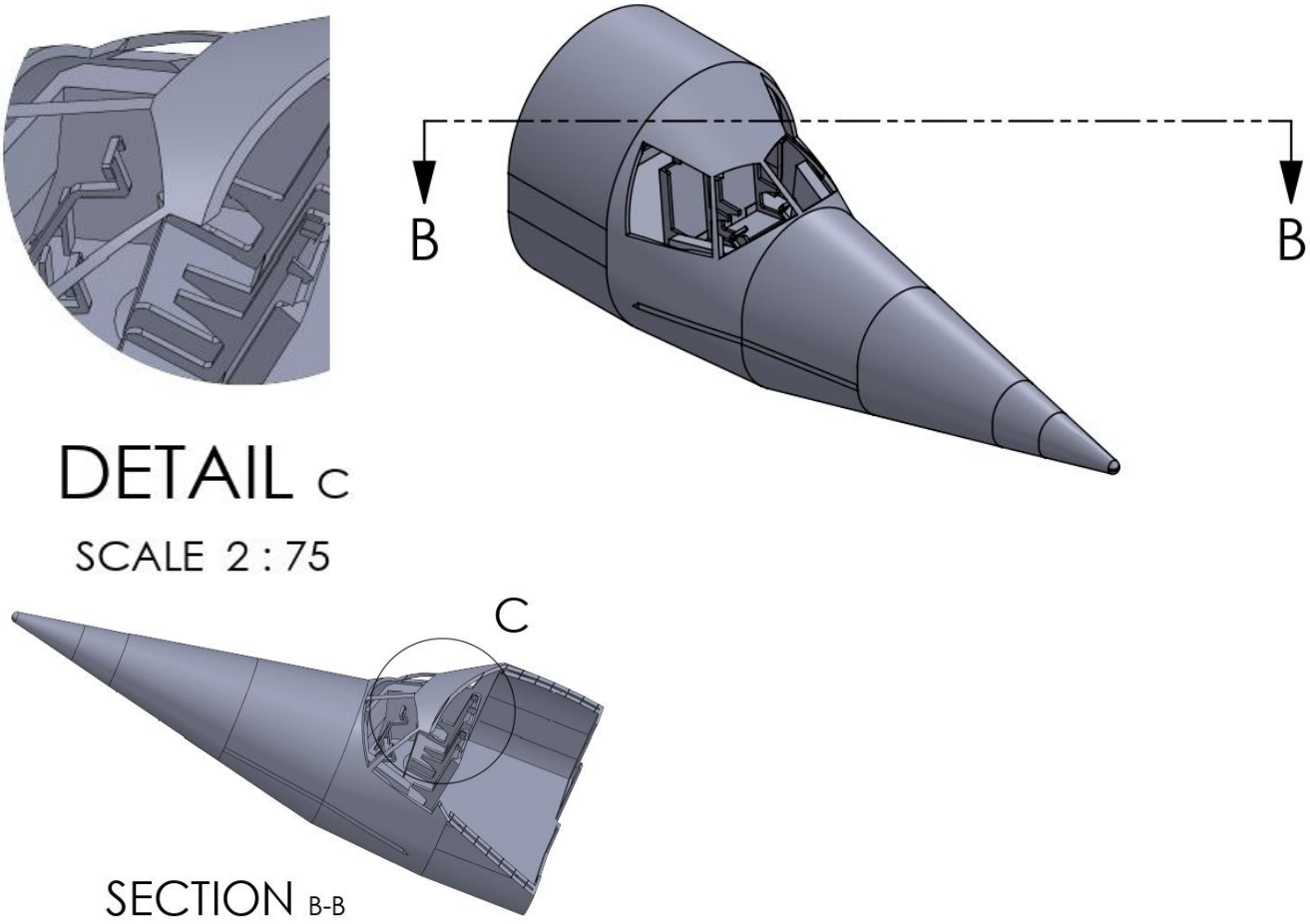

Figure 6.13. Isometric view of cockpit detailing the interiors

6.3 Layout design of the payload compartment:

Layout of fuselage ultimately relies on the payload or number of CubeSats to be delivered. To assess the performance with maximum payload capacity of X-69, dimensions 27U CubeSats along with that of canister dispenser is considered:

Table 6.3. Basic knowledge about payload

Parameters of Components	Quantity
Type of CubeSats	27U
Mass per payload (1 no. of 27U CubeSat)	54 kg (119 lbs.)
Dimensions $L \times W \times H$ ~	$34cm \times 35cm \times 36cm$
Canister Dispenser Dimensions	$15" \times 15" \times 15"$
Mass of CSD	About 500 grams
Number of CSD and CubeSats	24
Deploying method	Deployment from above

Preliminary design of fuselage is slightly referred to the fuselage design of SpaceShipTwo considering shape and visualization. Although since the mission is to deliver CubeSats, all passenger seats and equipment are unloaded emptying the fuselage and filling it with estimated layout of CubeSats as shown in fig 6.6 and fig 6.13 ultimately making it a payload compartment. Deployment phase is accompanied with coasting phase of X-69. While coasting, CubeSats will be deployed from upward direction with open sliding door maintaining fewer moving parts. A sliding door is advantageous since the depressurization of fuselage will be gradually achieved maintaining the structural integrity.

As discussed in section 6.1.3, it is quite impractical elongate the fuselage to accommodate the propulsion system separately. The rocket motor itself is about 45.5 ft long and 6 ft in diameter as shown in fig.6.7 which if installed after the fuselage will make the X-69 much longer than a sophisticated design. Therefore, considering the rocket motor diameter as base reference, the propulsion system is integrated underneath the payload compartment that avoids the unwanted extension of fuselage as shown in fig 6.6. All the safety measures are considered while designing the rocket motor that will be discussed later.

This section mostly consolidates on the layout of the payload. The deployment of the payload should be efficient enough to achieve their predefined trajectories. As a space-plane company, the basic contract would be signed as to a maximum altitude from where the successfully deployed CubeSat's controls are handed over to the customer for further trajectory and orbital transfers. Hence, the deployment of CubeSats is expected to very efficient. Considering these points,

a) The CSDs are placed 21 inches from each other transversely as shown in fig. 6.14 maintaining the distance between adjacent CubeSats to more than 22 inches including diagonal clearance of about 6.5 inches. The ejection mechanism is so efficient that CubeSat will scarcely perturb.

b) Looking from the side or front view, one might consider if the payload compartment door would obstruct the deploying CubeSats in either last rows. The door, vessel opening, and payload line are at least 4 inches far from each other creating free and non-interfering space for payload deployment as shown in fig. 6.14.

Fig. 6.14 shows the layout of CubeSats kept in casings. Fig. 6.15 and 6.16 are front and side view of fuselage respectively. Since X-69 is a low wing spaceplane, wing attachment can be seen at the lower side of the fuselage. Fig. 6.18 is 3D design of fuselage with payload and wing attachment.

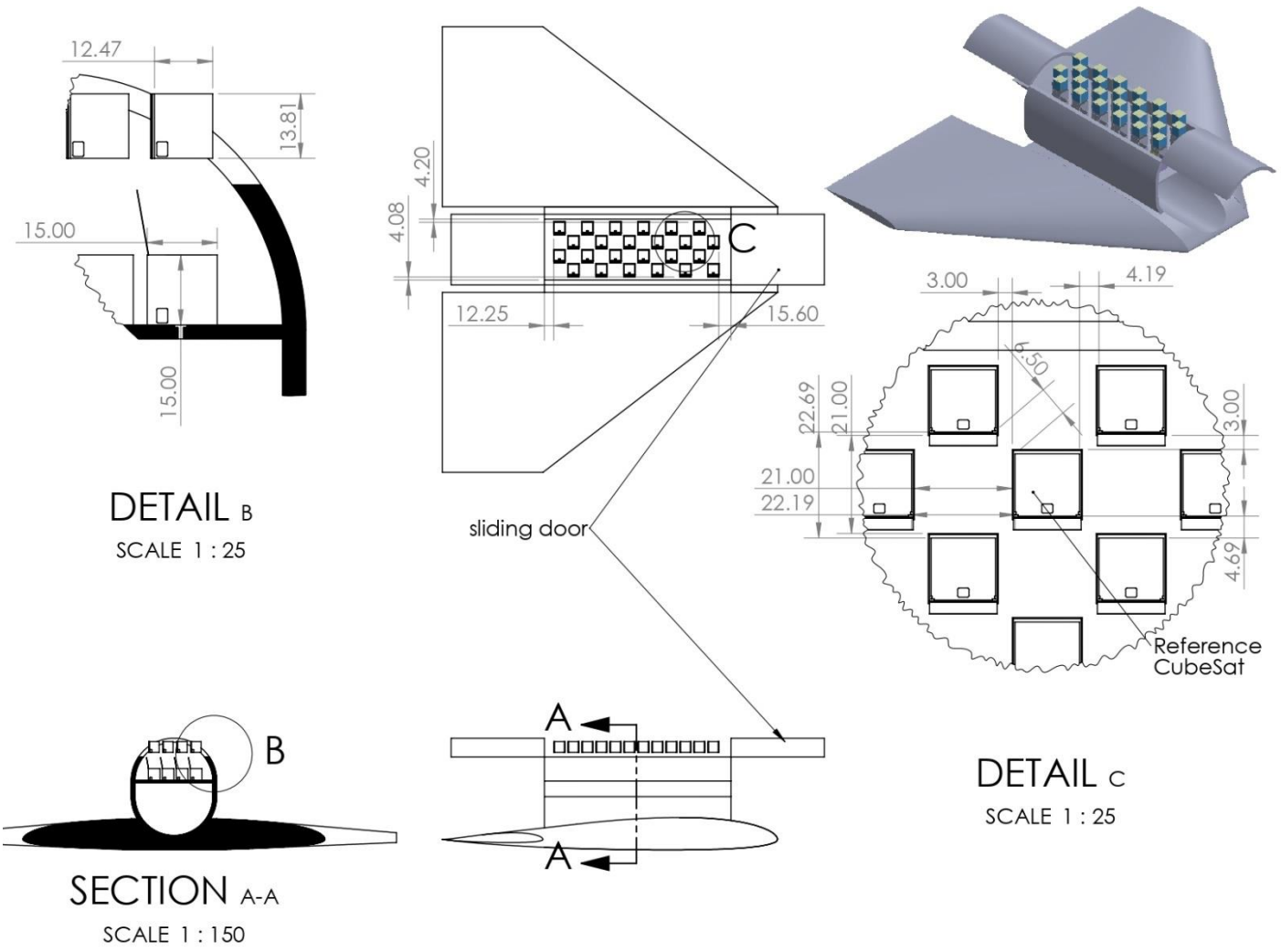

Figure 6.14. Payload deployment demonstration (all dimensions in inches)

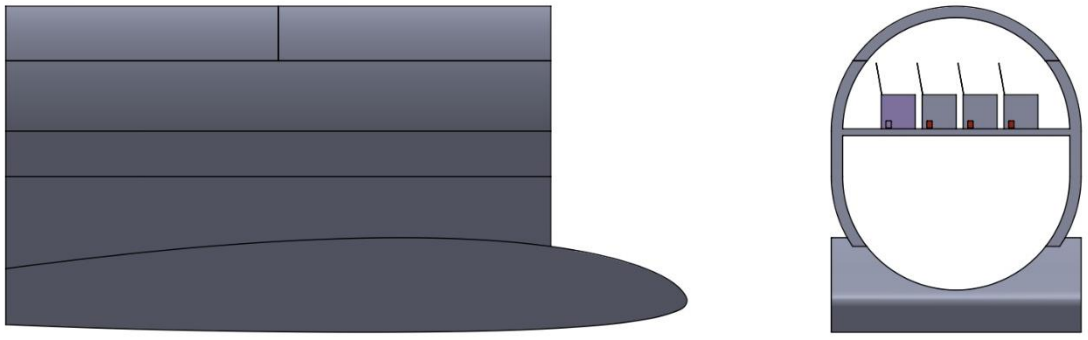

Figure 6.15. Front and side view of payload compartment with sliding door open

6.3.1 2D CAD models:

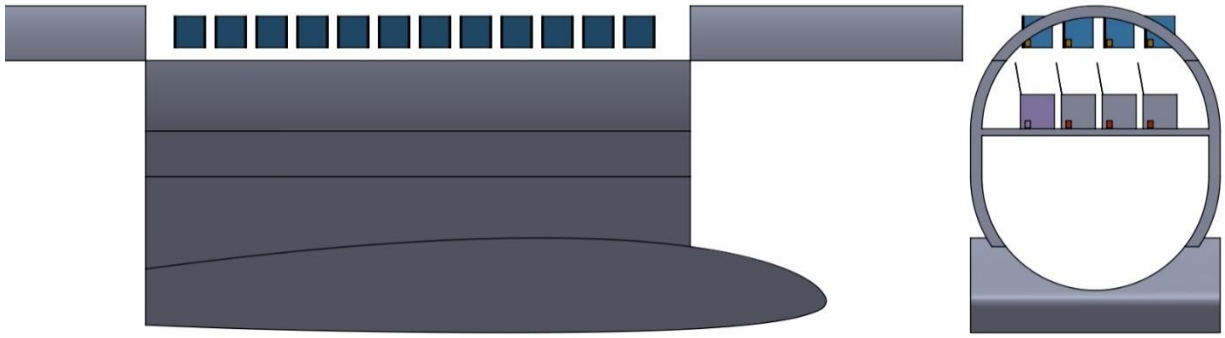

Figure 6.16.6. Top view of payload compartment with open and closed door respectively

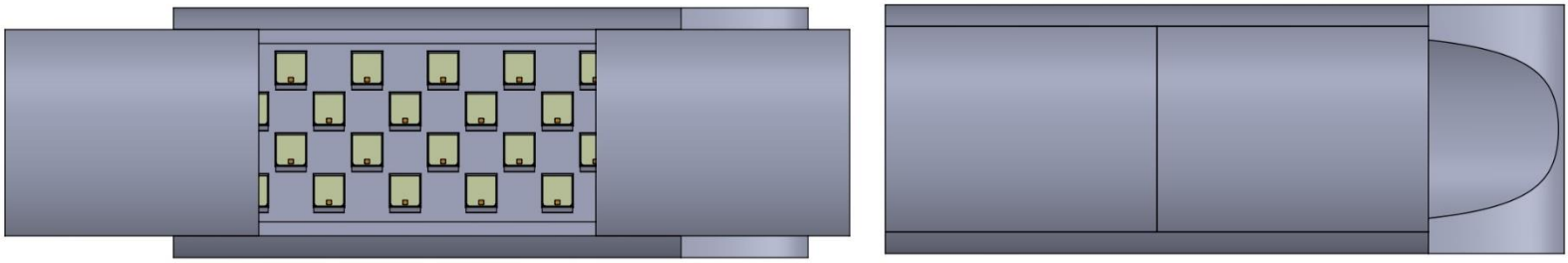

Figure 6.17. Front and side view of payload compartment with sliding door closed

6.3.2 3D CAD models:

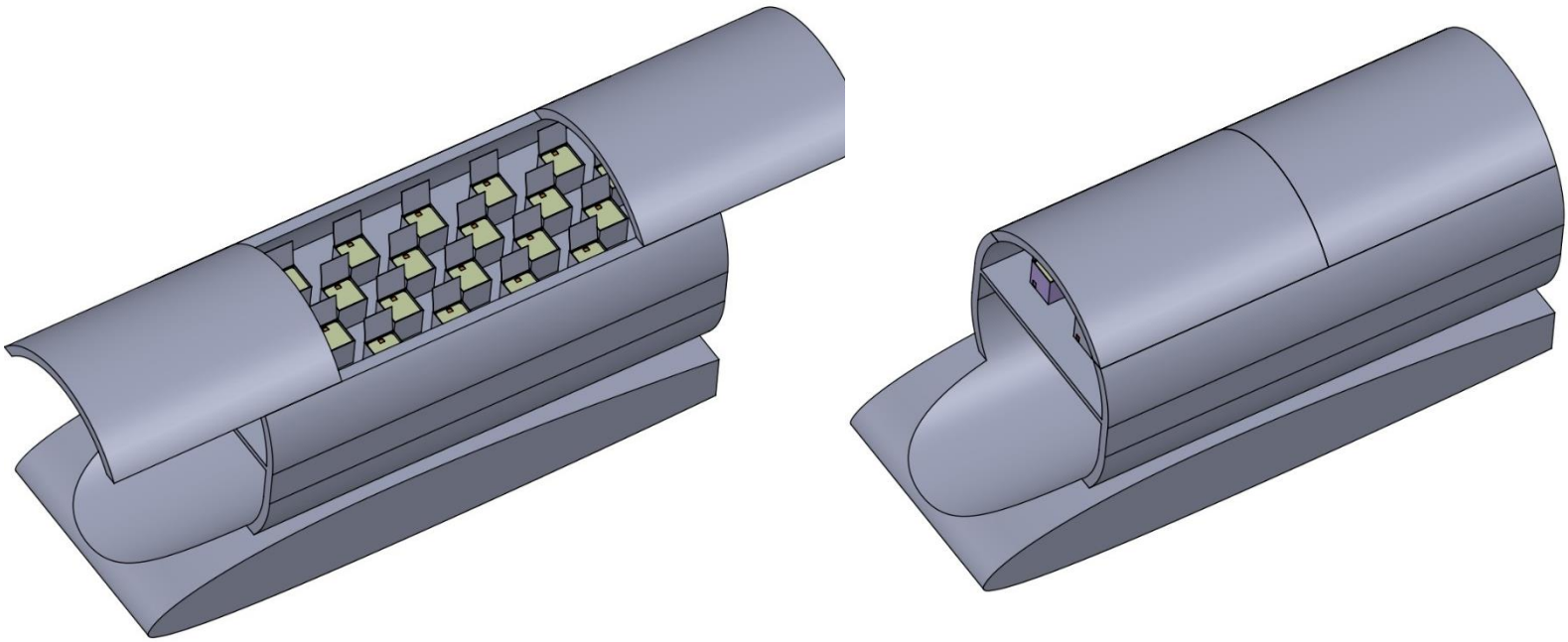

Figure 6.18. Isometric view of payload compartment with open and closed door respectively

6.4 Discussion:

There are some points needed to be considered to develop this prototype into more sophisticated reliable machine. The propulsion system and payload compartment have more scope in development since this project mostly concentrates only on CubeSats to consider the maximum payload capacity. Furthermore, the descent and landing completely relies on efficient wing aerodynamics and control surfaces as there won't be any propulsion system to govern these phases. The propellant for thrusters is installed in wing for rolling and in nose cone pitching and yawing.

Following are the aspects considered for the improvement in specific systems:

6.4.1 Improvements in Payload Compartment:

The basic mission specification describes that X-69 will have potential to bring back damaged satellites using efficient docking mechanism. This is possible if payload compartment allows more room for incoming payload as CSDs are fixed and integrated with the payload compartment. Unless the mission is solely to bring back damaged satellite including some coasting and space-walk, it is possible to modify the payload compartment up on mission requirement.

6.4.2 Improvements in Propulsion System Housing:

Hybrid rocket propulsion is one of the compact, efficient and robust propulsion systems for small spaceplanes. However, X-69 demands more research in propulsion system area that could give more sophisticated design to X-69 itself. Propulsion system design could be helpful to improve the aerodynamics, skin friction and drag during re-entry providing it more surface for deceleration. If propulsion system demands for extension of fuselage, the rear payload compartment can be kept reserved for incoming payload without affecting the main payload compartment.

7. Chapter 7 – Integration of Propulsion System

7.1 Introduction:

Nature of mission of any aircraft decides the selection of appropriate propulsion system. In case of X-69, the "spaceplane/ rocket-plane", its main mission is to successfully make it up to 110 km of altitude from earth surface into at least LEO. The normal jet engines however don't work at these higher altitudes. Therefore, a rocket engine is the way to go.

7.2 Selection of Propulsion System Type:

Before the selection process, it is necessary to understand the factors that play a vital role in:

7.2.1 Required Climb Rate and Maximum speed:

X-69 proposes to climb at supersonic speeds for very limited time period. The mission profile indicates climb phase which should be no longer than maximum 120 seconds.

7.2.2 Operating Altitude:

Flight phase of altitude will change constantly until X-69 makes it to LEO. However, the actual operating phase happens to be in coasting where the maneuvering of X-69 will controlled using RCS (Reaction Control System) thrusters. These thrusters are installed in wing and nose for roll and pitching & yaw respectively.

7.2.3 Range:

As for the climb phase, the range is about 100 km with continuous climb. The hybrid rocket motors allow to successfully achieve such mission profiles. Unlike solid propellant rockets, the hybrid ones can be controlled, by monitoring the oxidizer flow rate.

7.2.4 Installed Weight:

More research and another preliminary design process for rocket engine is required to obtain the accurate installed weight. This requires the experimented data for the analysis.

7.2.5 Reliability and Maintainability:

The rocket motor is expected to return empty after the mission completion. It simply consumes all solid propellant and liquid oxidizer by the end of climb phase. Therefore, it is convenient to replace the engine for the next mission quite conveniently. The fuselage itself has a separate rocket housing compartment that allows easy removal of the complete unit of propulsion system without disturbing the payload compartment.

7.2.6 Fuel Availability and Cost:

Considering the above points, the Hybrid Rocket engine fits the requirements. The hybrid engine consists of a solid propellant and liquid oxidizer. Solid propellant is either wax or detonating material which when mixed with oxidizers gives efficient burn and lift.

The actual estimation of rocket motor parameters have not been performed in this report due to lack of resources and reference material. However, up on research, since this demands the preliminary design process for rocket engine, the method of using Differential Evolution is recommended. Similar to regression method, D.E (differential evolution) algorithm requires pre-obtained data to define the population size which up on iteration narrows down to appropriate selection of rocket parameters. However, studying basic parameters of hybrid rocket engine and referring to engine of V.G's SpaceShipOne, following parameters are incorporated:

Table 7.1. Hybrid rocket parameters of SS1.

Parameters	Quantity
Maximum operating pressure	900 psia
Maximum vacuum thrust	250,000 lbf
Throat Diameter, initial	14.60 inches
Nozzle Expansion ratio, initial	12:1
Liquid Oxygen flow rate	420 – 600 lbm/sec (throttlable)
Fuel Weight	45,700 lbf
Burn time	80 sec – 90 sec
Speed at the end of the climb	Mach 2.5 – 3
Altitude at the end of the climb	100 km to 110 km
Solid propellant used	HTPB

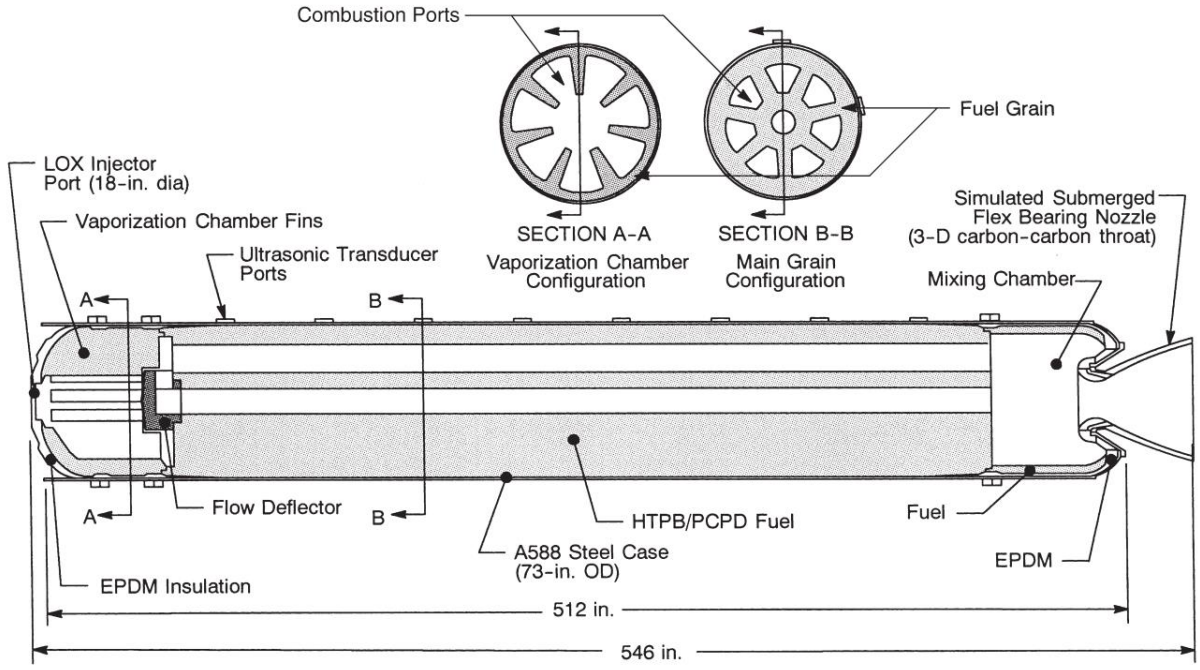

Figure 7.1. Hybrid rocket motor – grain details and dimensions

The grain size and pattern can be anything from star shaped to wheel shaped or one-hole grain. These parameters of grain depend up on grain boundary layer and fuel regression characteristics which is affected by various factors such as :

- Pressure and Temperature of gas or oxidizer
- Grain composition
- Combustion port
- Oxidizer mass flow rate
- Combustion port length
- Combustion port diameter

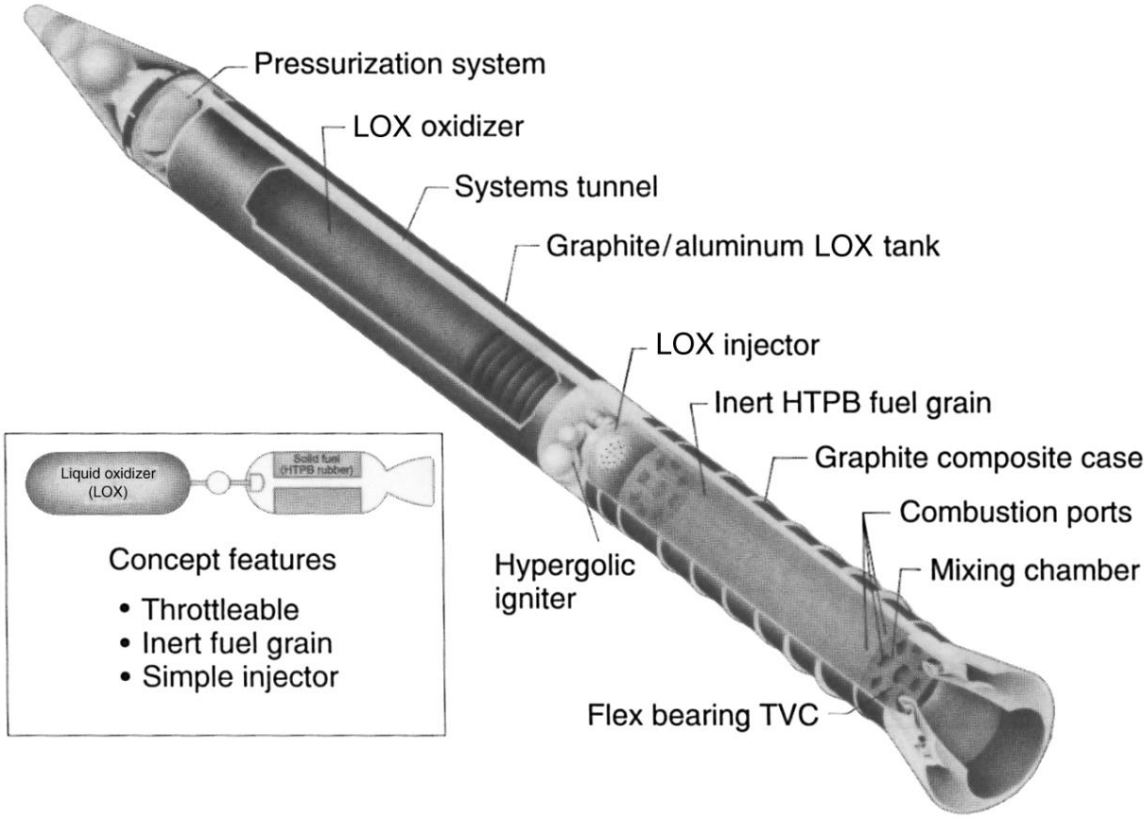

Figure 7.2. Schematic representation of a hybrid rocket.

7.3 Differential Evolution Algorithm:

DE was first proposed by Storn and Price (1997) at Berkeley as a new evolutionary algorithm. It uses a function called crossover to increase the diversity of the perturbed parameter vectors ensuring that the last vector gets at least one parameter from the previous one. As a population-based algorithm, the DE starts with a set of candidate solutions. The initial solutions are randomly generated over the problem space. The steps of DE algorithm can be described as follows:

- Initialize stochastic solutions as equation 7.1:

$$x_{ij} = x_{j-lowerlimit} + r\left(x_{j-upperlimit} - x_{j-lowerlimit}\right) \tag{7.1}$$

where, r is a random number, $r \in [0,1]$.

- Evaluate each initial solution against the objective function.
- Check the stopping criteria. Stop, if they are satisfied.
- For each solution x_i, create mutant solution x'_i as follows by randomly selecting three different solutions (R1, R2, R3) as equation 7.2.

$$x_i' = x_{RI} + F(x_{R3} - x_{R2}) \tag{7.2}$$

where, F is a mutation factor between [0,1].

- For each mutant solution, generate a trial solution x''_i by copying parameters either from the parent solution x_i or the mutant one x'_i as equation 7.3.

$$x''_{ij} = \{x\_\{i,j\}' \; if \;\; rand(0,1) < CR \\ x_{i,j} \qquad\qquad else\} \tag{7.1}$$

where, CR is a specified crossover factor between [0,1] and the subscript j refers to the jth dimension of the solution vector.

- Evaluate each trial solution against the objective function.
- Compare the objective function of the trial solution with that of the parent solution. Select the better solution to survive in the next generation.
- Repeat the steps four to seven until the population is filled.
- Update the best solution and go to step three.

7.3.1 Design Process:

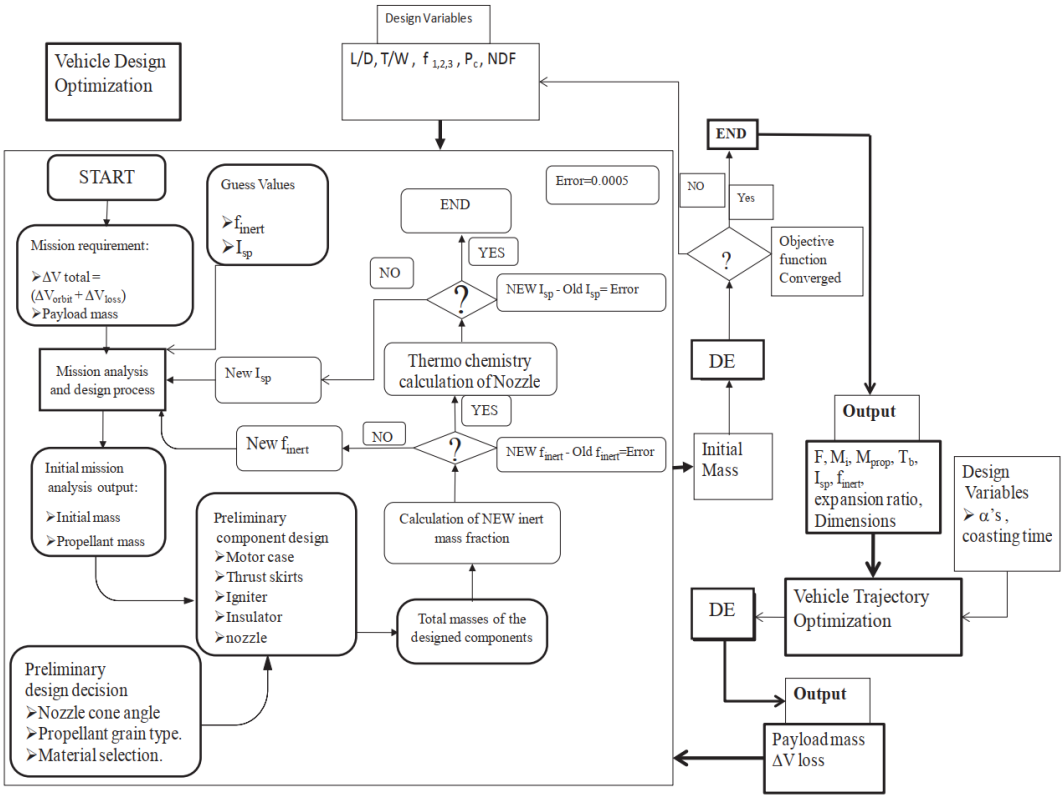

Figure 7.3. Chart of vehicle design and trajectory optimization of air-launch vehicle using DE.

- **Design Requirements:**
  - *Mission requirements:* Mission requirements are the target parameters to be achieved in the design process. Some requirements may be considered as constraints on the design, which are:
  - *Orbit and Altitude:* Main engine of X-69 should be able to insert X-69 at least into LEO.
  - *Payload Mass:* Collective payload mass for the engine is weight of components + mass of payload (CubeSats).
  - *Launch Conditions:* X-69 and hence its engine will be from a carrier aircraft at an altitude of 45,000 ft and speed of at least 300 m/s.
  - *Decisions:* Certain parameters should be defined to start the design process. They are selected based on published data of existing launch vehicles (e.g. Pegasus). However, some of them will be set as design variables in the optimization stage in order to find the optimal values. These parameters are: the number of stages (we have decided to use one stage: fixed), type of rocket in each stage (we choose hybrid rocket motor: fixed), chamber pressure (P_e), thrust-to-weight ratio (*T/W*), length to diameter ratio (*L/D*), *T/W & L/D* will be design variables in the optimization process.

- **Initial values:**
  - To start the design process, initial values for specific impulse (I_{sp}) and inert mass fraction (f_{inert}) are required. However, these values will change during the design loop processes until their values are converged. An initial value of total ΔV is also required to start the design process.

$$\Delta V = Speed\ at\ the\ end\ of\ climb - Speed\ when\ the\ rocket\ motor\ fires\ up$$
$$\Delta V = (1{,}020 - 300)\ m/s$$
$$\Delta V = 720 m/s$$

- **Design of micro air launch vehicle subcomponents:**
  - The required ΔV is used is mission analysis with initial specific impulse and inert mass fraction. The output of mission analysis is the initial values of propellant and inert masses using equations 7.4 and 7.5.

$$m_{prop} = \frac{m_{pay}\left(\frac{\Delta V}{e^{I_{sp}g_0} - 1}\right)(1 - f_{inert})}{1 - f_{inert}e^{\frac{\Delta V}{I_{sp}g_0}}} \tag{7.4}$$

$$m_i = m_{prop} + m_{payload} + m_{inert} \tag{7.5}$$

Note that the selected ΔV at the first step of the design will be taken based on some previously available data of Pegasus to start the design process. However, this ΔV will be replaced by the real value when the trajectory analysis is performed.

The propellant masses along with *T/W*, *L/D* and chamber pressure are used to design the geometry of the vehicle and to obtain the initial masses again and also to obtain the inert mass fraction. The vacuum thrust of the vehicle can be calculated using equation 7.6.

$$F = \dot{m}v + A_e P_e \tag{7.6}$$

Fig 7.4 illustrates the main components of the engine of X-69. Solid motor has classical architecture and is attached to the other stages by thrust skirts. The volume is calculated using the propellant mass and its density, a cylindrical motor case with half dome ends is selected for the design as shown in fig 7.4, the calculations are done using equations 7.7 to 7.12.

$$V_{CS} = \frac{m_{prop}}{n_v \rho prop} \tag{7.7}$$

$$V_{CS} = \pi D^3 \left[\frac{1}{6} + \frac{1}{4}\left(\frac{L}{D} - 1\right)\right] \tag{7.8}$$

Pressure vessel and skirt masses are calculated using Equation 7.9 to 7.12.

$$m_{pv} = \rho_{CS} t_{CS} D^2 \pi \left(1 + \frac{L_{cy}}{D}\right) b \tag{7.9}$$

$$m_{sk} = \rho_{CS} t_{CS} \pi D^2 \tag{7.10}$$

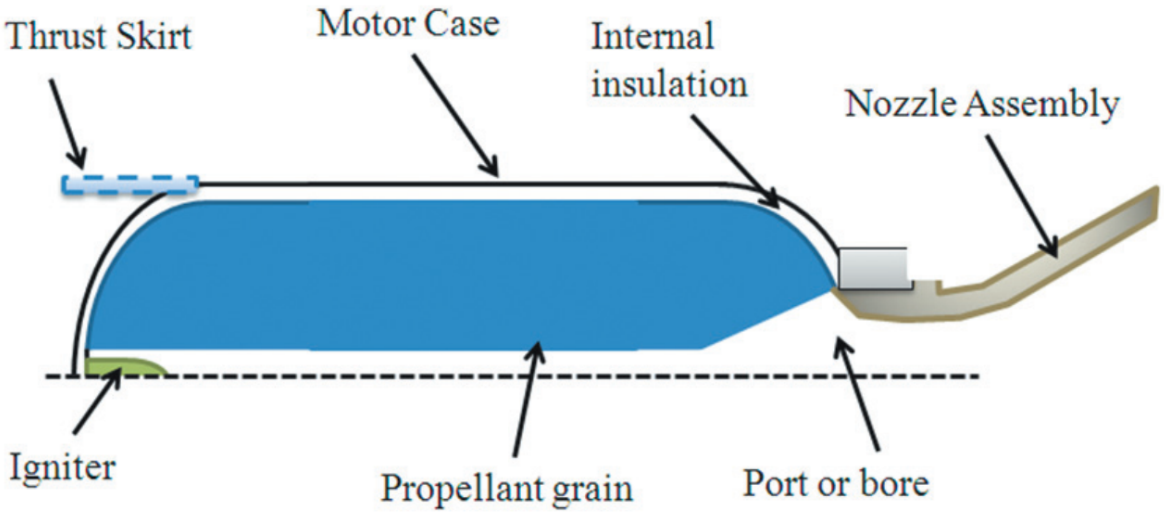

Figure 7.4. Main components of the solid rocket motor

Thus, the motor case mass is:

$$m_{CS} = 1.1\left(m_{SK} + m_{pv}\right) \tag{7.11}$$

Insulation mass of motor case is

$$m_{insul} = 1.788 \times 10^{-9} m_{prop}^{-1.33} t_b^{0.965} \left(\frac{L}{D}\right)^{-0.144} L_{sub}^{0.058} A_w^{2.69} \tag{7.12}$$

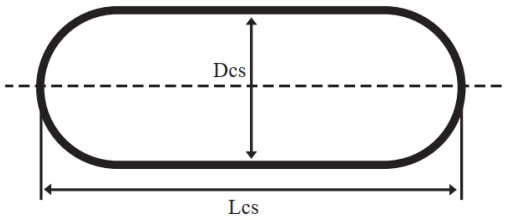

Figure 7.5. Sketch, length and diameter of the motor case

The nozzle parameters are shown in fig 7.6 and calculated using equations 7.13 to 7.20. Nozzle system mass may be calculated from equation 7.13.

$$m_{noz\ sys} = 1.5\left[0.256 \times 10^{-4}\left[\frac{\left(m_{prop}c^*\right)^{1.2}\epsilon^{0.3}}{P_c^{0.8}t_b^{0.6}tan\theta_{cn}}\right]\right] \tag{7.13}$$

The throat diameter and nozzle length are calculated using equations 7.14 and 7.15:

$$D_t = \sqrt{\frac{4c^*m_{prop}}{\pi t_b P_c}} \tag{7.14}$$

$$L_{noz} = \frac{D_e - D_t}{2tan\theta_{cn}} \tag{7.15}$$

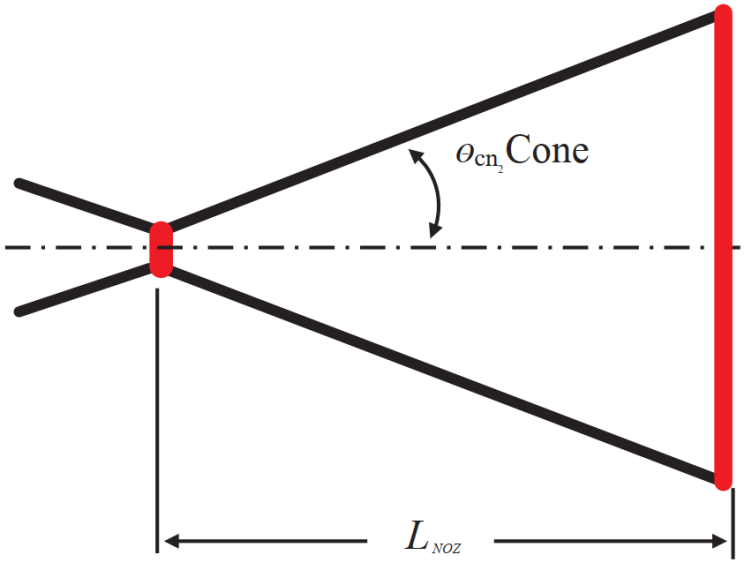

Figure 7.6. Sketch of nozzle design

In this work, the inert mass includes motor case, the insulation, the nozzle system masses, avionics, attitude control systems, etc. This may comprise an important fraction of the payload mass.

$$m_{inert} = m_{cs} + m_{insul} + m_{noz\ sys} \tag{7.16}$$

The inert mass fraction is calculated again using the new inert mass as in equation 7.17.

$$f_{inert} = \frac{m_{inert}}{m_{inert} + m_{prop} - m_{pay}} \tag{7.17}$$

If this new inert mass fraction is not the same as the initial values, then the new f_{inert} will be used in mission analysis and the same steps will be repeated until f_{inert} converges. When f_{inert} is converged, then the value of I_{sp} should be evaluated and compared with the initial values, if it is not the same, the whole previous procedure will be repeated until the solution of I_{sp} and f_{inert} converges. The calculation of the nozzle specific impulse is done using equations 7.18 and 7.19 from *George P. Sutton's Rocket Propulsion.*

$$\varepsilon = \frac{1}{M_e}\sqrt{\left[\left(\frac{2}{y+1}\right)\left(1+\frac{y-1}{2}\right)M_e^2\right]^{\frac{y+1}{y-1}}} \tag{7.18}$$

$$P_e = P_c\left[1+\frac{y-1}{2}M_e^2\right]^{\frac{y}{y-1}} \tag{7.19}$$

$$C_F = \sqrt{\left(\frac{2y^2}{y-1}\right)\left(\frac{2}{y+1}\right)^{\frac{y+1}{y-1}}\left[1-\left(\frac{P_e}{P_c}\right)^{\frac{y-1}{y}}\right]} + \frac{\varepsilon(P_e - P_a)}{P_c} \tag{7.20}$$

$$I_{sp} = \frac{\lambda C_F c^*}{g_0} \tag{7.21}$$

Output of the vehicle design is total mass, propellant mass, inert mass, specific impulse, inert mass fraction, dimensions, nozzle expansion ratio, thrust, mass flow rate and burning time.

In the case of a vehicle requiring real developments, the targeted payload mass should have a margin to cover inevitable losses during the development, which may cause a substantial loss in the targeted final mass.

- **Aerodynamic Model:**
  - Mission Datcom is the software used to obtain aerodynamic coefficients of lift and drag using the dimensions obtained from the design of X-69 subcomponents.

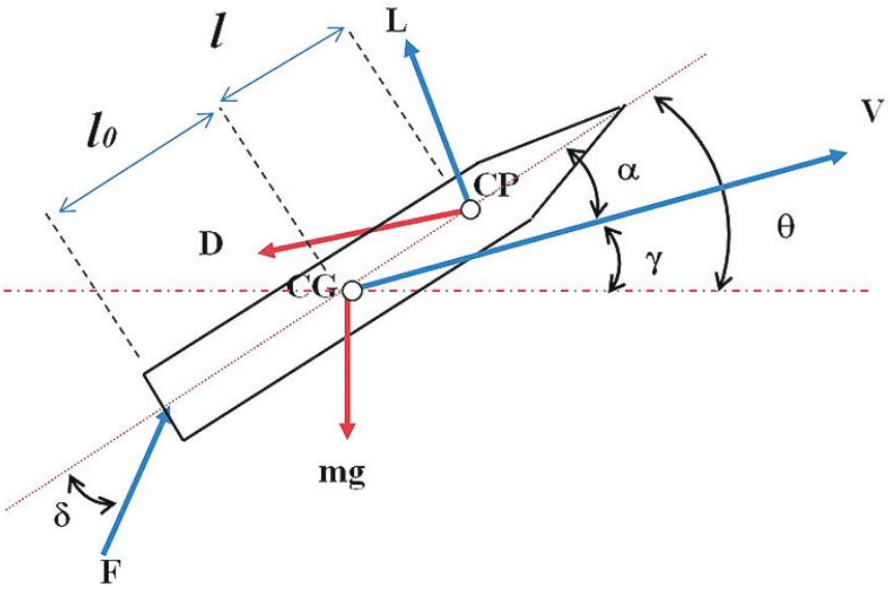

Figure 7.7. Two-dimensional body forces for flying vehicle

Since the aerodynamic coefficients are obtained, the trajectory model is done using the equations of motion 7.22 and 7.23.

$$m\frac{dV}{dt} = Fcos(\delta+\alpha) - mg \times sin\gamma - D \tag{7.22}$$

$$mv\frac{dv}{dt} = L + Fsin(\delta + \alpha) - mg \times cos\gamma + \frac{mV^2}{r}cos\gamma \quad (7.23)$$

The total ΔV, which is required from the launch vehicle, is calculated from equation 7.24.

$$\Delta V_{total} = V_{orbit} - V_{aircraft} + \Delta V_{loss} \quad (7.24)$$

where, ΔV_{loss} is the summation of drag, gravity, steering and performance losses expressed in equation 7.25.

$$\Delta V_{loss} = \Delta V_{drag} + \Delta V_{gravity} + \Delta V_{steering} + \Delta V_{performance} \quad (7.25)$$

In the equation 7.25, $\Delta V_{gravity}$ is the velocity needed to overcome the effect of the gravity and gain altitude and ΔV_{drag} is the loss due to drag that is profound at low altitudes, but become negligible at high altitudes. $\Delta V_{steering}$ is the velocity needed to steer and turn the vehicle along the trajectory. $\Delta V_{performance}$ is the velocity loss due to ideal performance assumptions, since vacuum performance is assumed during the design, whereas the actual rocket performance is reduced by atmospheric pressure.

7.4 Discussion:

Due to unavailability of data reference of Pegasus and Mission Datcom (a military-based software), the calculation for rocket parameters have not been proposed yet. However, the differential evolution algorithm is appropriate method to obtain optimal rocket engine parameters for X-69.

The propulsion system for RCS thrusters have propellant installed in the wing. As discussed earlier, the disposition of RCS thrusters is on wing and in nose to control roll and pitch & yaw respectively. The computation amount of propellant required is evaluated by ΔV defined by the mission profile during coasting. If the mission requires an orbital transfer, ΔV might increase requiring more propellant.

8. Chapter 8 – Wing, High Lift system and Lateral Control Design

8.1 Introduction:

A quick look back on the mission profile, parameters obtained from performance constraints, weight sizing and basic configuration studies are used to create and optimize wing planform for X-69. The previous parameters give an estimate for wing loading during landing, cruise and gliding. This report studies detailed wing design considering various characteristics. The procedure follows from *Roskam's Aircraft Design vol III*, a step-by-step procedure to carry out the wing design. Other wing components such as tail, spoilers, elevons and stabs are also estimated.

8.2 Wing Configuration:

8.2.1 Wing size:

Due to low wing loading as discussed in performance constraints, wing of X-69 are preferred with small size forming a delta-wing similar to that traditional space shuttles. Moreover, large size wing cannot sustain their structural integrity in supersonic and hypersonic regimes during climb and re-entry respectively.

Using equation from *Roskam's Aircraft Design Vol III*, for landing field length and following assumptions that weight of X-69 should drop to approximately 40% of its take-off weight W_{TO} during landing approach as the rocket fuel will be completely burnt and deployed payload with total wing area, S = 659.56 ft^2 (= 900 ft^2 including spoilers attached to the wing),we get the wing loading at landing

$$\left(\frac{W}{S}\right)_L = \frac{0.4 \times W_{TO}}{S} \tag{8.1}$$

$$\left(\frac{W}{S}\right)_L = \frac{0.4 \times 13{,}870}{659.56}$$

$$\left(\frac{W}{S}\right)_L = 8.42 lb/ft^2$$

Therefore, the landing field equation follows as:

$$S_L = 429(W/S)_L / C_{L_{max_L}} \tag{8.2}$$

$$S_L = 429 \times 8.42 / C_{L_{max_L}}$$

Considering the $C_{L_{max_L}}$ from performance constraints in the range of 1.7 to the design point 2.7, the table 8.1 and plot in fig 8.1 estimates respective field lengths

Table 8.1. Field length at specific $C_{L_{max_L}}$

Landing Field Length, S_L in ft	$C_{L_{max_L}}$
2124.811765	1.7
1901.147368	1.9
1720.085714	2.1
1570.513043	2.3
1444.872	2.5
1337.844444	2.7

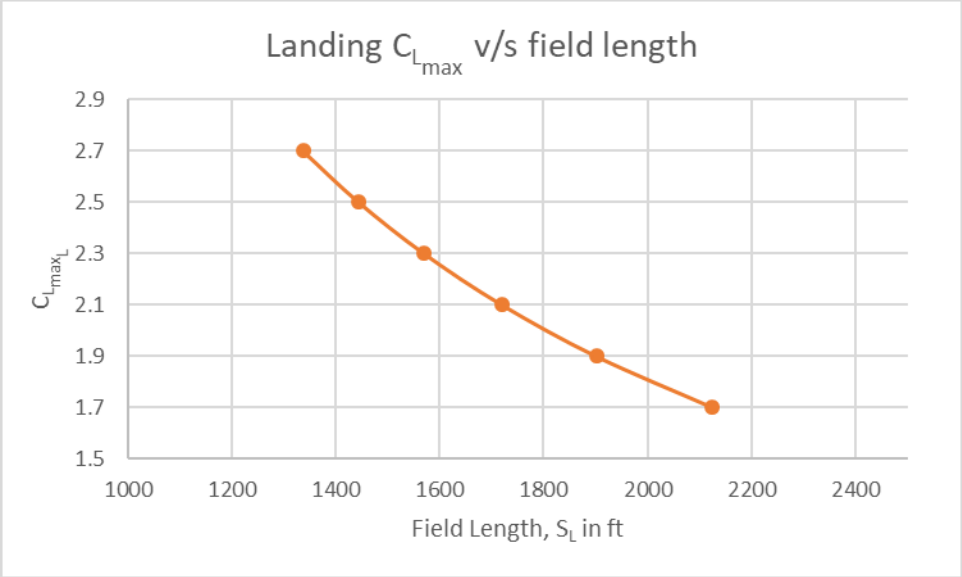

Figure 8.1. Field length estimation

Secondly, it is efficient to achieve cruise performance with a cruise flight close to $(L/D)_{max}$.

An appreciation for the effect of wing loading on $(L/D)_{max}$ can be obtained as follows:

$$(L/D)_{max} = \sqrt{\frac{\pi * A * e}{4 * C_{D_0}}} \tag{8.3}$$

with:

$$C_{D_0} = 1/S\left(10^{\left[a+b*log_{10}\left[10^{(c+d*log_{10}W_{TO})}+k_{ww}*(S-S_{baseline})\right]\right]}\right) \tag{8.4}$$

Equations (8.3) and (8.4) can be used to study the effect of varying wing area (wing loading) on $(L/D)_{max}$ for X-69.
Hence to perform such a study, the following input is referred
Aspect ratio, A = 2.18
Oswald's efficiency, e = 0.8
Regression constants that we obtained in chapter 4 (performance constraints) are as follows:
a = -2.523,
b = 1,
c = 0.2263,
d = 0.6977
Take-off Weight, W_{TO} = 13,870 lbs.
Baseline Wing Loading, $(W/S)_{baseline}$
k_{ww} = 1.85 (approximately)

The constant k_{ww} accounts for that part of the wing which is buried in the fuselage that does not contribute to the wetted area,
The value for $S_{baseline}$ in equation (8.4) follows from:

$$S_{baseline} = \frac{W_{TO}}{\left(\frac{W}{S}\right)_{baseline}} \tag{8.5}$$

The lift coefficient at $(L/D)_{max}$ follows from:

$$C_{L_{(L/D)max}} = \sqrt{C_{D_0} \pi A.e} \tag{8.6}$$

Therefore, solving from equation (8.3) to (8.6) up on substituting the respective values, we get following table 8.2 and plot of wing loading and $(L/D)_{max}$ at cruise flight in fig 8.2.

Table 8.2. Effect of wing loading on cruise flight parameters

$(W/S)_{baseline}$	$(L/D)_{max}$	$C_{L_{(L/D)max}}$
15	20.5816	0.13312
30	19.56008	0.140072
45	19.35549	0.141553
60	19.2662	0.142209
75	19.21604	0.14258
90	19.18388	0.142819

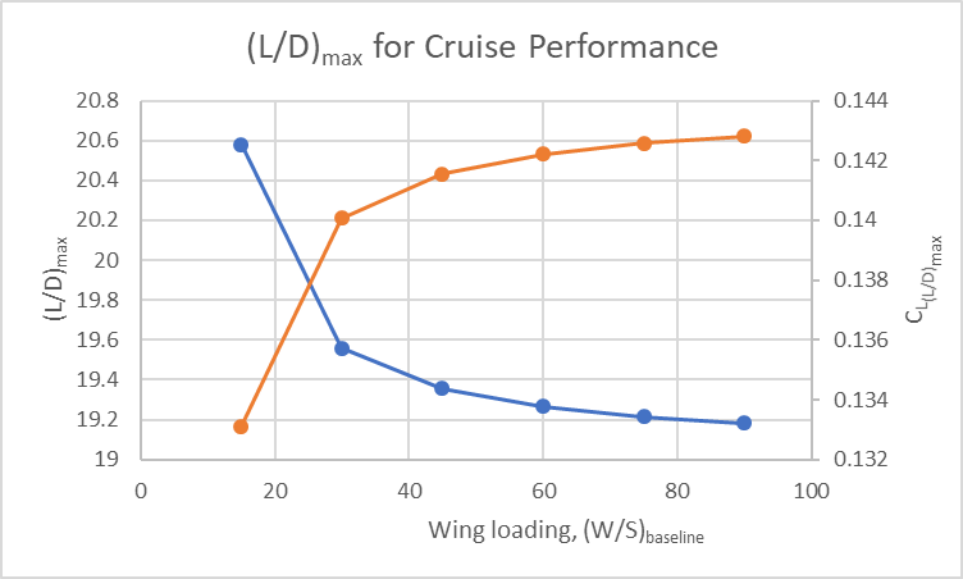

Figure 8.2. Effect of wing loading on cruise flight parameters

Another major factor that could affect the wing parameters in terms of performance constraints is *Ride through turbulence* which has a significant effect on wing loading especially on X-69 during climb and re-entry. The climb cannot extend more than 3 minutes (max) however the re-entry is to optimal to achieve required deceleration for efficient gliding. Diving with hypersonic speeds is just another ride through turbulence that has keep extending to kill the acceleration. Hence during this phase, the wing structure should be intact maintaining the structural integrity. Thus, the spoilers come into the picture playing a major role which will be explained further.

The equation referred from *Roskam's,* ride response to turbulence is proportional to the parameter n_α, and is given by,

$$n_\alpha = \frac{\bar{q} C_{L_\alpha}}{W/S} \tag{8.7}$$

The above equation when related to X-69 performance requires more research considering hypersonic parameters since the equation clearly mentions that lower wing loading yields higher values ride response n_α which translates into "poor" ride qualities. It quantitively clarifies poor ride qualities however it is required to develop the wing that improve the turbulence response extending the time required for X-69 to deceleration.

8.2.2 Low Wing Configuration:

X-69 incorporates a low wing configuration considering various aspects such as mission profile & improving performance constraints, similar trending spaceplanes (or space shuttles), advantages and disadvantages. Most of the space-vehicles, except X-15A-2 and 5-10% of other, have low wing configuration since they offer good visibility and accessibility during coasting in space and deploying payload as studied in fuselage section, combines with ventral part of the fuselage providing more surface for ablative material to fight with hypersonic temperatures and pressures, lower ground clearance for quick bailing out, etc.

8.2.3 Numerical parameters:

Rest of the parameters are computed and obtained using AAA software and some of the basic relations for wing design. The parameters in fig 8.3 are for the basic wing excluding the spoiler as follows:

Input Parameters

b_w	47.06 ft	c_{t_w}	7.82 ft	X_{apex_w}	23.25 ft
c_{r_w}	27.00 ft	$\Lambda_{c/4_w}$	37.2 deg	Y_{offset_w}	4.58 ft

Output Parameters

S_w	659.65 ft^2	λ_w	0.29	y_{mgc_w}	7.73 ft	Λ_{LE_w}	45.4 deg
AR_w	2.18	$\bar{c}_w$	19.17 ft	x_{mgc_w}	7.83 ft	Λ_{TE_w}	0.0 deg

Straight Tapered Wing Geometry: Output Parameters

Panel	c_r ft	c_t ft	X_r ft	X_t ft	Y_r ft
1	27.0000	7.8200	23.2508	42.4332	4.5833

Figure 8.3. I/O for wing parameters from AAA

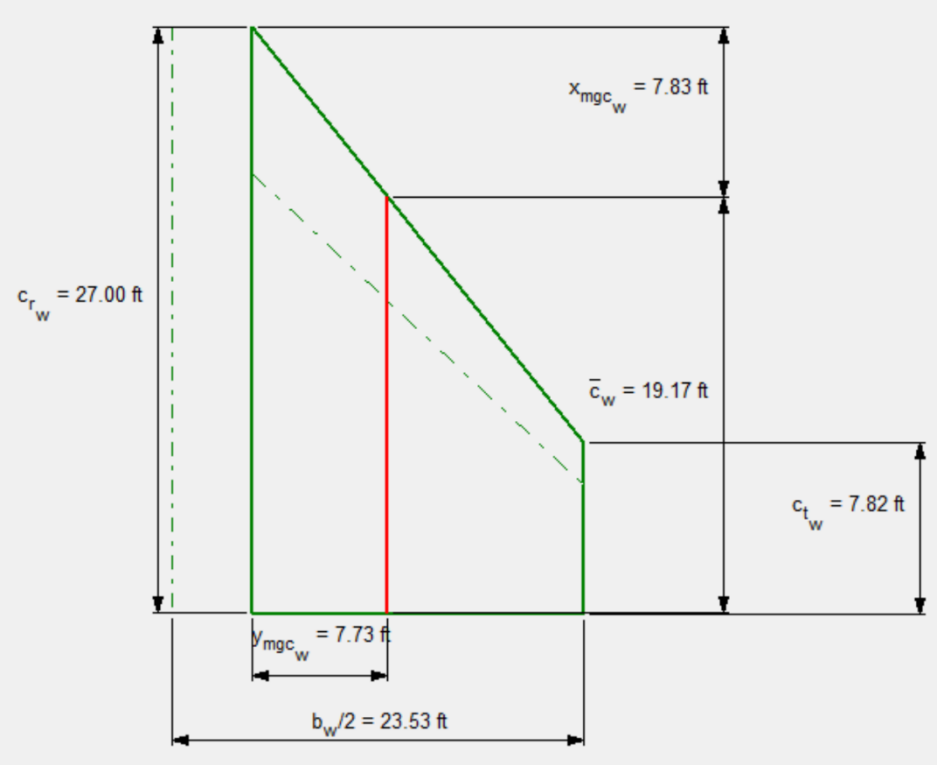

Figure 8.4. Wing geometry without spoiler

The basic wing layout output without spoiler can be seen in fig 8.4. The root chord, $c_{r_w} = 27\ ft$ and tip chord, $c_{t_w} = 7.82\ ft$ are desired and a constrained maintaining the aspect ratio of 2.18 and span area of 659.56 ft^2.
From fig 8.3 and previous data,

$$A_{without\ spoilers} = 2.18$$

Hence, wingspan, b_w with wing area, $S_w = 659.56 ft^2$ (excluding the spoilers).

$$b_w = 47.0556 ft$$

$$\lambda = \frac{c_t}{c_r} = \frac{7.8155}{27}$$

$$\lambda = 0.29$$

Therefore, the aspect ratio, A = 2.18 and taper ratio, $\lambda = 0.29$ will be considered for further computation of aerodynamic parameters with influential span area, $S_{w_{with\ spoiler}} = 1{,}114.32 ft^2$ since the spoiler is simply a flat plate.

Taper ratio, λ = 0.29 is close desired to contain the rolling thrusters' components and propellant

Sweep angle, $\Lambda = 37.215°$ is preferred to keep the trailing edge of the wing perpendicular to the longitudinal axis of X-69 forming a delta-wing configuration.
Twist angle, $\varepsilon = 0^o - 2°$, A twist angle gives efficiency in deceleration in hypersonic regime.

Dihedral angle, $\Gamma = 0°$
Incidence angle, $i_w = 0°$
Average thickness ratio, $t/c = 0.0966$

Wing Aerodynamic center will in estimation of empennage parameters.

Hence, to calculate mean aerodynamic center of wing of X-69, we have
Mean aerodynamic chord, MAC is

$$MAC = \bar{C} = \frac{2}{3} \times c_{root} \times \frac{1 + \lambda + \lambda^2}{1 + \lambda} \tag{8.8}$$

$$MAC = \bar{C} = \frac{2}{3} \times 27.00ft \times \frac{1 + 0.29 + 0.29^2}{1 + 0.29}$$

$$MAC = \bar{C} = 19.1698\, ft$$

y-location of MAC on each half of the wing is,

$$\bar{Y} = \frac{b_{exposed}}{6} \times \frac{1 + 2 \times 0.29}{1 + 0.29} \tag{8.9}$$

$$\bar{Y} = \frac{(47.0556 - 9.1667)\, ft}{6} \times \frac{1 + 2 \times 0.29}{1 + 0.29}$$

$$\bar{Y} = 7.73ft$$

And according to Raymer's section 4.6, *Wing Geometry,* X-location of the aerodynamic center for a supersonic wing is,

$$x_{ac} = 0.408 \times \bar{C} \tag{8.10}$$
$$x_{ac} = 0.408 \times 19.1698$$
$$\mathrm{x_{ac}} = 7.823 \text{ ft}$$

However, it is attempted to add spoilers in AAA using an aileron feature to account for aerodynamic parameters of spoiler along with the wing.

To add spoiler effect in AAA software, the aileron feature is used to plot spoiler as shown in fig 8.5. This extends the total span area, $S_w = 1{,}114.32ft^2$ and reduces the aspect ratio, *A=1.29* which will be considered for further computation of aerodynamic parameters. However, the spoiler is a flat plate hinged to the wing where elevons on Horizontal Tail will do the function of rolling,

The spoiler input parameters are maintained such that the root and tip chord of spoiler are 12 ft spanning equally with the wing. The input and output parameters can be referred in fig 8.6. Being a low wing configuration, the wing will attach to fuselage using either spar or bi-plane structure which can be referred in fuselage section. This configuration allows the space for housing the main landing gears retracting inwards. The space towards cockpit can be used to accommodate the avionics of the system making it compact but reliable.

Up on adding the spoiler to the wing, the parameters updated are as follows:

$$A_{with\ spoilers} = 1.29$$

Hence, wing span, b_w with wing area, $S_w = 1{,}114.32\ ft^2$ (including the spoilers).

$$b_w = 47.0556ft$$

$$\lambda = \frac{c_t}{c_r} = \frac{19.82}{39}$$

$$\lambda = 0.51$$

Therefore, the aspect ratio, $A_{with\ spoiler} = 1.29$ and taper ratio, $\lambda_{\text{withspoiler}} = 0.51$ will be considered for further computation of aerodynamic parameters with influential span area, $S_{w_{with\ spoiler}} = 1{,}114.32ft^2$ since the spoiler is simply a flat plate.

Taper ratio, λ = 0.51 is close desired to contain the rolling thrusters' components and propellant.

Sweep angle, $\Lambda = 37.215°$ is preferred to keep the trailing edge of the wing perpendicular to the longitudinal axis of X-69 forming a delta-wing configuration.

Twist angle, $\varepsilon = 0^o - 2°$, A twist angle gives efficiency in deceleration in hypersonic regime.

Dihedral angle, $\Gamma = 0°$
Incidence angle, $i_w = 0°$
Average thickness ratio, $t/c = 0.0966$

Wing Aerodynamic center will in estimation of empennage parameters.

Hence, to calculate mean aerodynamic center of wing of X-69, we have

Mean aerodynamic chord, MAC is

$$MAC = \bar{C} = \frac{2}{3} \times c_{root} \times \frac{1 + \lambda + \lambda^2}{1 + \lambda}$$

$$MAC = \bar{C} = \frac{2}{3} \times 39.00ft \times \frac{1 + 0.51 + 0.51^2}{1 + 0.51}$$

$$MAC = \bar{C} = 30.48\ ft$$

y-location of MAC on each half of the wing is,

$$\bar{Y} = \frac{b_{exposed}}{6} \times \frac{1 + 2 \times 0.51}{1 + 0.51}$$

$$\bar{Y} = \frac{(47.0556 - 9.1667)\ ft}{6} \times \frac{1 + 2 \times 0.51}{1 + 0.51}$$

$$\bar{Y} = 8.4478\ ft$$

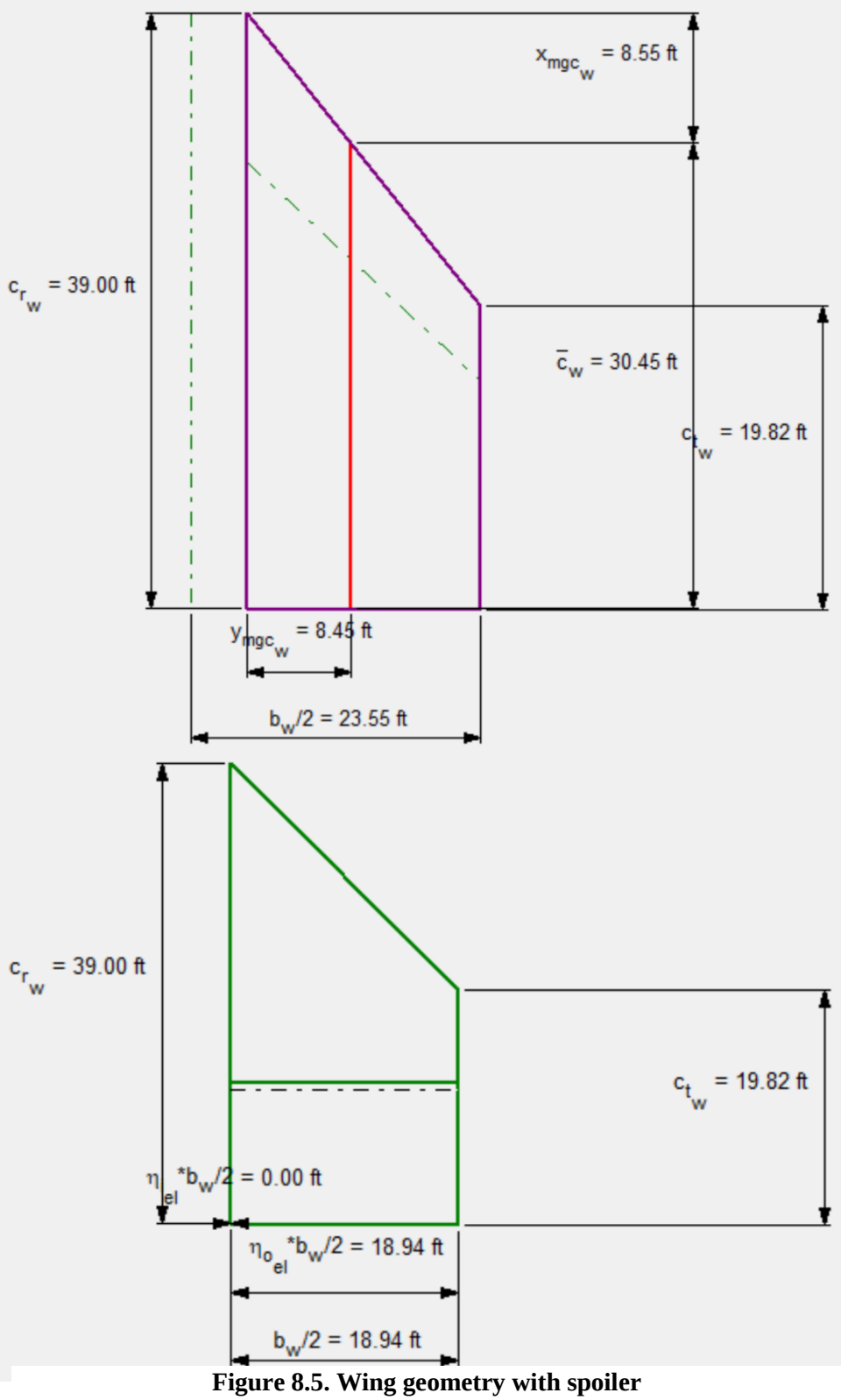

Figure 8.5. Wing geometry with spoiler

Table 8.3. I/O parameters for wing with spoiler in aileron feature of AAA

Parameters	Quantity
Spoiler Chord to Wing Chord Ratio at the Spoiler Inboard Station, $(c_{el}/c_w)_i = (c_{sp}/c_w)_i$ Spoiler root chord length, $c_{r_{sp}} = c_{r_{el}}$	$(c_{sp}/c_w)_i = 30.77\%$ $c_{r_{sp}} = 0.3077 \times 39\ ft$ $c_{r_{sp}} = 12\ ft$
Spoiler (Spoiler) Chord to Wing Chord Ratio at the Spoiler Outboard Station, $(c_{el}/c_w)_o = (c_{sp}/c_w)_o$ Spoiler root chord length, $c_{t_{sp}} = c_{t_{el}}$	$(c_{sp}/c_w)_o = 60.55\%$ $c_{t_{sp}} = 0.6055 \times 39\ ft$ $c_{t_{sp}} = 12\ ft$
Spoiler Root Hingeline Location in Terms of Spoiler Root Chord, $(x_{hl}/c)_{i_{el}} = (x_{hl}/c)_{i_{sp}}$ Spoiler Chord Forward of Hinge at Spoiler Inboard Station, $c_{b_{i_{sp}}} = c_{b_{i_{el}}}$	$(x_{hl}/c)_{i_{el}} = 5\%$ $c_{b_{i_{sp}}} = 0.05 \times 12\ ft$ $c_{b_{i_{sp}}} = 0.6ft$
Spoiler Root Hingeline Location in Terms of Spoiler Root Chord, $(x_{hl}/c)_{o_{el}} = (x_{hl}/c)_{o_{sp}}$ Spoiler Chord Forward of Hinge at Spoiler Inboard Station, $c_{b_{o_{sp}}} = c_{b_{o_{el}}}$	$(x_{hl}/c)_{o_{el}} = 5\%$ $c_{b_{o_{sp}}} = 0.05 \times 12\ ft$ $c_{b_{o_{sp}}} = 0.6ft$
Spoiler Chord Aft of Hinge at Spoiler Inboard Station, $c_{f_{i_{el}}} = c_{f_{i_{sp}}}$	$c_{f_{i_{sp}}} = 11.4ft$
Spoiler Chord Aft of Hinge at Spoiler Inboard Station, $c_{f_{o_{el}}} = c_{f_{o_{sp}}}$	$c_{f_{o_{sp}}} = 11.4ft$
Average Spoiler Chord to Wing Chord Ratio aft of Hinge Line, $c_{el}/c_w = c_{sp}/c_w$	$c_{sp}/c_w = 43.377\%$ $c_{sp} = 0.43377 \times 39ft$ $c_{sp} = 16.917ft$
Spoiler Mean Geometric Chord, $(\bar{c})_{el} = (\bar{c})_{sp}$	$(\bar{c})_{sp} = 11.4ft$
Spoiler Planform Area, $S_{el} = S_{sp}$	$S_{sp} = 11.4 \times 18.94ft$ $S_{sp} = 216.144ft^2$

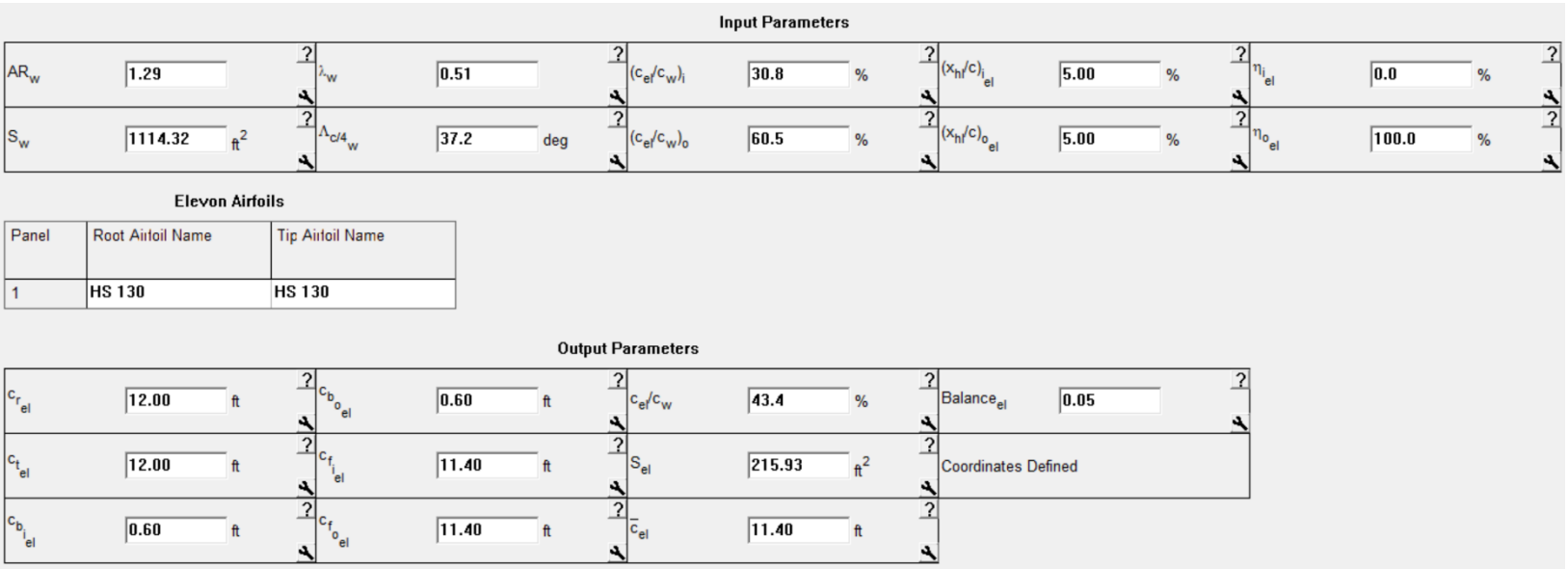

Figure 8.6. I/O parameters of wing with spoilers

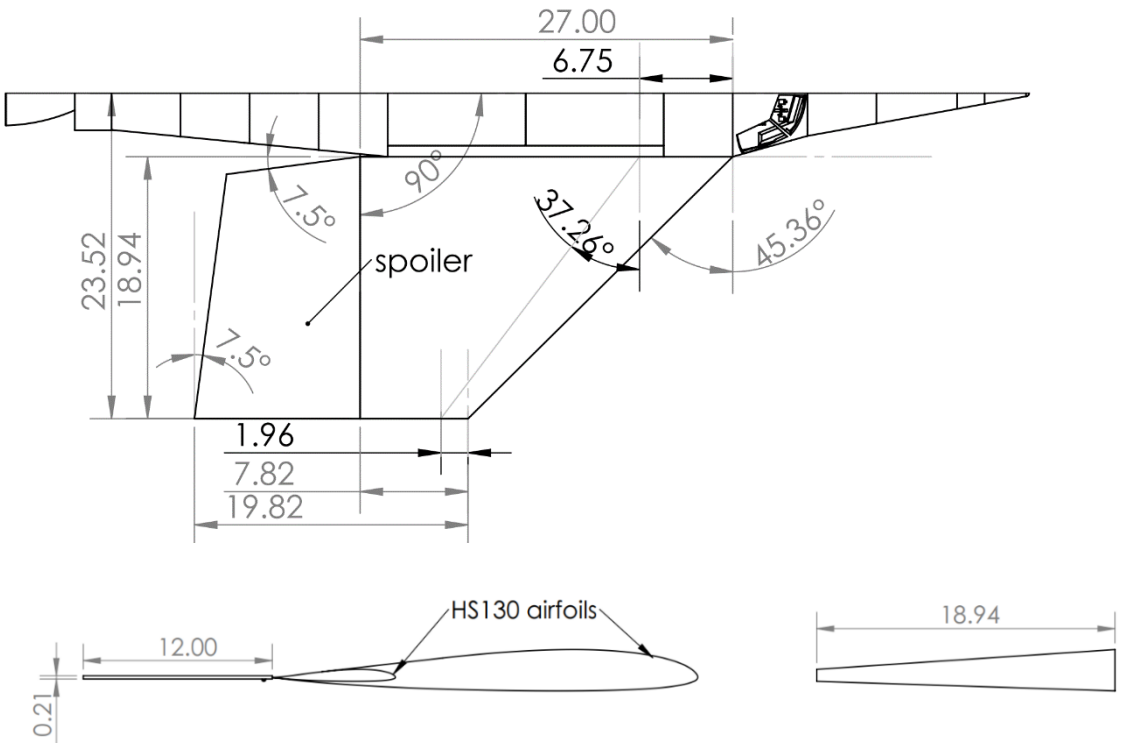

Figure 8.7. Wing-spoiler configuration dimensions

8.2.4 Function of Spoiler

The spoiler plays significant role during the re-entry phase of X-69. The configuration is demonstrated in fig. 8.8 and 8.9.

A simple example of a badminton shuttle cock can be considered to understand the working of spoiler. The shuttle cock always lands on its hard, solid surface vertically (perpendicular to the ground surface) no matter how player hits the shuttle cock. It simply lands vertically due the feathers around it that guide aerodynamically to stay vertically stable.

Similar concept is used for X-69's wing-spoiler configuration where the spoiler lifts and locks gradually up to 65^o angle directing and stabilizing X-69. It also decelerates the hypersonic speeds to subsonic speeds suitable for further glide and landing phases. X-69 will be at around -10 to -20^o angle of attack during re-entry. The ablative surface under the wing will help to tackle high temperatures and pressures. The spoiler locked at 65^o feather angle will create a wake in the air flow providing high drag slowing the vehicle to subsonic speeds.

It can be in fig. 8.6 and 8.7 the wing-spoiler configuration with spoiler at 0^o and 65^o angle with respect to horizontal plane of the wing. This configuration further adds the twin tailboom with control surfaces such as horizontal and vertical stabilizers, elevons and rudders that will be explained in empennage section.

Figure 8.8. Spoiler back at 0^o during normal flight

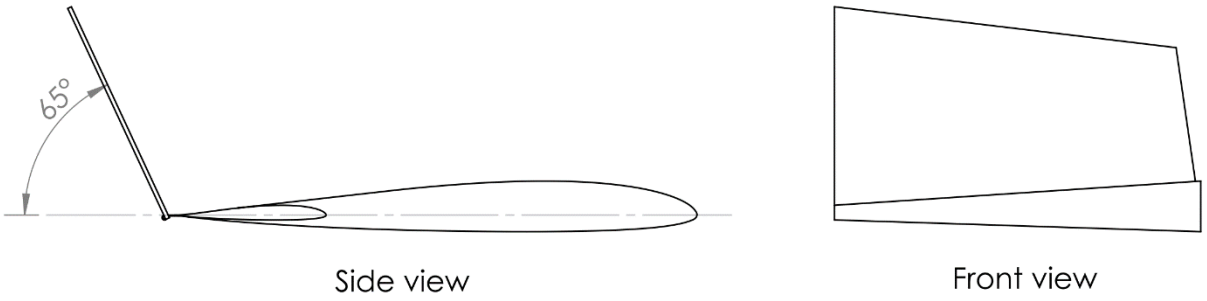

Figure 8.9. Spoiler locking at 65º angle during re-entry

Fig 8.8 shows the look of above configuration with both wings and fuselage. As mentioned earlier, the twin tailboom will be attached to tip of the wing connecting with spoiler. The twin tailboom consequently allows to accommodate for control surfaces giving the Y-location of horizontal stabilizers equal to the half of the wing space from the center of the fuselage.

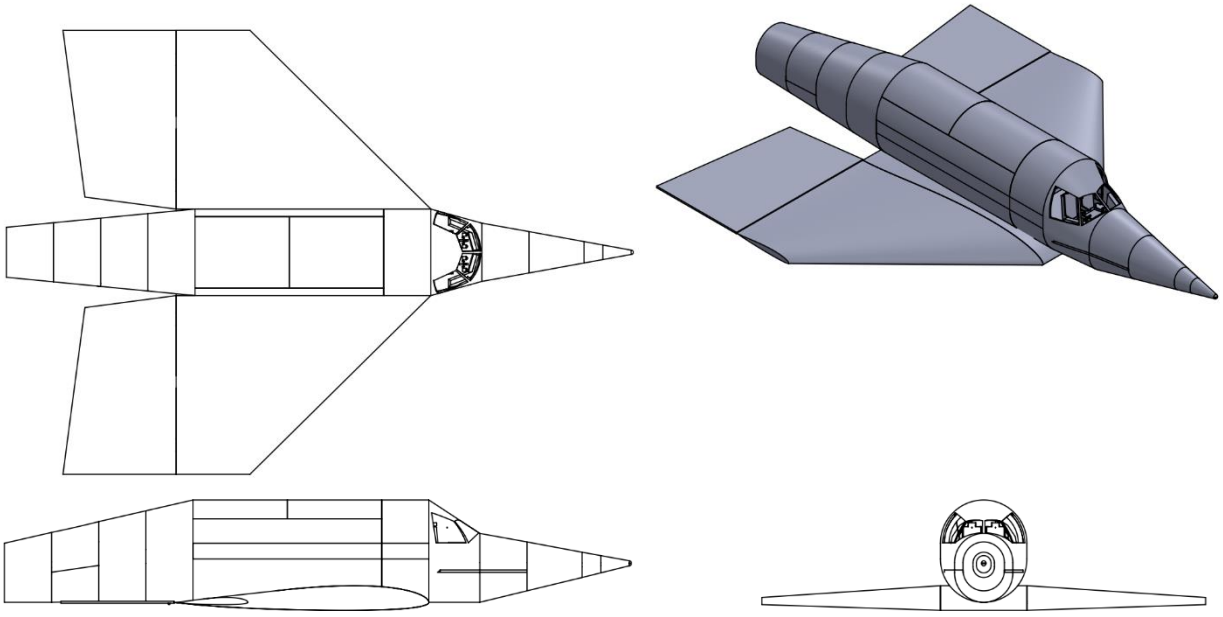

Figure 8.10. Complete configuration during normal flight

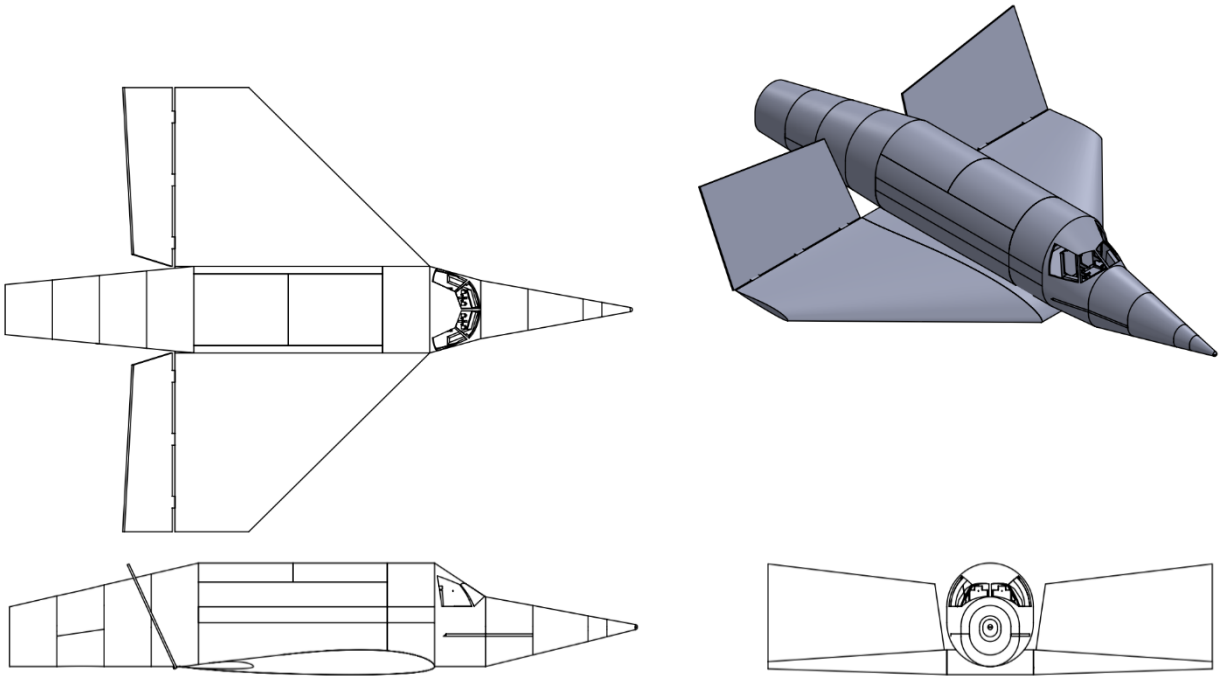

Figure 8.11. Complete configuration during re-entry in hypersonic regime

8.2.5 Airfoil selection:

The basic type of airfoil used for X-69 wing falls into slope soaring category. In this category there are many newly documented airfoils such as HS130, JWL-065, MH45 etc. MH45 delivers better speed performance but its sinking rate increases with higher wing loading and gives very poor gliding performance. Also, this airfoil is not recommended for low aspect ratio wing. JWL- 065 is mostly recommended for high aspect ratio wings, where elevator is used to rise speed. For X-69 use of elevons is crucial to maintain roll when it glides after re-entry. HS130 is well-known for very fast planks such as dynamic soaring slope soaring. X-69 will dive into earth's atmosphere at very re-entry speeds. Following fig 8.4 is the image of HS130 airfoil and its analyses from Xfoil.

From the performance point of view, the role of wing is to glide and land safely where launch and climb is solely governed by rocket motor. The lower edge of the airfoil can provide better performance during re-entry at hypersonic speeds due to better pressure distribution which can up on analysis of the airfoil.

Furthermore, XFLR5 have been used to estimate the lift, drag and glide ratio at various angle of attacks. This analysis is performed on HS130 airfoil to examine its aerodynamic performance. Fig. 8.3 shows the imported airfoil and pressure distribution at 0^o angle of attack at Mach 0 and Reynolds number 100,000.

Fig.8.6 gives the estimate of $C_{l_{max}}$ which lies between 1.0 to 1.2 at rising Reynolds number at approximately 12^o to 12.5^o angle of attack. This analysis resembles when X-69 descends from 80,000 ft of altitude.

Plots for Mach 0.2 and 0.3 can referred from Appendix C. X-69 is expected to decelerate from re-entry to approach velocity VA by the time it reaches to landing stage. This approach speed should be between 130 knots to 140 knots or 0.2 to 0.3 Mach. Hence using XFLR5 in appendix C, plots for lift and drag coefficient and angle of attack are computed which shows wing configuration still has stable aerodynamic parameters at similar Reynolds number and different speeds.

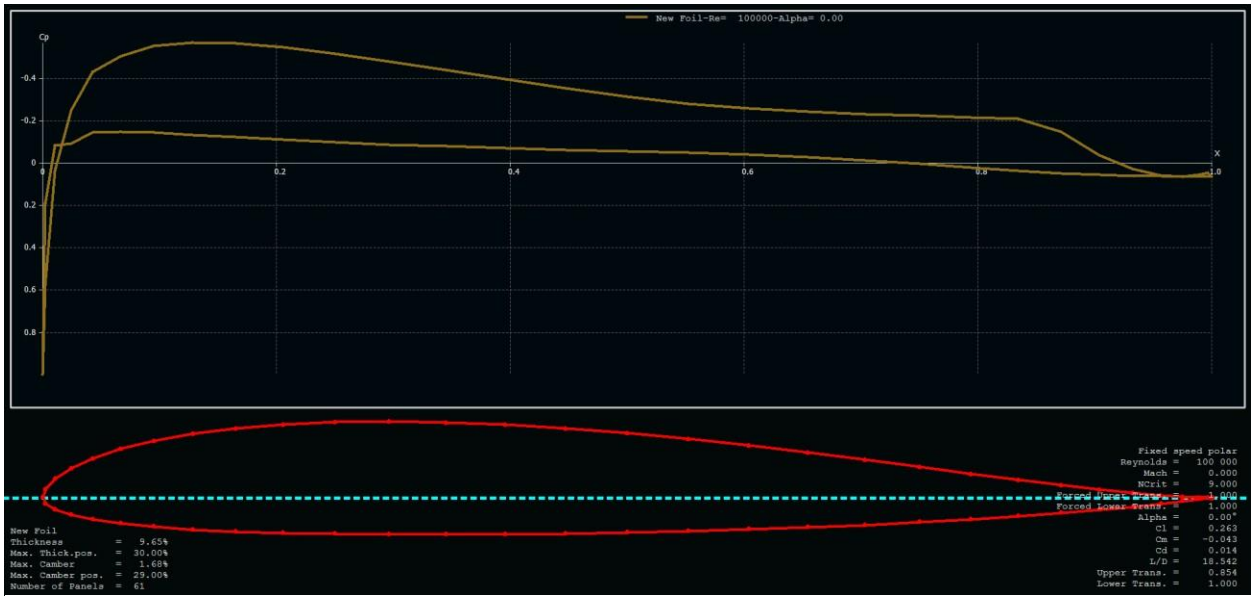

Figure 8.13. Pressure distribution on HS130 airfoil using XFLR5

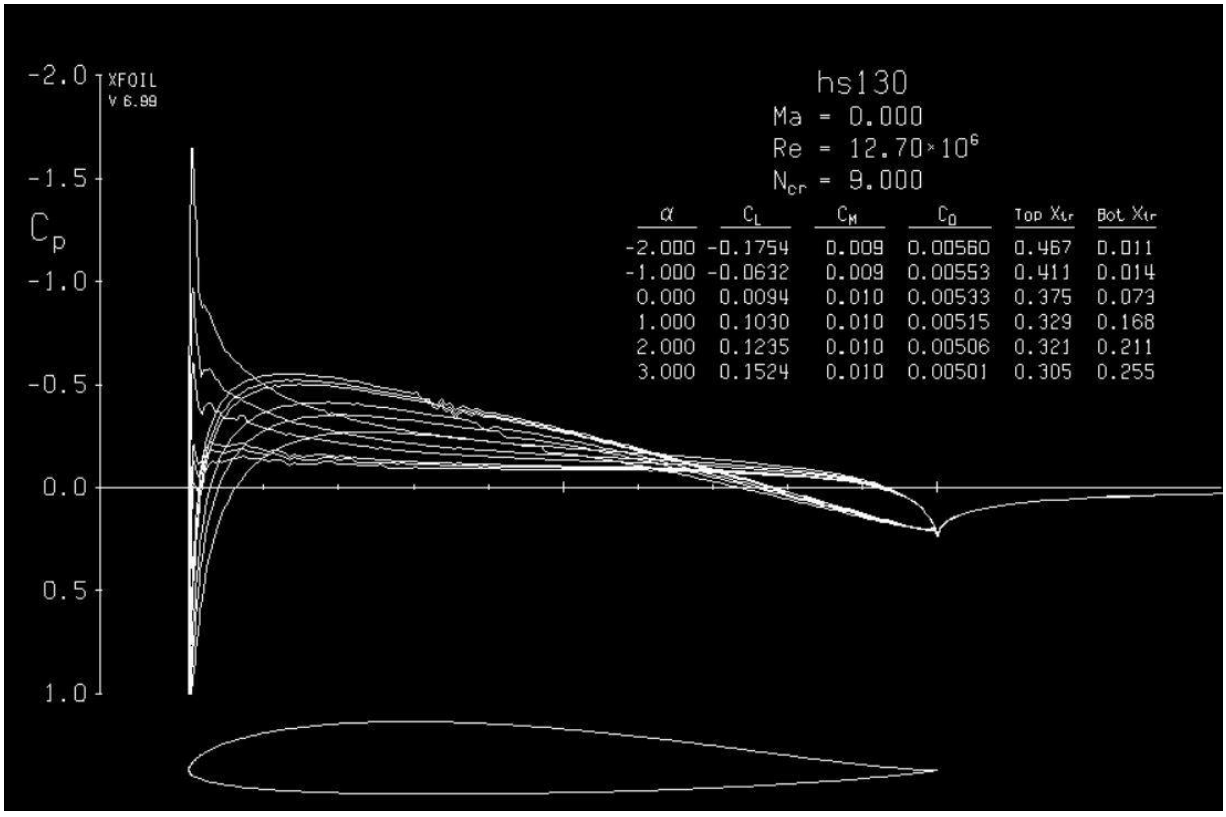

Figure 8.12. HS130 airfoil and pressure distribution at various AoA using Xfoil

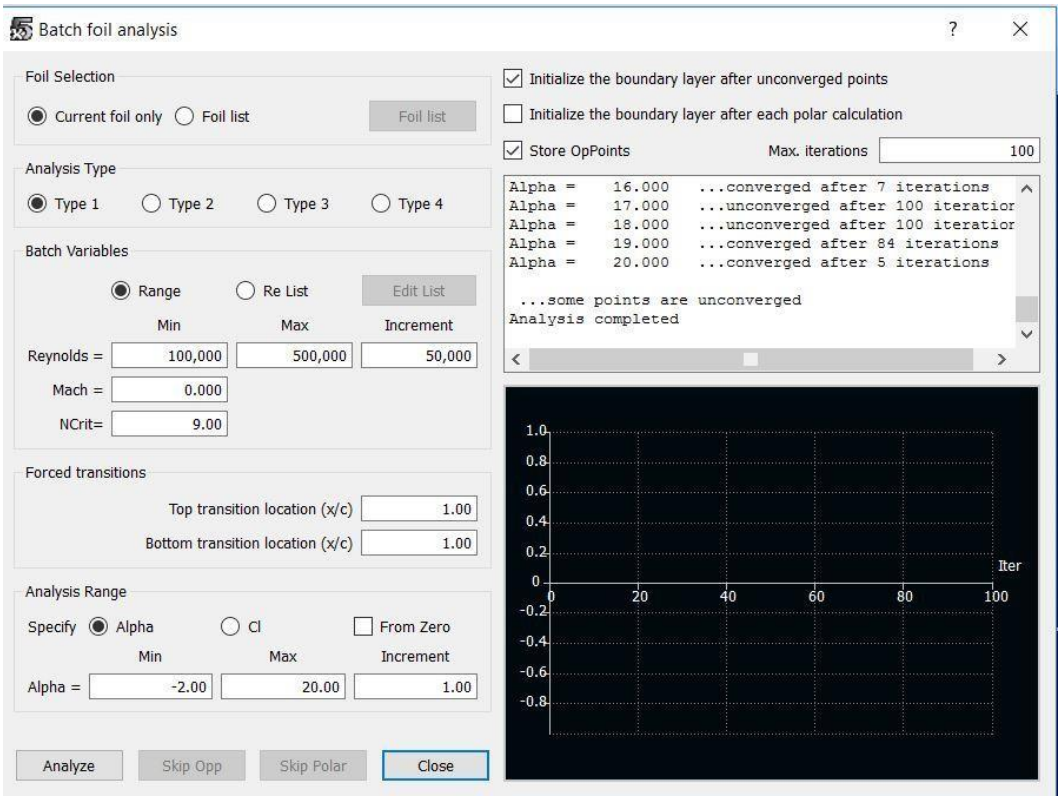

Figure 8.14. Batch analysis inputs in XFLR5 to compute aerodynamic coefficients

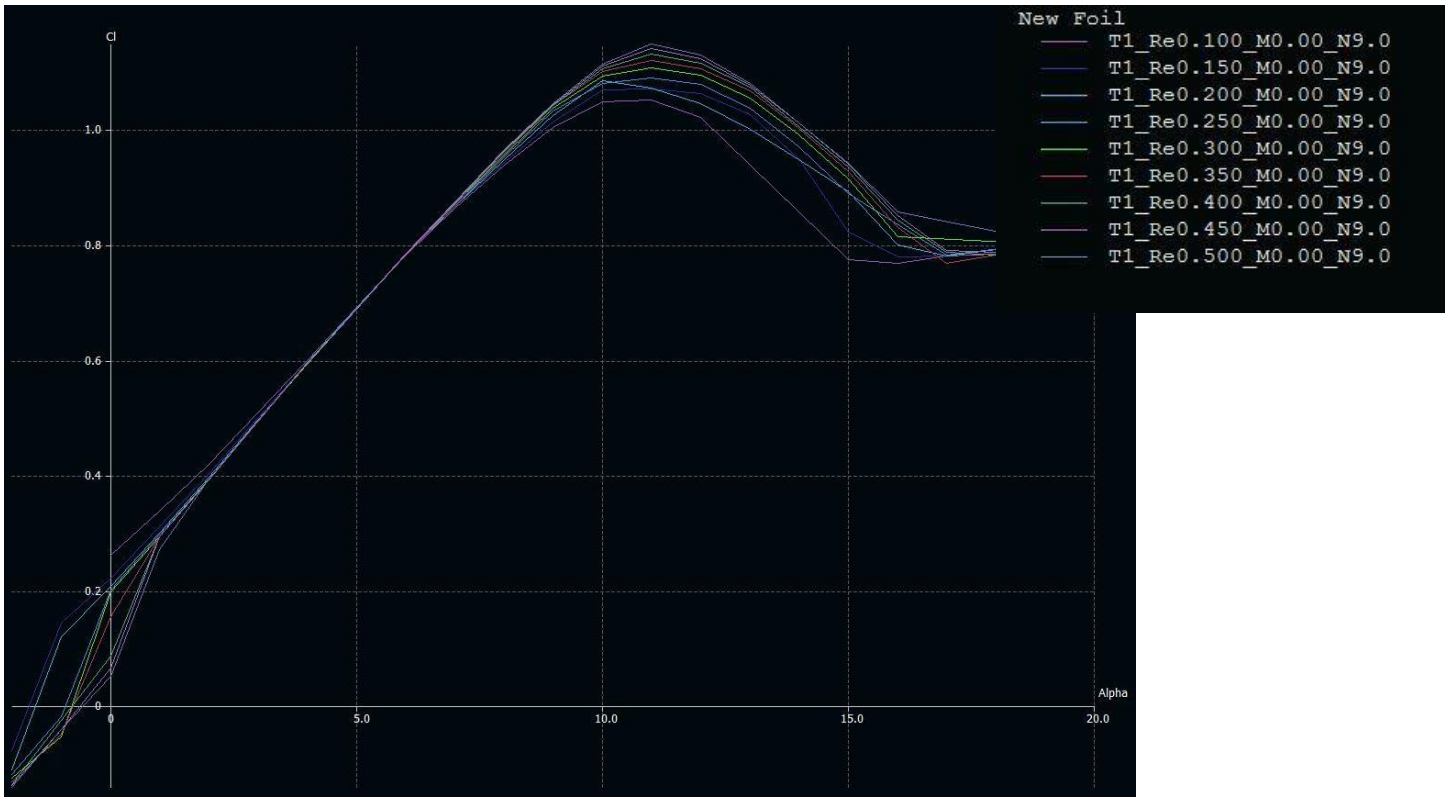

Figure 8.15. Coefficient of lift v/s AoA at various reynolds number and mach 0.0

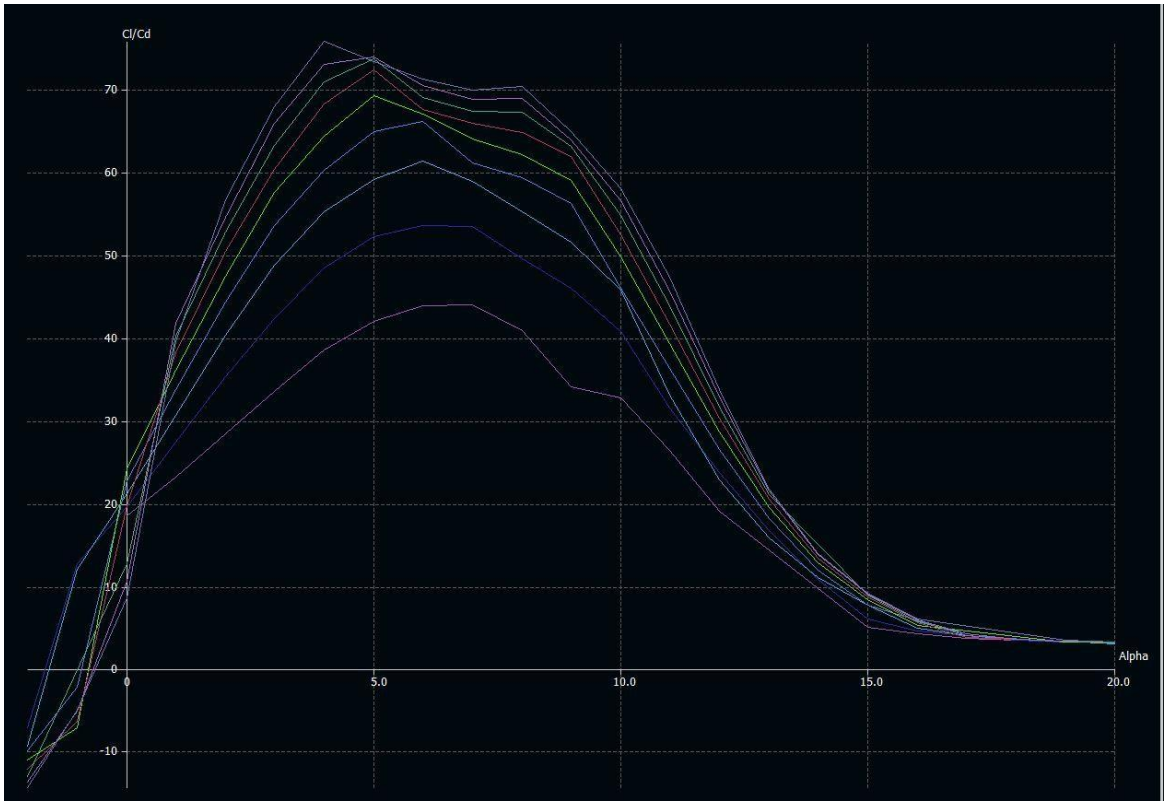

Figure 8.17. C_l/C_d (glide ratio) v/s angle of attack at similar conditions

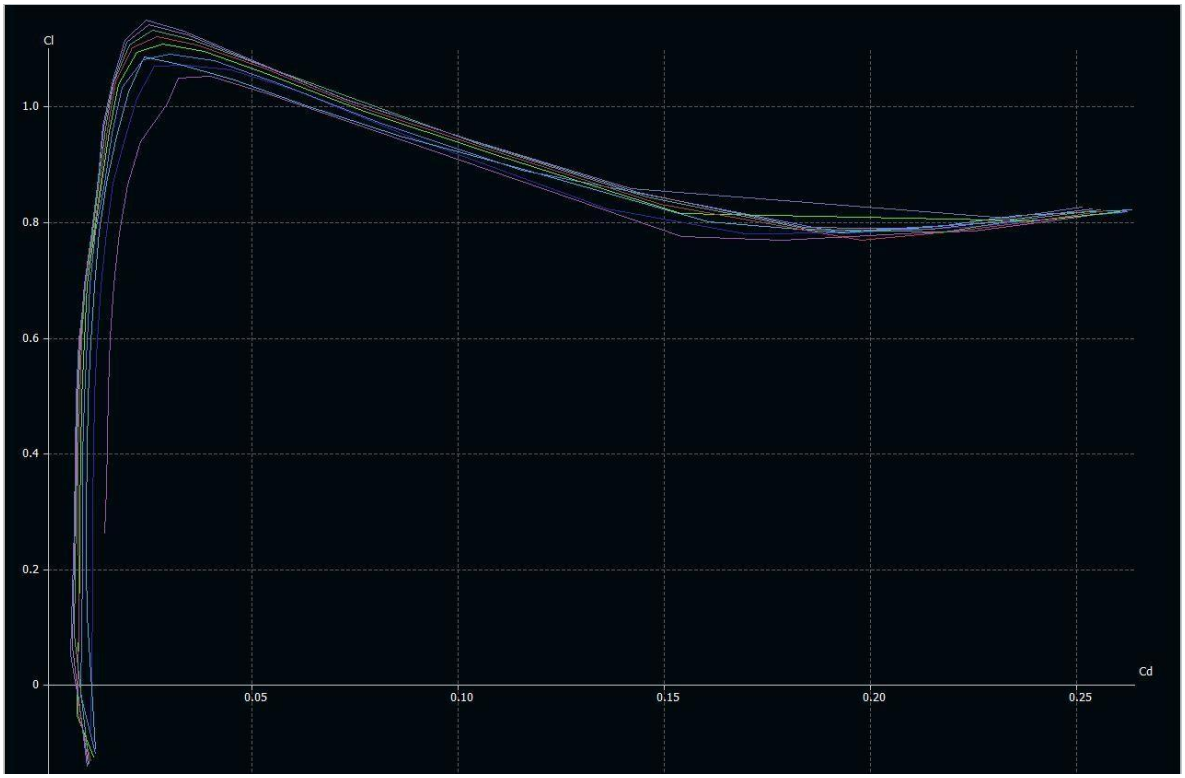

Figure 8.16. Lift v/s Drag coefficients at similar condition as above

8.2.6 Estimation of Weight of Wing:

Using USAF Method from *Roskam*, the following equation that applies to light and utility type airplanes with performance up to about 300 kts. X-69 locks back its feathers to normal position at gliding, descent and near-landing approach phase where its speed is ranges between 130 kts to 140 kts. Hence considering maximum speed, V_H = 140 kts.

$$W_W = 96.948\left[\left(\frac{W_{TO}n_{ult}}{10^5}\right)^{0.65}\left(\frac{A}{cos\Lambda_{\frac{1}{4}}}\right)^{0.57}\left(\frac{S}{100}\right)^{0.61}\left(\frac{1+\lambda}{2\left(\frac{t}{c}\right)_m}\right)^{0.36}\left(1+\frac{V_H}{500}\right)^{0.5}\right]^{0.993} \quad (8.11)$$

From the previous above data,

$$W_{TO} = 13{,}870\ lbs, n_{ult} = 7, A = 2.18, \Lambda_{\frac{1}{4}} = 37.215°, S = 1{,}114.32 ft^2\ V_H = 140 kts$$

$$W_W = 96.948\left[\left(\frac{13{,}870 \times 7}{10^5}\right)^{0.65}\left(\frac{2.18}{cos37.215}\right)^{0.57}\left(\frac{1{,}114.32}{100}\right)^{0.61}\left(\frac{1+0.29}{2\times 0.0966}\right)^{0.36}\left(1+\frac{140}{500}\right)^{0.5}\right]^{0.99:}$$

$$W_W = 1{,}614.067\ lbs$$

8.3 Design of the high-lift devices:

X-69 being a prototype at this level does not have high-lifting devices such as flaps and slats except spoilers. However, the primary function of spoiler is to create more drag during re-entry for deceleration whereas the application of regulars on any airplane is to kill the lift to stabilize the landing. Nonetheless, X-69 will be under research with the scope to improve its aerodynamics optimally using high-lifting devices. The climb is solely governed by rocket motor propulsion. Re-entry is initiated by reaction control thrusters and spoilers and lateral control surfaces for maneuvering followed by simple approach for landing. There are no flaps and slats on the wing of X-69 to enhance the lift currently.

The spoilers along with the boom configuration are locked at 65^o position with respect to longitudinal axis at re-entry altitude. When it descends and approaches to around 70,000 ft to 80,000 ft, the spoilers and the boom configurations are set back to normal position from where X- 69 glides back to land. Its mission profile is like that of SpaceShipTwo where its speed approaches to around Mach 0.5 – Mach 0.6 at altitude of 50,000 ft to 60,000 ft. While re-entry, X-69 itself is at high angle of attack to completely dominate its dorsal surface to yield drag.

8.4 Discussion:

Aerodynamic performance of X-69 depends up on various components of aircraft and mission profile. X-69 is completely different type of plane as compared to conventional airplanes considering its application, mission profile and various other factors. It is an attempt to seek for new method to fly to space and come back for re-usability.

Considering all above aspects, the design of X-69 aerodynamics relies on wing, spoilers, horizontal stabilizers and elevons. To study wing design, theories from *Roskam* are followed to estimate wing sizing, aerodynamic capabilities. Although other than wing, elevons, stabs and spoilers play a very vital role to

make X-69 complete the mission. This report limits to the estimation of design of wing only. Although attempts will be made to estimate parameters of spoilers, elevons and stabs based on their functions.

Ultimately, the purpose of spoiler is to create optimum amount of drag enhancing the deceleration generated by lower surface of aircraft while re-entry. This drag makes aircraft unstable hence twin- tail boom consisting of elevons and stabs helps it stabilize perturbed motion of X-69 due to drag.

8.5 Conclusions:

The basic parametric wing design is presented in this report. This defines the preliminary layout of wing. Although it is keenly desired to do CFD on the wing to understand climb and gliding performance. X-69 does not contain flaps and slats while landing. Spoiler solely governs the approach speed that results into precise landing. The roll is governed by elevons mounted on horizontal tail.

Spanwise distribution of lift on wing at 5° AoA and Mach 0.485 can be seen in fig. 8.17. This lift distribution is when the spoiler is not locked at feather-lock position at 0° to the X-axis.

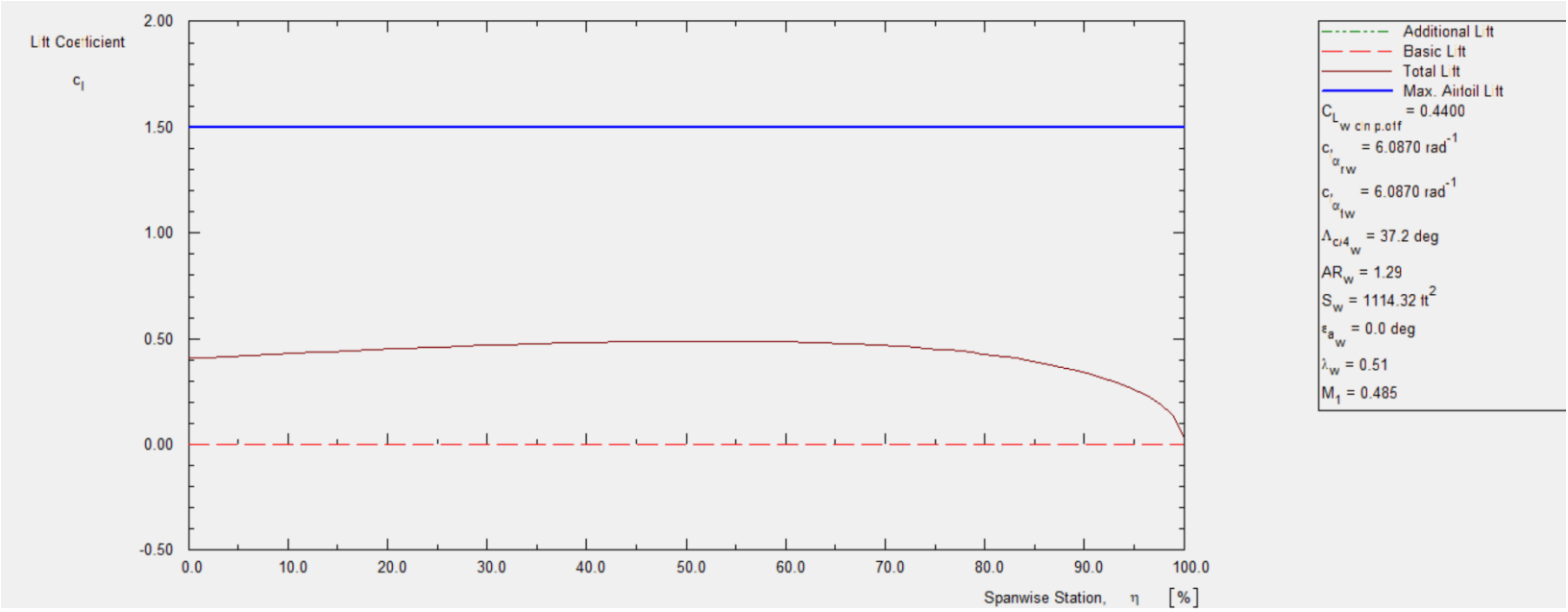

Figure 8.18. Spanwise lift distribution

9. Chapter 9. Empennage Layout Design

9.1 Introduction:

This section evaluates the empennage layout, components included in the empennage and their sizing and their functions during the flight of X-69. Since X-69's overall return phase that includes re-entry, glide, descent and landing are un-powered, the flight demands the stability in its dynamics. At the same time, it is also important to keep the design X-69 compact, good looking and aesthetically efficient. Therefore, following components and prospective design might fulfill the requirements:

The major components of empennage are:

1) Horizontal Stabilizers (also called as stabilators)
2) Elevons (function like elevators)
3) Vertical Stabilizers
4) Rudders
5) Twin Tailboom
6) Fin (optional)

The basic layout of empennage of X-69 is extended section longitudinally with the help of twin tailboom attached at the tip end of the spoilers. The vertical stabilizers are attached along the tailboom whereas the horizontal stabilizers are attached outwards. The twin boom gives optimal lateral stability will smooth rolling capabilities. Since the boom is attached to the spoiler, the complete configuration lifts to 65° locking position during hypersonic re-entry which will illustrated further in details. The layout also features an optional component, called fin attached on twin boom against the horizontal stabilizer inwards.

Following sections discusses the design of each component in details:

9.2 Horizontal Tail

Design parameters are obtained using various tools such as AAA and Solid Works. Considering the overall layout of the horizontal tail, basic input parameters are as follows:

Table 9.1. Input parameters for horizontal tail

Parameters	Quantity
Horizontal tail span, b_h	67 ft
Horizontal tail root chord length, c_{r_h}	8.00 ft
Horizontal tail tip chord length, c_{t_h}	2.23 ft
Horizontal tail quarter-chord sweep angle, $\Lambda_{(c/4)_h}$	23.4721°
X-coordinate of Horizontal tail apex, X_{apex_h}	85 ft
Y-coordinate of the equivalent horizontal tail root chord offset from centerline, Y_{off_h}	23.5283 ft

The above input parameters are obtained from SolidWorks giving the layout estimate of the horizontal tail. The layout diagram is shown in fig. 9.1.

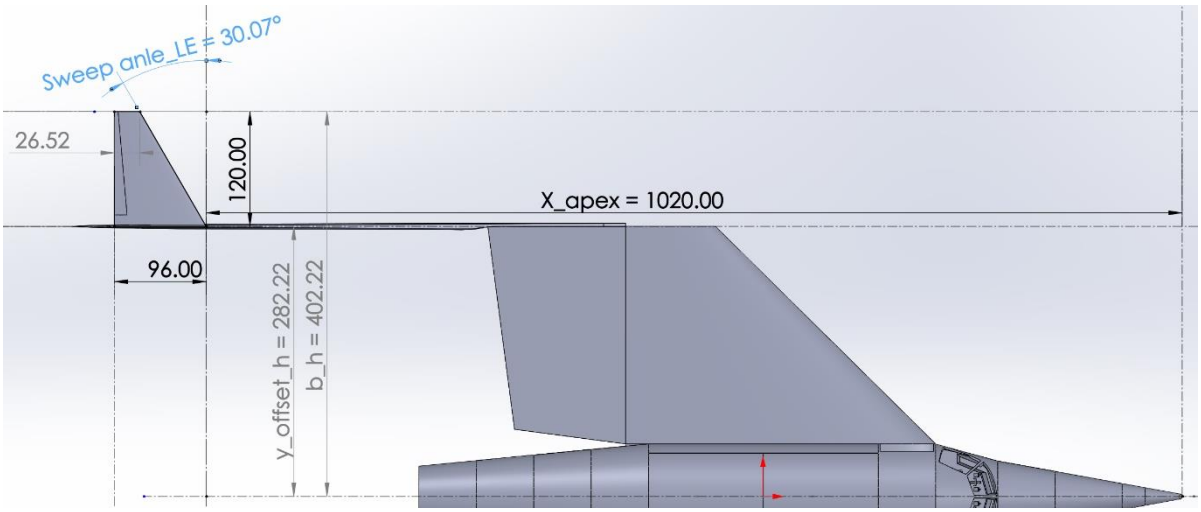

Figure 9.1. Horizontal tail input layout estimate in inches

Output parameters yielded by AAA are as follows in the table 9.2:

Table 9.2. Output parameters of horizontal tails

Parameters	Quantity
Horizontal tail span area, S_h	101.98 ft^2
Horizontal tail Aspect ratio, AR_h	3.90
Horizontal taper ratio, λ_h	0.28
Horizontal tail mean (geometric) aerodynamic chord (MAC or MGC), $\bar{c}_h$	5.656 ft
Y-distance between the Horizontal tail apex and Horizontal tail mean (geometric) aerodynamic chord, y_{mgc_h} or y_{mac_h}	4.048 ft
X-distance between the Horizontal tail apex and Horizontal tail MGC, x_{mgc_h}	2.34 ft
Leading edge Sweep Angle, Λ_{LE_h}	30.07833°
Trailing edge sweep angle, Λ_{TE_h}	0.0°

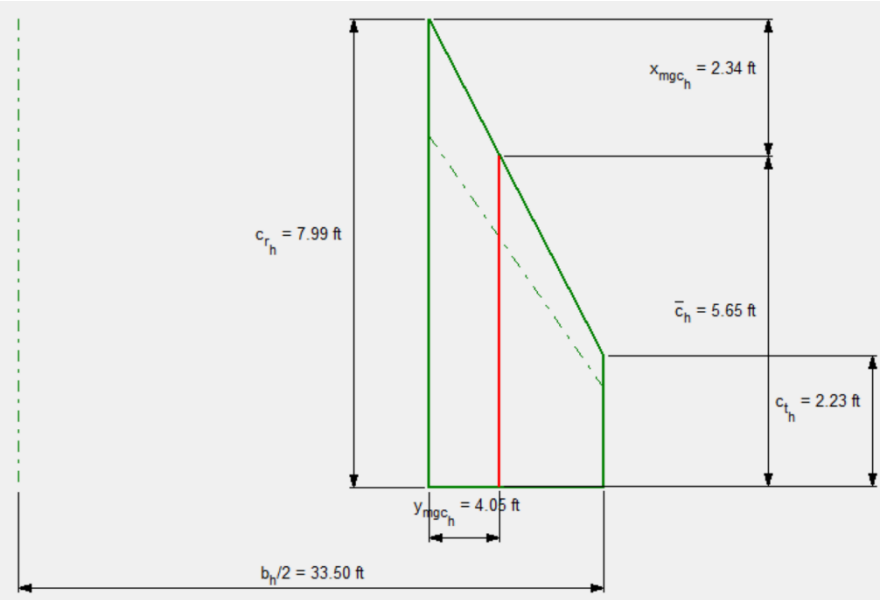

Figure 9.2. Output parameters plot horizontal tail

The trailing edge of the tail is intentionally kept perpendicular to the fuselage to keep the design easy for dynamics and hence for the manufacturing. Furthermore, the straightness at the trailing edge can provide smooth movement for the elevons as described below:

9.3 Elevons (Elevators)

Elevons can be used to control the longitudinal and lateral stability of X-69. Their function is combination of ailerons and elevators, hence the "Elevons". The design input for elevons are follows:

Table 9.3. Input parameters for elevator and elevator tab design

Parameters	Quantity
Horizontal tail Aspect ratio, AR_h	3.90
Horizontal tail span area, S_h	101.98 ft^2
Horizontal taper ratio, λ_h	0.28
Horizontal tail quarter-chord sweep angle, $\Lambda_{(c/4)_h}$	23.4721^o
Inboard station elevator chord length to horizontal tail chord, $(c_e/c_h)_i$	15 %, $c_{e_i} = 0.15 \times c_{h_i}$ $c_{e_i} = 0.15 \times 8$ $c_{e_i} = 1.2ft$
Outboard station elevator chord length to horizontal tail chord, $(c_e/c_h)_o$	15%, $c_{e_O} = 0.15 \times c_{h_o}$ $c_{e_o} = 0.15 \times 2.23$ $c_{e_o} = 0.3345ft$
Elevator root inboard hingeline location, $(x_{hl}/c)_{i_e}$	10%, $x_{hl_{i_e}} = 0.1 \times c_{e_i}$ $x_{hl_{i_e}} = 0.1 \times 1.2ft$ $x_{hl_{i_e}} = 0.12ft$
Elevator tip outboard hingeline location, $(x_{hl}/c)_{o_e}$	10%, $x_{hl_{o_e}} = 0.1 \times c_{e_o}$ $x_{hl_{o_e}} = 0.1 \times 0.3345$ $x_{hl_{o_e}} = 0.03345ft$
Elevator inboard station in terms of H.T. half span, η_{i_e}	10%, $y_{i_e} = 0.1 \times (b_h/2)$ $y_{i_e} = 0.1 \times 67/2$ $y_{i_e} = 3.35ft$
Elevator outboard station in terms of H.T half span, η_{o_e}	100%, $y_{o_e} = 1 \times b_h/2$ $y_{o_e} = 33.5ft$
Elevator tab inboard station in terms of H.T half span, $\eta_{i_{et}}$	15%, $y_{i_{et}} = 0.15 \times (b_h/2)$ $y_{i_{et}} = 0.15 \times 67/2$ $y_{i_{et}} = 5.025ft$
Elevator tab outboard station in terms of H.T half span, $\eta_{o_{et}}$	85%, $y_{o_{et}} = 0.85 \times (b_h/2)$ $y_{o_{et}} = 0.85 \times (67/2)$ $y_{o_{et}} = 28.475ft$

Parameters	Quantity
Average elevator tab chord, c_{et}	30%, $c_{et} = 0.3 \times c_e$ $c_{et} = 0.3 \times (c_{e_i} + c_{e_o})/2$ $c_{et} = 0.3 \times (1.2 + 0.3345)/2$ $c_{et} = 0.23ft$
Average elevator tab aft chord, $c_{r_{et}}$	20%, $c_{r_{et}} = 0.2 \times 0.23$ $c_{r_{et}} = 0.046ft$

The above parametric significance can be referred in pictorial representation from fig 9.3. The fig shows X and Y location of elevator and hingeline. The elevator chord lengths are defined in percentage of the horizontal tail that includes taper ratio in terms of inboard and outboard station.
where, in our case, taper ratio for elevator becomes $\lambda_e = 0.3345/1.2 = 0.2787$
Similarly, X-location of elevator inboard and outboard are $x_{hl_{i_e}} = 0.12ft$ and $x_{hl_{o_e}} = 0.03345ft$ respectively.

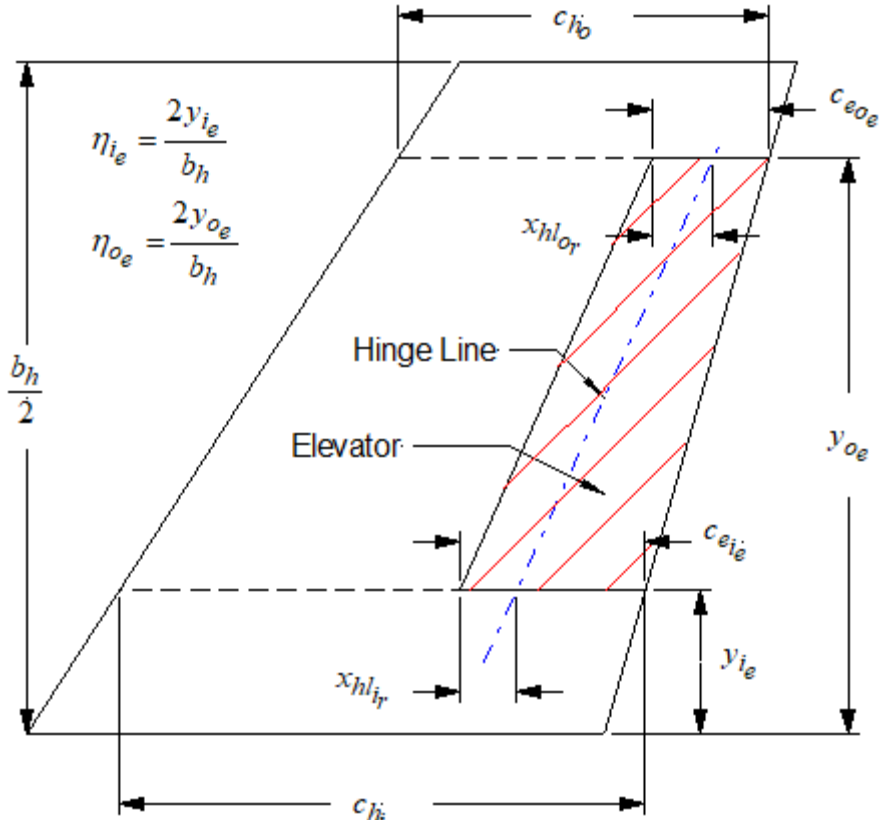

Figure 9.3. Definition of elevator parameters

The airfoils used for horizontal tail are NACA 64-206 both at the root and the tip. The airfoil is thin, uniform, that makes it a fit candidate for horizontal application.
Parameters for elevator tabs are referred from AAA theory represented in fig. 9.5. The root chord length of elevator tab, $c_{et} = 0.23ft$ tapering outwards at the ratio of 0.3.

Figure 9.4. NACA 64-206 airfoil used for horizontal stabilizer

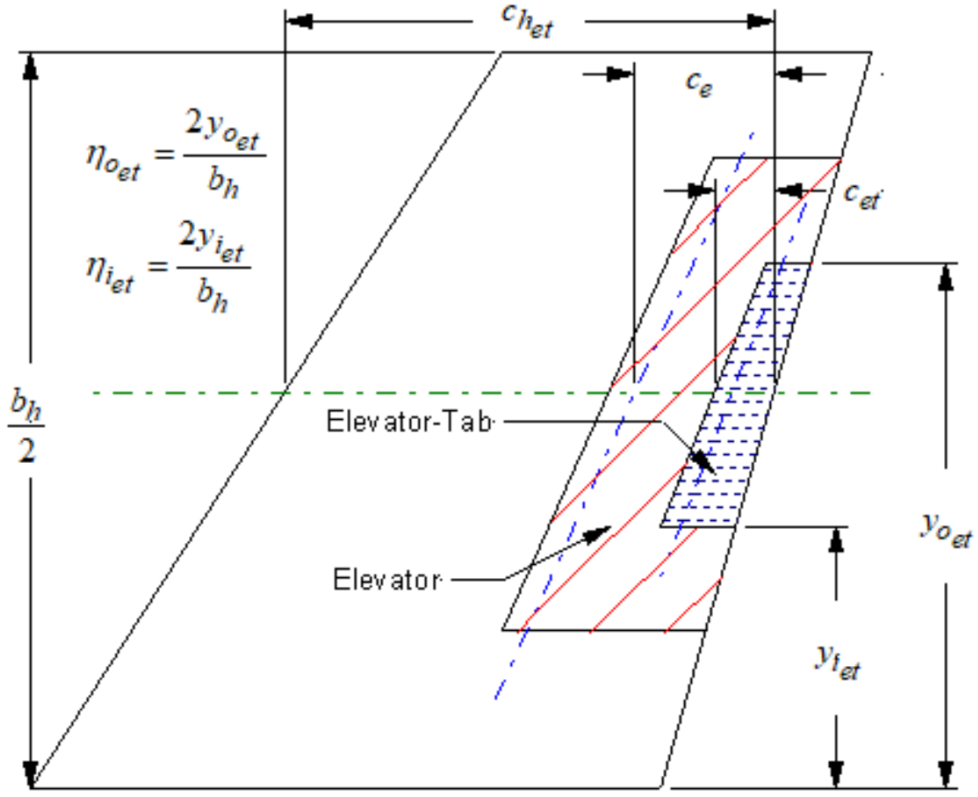

Figure 9.5. Definition of elevator tab parameters

Input Parameters

AR_h	3.90	$\Lambda_{c/4_h}$	23.5	deg	$(x_{hf}/c)_{i_e}$	10.00	%	η_{o_e}	100.0	%	c_{et}/c_e	30.0	%
S_h	101.98	ft^2	$(c_e/c_h)_i$	15.0	%	$(x_{hf}/c)_{o_e}$	10.00	%	$\eta_{i_{et}}$	15.0	%	$(c_f/c)_{et}$	20.0	%
λ_h	0.28		$(c_e/c_h)_o$	15.0	%	η_{i_e}	10.0	%	$\eta_{o_{et}}$	85.0	%			

Elevator Airfoils

Panel	Root Airfoil Name	Tip Airfoil Name
1	NACA 64-206	NACA 64-206

Figure 9.6. Input parameters for horizontal tail

Output parameters of Horizontal tail are as follows:

Table 9.4. Output parameters of horizontal tail

Parameters	Quantity
Elevator root chord length, c_{r_e}	1.11 ft
Elevator tip chord length, c_{t_e}	0.33 ft
Elevator Chord Forward of Hinge at Elevator Inboard Station, $c_{b_{i_e}}$	0.11134 ft
Elevator Chord Forward of Hinge at Elevator Outboard Station, $c_{b_{o_e}}$	0.0334 ft
Elevator Chord Aft of Hinge at Elevator Inboard Station, $c_{f_{i_e}}$	1.0021 ft
Elevator Chord Aft of Hinge at Elevator Outboard Station, $c_{f_{o_e}}$	0.3006 ft
Average Elevator Chord to H.T Chord ratio aft of Hingeline, c_e/c_h	13.5%
Elevator Planform Area, S_e	11.69 ft^2
Elevator MAC, $\bar{c}_e$	0.7397 ft
Elevator Balance based on Control Surface Area Forward and Aft of Hingeline, $Balance_e$	0.111

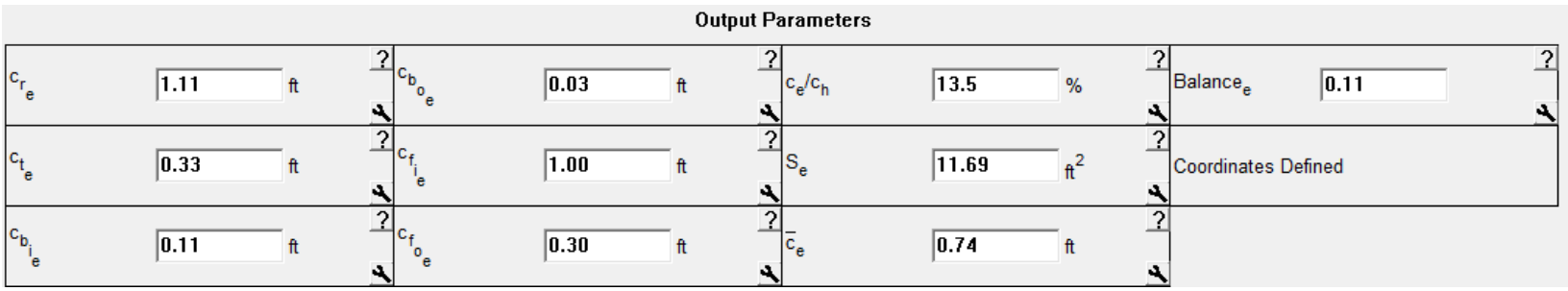

Figure 9.7. Output parameters of horizontal tail

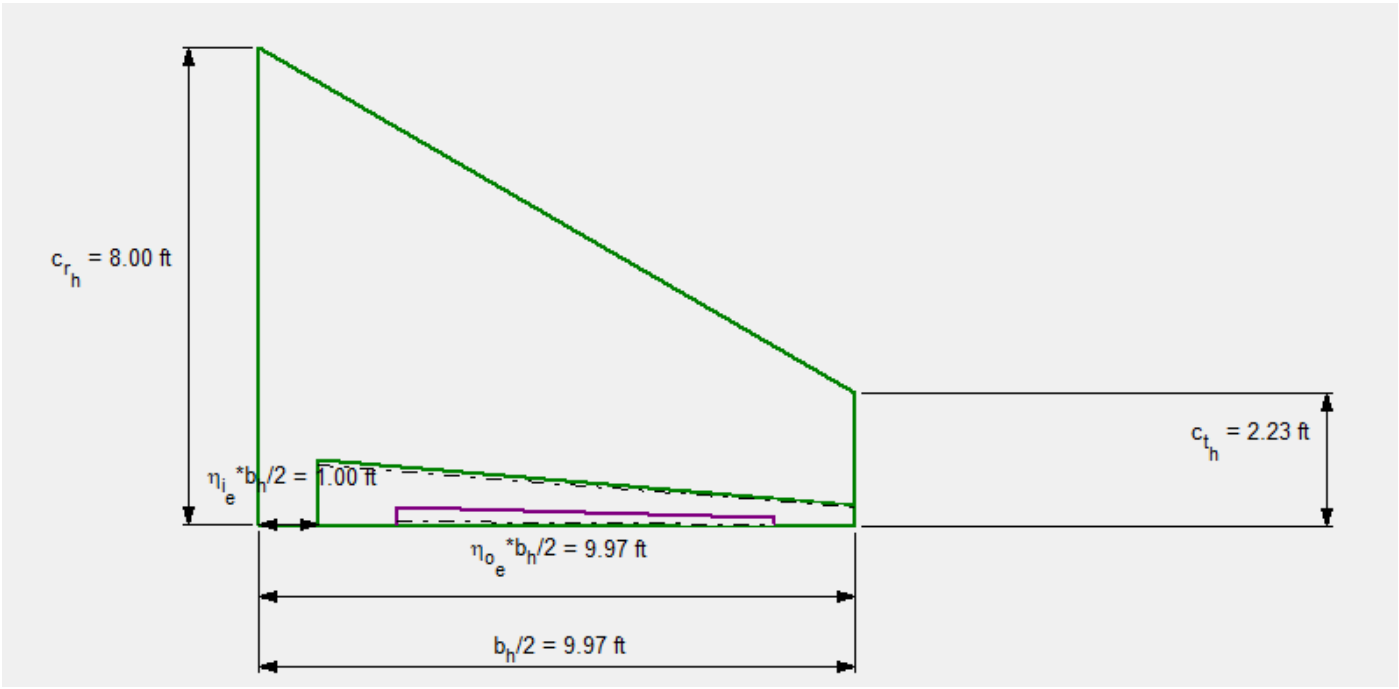

Figure 9.8. Horizontal tail plotted used AAA output parameters

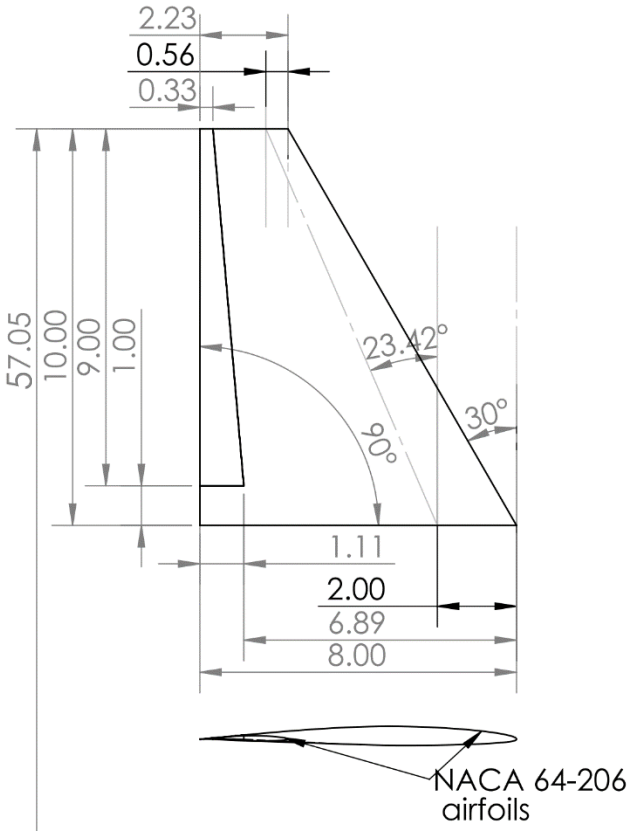

Figure 9.9. All dimensions of horizontal tail in one plot in ft.

9.4 Vertical Tail

Design parameters are obtained using various tools such as AAA and Solid Works. Considering the overall layout of the vertical tail, basic input parameters are as follows:

Table 9.5. Input parameters for vertical tail

Parameters	Quantity
Vertical tail span, b_v	6.67 ft
Vertical tail root chord length, c_{r_v}	6.67 ft
Vertical tail tip chord length, c_{t_v}	3.33 ft
Vertical tail quarter-chord sweep angle, $\Lambda_{(c/4)_v}$	40.00°
X-coordinate of Vertical tail apex, X_{apex_v}	86.89 ft
Z-coordinate of the equivalent Vertical tail root chord offset from centerline, Z_{apex_v}	5.00 ft

The above input parameters are obtained from SolidWorks giving the layout estimate of the Vertical tail. The layout diagram is shown in fig. 9.10.

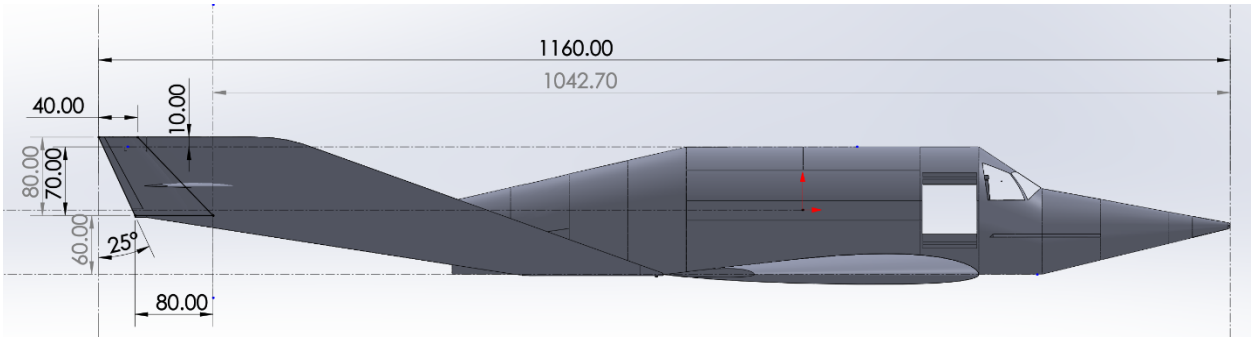

Figure 9.10. Vertical tail layout estimate in inches

Output parameters yielded by AAA are as follows in the table 9.6:

Table 9.6. Output parameters for vertical tail

Parameters	Quantity
Vertical tail span area, S_v	33.33 ft^2
Vertical tail Aspect ratio, AR_v	1.33
Vertical taper ratio, λ_v	0.5
Vertical tail mean (geometric) aerodynamic chord (MAC or MGC), $\bar{c}_v$	5.19 ft
Y-distance between the Vertical tail apex and Vertical tail mean (geometric) aerodynamic chord, z_{mgc_v} or z_{mac_v}	2.96 ft
X-distance between the Vertical tail apex and Vertical tail MGC, x_{mgc_v}	2.42 ft
Leading edge Sweep Angle, Λ_{LE_v}	44.02°
Trailing edge sweep angle, Λ_{TE_v}	24.95°

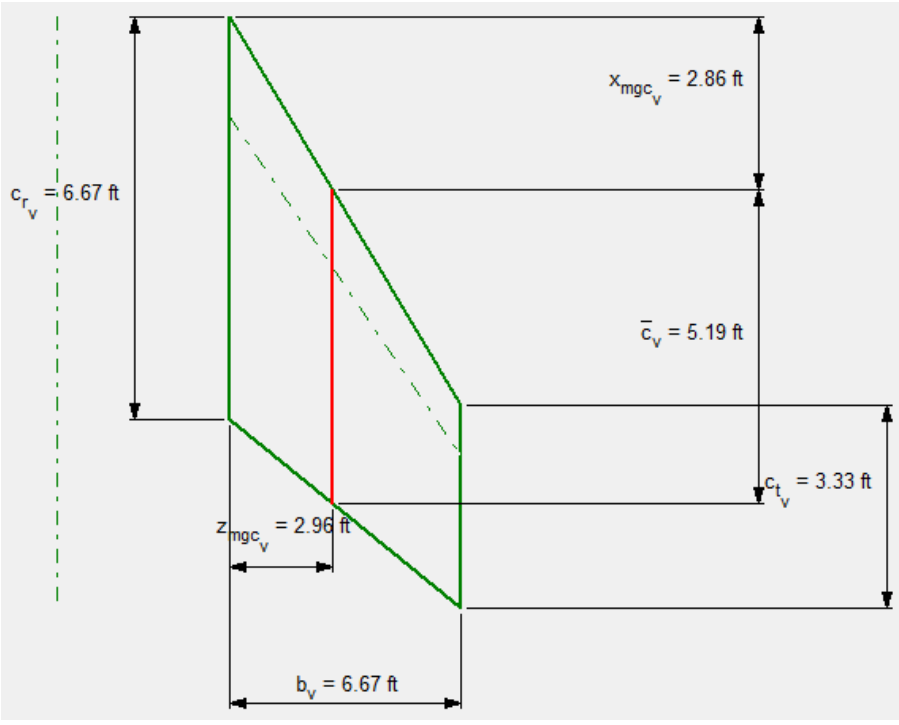

Figure 9.11. Output parameters plot for vertical tail

9.5 Rudders

Rudders can used to control lateral and directional stability. They assist to achieve smooth yawing and rolling when accompanied with wing. The design input for rudders are as follows:

Table 9.7. Input parameters for rudder and rudder tab design

Parameters	Quantity
Vertical tail Aspect ratio, AR_v	1.33
Vertical tail span area, S_v	33.33 ft^2
Vertical taper ratio, λ_v	0.5
Vertical tail quarter-chord sweep angle, $\Lambda_{(c/4)_v}$	40.00^o
Inboard station elevator chord length to Vertical tail chord, $(c_r/c_v)_i$	15 %, $c_{r_i} = 0.15 \times c_{v_i}$ $c_{r_i} = 0.15 \times 6.67$ $c_{r_i} = 1.0005ft$
Outboard station elevator chord length to Vertical tail chord, $(c_r/c_v)_o$	15%, $c_{r_O} = 0.15 \times c_{v_o}$ $c_{r_o} = 0.15 \times 3.33$ $c_{r_o} = 0.4995ft$
Elevator root inboard hingeline location, $(x_{hl}/c)_{i_r}$	10%, $x_{hl_{i_r}} = 0.1 \times c_{r_i}$ $x_{hl_{i_r}} = 0.1 \times 1.0005ft$ $x_{hl_{i_r}} = 0.1ft$
Elevator tip outboard hingeline location, $(x_{hl}/c)_{o_r}$	10%, $x_{hl_{o_r}} = 0.1 \times c_{r_o}$ $x_{hl_{o_r}} = 0.1 \times 0.4995$ $x_{hl_{o_r}} = 0.04995ft$
Elevator inboard station in terms of V.T. half span, η_{i_r}	10%, $y_{i_r} = 0.1 \times (b_v/2)$ $y_{i_r} = 0.1 \times 6.67/2$ $y_{i_r} = 0.335ft$
Elevator outboard station in terms of V.T half span, η_{o_r}	100%, $y_{o_r} = 1 \times b_v/2$ $y_{o_r} = 3.35ft$
Elevator tab inboard station in terms of V.T half span, $\eta_{i_{rt}}$	15%, $y_{i_{rt}} = 0.15 \times (b_v/2)$ $y_{i_{rt}} = 0.15 \times 6.67/2$ $y_{i_{rt}} = 0.50025ft$
Elevator tab outboard station in terms of V.T half span, $\eta_{o_{rt}}$	85%, $y_{o_{rt}} = 0.85 \times (b_v/2)$ $y_{o_{rt}} = 0.85 \times (6.67/2)$ $y_{o_{rt}} = 2.83475ft$
Average rudder tab chord, c_{rt}	30%, $c_{rt} = 0.3 \times c_r$ $c_{rt} = 0.3 \times (c_{r_i} + c_{r_o})/2$ $c_{rt} = 0.3 \times (1 + 0.5)/2$ $c_{rt} = 0.225ft$

Parameters	Quantity
Average rudder tab aft chord, $c_{r_{rt}}$	20%, $c_{r_{rt}} = 0.2 \times 0.225$ $c_{r_{rt}} = 0.045ft$

The above parametric significance can be referred in pictorial representation from fig 9.3. The fig shows X and Y location of elevator and hingeline. The elevator chord lengths are defined in percentage of the horizontal tail that includes taper ratio in terms of inboard and outboard station.
where, in our case, taper ratio for elevator becomes $\lambda_e = 0.3345/1.2 = 0.2787$
Similarly, X-location of elevator inboard and outboard are $x_{hl_{i_e}} = 0.12ft$ and $x_{hl_{o_e}} = 0.03345ft$ respectively.

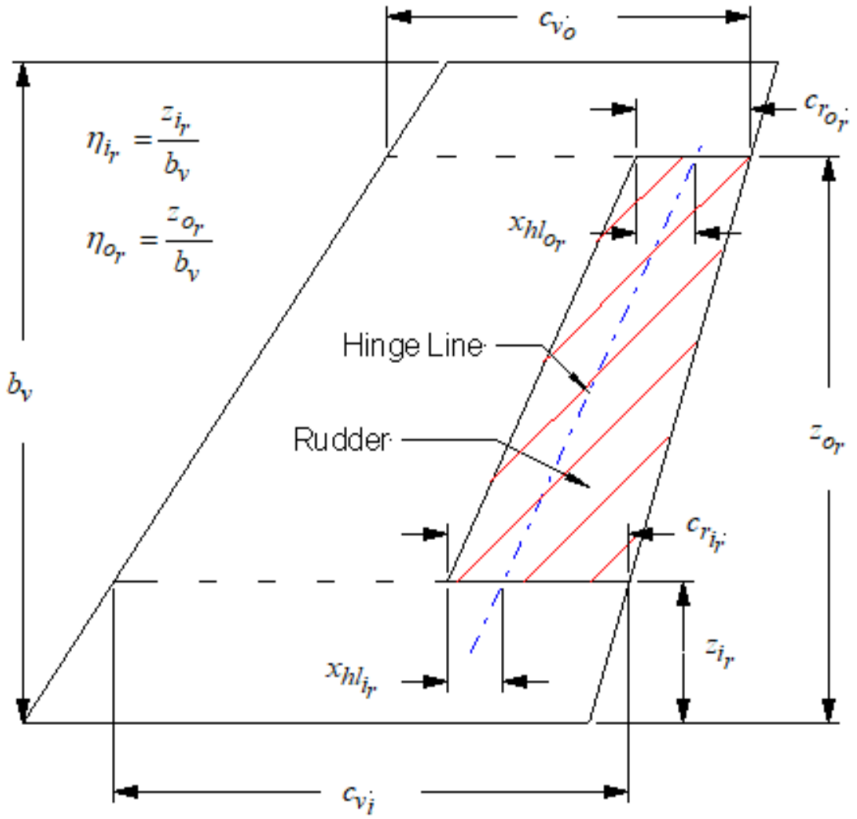

Figure 9.12 Definition of rudder parameters

The airfoils used for horizontal tail are NACA 0006 both at the root and the tip. The airfoil is thinner than NACA 64-206 that can accommodate well in the twin boom, uniform, that makes it a fit candidate for vertical tail application.
Parameters for elevator tabs are referred from AAA theory represented in fig. 9.14. The root chord length of elevator tab, $c_{rt} = 0.225ft$ tapering outwards at the ratio of 0.3.

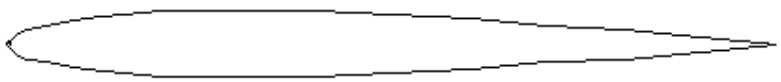

Figure 9.13 NACA 0006 airfoil used for vertical tail

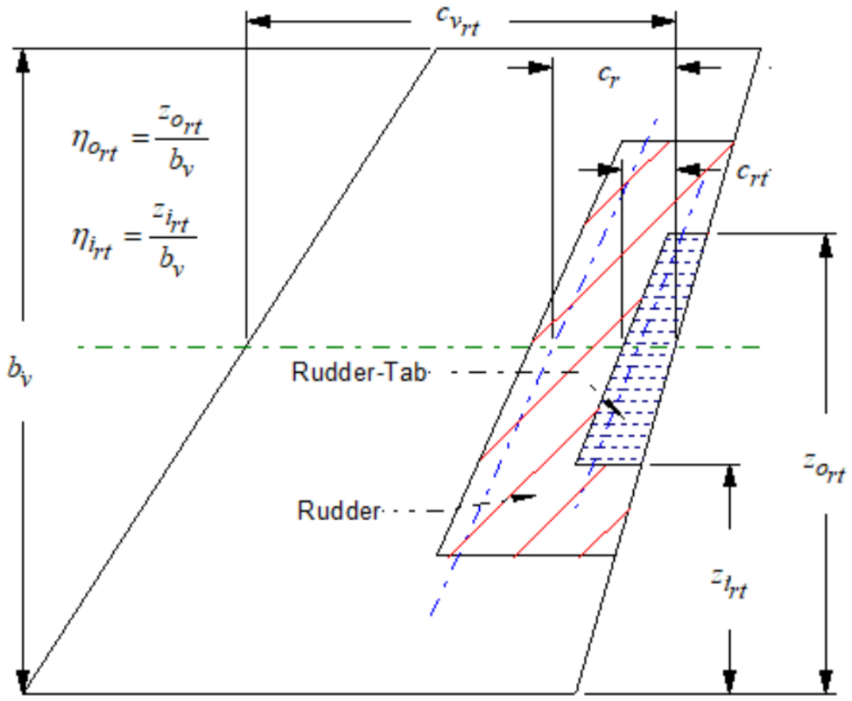

Figure 9.14. Definition of rudder tab parameters

Input Parameters

AR_v	1.33	$\Lambda_{c/4_v}$	40.0	deg	$(x_{hl}/c)_{i_r}$	10.00	%	η_{o_r}	100.0	%	c_{rt}/c_r	30.0	%
S_v	33.33	ft^2	$(c_r/c_v)_i$	15.0	%	$(x_{hl}/c)_{o_r}$	10.00	%	$\eta_{i_{rt}}$	15	%	$(c_f/c)_{rt}$	20.0	%
λ_v	0.50		$(c_r/c_v)_o$	15.0	%	η_{i_r}	10.0	%	$\eta_{o_{rt}}$	85.0	%			

Rudder Airfoils

Panel	Root Airfoil Name	Tip Airfoil Name
1	NACA 0006	NACA 0006

Figure 9.15. Input parameters for rudder tab

Output parameters of Vertical Tail are as follows:

Table 9.8. Input parameters for vertical tail

Parameters	Quantity
Rudder root chord length, c_{r_r}	0.95 ft
Rudder tip chord length, c_{t_r}	0.5 ft
Rudder Chord Forward of Hinge at Rudder Inboard Station, $c_{b_{i_r}}$	0.10 ft
Rudder Chord Forward of Hinge at Rudder Outboard Station, $c_{b_{o_r}}$	0.05 ft
Rudder Chord Aft of Hinge at Rudder Inboard Station, $c_{f_{i_r}}$	0.86 ft
Rudder Chord Aft of Hinge at Rudder Outboard Station, $c_{f_{o_r}}$	0.45 ft
Average Rudder Chord to H.T Chord ratio aft of Hingeline, c_r/c_v	13.5%
Rudder Planform Area, S_r	3.91 ft^2
Rudder MAC, $\bar{c}_r$	0.68 ft
Rudder Balance based on Control Surface Area Forward and Aft of Hingeline, $Balance_r$	0.111

Output Parameters

c_{r_r}	0.95 ft	$c_{b_{o_r}}$	0.05 ft	c_r/c_v	13.5 %	Balance$_r$	0.11
c_{t_r}	0.50 ft	$c_{f_{i_r}}$	0.86 ft	S_r	3.91 ft^2	Coordinates Defined	
$c_{b_{i_r}}$	0.094999999 ft	$c_{f_{o_r}}$	0.45 ft	$\bar{c}_r$	0.68 ft		

Figure 9.16. Output parameters of rudder tab

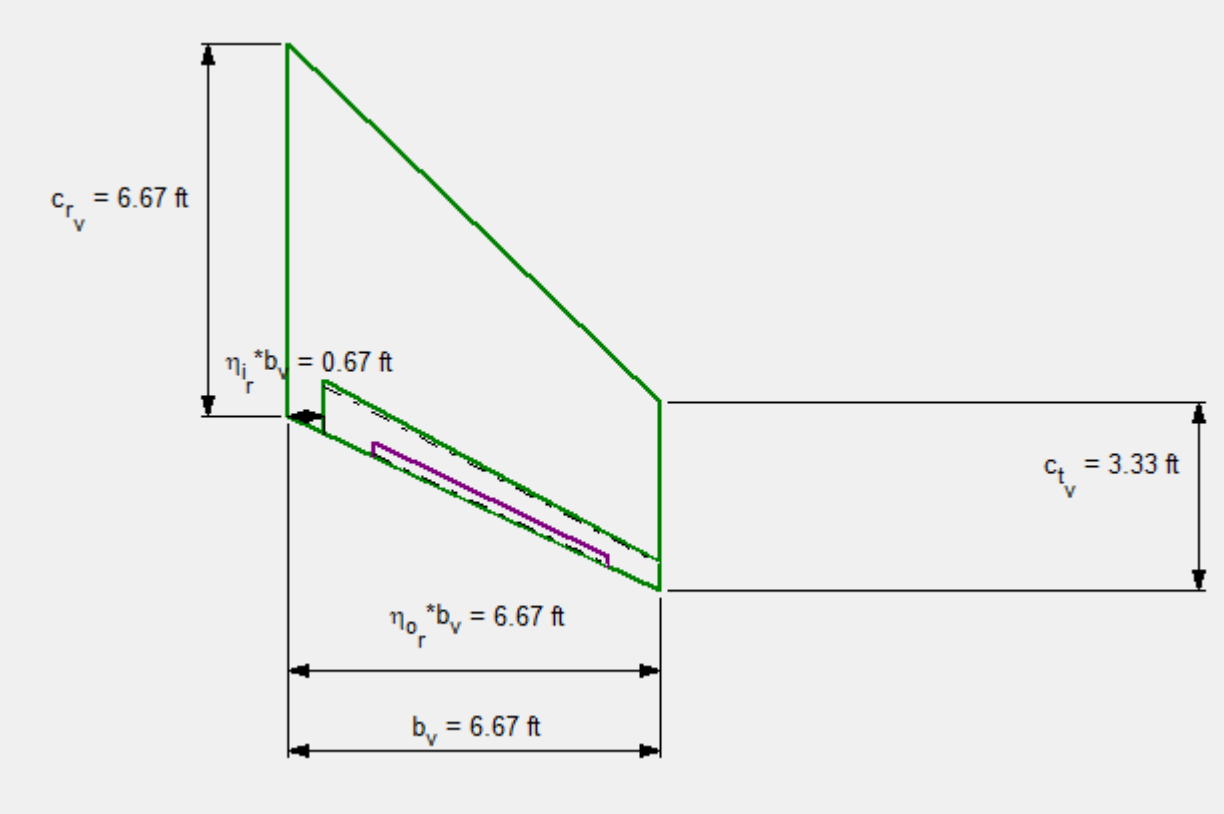

Figure 9.17. Output parameters plotted of vertical tail

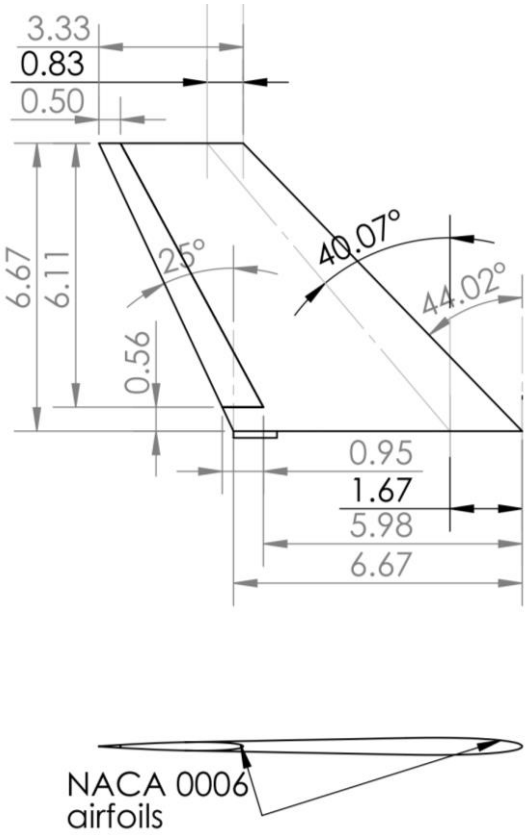

Figure 9.18. All dimensions for vertical tail in plot in ft.

9.6 Tail Boom (Twin Boom)

All above components are ultimately to the extended member called tail boom. The vertical tail is extremely challenging to install directly on fuselage due to the propulsion system. The vibrations and exhaust heat rocket from the rocket motor would compromise the structural integrity of the vertical tail. Moreover, it will reduce the life-span empennage components. Therefore, it is convenient to install the empennage on the tail boom away from the line of exhaust.

Length of tail boom enhances the longitudinal and lateral stability of X-69. The design procedure used for tail boom is combination of that of fuselage and empennage. Using SolidWorks, following layout is established.

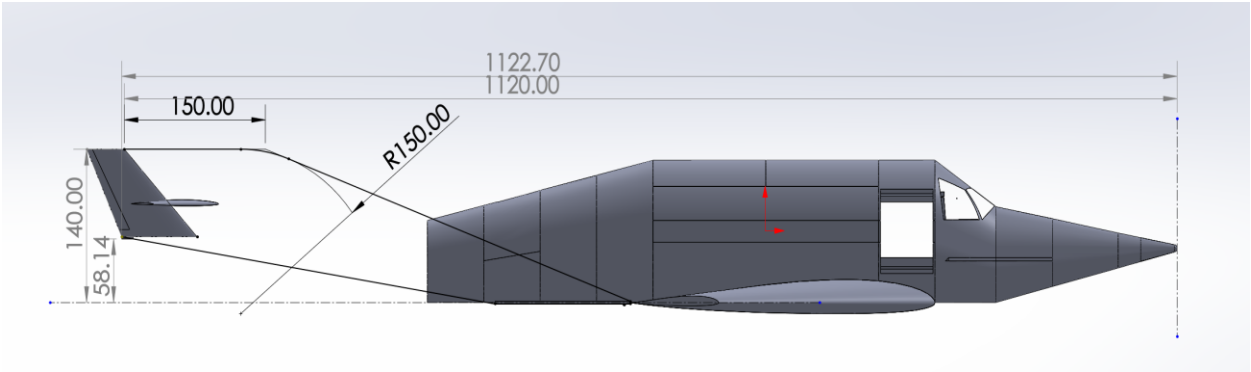

Figure 9.19. Layout estimate of tail boom in inches

The assembly of the tail boom is simply connecting the nose end to the spoiler and tail end to the vertical stabilizer. The layout estimates essentially helped to understand tailboom curve boundary limits.

The cross-sections of the tail boom at about 24 locations have been obtained using Cross-section parameters method from AAA.

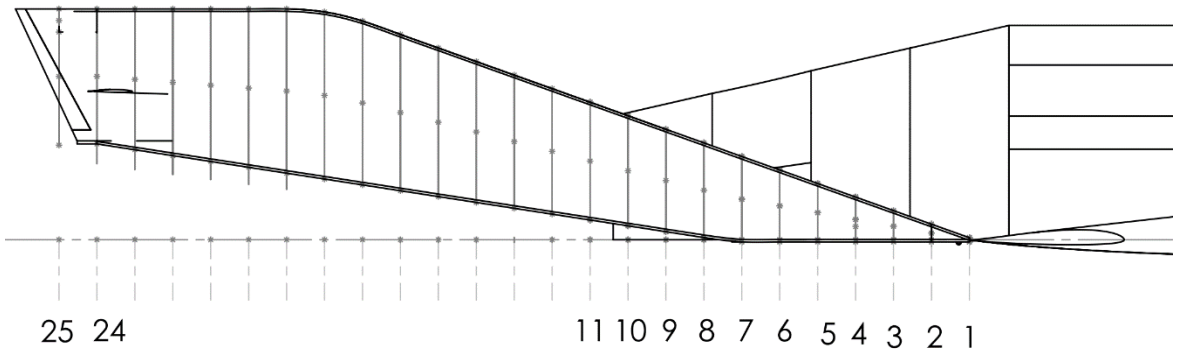

Figure 9.20. X-locations for tail boom

The cross section at each of 25 panels are defined using Cross-section parameters method as shown in fig. 9.21, referring all the components such as Y and Z co-ordinates from the apex or nose. The perimeter plot similar to the fuselage can be obtained from the output parameter from AAA.

The tailboom has major effect on the aerodynamic parameters of its own and X-69 as a whole. The wetted area of both tailboom is about 1,067.5 ft^2. Fig below shows the cross section of tailboom at various stations from nose to the tail.

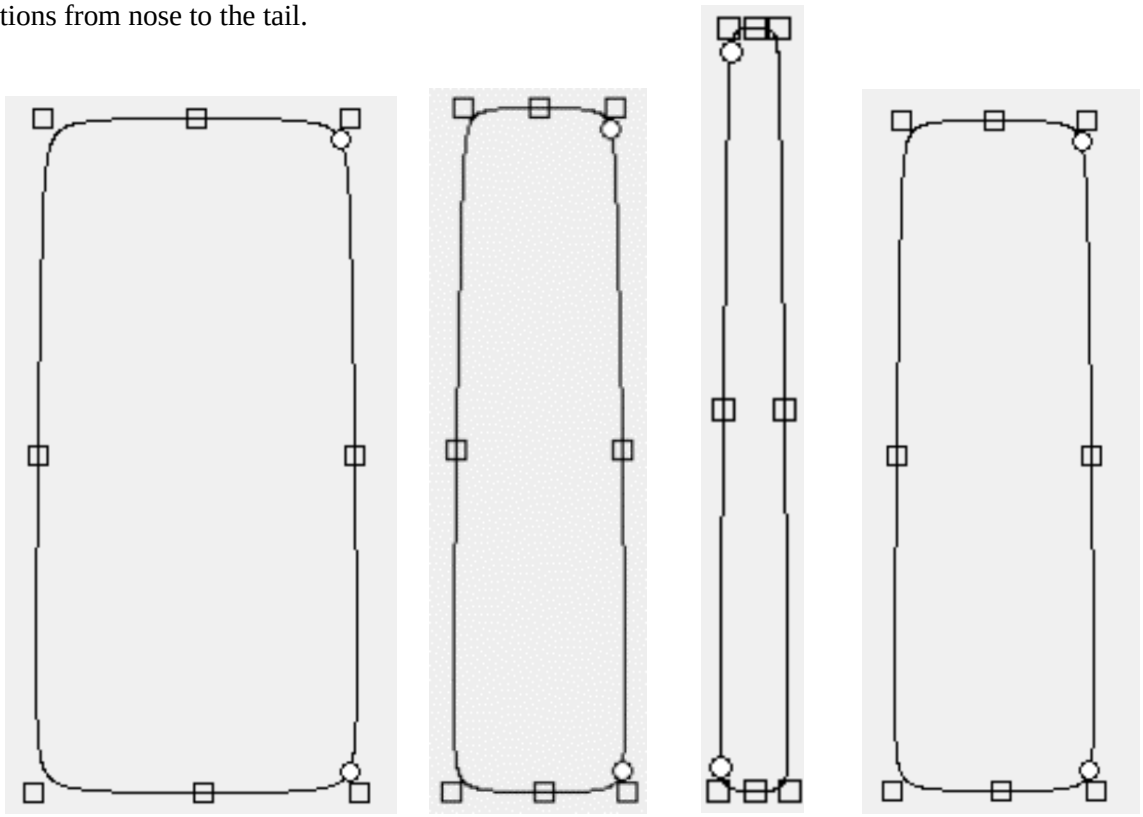

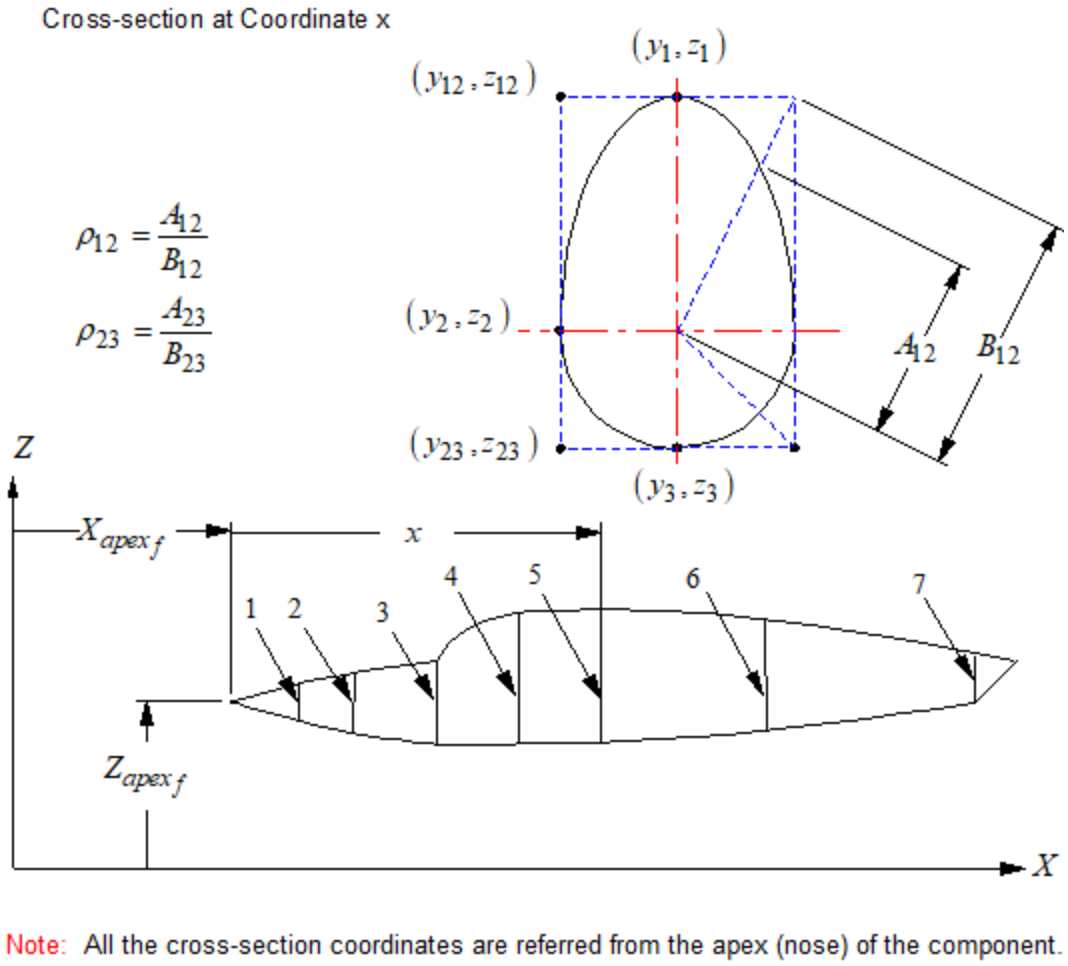

Figure 9.21. Fuselage cross-section parameters.

After obtaining above co-ordinates of y and z, they become input parameters for AAA cross-section dialog box which limits to maximum of 90 stations. 25 panels plotted in fig. 9.20 are sub-divided into 90 stations.

Appendix 9.1 can be referred for co-ordinates for the creation of airplane bodies such as fuselage, tail booms, nacelles, etc. Fig. 9.22 shows the input parameters of tail boom.

Table 9.9. Input parameters of tailboom

Parameters	Quantity
X-coordinate of Tailboom Nose, $X_{nose_{tb}}$	42.4459 ft
Y-coordinate of Tailboom Nose, $Y_{nose_{tb}}$	18.94 ft = half of wing span
Z- coordinate of Tailboom Nose, $Z_{nose_{tb}}$	3.5 ft
Incidence angle of tailboom, i_{tb}	0^o
Tailboom toe angle, Ψ_{tb}	90^o
Tailboom camber angle, Γ_{tb}	0^o

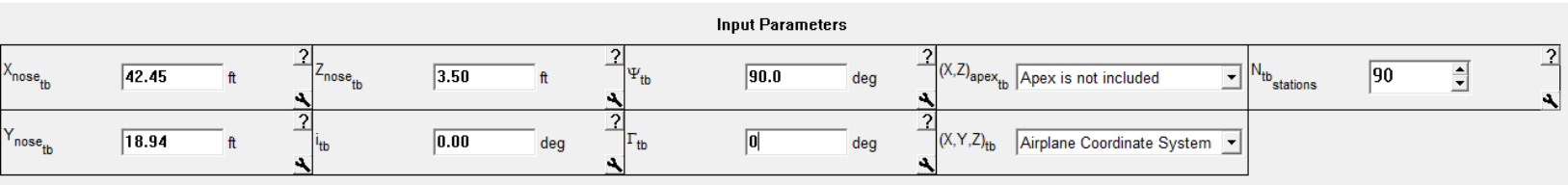

Figure 9.22. Input parameters of tailboom in AAA

The output yielded is as follows:

Table 9.10. Output parameters of tailboom

Parameters	Quantity
Length of tailboom, l_{tb}	46 ft
Tailboom Base Area, $S_{b_{tb}}$	1.041 ft^2
Tailboom Maximum Frontal Area, $S_{tb_{max}}$	1.418 ft^2
Tailboom Planform Area, $S_{plf_{tb}}$	7.95 ft^2
Tailboom wetted area, $S_{wet_{tb}}$	538.39 ft^2
Tailboom Wetted area of all tailbooms combined, $S_{wet\Sigma tb}$	1066.25 ft^2

Horizontal and vertical tail are buried in the tailboom.

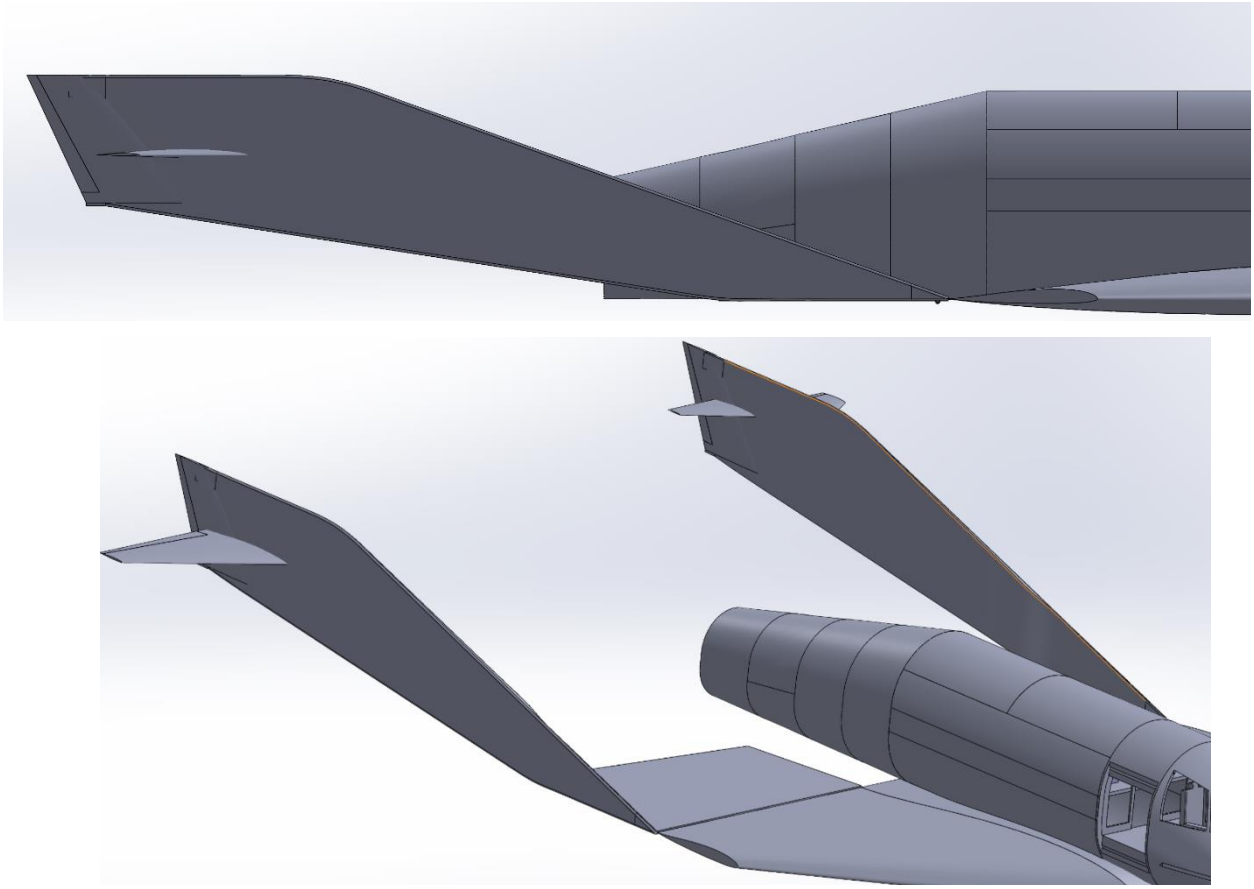

Figure 9.23. Tailboom final output using AAA and SolidWorks

9.7 Fins

Fins are optional components for X-69. Fins enhance the controls in rolling and pitching balancing the airflow at inner side of the tailboom. Fins are installed burying into the tailboom as for H.T and V.T. Fig. 9.24 shows diagram of fins.

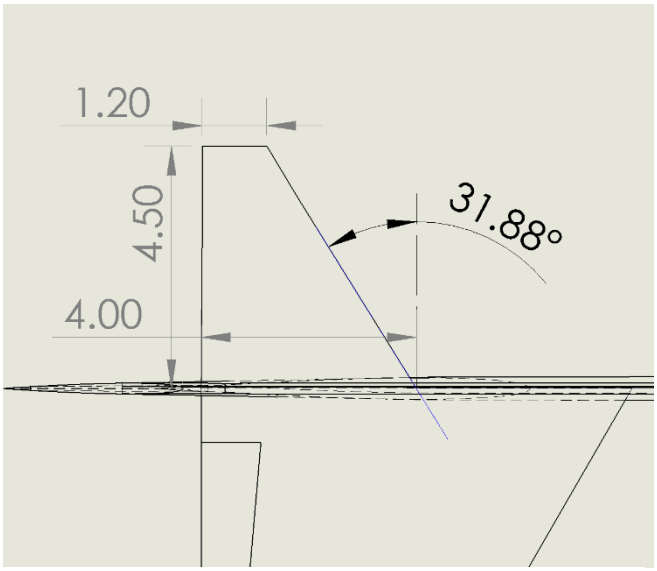

Figure 9.24. Fin

9.8 Volume Coefficients:

Using above information of wing and empennage, the volume coefficients can be obtained. Parameters such moment arms and quarter-chord lengths can be obtained from fig 8.25.

For volume coefficient of H.T, $\overline{V_h}$, we have

$$\overline{V_h} = \frac{x_h S_h}{S\bar{C}} \tag{9.1}$$

where,

x_h = 44.35 ft

S_h = 101.98 ft^2

S = 1,114.32 ft^2

$\bar{C}$= 30.45 ft

Hence,

$$\overline{V_h} = \frac{44.35 \times 101.98}{1{,}114.32 \times 30.45}$$

$$\overline{V_h} = 0.1333$$

For volume coefficient of V.T, $\overline{V_v}$, we have

$$\overline{V_v} = \frac{x_v S_v}{Sb} \tag{9.2}$$

where,
x_v = 46.75 ft
S_v = 33.33 ft^2
S = 1,114.32 ft^2
b = 47.0556 ft
Hence,

$$\bar{V}_v = \frac{46.75 \times 33.33}{1{,}114.32 \times 47.0556}$$

$$\bar{V}_v = 0.0297$$

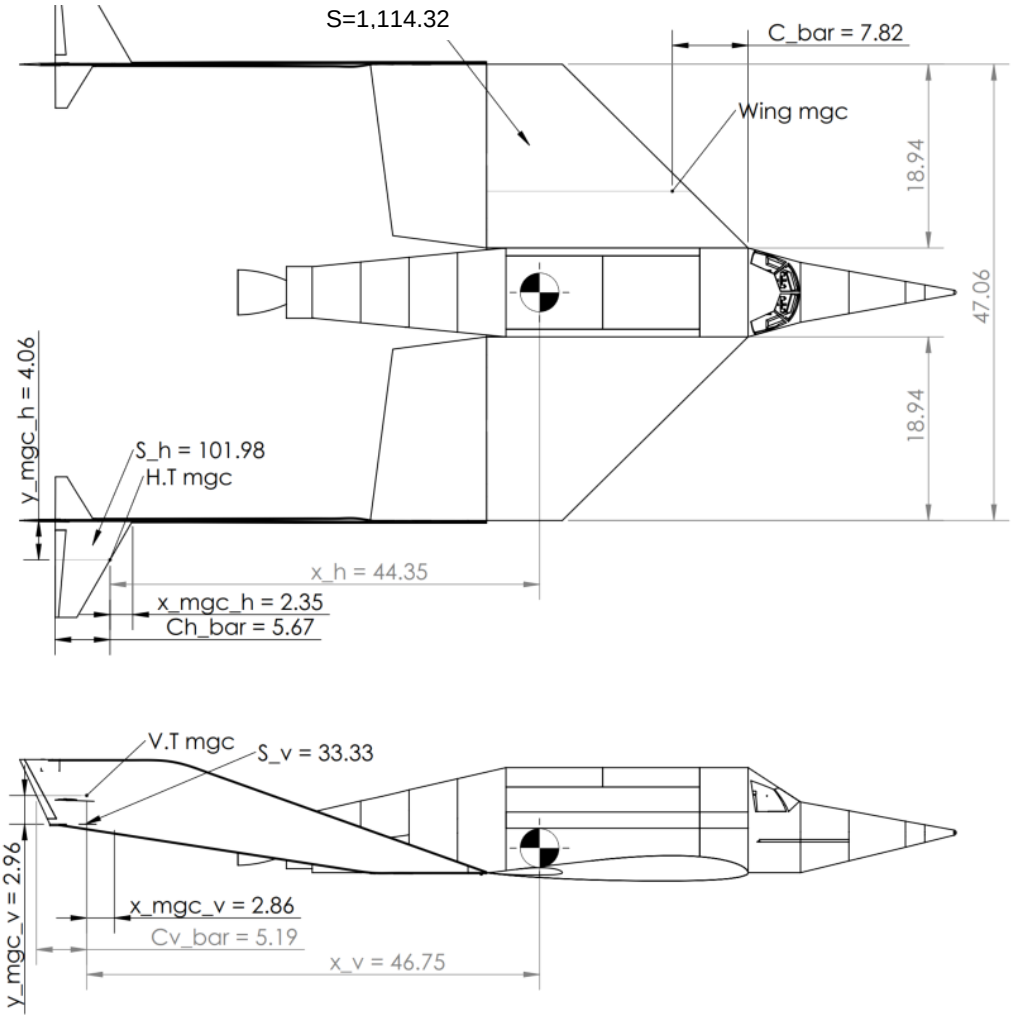

Figure 9.25. Volume coefficients parameters

9.9 Discussion

The empennage layout ultimately includes above components such as Horizontal tail, Elevons, Vertical tail, Rudders, Fins installed on Tailboom. The entire configuration can rotate from 0 to 65^{o} along with the spoiler. The rotation of empennage assuages the high pressure and temperature air flow emerging from the tail boom. There is an ablative material applied on dorsal part of X-69 on wings, fuselage, spoiler and empennage that works as heat shield during re-entry. The re-entry itself is decelerated by the aforementioned feather-lock mechanism which is shown in following figure.

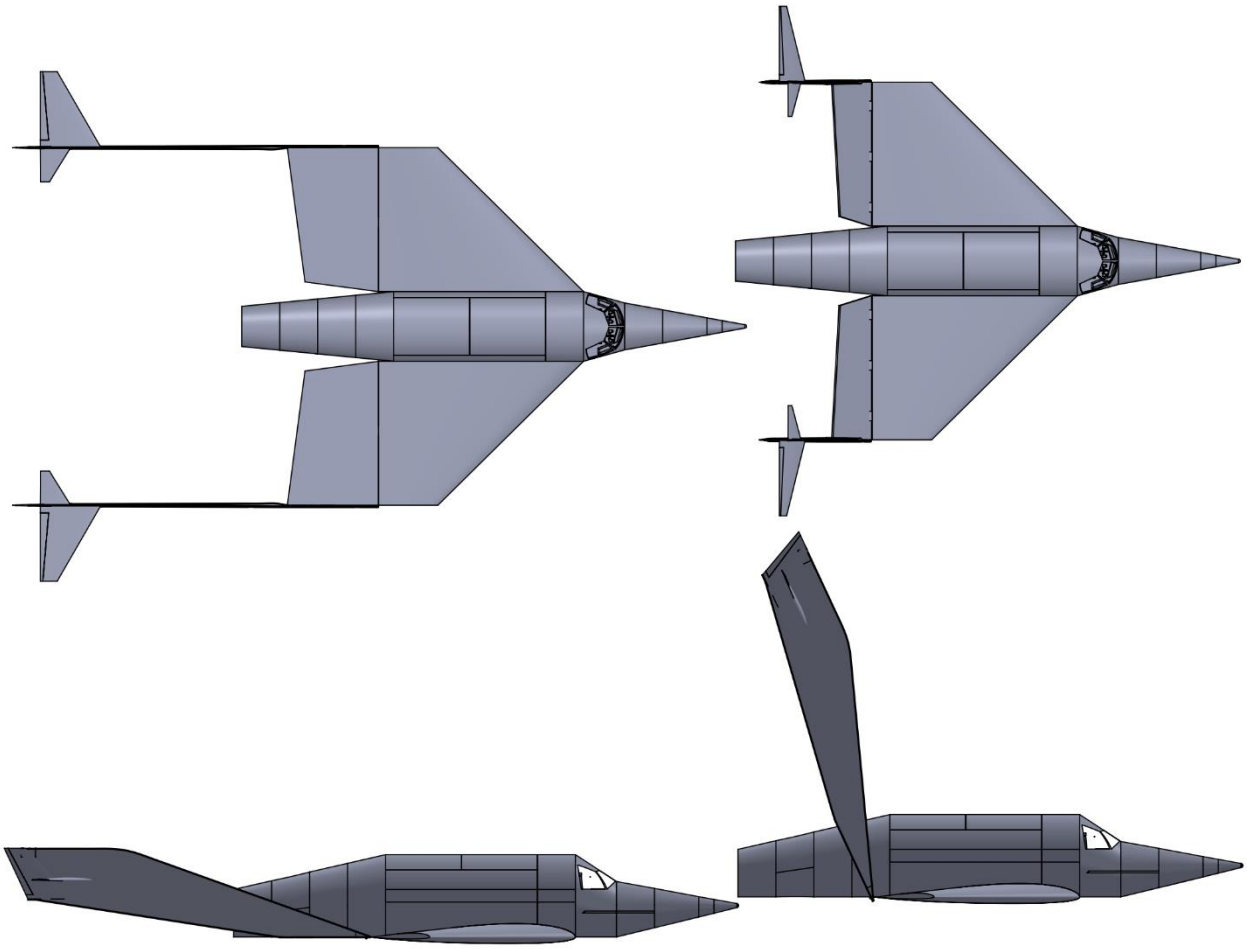

Figure 9.26. All assembled normal and feather-locked top and side view

9.10 Conclusion

The empennage configuration is quite sophisticated allowing easy design and manufacturing. Stability and control will allow us to understand the efficiency of horizontal and vertical tail and to incorporate trim conditions. As a recommendation for future improvement, it is possible to make X-69 a self-take-off spaceplane using its own engines. This gives more room for changes in design itself. The space between tailboom and the fuselage can be used for jet engines buried into the delta shaped body giving more span area.

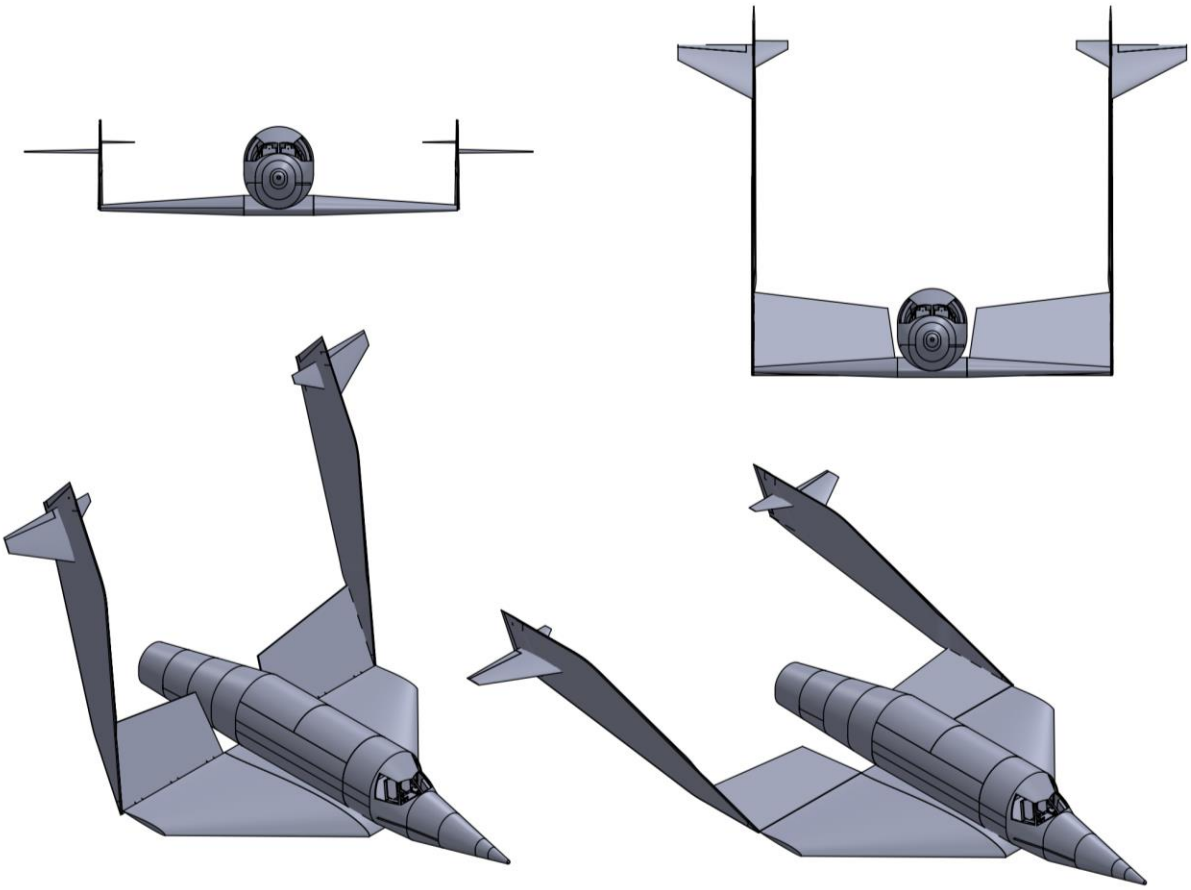

Figure 9.27. All assembled normal and feather-locked front and 3D isometric view

10. Chapter 10. Landing Gear Design and Weight & Balance Analysis

10.1 Introduction:

After successful estimation of major components of X-69, it is time to compute estimation for landing layout. Since X-69 is a low wing spaceplane, it gives an advantage to conveniently install main landing gear under the wing which will be discussed further. Moreover, ground clearance has to very optimal. Weight and balance analysis play major role in deciding landing gear sizing.

Landing gears usually bear 3 types load:

- Vertical loads: Primarily caused by non-zero touch-down rates and taxiing over rough surfaces.
- Longitudinal loads: Primarily caused by 'spin-up' loads braking loads and rolling friction loads.
- Lateral loads: Primarily caused by 'crabbed landings', cross-wind taxiing and ground turning.

A class I method for landing gear sizing and disposition will be used as follows:

10.1.1 Type of landing gear system:

A retractable type of landing gear system will be used since it's a "Spaceplane" that deals with Supersonic and Hypersonic regimes.

10.1.2 Overall Landing gear configuration:

The configuration of landing gear system adopted is a combination of wheel at main gear and possibly a skid at nose. A nose-skid is choosing due to size constraints and lack of space for any basic load bearing wheel to accommodate in nose. Also, nose will house thrusters as discussed earlier therefore nose-skid is decided.

10.1.3 Disposition of Landing gear

A disposition of landing gear is attempted using weight and balance statement extending the process to decide on a preliminary landing gear strut disposition. Using the overall C.G of X-69, the geometric criteria such as Tip-over Criteria and Ground Clearance Criteria are attempted to be met.

Especially for a Tip-over longitudinal criteria in tricycle type gears, the main landing gear must be behind the aft C.G location maintaining the angle of 15^{o} or more between the main gear and the aft C.G. Fig 10.1 shows the rough sketch of the possible layout for landing gears where the length of strut becomes 72 inches that satisfies tip-over criteria. The main gear will be installed under the wing retracting inwards towards fuselage. Point labeled as "main gear position" will be the location of main gear strut that gives enough space for wheel and the strut under the fuselage up on retraction. Moreover, the wing taper and thickness ratio also satisfies the criteria.
For the nose-skid, the strut should work efficient with 60^{o} full retraction angle as shown in fig. 10.1. This gives the length of nose-skid to about 132 inches.

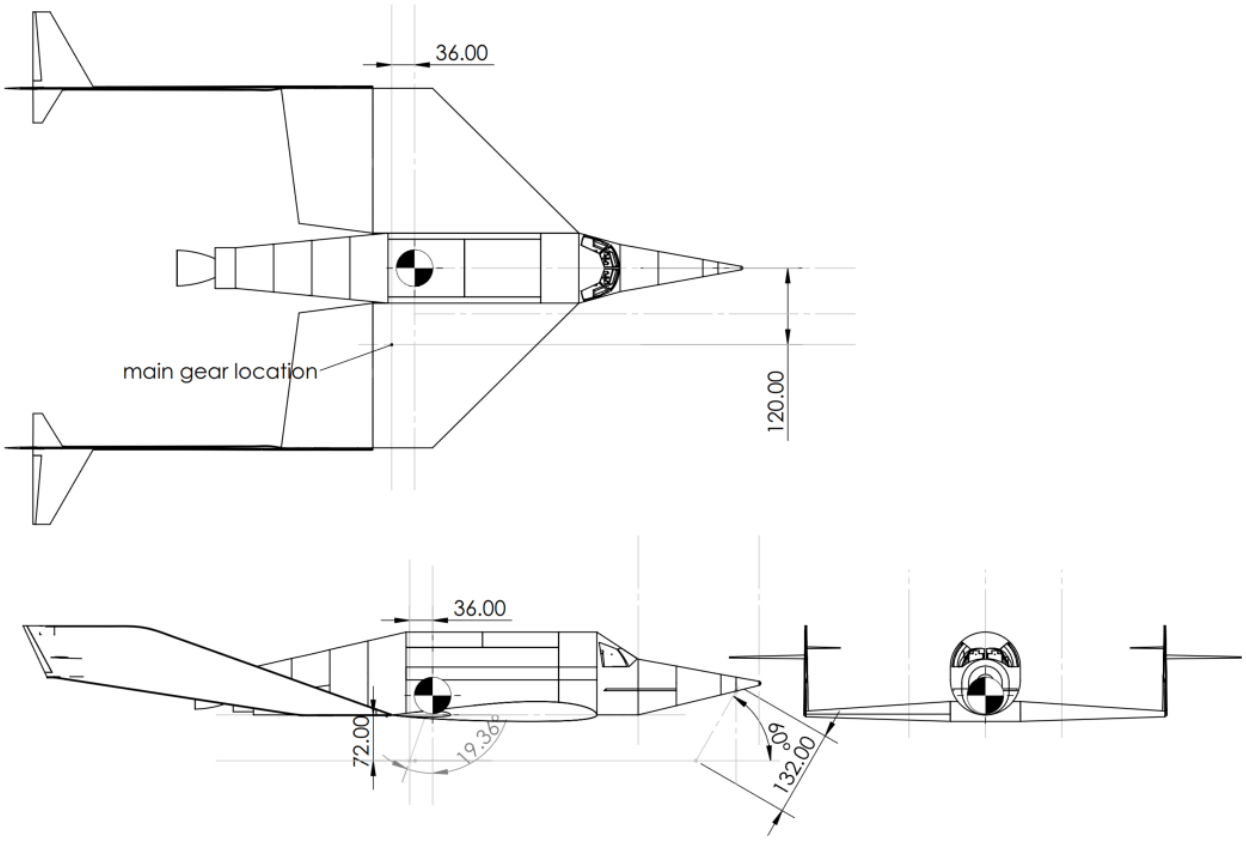

Figure 10.1. A rough C.G sketch for preliminary landing gear disposition

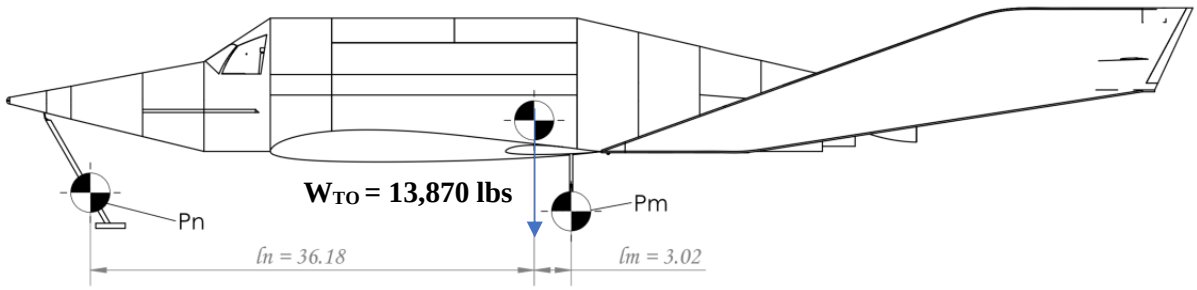

Figure 10.2. C.G locations of main gear and nose skid

We can now use take-off weight, W_{TO} = 13,870 lbs. to calculate the loads on nose skid, P_n and main gear, P_m. C.G locations are obtained from fig 10.2 with l_n = *36.18 ft* and l_m = 3.02 ft. Dimensions of the main gear are referred from *Roskam's Aircraft Design vol III, table 10.2 under Agriculture plane section* with $D_t \times b_t = 22inch \times 8inch$ and nose skid at 60° angle with longitudinal axis. Since X-69 has tricycle type landing gear system, the maximum static load per strut are as follows:

Nose Skid –

$$P_n = \frac{W_{TO} l_m}{(l_m + l_n)} \quad (10.1)$$

$$P_n = \frac{13{,}870 \times 3.02}{(36.18 + 3.02)}$$

$$P_n = 1{,}068.56 lbs.$$

Main Gear Strut: with coefficient $n_s = 2$,

$$P_m = \frac{W_{TO} l_n}{n_s (l_m + l_n)} \quad (10.2)$$

$$P_m = \frac{13{,}870 \times 36.18}{2 \times (36.18 + 3.02)}$$

$$P_m = 6{,}400.7 lbs.$$

Therefore, the gear load ratios are,

$$\frac{P_n}{W_{TO}} = \frac{1{,}068.56}{13{,}870}$$

$$\frac{P_n}{W_{TO}} = 0.07704$$

$$\frac{2.P_m}{W_{TO}} = \frac{2 \times 6{,}400.7}{13{,}870}$$

$$\frac{P_m}{2.W_{TO}} = 0.923$$

10.2 Weight and Balance Analysis:

10.2.1 Class I Weight and Balance Method:

Class I method from *Roskam's* Chapter 10 is used to estimate weight and balance. We will need an initial component breakdown as shown in fig 10.3 and table 10.1.

Table 10.1. Component breakdown

Item Number	Component Name
1	Cockpit
2	Payload Compartment
3	Payload (including 24 Canisters and CubeSats)
4	Payload Dispensing Sliding doors
5	Rocket Housing
6	Hybrid Rocket Motor (propulsion system)
7	Wing
8	Spoiler
9	Tailboom
10	Horizontal Stabilizers (H.T)

Item Number	Component Name
11	Elevons(H.T)
12	Vertical Stabilizers (V.T)
13	Rudders (V.T)
14	Fins
15	Main Landing Gears
16	Nose Skid

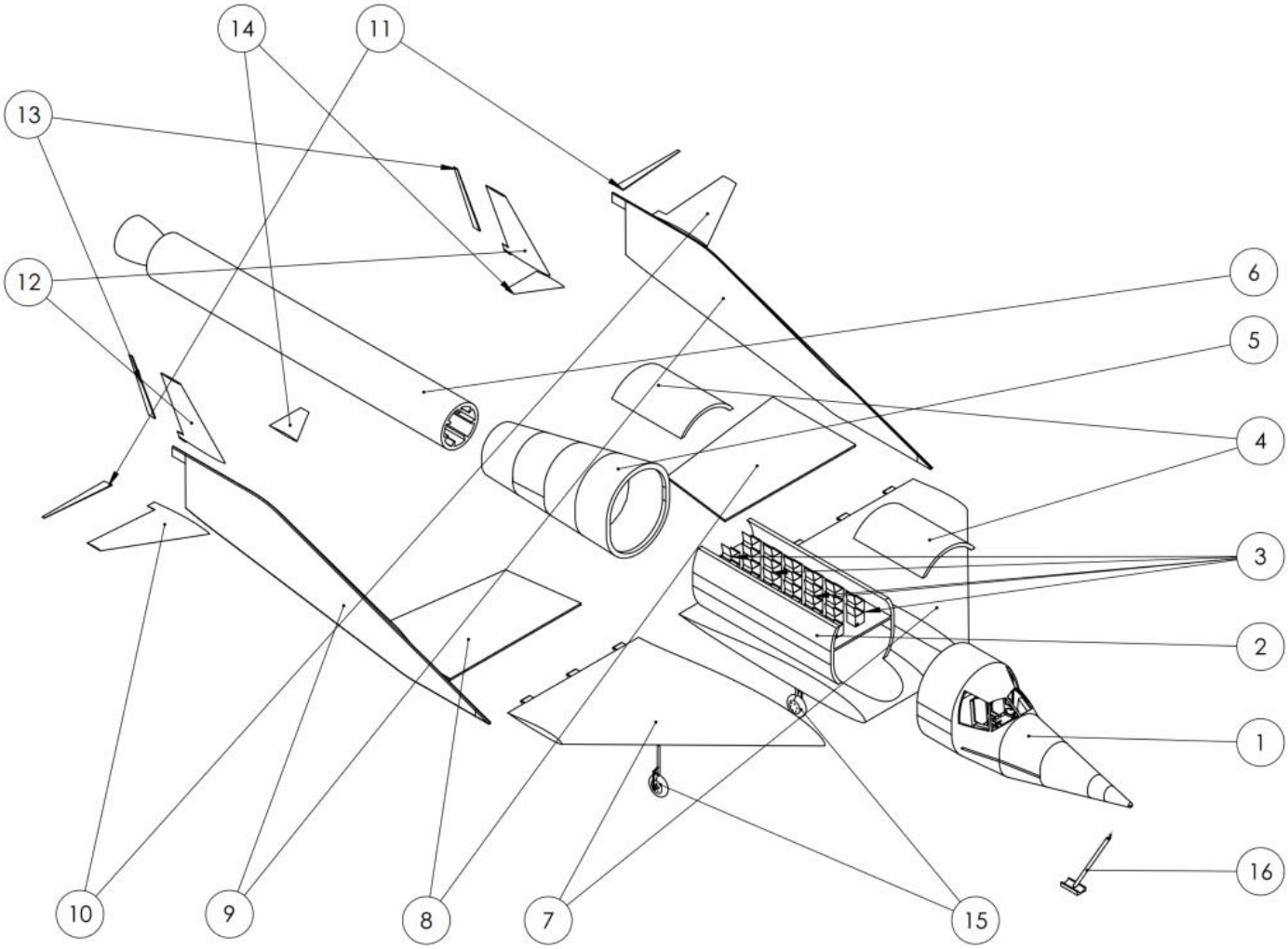

Figure 10.3. Component breakdown

10.2.2 Estimation of the Center of Gravity location for the airplane:

To estimate the C.G location of major components and complete X-69, according to *Roskam*, the nomenclature widely used in the aircraft industries is applied for X-69.

- X-axis as defined in fig 10.5 is referred to as Fuselage Station (F.S).
- Y-axis as defined in fig 10.4 is referred to as Wing Buttock line (W.L or W.B.L)
- Z-axis as defined in fig 10.6 is referred to as Water lines (W.L), the term carry-over from ship building industry.

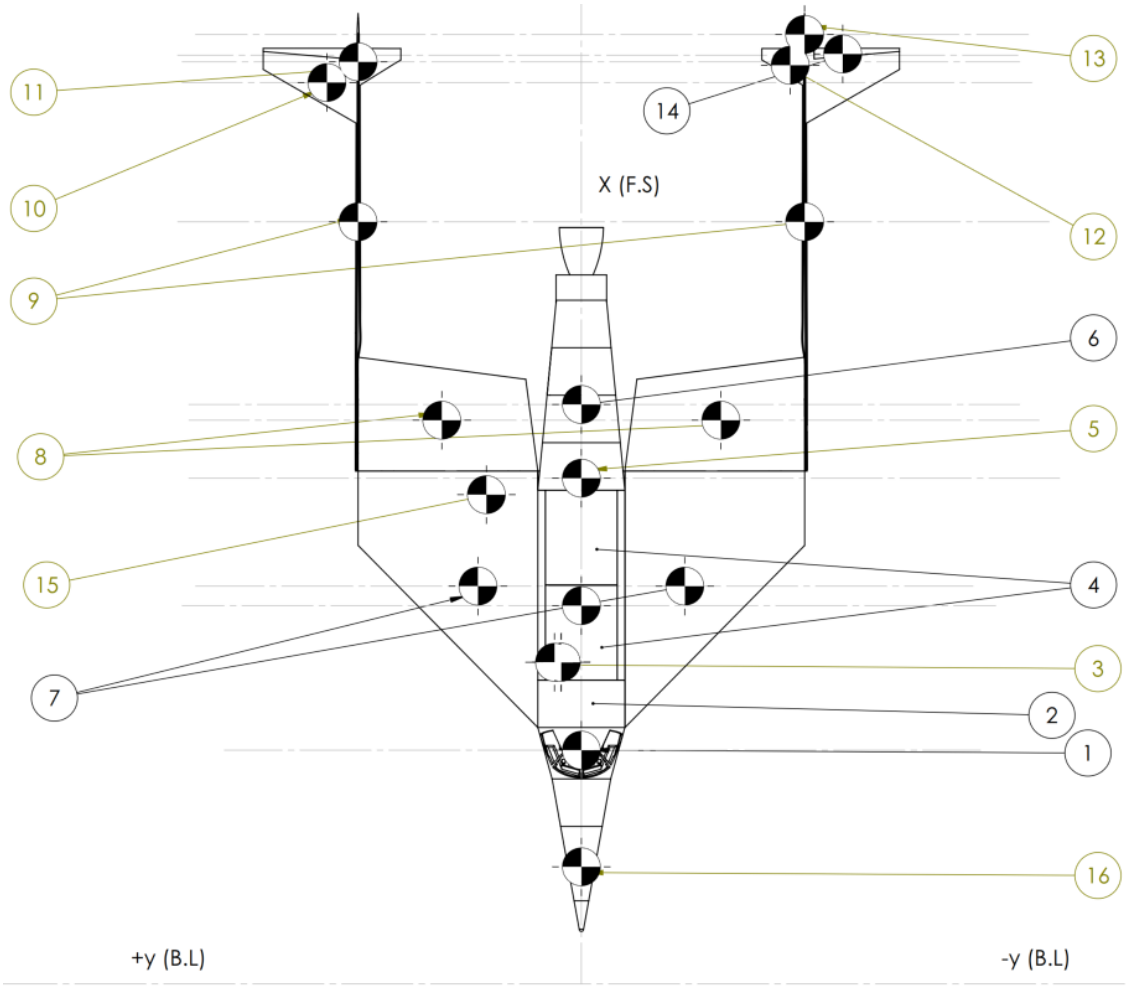

Figure 10.5. Top view of X-69 for C.G locations

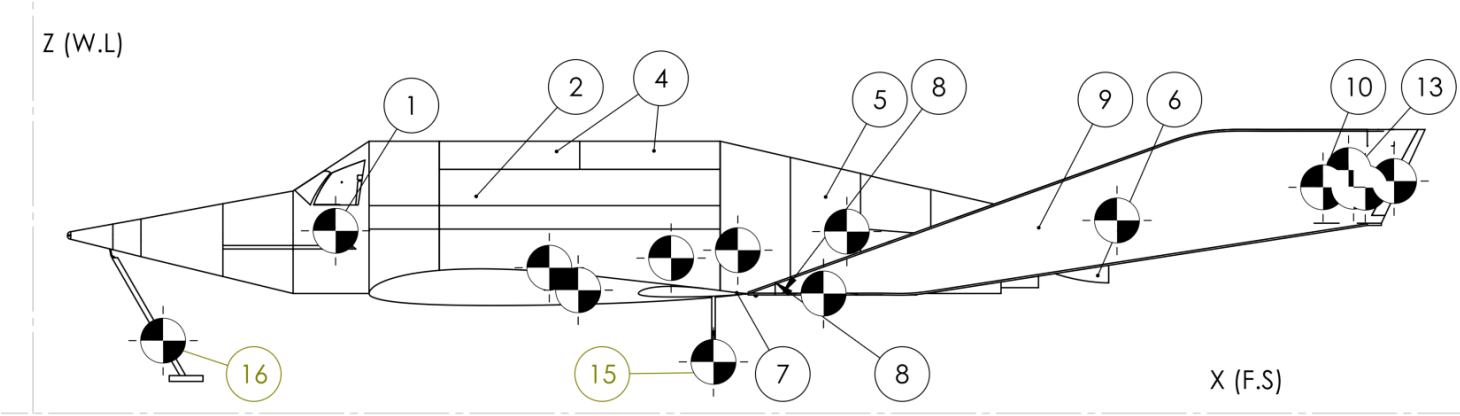

Figure 10.4. Side view of X-69 for C.G locations

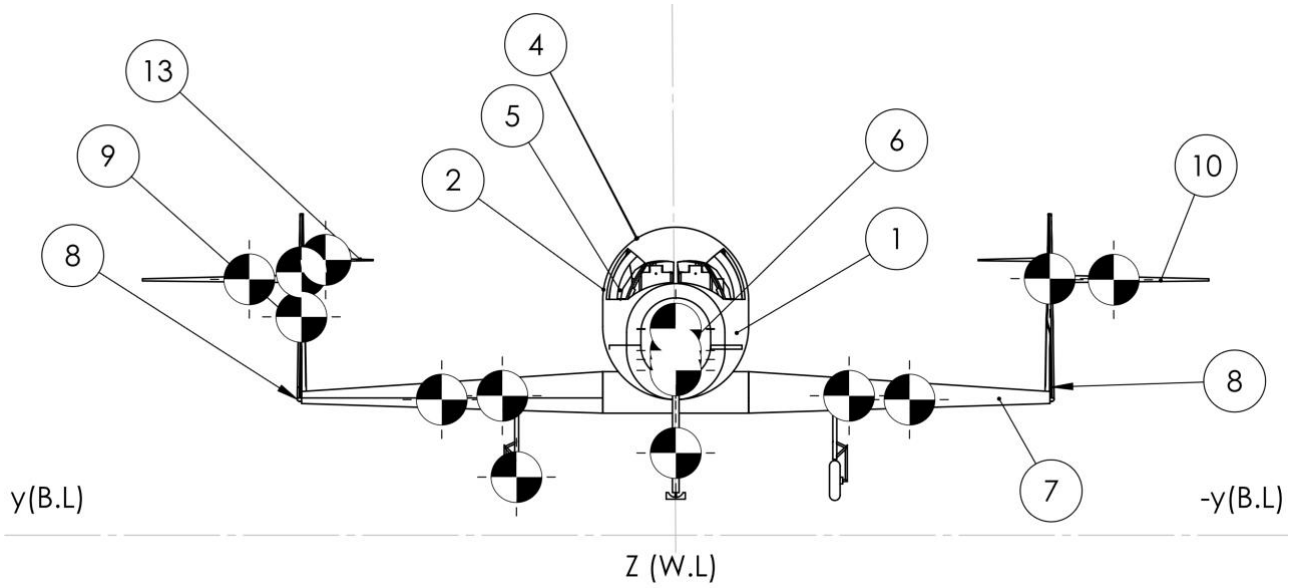

Figure 10.6 Front view of X-69 for C.G locations

10.2.3 Location of C.G.s of major components:

Following are the C.G.s of major components such as cockpit, payload compartment, rocket housing, rocket motor, wing, horizontal tail and elevons combined, vertical tail and rudders combined, tailboom, spoiler, main gear and nose skid.

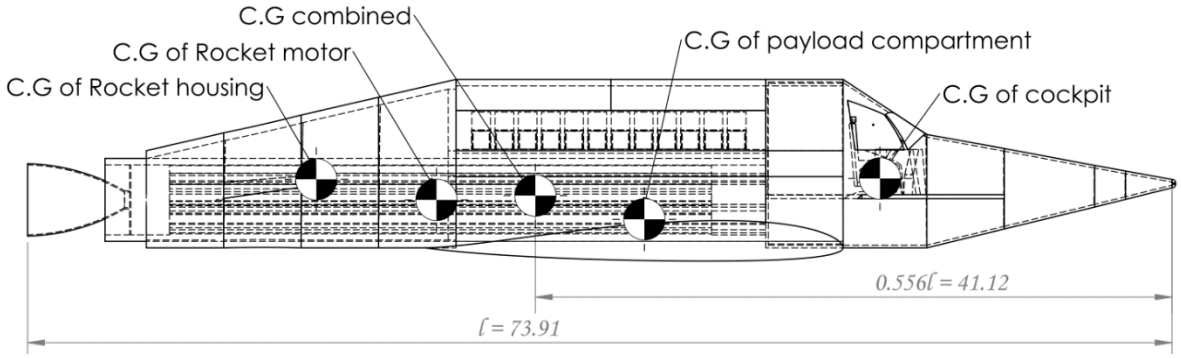

Figure 10.7.C.G of fuselage with above components combined

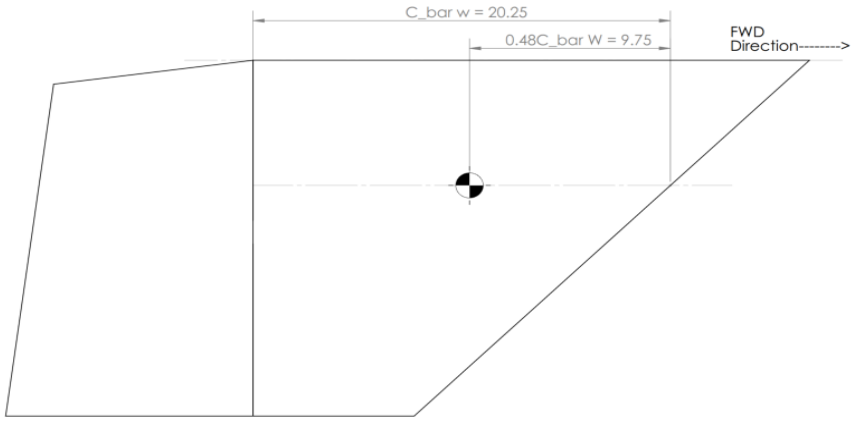

Figure 10.8 C.G location of wing with spoiler

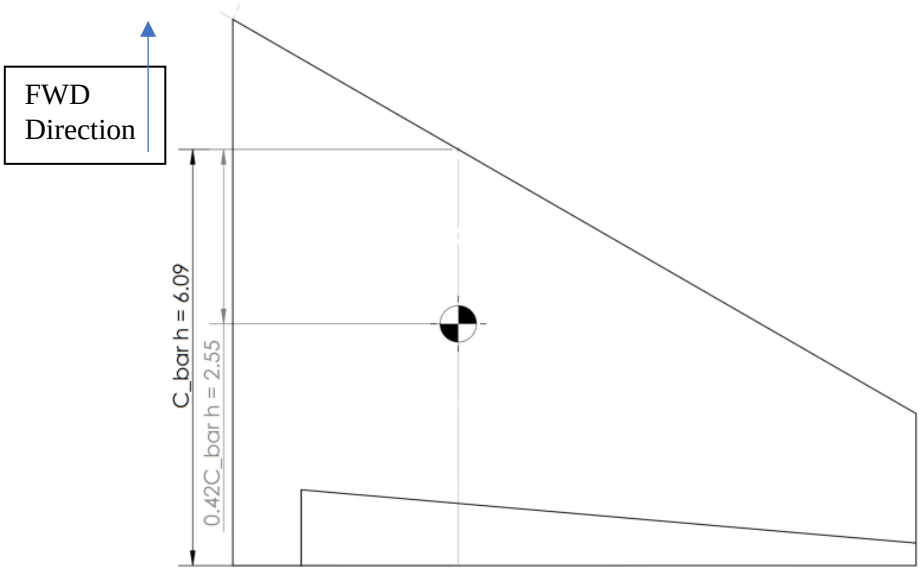

Figure 10.9 C.G location of horizontal tail

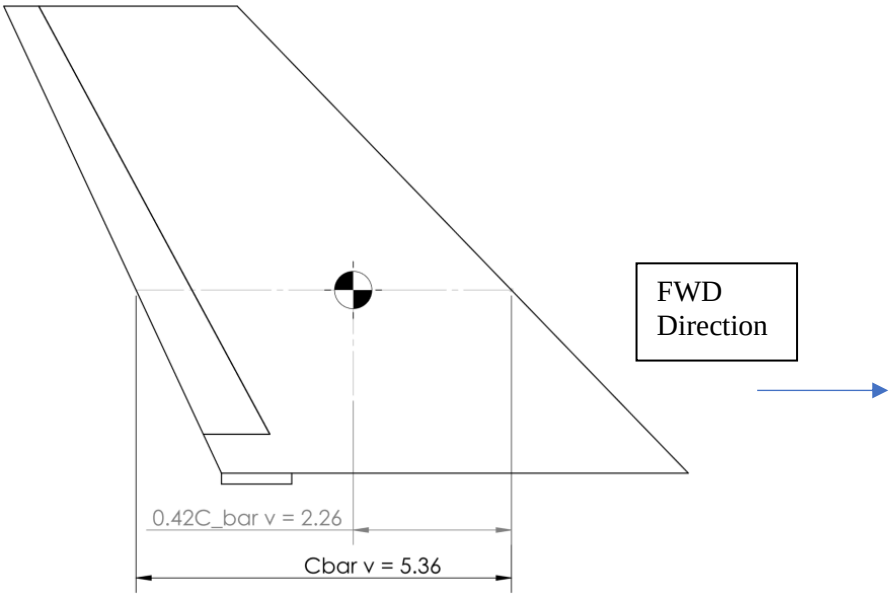

Figure 10.10 C.G location of vertical tail

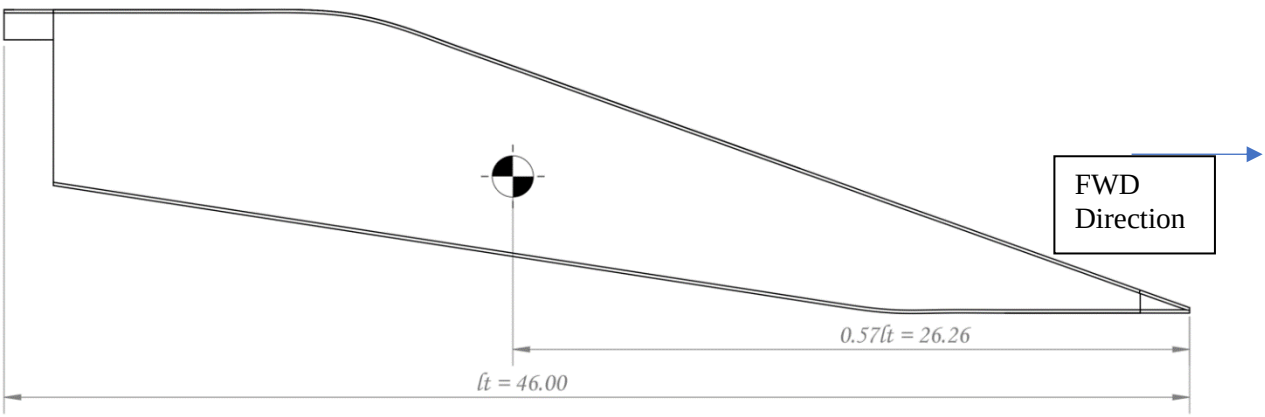

Figure 10.11. C.G location of tailboom

10.2.4 Class I Method for Estimation of Airplane Components Weight

Revising the overall weight values for the airplane from weight sizing in table 10.2. Structure Weight, W_{struct} for X-69 is referred and averaged from similar airplanes weight data from *Roskam's Airplane Design vol V, Appendix A13.1a & b* under North American X-15 which has similar mission profile to that of X-69. The average weight fractions can be referred from table 10.3.

Table 10.2. Component weight list

Type	**Weight**
Gross Take-off Weight, W_{TO}	13,870 lbs.
Empty Weight, W_E	8,418.8 lbs.
Mission Fuel Weight, W_F	1,720.75 lbs.
Payload Weight, W_{PL}	3,310 lbs.
Crew Weight, W_{crew}	350 lbs.
Trapped fuel and oil weight, W_{tfo}	160 lbs. (slivers of solid propellant)
Flight Design Gross Weight, GW	13,870 lbs.
Structure Weight, W_{struct}	
Wing Group	1,500 lbs. (including spoilers)
Empennage Group	1300 lbs.
Fuselage Group	3,500 lbs.
Engine Section	190 lbs. (hybrid rocket motor)
Landing Gear (main gear and nose skid)	400 lbs.
Structural Total	**6,890 lbs.**
Powerplant Weight, W_{plt}	
Engine	500 lbs.
Fuel System	1,200 lbs.
Propeller Instrument	0
Propulsion System	150 lbs.
Powerplant Total	**1,850 lbs.**
Fixed Equipment Weight, W_{feq}	
Avionics & Instruments	170 lbs.
Surface controls	1,180 lbs.
Pneumatic systems	240 lbs.
Electrical System	140 lbs.

Type	Weight
Fixed Equipment Weight, W_{feq}	
Electronics	175 lbs.
Test Instrumentation Ballast	1,000 lbs.
Air Conditioning System	200 lbs.
Furnishings	450 lbs.
Auxiliary Gears	10 lbs.
Fixed Equipment Weight, W_{feq}`	**3,565 lbs.**

Only weights of wing, empennage, fuselage, landing gear. Powerplant and fixed equipment are considered.

The ratio for empty weight/GW = 8,418.8/13,870 = 0.61 which is lower than of North American X-15 with empty weight/GW = 0.949 due to higher payload for X-69, the above component weights are adjusted to meet X-69's empty weight's requirements:

Table 10.3. Adjustments for estimated component weights

Type	First Weight estimate	Adjustment	Class I weight
Gross Take-off Weight, W_{TO}	13,870 lbs.		13,870 lbs.
Empty Weight, W_E	8,418.8 lbs.		8,420 lbs.
Mission Fuel Weight, W_F	1,720.75 lbs.		1,720.75 lbs.
Payload Weight, W_{PL}	3,310 lbs.		3,310 lbs.
Crew Weight, W_{crew}	350 lbs.		350 lbs.
Trapped fuel and oil weight, W_{tfo}	160 lbs. (slivers of solid propellant)		160 lbs.
Flight Design Gross Weight, GW	13,870 lbs.		13,870 lbs.
Structure Weight, W_{struct}			
Wing Group	1,500 lbs. (including spoilers)	-200 lbs.	1,300 lbs.
Empennage Group	1,300 lbs.	-100 lbs.	1,200 lbs.
Fuselage Group	3,500 lbs.	-2000 lbs.	1,500 lbs.
Engine Section	190 lbs. (hybrid rocket motor)	0 lbs.	190 lbs.
Landing Gear (main gear and nose skid)	400 lbs.	-150 lbs.	250 lbs.
Structural Total	**6,890 lbs.**	**-1,600 lbs.**	**4,440 lbs.**
Powerplant Weight, W_{plt}			
Engine	500 lbs.	0 lbs.	500 lbs.
Fuel System	1,200 lbs.	-400 lbs.	800 lbs.
Propeller Instrument	0	0 lbs.	0 lbs.
Propulsion System	150 lbs.	0 lbs.	150 lbs.
Powerplant Total	**1,850 lbs.**	**-400 lbs.**	**1,450 lbs.**
Fixed Equipment Weight, W_{feq}			
Avionics & Instruments	170 lbs.	-20 lbs.	150 lbs.
Surface controls	1,180 lbs.	-180 lbs.	1,000 lbs.
Pneumatic systems	240 lbs.	-90 lbs.	150 lbs.
Electrical System	140 lbs.	-40 lbs.	100 lbs.
Electronics	175 lbs.	-55 lbs.	120 lbs.
Test Instrumentation Ballast	1,000 lbs.	-500 lbs.	500 lbs.
Air Conditioning System	200 lbs.	-50 lbs.	150 lbs.

Type	First Weight estimate	Adjustment	Class I weight
Furnishings	450 lbs.	-100 lbs.	350 lbs.
Auxiliary Gears	10 lbs.	0 lbs.	10 lbs.
Fixed Equipment Weight, W_{feq}`	**3,565 lbs.**	**-1,035 lbs.**	**2,530 lbs.**

With the weight fractions as follows:

Table 10.4. Weight fractions

Type	Weight or Weight fraction
Flight Design Gross Weight, GW	13,870 lbs.
Structure/GW	0.32
Powerplant/GW	0.105
Fixed Equipment/GW	0.182
Empty Weight/GW	0.61
Wing Group/GW	0.094
Empennage Group/GW	0.0865
Fuselage Group/GW	0.12
Engine Section/GW	0.0137
Landing Gear/GW	0.01802

Following figures 10.12 and 10.13 show C.G locations of all components with respect to X and Z-axis namely Fuselage Station (F.S) and Water lines (W.L) respectively.

Table 10.5. Component weight and coordinate data

Component	Weight, lbs.	x, ft	Wx, ft.lbs.	y, ft	Wy, ft.lbs.	z, ft	Wz, ft.lbs.
Wing Group	1,500	36.20	54,300	0	0	9.95	14,925
Empennage Group	1,300	91.41	1,18,833	0	0	17.30	22,490
Fuselage Group	3,500	41.69	1,45,915	0	0	12.72	44,520
Landing gear	400	45.83	18,332	0	0	4.84	1,936
Engine	1,850	47.56	87,986	0	0	12.79	23,661.5
Fixed Equipments	3,565	18.22	64,954.3	0	0	14.17	50,516.05
Empty weight	8,418.8	41.69	8,460	0	0	12.72	107,087.14
TFO	160	36.20	5,792	0	0	12.79	2,046.4
Fuel	1,720.75	47.56	81,838.87	0	0	12.79	81,838.9
Payload	3,310	34.14	1,13,003.4	0	0	12.79	42,335
Take-off Weight	13,870	47.56	6,59,657.2	0	0	12.79	177,397.3
Pilot	350	36.20	12,670	0	0	14.17	5,000

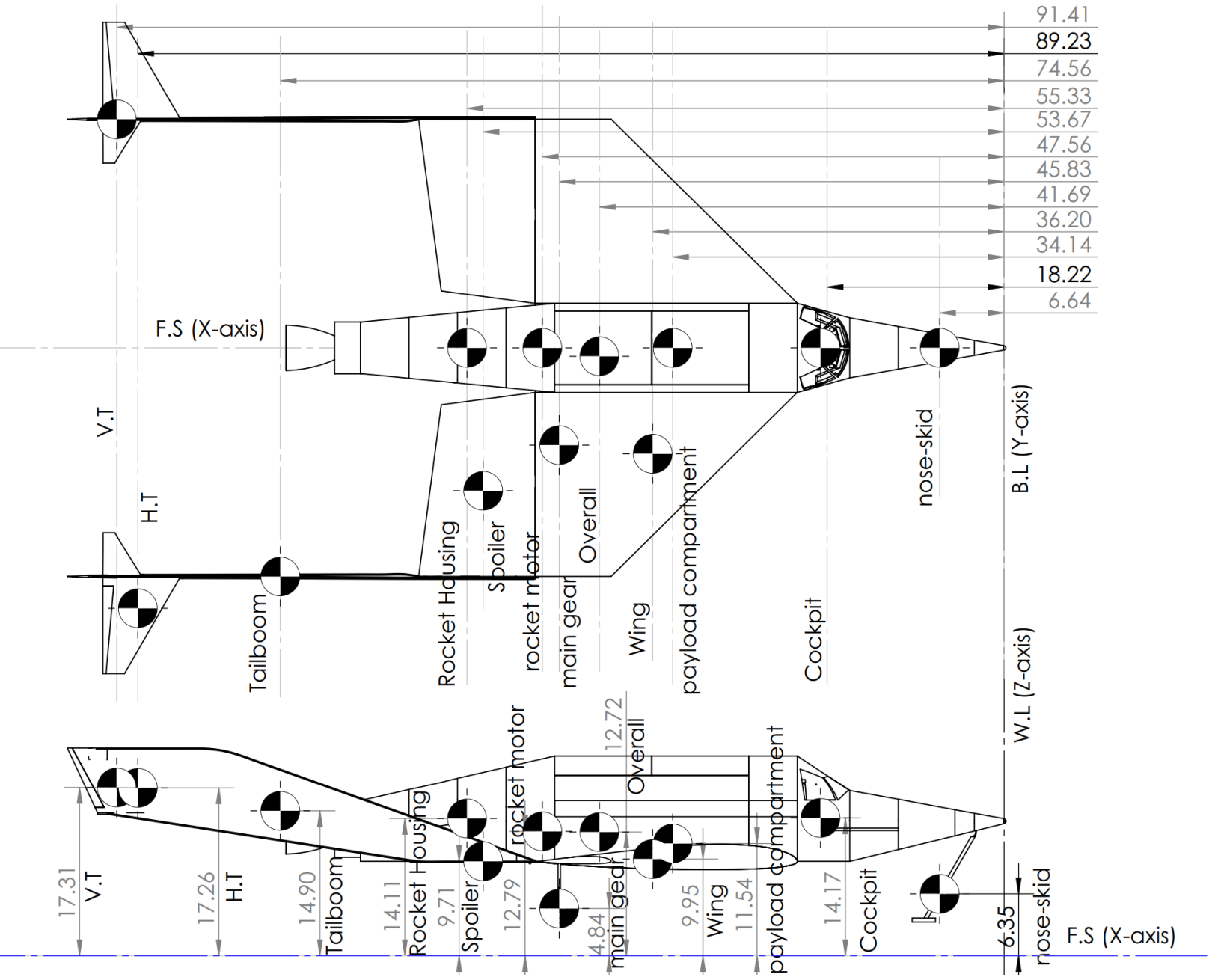

Figure 10.12. C.G data

Using AAA, we get the C.G excursion with respect to X-axis (F.S). Similar empty weight adjustments have been made while inputting empty weights using "From Fractions". As the AAA demands for C.G.s, fig 10.12 is referred for X and Z axis.

Figures 10.13 to 10.16 shows the input parameters supplied to the software and obtained output parameters followed by C.G excursion plot in X-direction along the Fuselage Station.

Empty Weight Table

Component	Weight lb	X_{cg} ft	Y_{cg} ft	Z_{cg} ft
Fuselage Group	1700.0	41.69	0.00	12.72
Wing Group	1300.0	36.20	0.00	9.95
Empennage Group	1200.0	91.41	0.00	17.30
Landing Gear Group	240.0	45.83	0.00	4.84
Nacelle Group	0.0			
Powerplant Group	1450.0	47.56	0.00	12.79
Fixed Equipment Group	2530.0	18.22	0.00	14.17

Output Parameters

$W_{structure}$	4440.0 lb	$X_{cg_{structure}}$	ft	$Y_{cg_{structure}}$	ft	$Z_{cg_{structure}}$	ft
W_E	8420.0 lb	X_{cg_E}	41.69 ft	Y_{cg_E}	0.00 ft	Z_{cg_E}	12.79 ft

Figure 10.14. Empty weight inputs as referred from table 10.3

W_E	8420.0 lb	X_{cg_E}	41.69 ft	Y_{cg_E}	0.00 ft	Z_{cg_E}	12.79 ft

Loading Table

Component	Weight lb	X_{cg} ft	Y_{cg} ft	Z_{cg} ft
Crew	350.0	36.20	0.00	14.17
Trapped Fuel and Oil	64.4	47.56	0.00	12.79
Mission Fuel Group 1	1358.9	47.56	0.00	12.79
Mission Fuel Group 2	0.0	0.00	0.00	0.00
Passenger Group 1	0.0	0.00	0.00	0.00
Passenger Group 2	0.0	0.00	0.00	0.00
Passenger Group 3	0.0	0.00	0.00	0.00
Passenger Group 4	0.0	0.00	0.00	0.00
Baggage	0.0	0.00	0.00	0.00
Cargo	3310.0	34.14	0.00	12.79
Military Load Group 1	0.0	0.00	0.00	0.00
Military Load Group 2	0.0	0.00	0.00	0.00

Output Parameters

$W_{current}$	13503.2 lb	X_{cg}	40.32 ft	Y_{cg}	0.00 ft	Z_{cg}	12.83 ft

Figure 10.13. Total aircraft center of gravity

Input Parameters

W_{PL}	3310.0 lb	$X_{cg_{mg}}$	45.83 ft	x_{mgc_w}	7.83 ft
$W_{PL_{exp}}$	0.0 lb	X_{apex_w}	23.25 ft	$\bar{c}_w$	19.17 ft

C.G. Excursion Table

Component	Weight lb	X_{cg} ft	Load (1-13)	Unload (1-13)
Empty Weight	8420.0	41.69	1	13
Crew	350.0	36.20	2	12
Trapped Fuel and Oil	64.4	47.56	3	11
Mission Fuel Group 1	1358.9	47.56	4	10
Mission Fuel Group 2	0.0	0.00		
Passenger Group 1	0.0	0.00		
Passenger Group 2	0.0	0.00		
Passenger Group 3	0.0	0.00		
Passenger Group 4	0.0	0.00		
Baggage	0.0	0.00		
Cargo	3310.0	34.14	5	9
Military Load Group 1	0.0	0.00		
Military Load Group 2	0.0	0.00		

Output Parameters

$W_{current}$	13503.2 lb	X_{cg}	40.32 ft

Figure 10.15. C.G excursion plot input for x-direction with X_{cg}

10.3 Discussion

Fig. 10.9 gives the excursion plot with the main gear and wing mean aerodynamic chord. The cargo component is nothing but a payload for the case of X-69 with total payload weight of 3,310 lbs. Also, while considering a payload C.G, instead of one canister and CubeSat, total weight of 24 canisters and CubeSats with C.G location at the center with respect to the payload area. The most aft C.G is well forward of the main landing gear contact point at 42.5 ft and the most forward C.G is at 41.5 ft referring from the C.G excursion plot in fig 10.9.

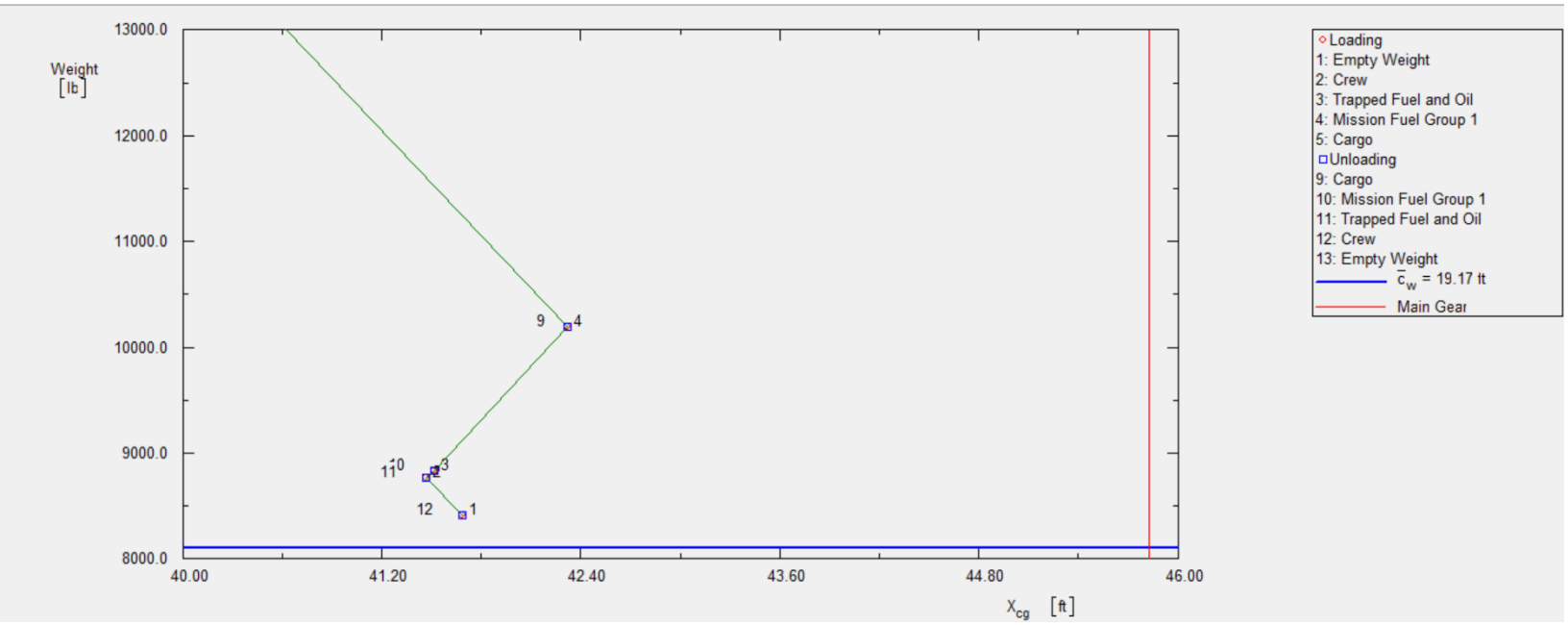

Figure 10.16. C.G excursion plot for X-69

10.4 Conclusion

From the Class I weight and balance analysis, it appears that the gear configuration will be satisfactory from a weight and balance viewpoint. It is acceptable to move forward with above landing gear configuration that will have main gears under the wing and nose-skid. The main gear up on retraction swiftly accommodates in the dorsal part of the fuselage.

11. Chapter. 11 Stability and Control Analysis

11.1 Introduction

This part of the report examines whether the configurations incorporated to X-69 has a satisfactory stability and control characteristics. As usual this estimation is done using Class I method for stability and control analysis. The method as referred deals with about 16 steps among most of the steps are not eligible due to their operating conditions and mission profile. The steps sub-divided into:

- Static longitudinal stability (Longitudinal X-plot)
- Static directional stability (Directional X-plot)
- Minimum control speed with one engine out. This step is skipped since powered phase of the flight is only climb using hybrid rocket engine with one-time firing capabilities with rest flight unpowered.

11.2 Static Longitudinal Stability

To carry longitudinal analysis, we need two curves represented as "legs" against X-plot.

1) The c.g leg represents the rate at which the c.g moves aft (fwd) as a function of horizontal tail area.
2) The a.c leg represents the rate at which the a.c moves aft (fwd) as a function of horizontal tail area.

The c.g and a.c leg are computed with the help of AAA program. This assists to determine the proposed configuration of X-69 will have satisfactory stability and control characteristics. The static margin is found using the area of the lifting surface which has been determined earlier to check whether the X-69 is inherently stable. Inherent stability is required of all airplanes which do not rely on a feedback augmentation system for their stability. X-69 however falls in the category where minimum 5% of static margin is desired. This allows to incorporate the feedback augmentation system into the configuration to provide relaxed stability to the airplane.

The static margin is computed considering the variation of X-69 c.g with horizontal tail, $dX_{cg}/dS_h = 0.02062 ft^{-1}$.

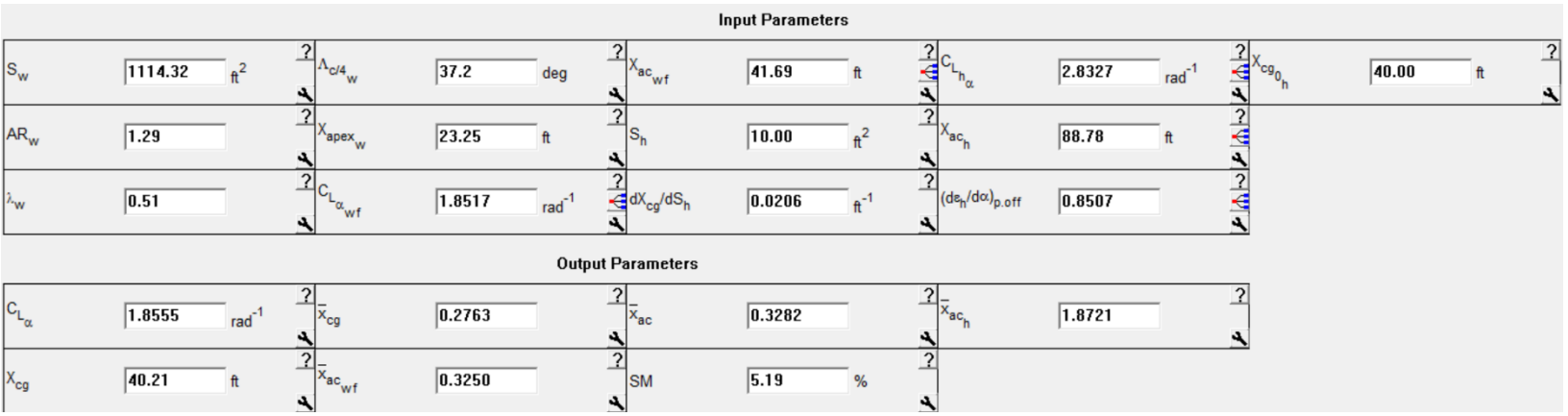

Figure 11.1. Static margin calculation

Table 11.1. X-locations of c.g and a.c in terms of wing aerodynamic chord

S_h	$\bar{x}_{cg}$	$\bar{x}_{ac}$
0	0.2695	0.325
10	0.2763	0.3282
20	0.283	0.3313
30	0.2898	0.3345
40	0.2966	0.3376
50	0.3034	0.3407
60	0.3101	0.3438
70	0.3169	0.3469
80	0.3237	0.35
90	0.3305	0.353
100	0.3372	0.3561
101.99	0.3386	0.3567
110	0.344	0.3591
120	0.3508	0.3621
130	0.3576	0.3652
140	0.3643	0.3682
150	0.3711	0.3711
160	0.3779	0.3741
170	0.3847	0.3771
180	0.3914	0.38
190	0.3982	0.383
200	0.405	0.3859
210	0.4118	0.3888
220	0.4185	0.3918
230	0.4253	0.3946
240	0.4321	0.3975
250	0.4389	0.4004

From the longitudinal X-plot in fig 11.3, we can observe that X-69 is longitudinally unstable without a horizontal tail. At the horizontal tail area of 101.99 ft^2, the level of instability is $0.0181\bar{c}_w$ where X-69 is designed to a level of instability of $0.3567\bar{c}_w$ at its aft c.g. Hence, for the purpose of p.d. study a level of instability of $0.0181\bar{c}_w$ is arbitrarily selected.

Using the aft c.g leg of fig. 11.2, it is found that the longitudinal stability augmentation system must generate a value of incremental static margin of:

$$\Delta SM = 0.0181 + 0.05 = 0.0681$$

The total airplane lift curve slope was computed to be: $C_{L_\alpha} = 1.8904\, rad^{-1}$. The value of the elevon control power derivative was found to be: $C_{m_{\delta_e}} = -0.0289\, rad^{-1}$.

With these values and with equation 11.1, it follows that: $k_\alpha = -0.1833$ which is an acceptable value of feedback gain. The horizontal tail area of 101.99 ft^2 will be kept.

$$k_\alpha = (\Delta SM).\, C_{L_\alpha}/C_{m_{\delta_e}} \tag{11.1}$$

where,

$$C_{L_\alpha} = C_{L_{\alpha_{wf}}} + C_{L_{\alpha_h}}(1 - d\varepsilon/d\alpha)(S_h/S)$$

Input Parameters

S_w	1114.32	ft^2	$\Lambda_{c/4_w}$	37.2	deg	$X_{ac_{wf}}$	41.69	ft	$C_{L_{h_\alpha}}$	2.8327	rad^{-1}	$C_{m_{\delta_e}}$	-0.0289	rad^{-1}
AR_w	1.29		X_{apex_w}	23.25	ft	S_h	101.99	ft^2	X_{ac_h}	88.78	ft	$C_{m_{i_h}}$	-0.3288	rad^{-1}
λ_w	0.51		$C_{L_{\alpha_{wf}}}$	1.8517	rad^{-1}	dX_{cg}/dS_h	0.0206	ft^{-1}	$(d\varepsilon_h/d\alpha)_{p.off}$	0.8507		$X_{cg_{0_h}}$	40.00	ft

Output Parameters

C_{L_α}	1.8904	rad^{-1}	$\bar{x}_{cg}$	0.3386		$\bar{x}_{ac}$	0.3567		K_α	-0.18	
X_{cg}	42.10	ft	$\bar{x}_{ac_{wf}}$	0.3250		SM	1.81	%	$\bar{x}_{ac_h}$	1.8721	

Figure 11.3. Class I longitudinal gain calculation

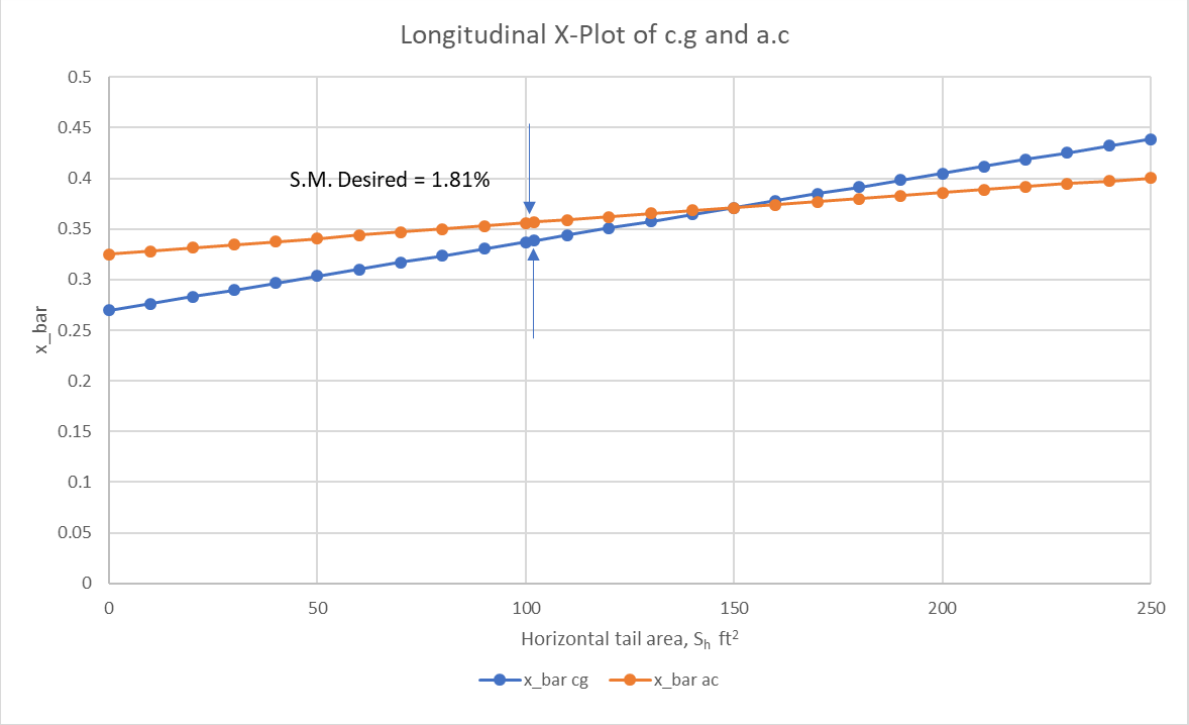

Figure 11.2. Longitudinal plot of c.g and a.c

11.3 Static Directional Stability

Similar to the longitudinal, the static directional stability is determined using directional X-plot of X-69 which contains a c.g leg with respect to weight per ft^2 of the vertical tail. The X-69 has twin booms with twin vertical tail attached. The C_{n_β} leg of the X-plot follows from:

$$C_{n_\beta} = C_{n_{\beta_{wf}}} + C_{L_{\alpha_V}}.(S_v/S)(x_v/b)$$

Using AAA's directional stability, the c.g leg is computed which can be referred from table 11.2 and plot in fig 11.5. The values in table 11.2 are obtained from following inputs as shown in fig 11.4.

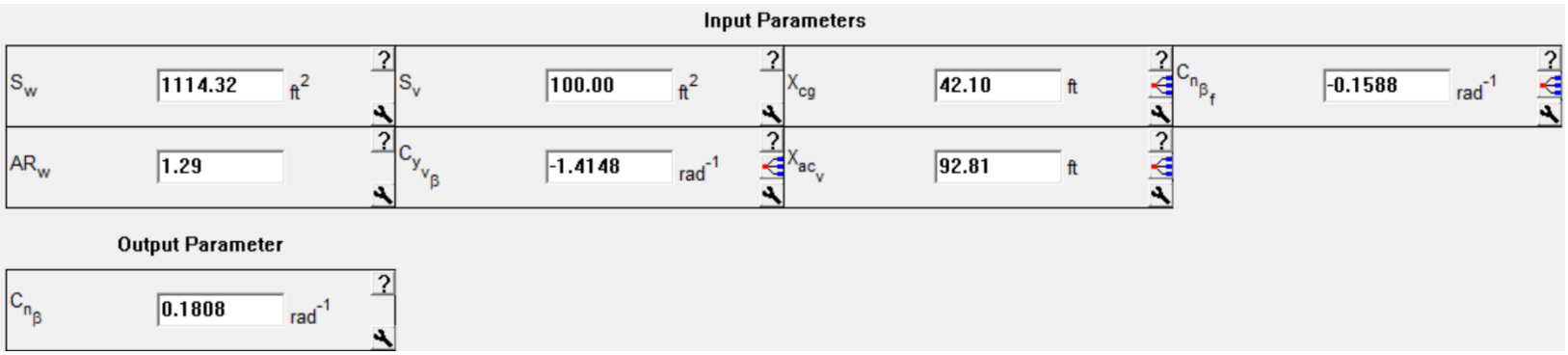

Figure 11.4. I/O for directional stability

Table 11.2. X-location of c.g. in directional stability

S_v	C_{n_β}
0	-0.1588
10	-0.1248
20	-0.0909
30	-0.0569
33.33	-0.0456
40	-0.0229
50	0.011
60	0.045
70	0.079
80	0.1129
90	0.1469
100	0.1808

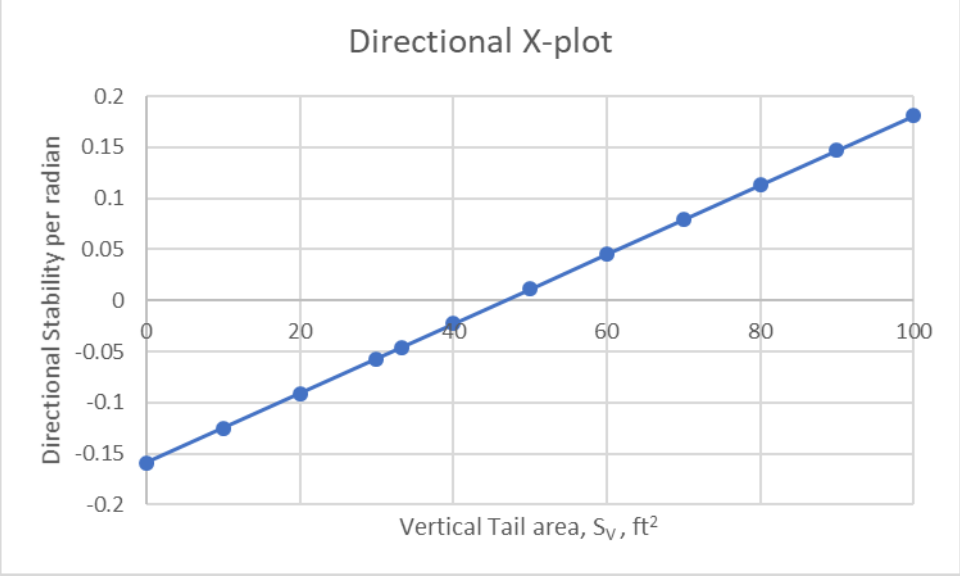

Figure 11.5. Directional x-plot of X-69

From plot fig 11.5, we can observe that the vertical tail of the X-69 renders the airplane directionally unstable at a level of $C_{n_\beta} = -0.0456\, rad^{-1}$. Desired is a 'de-facto" level of 0.0010. The decrement of 0.0466 must be provided by the sideslip feedback system.

The rudder control system power derivative of the X-69 was computed to be: $C_{n_{\delta_r}} = 0.003\, rad^{-1}$. With the help of equation 11.2, the feedback gain can be computed to be: $k_\beta = 33.91 rad/rad$

$$k_\beta = \left(\Delta C_{n_\beta}\right) / \left(C_{n_{\delta_r}}\right) \tag{11.2}$$

12. Chapter 12. Drag Polar Estimation

The drag polar estimation accounts for wetted area of the airplane split it into major components such as fuselage and tailbooms, wing, empennage and other components. The method used is a Class I method for drag polar determination.

In this method, above major components of the X-69 are enlisted below along with their wetted areas computed from AAA using following equations:

12.1 Wing

Wetted area of the wing is given by,

$$S_{wet_w} = 2.S_{net_w}.\left(1 + \frac{\left(\frac{t}{c}\right)_{f_w}}{4}\right)\left(\frac{1 + \tau_w.\lambda_{exp_w}}{1 + \lambda_{exp_w}}\right) \tag{12.1}$$

where,

S_{wet_w} = Wetted area of the wing,

S_{net_w} = Net planform area of the wing,

$\left(\frac{t}{c}\right)_{f_w}$ = The thickness ratio at the fuselage,

λ_{exp_w} = Exposed taper ratio of the wing,

τ_w = ratio of the tip thickness ratio to the thickness ratio at the fuselage

Using the wing estimated parameters such as shown in I/O fig 12.1, the wetted area of the wing can be estimated:

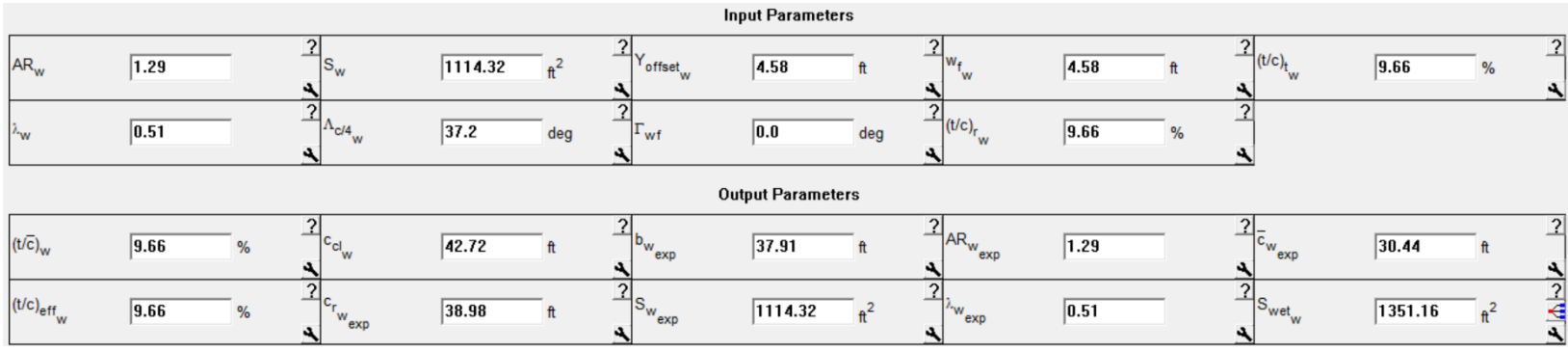

Figure 12.1. I/O parameters to compute wetted area of the wing

12.2 Fuselage

Wetted area of the fuselage is given by,

For fuselage with cylindrical mid-sections:

$$S_{wet_f} = \pi.D_f.l_f.\left(1 - \frac{2}{\lambda_f}\right)^{2/3}\left(1 + \left(\frac{1}{\lambda_f}\right)^2\right) \tag{12.2}$$

where,

S_{wet_f} = Wetted area of the fuselage.

$\lambda_f = l_f/D_f$, the fuselage fineness ratio

The above parameters are computed in fuselage section using AAA as shown in fig 12.2 to 12.4. The perimeter plot of the fuselage including nose, cockpit, payload compartment and rocket housing is plotted against the fuselage station F.S. The 90 stations can be referred from the appendix 11 including the perimeter output.

Input Parameters

X_{apex_f}	0.00 ft	i_f	0.00 deg	X_{apex_h}	85.00 ft	c_{r_v}	6.67 ft	$N_{f_{stations}}$	90		
Y_{apex_f}	0.00 ft	X_{apex_w}	23.25 ft	c_{r_h}	7.99 ft	$(X,Z)_{apex_f}$	Apex is not included				
Z_{apex_f}	7.50 ft	c_{r_w}	38.98 ft	X_{apex_v}	86.89 ft	$(X,Y,Z)_{fus}$	Fuselage Coordinate System				

Fuselage Table: double click for Cross-Section Dialog

Fuselage	x_{fus_1} ft	y_{fus_1} ft	z_{fus_1} ft	y_{fus_2} ft	z_{fus_2} ft	y_{fus_3} ft	z_{fus_3} ft	$y_{fus_{12}}$ ft	$z_{fus_{12}}$ ft	$\rho_{fus_{12}}$	$y_{fus_{23}}$ ft	$z_{fus_{23}}$ ft	$\rho_{fus_{23}}$	A_{fus_i} ft^2	s_{fus} ft
Section	Input	Input	Input	Input	Input	Input	Input	Input	Input	Input	Input	Input	Input	Output	Output
1	1.2588	0.0000	0.2305	0.2283	-0.0383	0.0000	-0.3071	0.2280	0.2305	0.7077	0.2280	-0.3071	0.7077	0.19	1.5647
2	2.0143	0.0000	0.3679	0.3656	-0.0632	0.0000	-0.4944	0.3654	0.3679	0.7077	0.3654	-0.4944	0.7077	0.50	2.5082
3	2.7727	0.0000	0.5053	0.5029	-0.0882	0.0000	-0.6817	0.5028	0.5053	0.7077	0.5028	-0.6817	0.7077	0.94	3.4516

Figure 12.2. Input parameters for fuselage wetted area

Output Parameters

l_f	67.50 ft	S_{B_s}	565.57 ft^2	S_o	88.68 ft^2	Z_{fc_w}	8.75 ft				
$h_{f_{max}}$	10.83 ft	S_{plf_f}	478.89 ft^2	V_f	3793.18 ft^3	h_{f_w}	10.83 ft				
$w_{f_{max}}$	9.17 ft	S_{wet_f}	1773.42 ft^2	X_{c_f}	38.71 ft	$D_{f_{max_w}}$	10.63 ft				
S_{b_f}	26.01 ft^2	X_1	24.01 ft	$h_{f_{0.25}}$	7.21 ft	h_{f_h}	0.00 ft				
$S_{f_{max}}$	88.68 ft^2	X_o	38.76 ft	$h_{f_{0.75}}$	10.26 ft	D_{f_h}	0.00 ft				

Figure 12.3. Output parameters of fuselage with wetted area

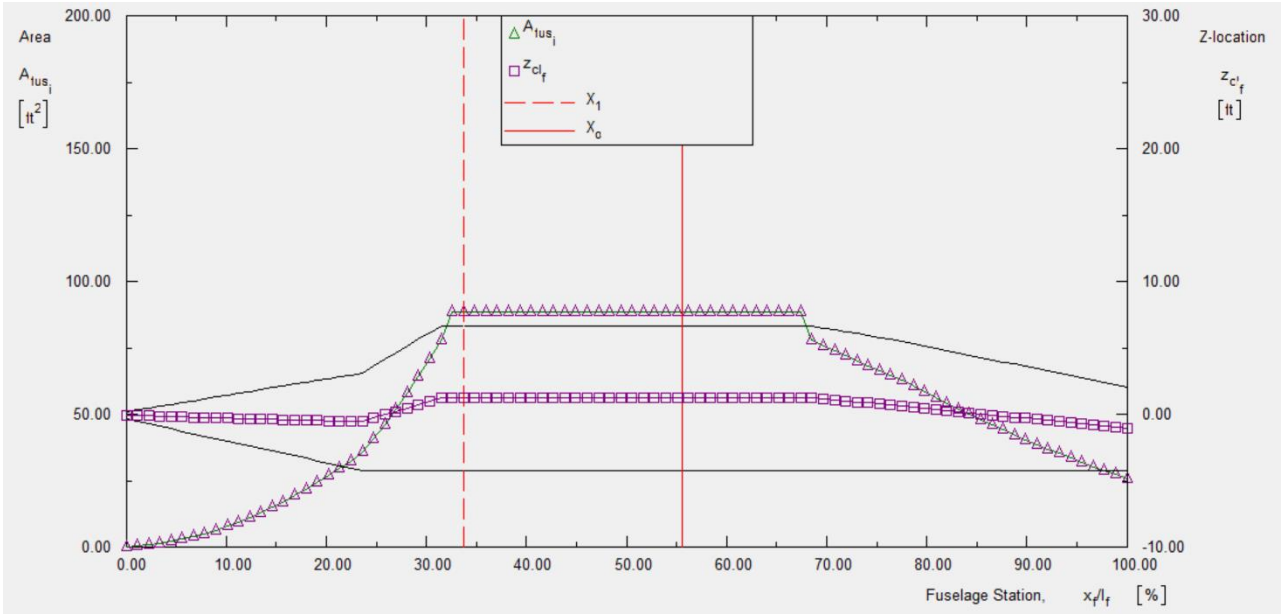

Figure 12.4. Perimeter plot

12.3 Tailbooms

Wetted area of the tailboom is computed similar to that of fuselage, which is given by,
For fuselage with cylindrical mid-sections:

$$S_{wet_{\Sigma\, tb}} = \pi . D_{tb} . l_{tb} . \left(1 - \frac{2}{\lambda_{tb}}\right)^{2/3} \left(1 + \left(\frac{1}{\lambda_{tb}}\right)^2\right) \tag{12.3}$$

where,
$S_{wet_{\Sigma\, tb}}$ = Total Wetted area of the two Tailbooms.
$\lambda_{tb} = l_{tb}/D_{tb}$, the fuselage fineness ratio

Input Parameters

$X_{nose_{tb}}$	42.45 ft	$Z_{nose_{tb}}$	5.00 ft	Ψ_{tb}	90.0 deg	$(X,Z)_{apex_{tb}}$	Apex is not included	$N_{tb_{stations}}$	90		
$Y_{nose_{tb}}$	18.94 ft	i_{tb}	0.00 deg	Γ_{tb}	0.0 deg	$(X,Y,Z)_{tb}$	Airplane Coordinate System				

Tailboom 1 Table, double click for Cross-Section Dialog

Station	x_{tb_1} ft	y_{tb_1} ft	z_{tb_1} ft	y_{tb_2} ft	z_{tb_2} ft	y_{tb_3} ft	z_{tb_3} ft	$y_{tb_{12}}$ ft	$z_{tb_{12}}$ ft	$\rho_{tb_{12}}$	$y_{tb_{23}}$ ft	$z_{tb_{23}}$ ft	$\rho_{tb_{23}}$	A_{tb_i} ft^2	s_{tb} ft
Section	Input	Input	Input	Input	Input	Input	Input	Input	Input	Input	Input	Input	Input	Output	Output
1	48.4708	23.5300	3.0342	23.6617	2.9300	23.5300	2.8258	23.6617	3.0342	0.9350	23.6617	2.8258	0.9350	0.05	0.8931
2	48.9877	23.5300	3.2184	23.6635	3.0221	23.5334	2.8258	23.6617	3.2184	0.9350	23.6653	2.8258	0.9350	0.10	1.2435
3	49.5045	23.5300	3.4027	23.6653	3.1143	23.5367	2.8258	23.6617	3.4027	0.9350	23.6689	2.8258	0.9350	0.15	1.5986

Figure 12.5. Input parameters for tailboom wetted area

The above parameters are computed in tailboom section using AAA as shown in fig 12.5 to 12.7. The perimeter plot of the tailboom including nose, body and tail is plotted against the fuselage station F.S. The 90 stations can be referred from the appendix 11 including the perimeter output.

Output Parameters

Coordinates Defined	$S_{b_{tb}}$	1.05 ft^2	$S_{plf_{tb}}$	7.95 ft^2	$S_{wet_{\Sigma tb}}$	1067.50 ft^2	
l_{tb} 46.00 ft	$S_{tb_{max}}$	1.43 ft^2	$S_{wet_{tb}}$	539.03 ft^2			

Figure 12.6. Output parameters of tailboom with wetted area

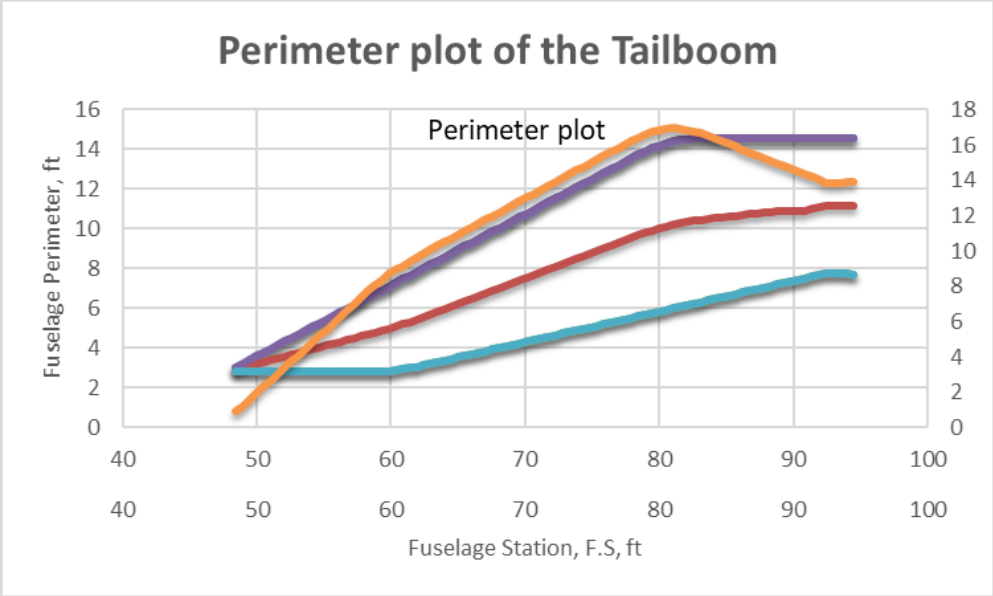

Figure 12.7. Perimeter plot of tailboom

12.4 Horizontal Tail

Wetted area of the Horizontal tail is given by,

$$S_{wet_h} = 2.S_{net_h}.\left(1 + \frac{\left(\frac{t}{c}\right)_{f_h}}{4}\right)\left(\frac{1 + \tau_h.\lambda_{exp_h}}{1 + \lambda_{exp_h}}\right) \tag{12.4}$$

where,
S_{wet_h}= Wetted area of the Horizontal Tail
S_{net_h}= Net planform area of the Horizontal Tail,
$\left(\frac{t}{c}\right)_{f_h}$ = The thickness ratio at the fuselage,
λ_{exp_h}= Exposed taper ratio of the Horizontal Tail,
τ_h= ratio of the tip thickness ratio to the thickness ratio at the fuselage

Using the H.T estimated parameters such as shown in I/O fig 12.8, the wetted area of the H.T can be estimated:

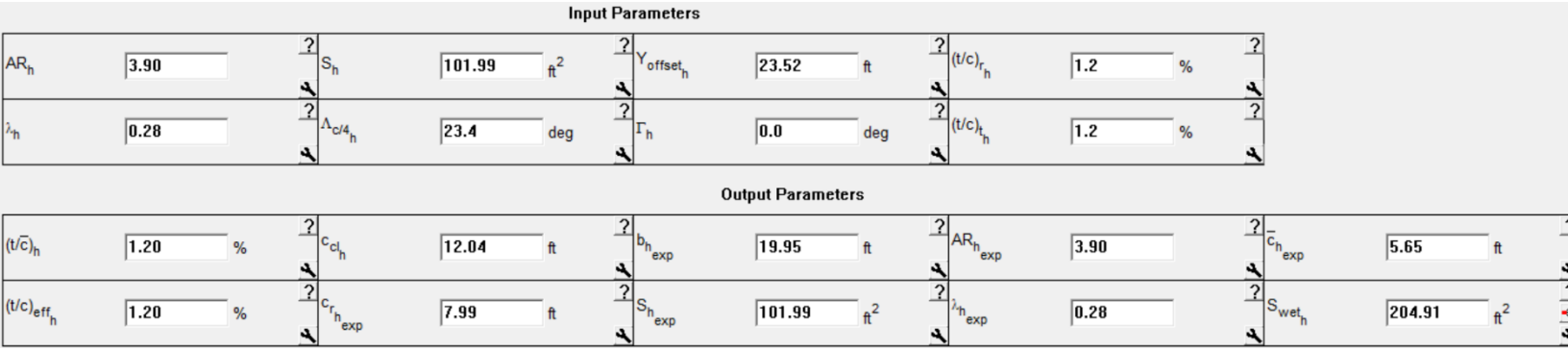

Figure 12.8. I/O parameters to compute the wetted area of H.T

12.5 Vertical Tail

Wetted area of the Vertical tail is given by,

$$S_{wet_v} = 2.S_{net_v}.\left(1 + \frac{\left(\frac{t}{c}\right)_{f_v}}{4}\right)\left(\frac{1 + \tau_v.\lambda_{exp_v}}{1 + \lambda_{exp_v}}\right) \tag{12.5}$$

where,
S_{wet_v}= Wetted area of the Vertical Tail
S_{net_v}= Net planform area of the Vertical Tail,
$\left(\frac{t}{c}\right)_{f_v}$ = The thickness ratio at the fuselage,
λ_{exp_v}= Exposed taper ratio of the Vertical Tail,
τ_v= ratio of the tip thickness ratio to the thickness ratio at the fuselage

Using the V.T estimated parameters such as shown in I/O fig 12.9, the wetted area of the V.T can be estimated:

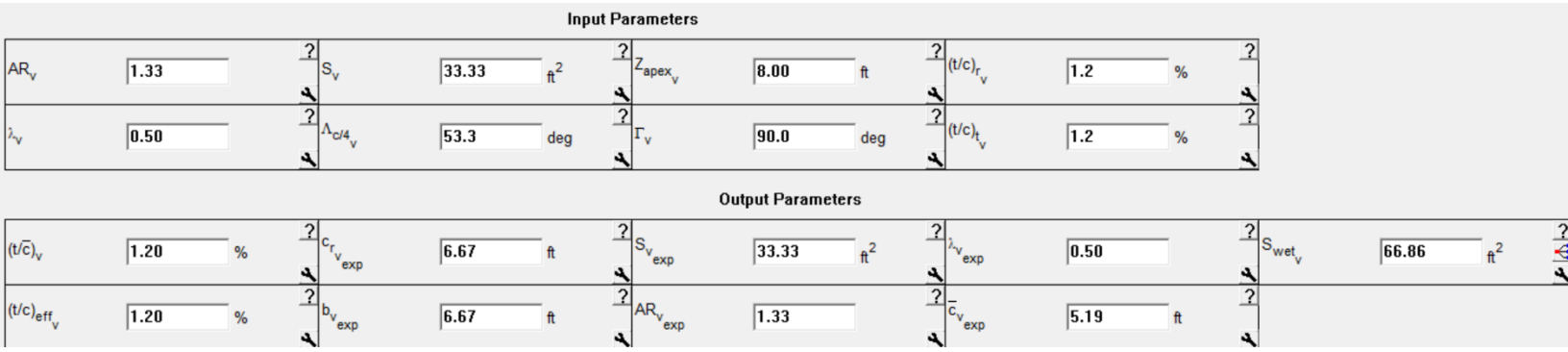

Figure 12.9. I/O parameters to compute the wetted area of V.T

12.6 Total Wetted Area

Total wetted area is computed adding all above wetted areas as shown in table 12.1.

Table 12.1. Wetted areas of major components of X-69

Component	Wetted Area, ft^2
Fuselage, S_{wet_f}	1,773.42 ft^2
Wing including spoilers, S_{wet_w}	1,351.16 ft^2
Tailbooms, $S_{wet_{\Sigma tb}}$	1,067.5 ft^2
Horizontal Tail, S_{wet_h}	204.91 ft^2
Vertical Tail, S_{wet_v}	66.86 ft^2
Total, S_{wet}	**4,530.70 ft^2**

13. All View of X-69 CargoSat

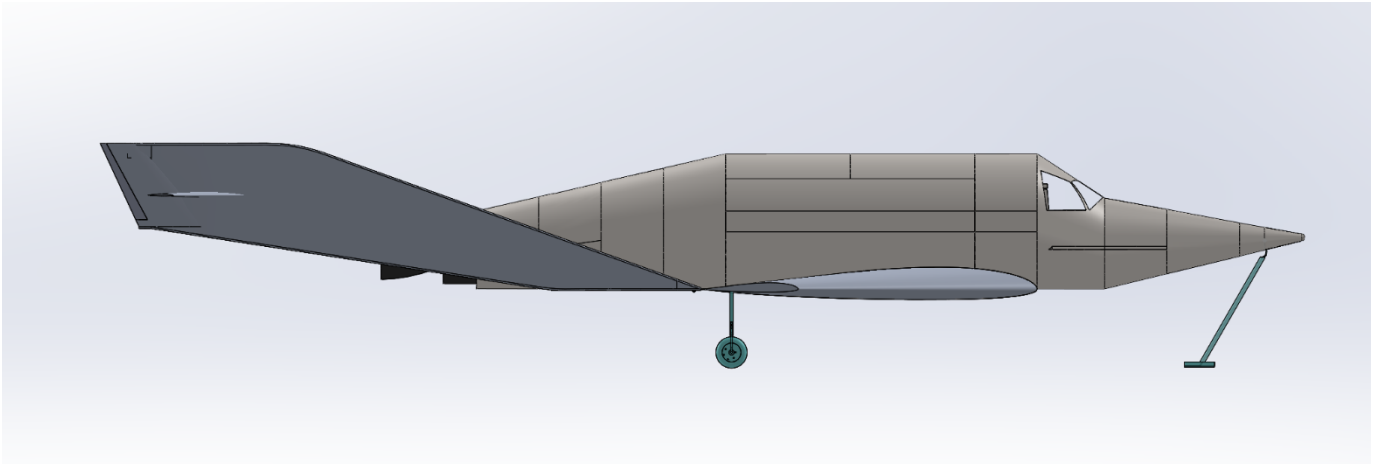

Figure 13.1. Side view of X-69 CargoSat

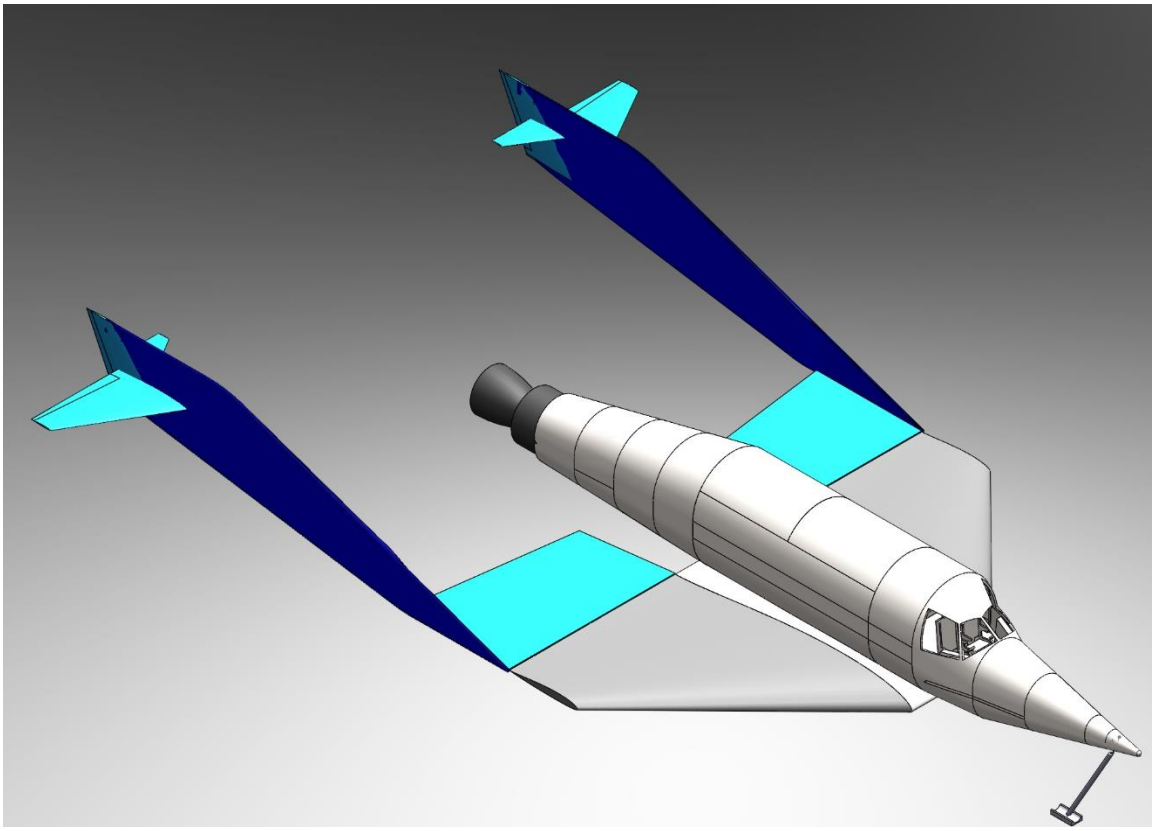

Figure 13.2. Isometric view X-69 CargoSat

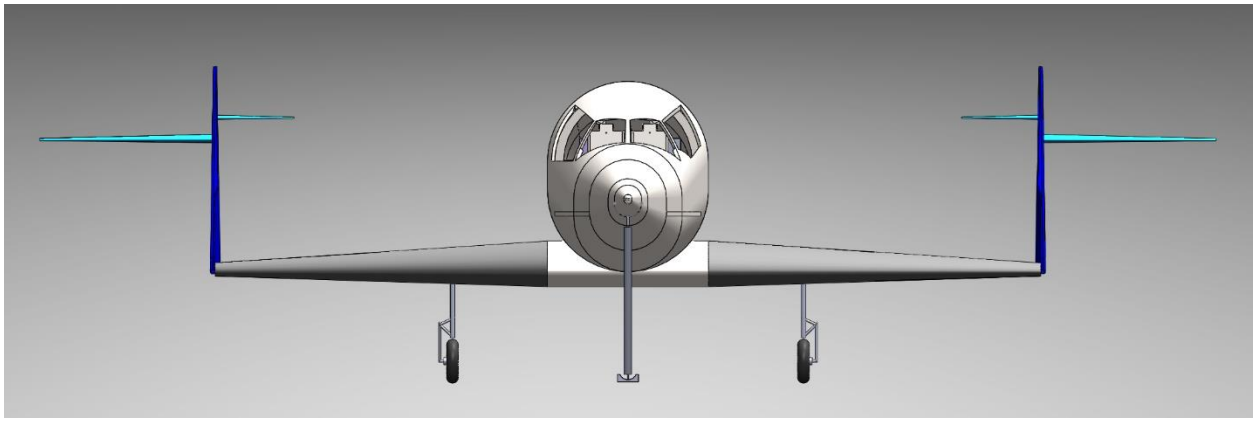

Figure 13.4. Front view of X-69 CargoSat

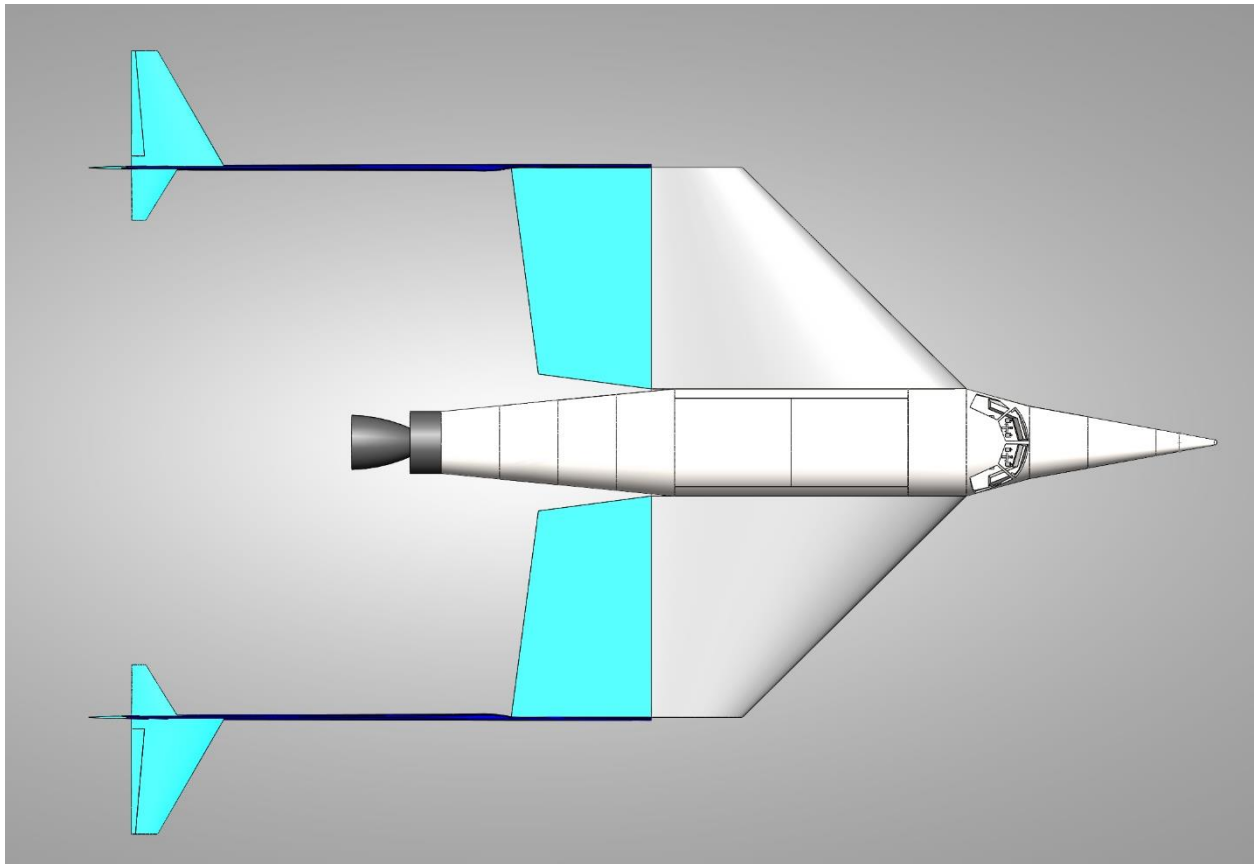

Figure 13.3. Top view of X-69 CargoSat

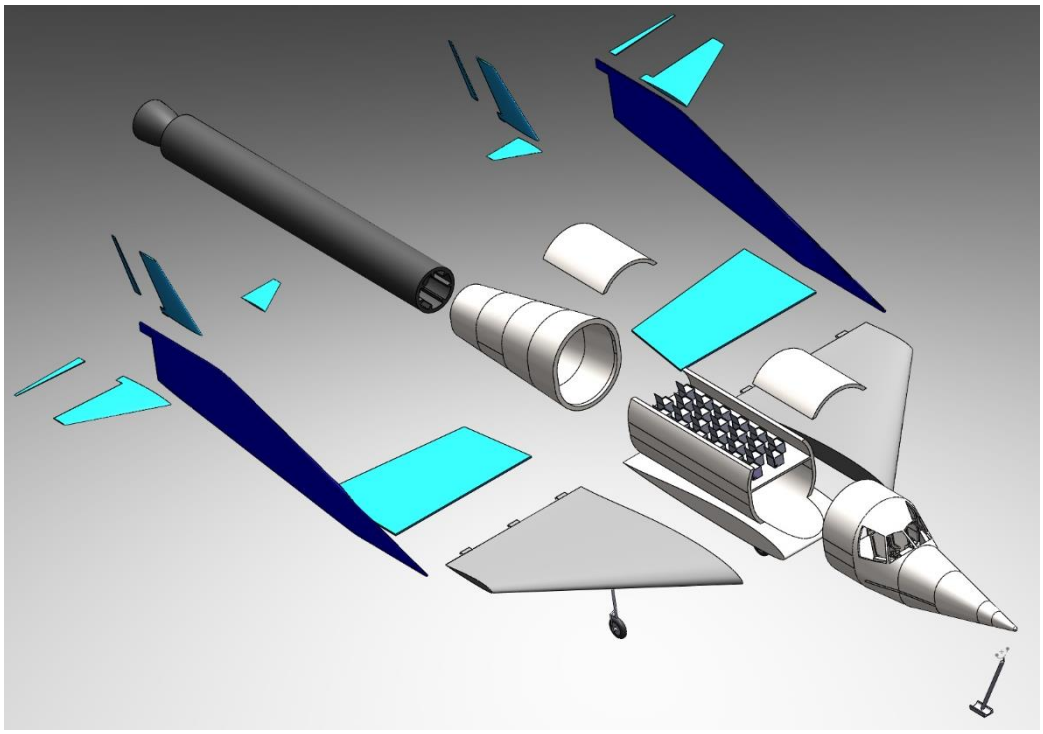

Figure 13.6. Exploded view of X-69 CargoSat

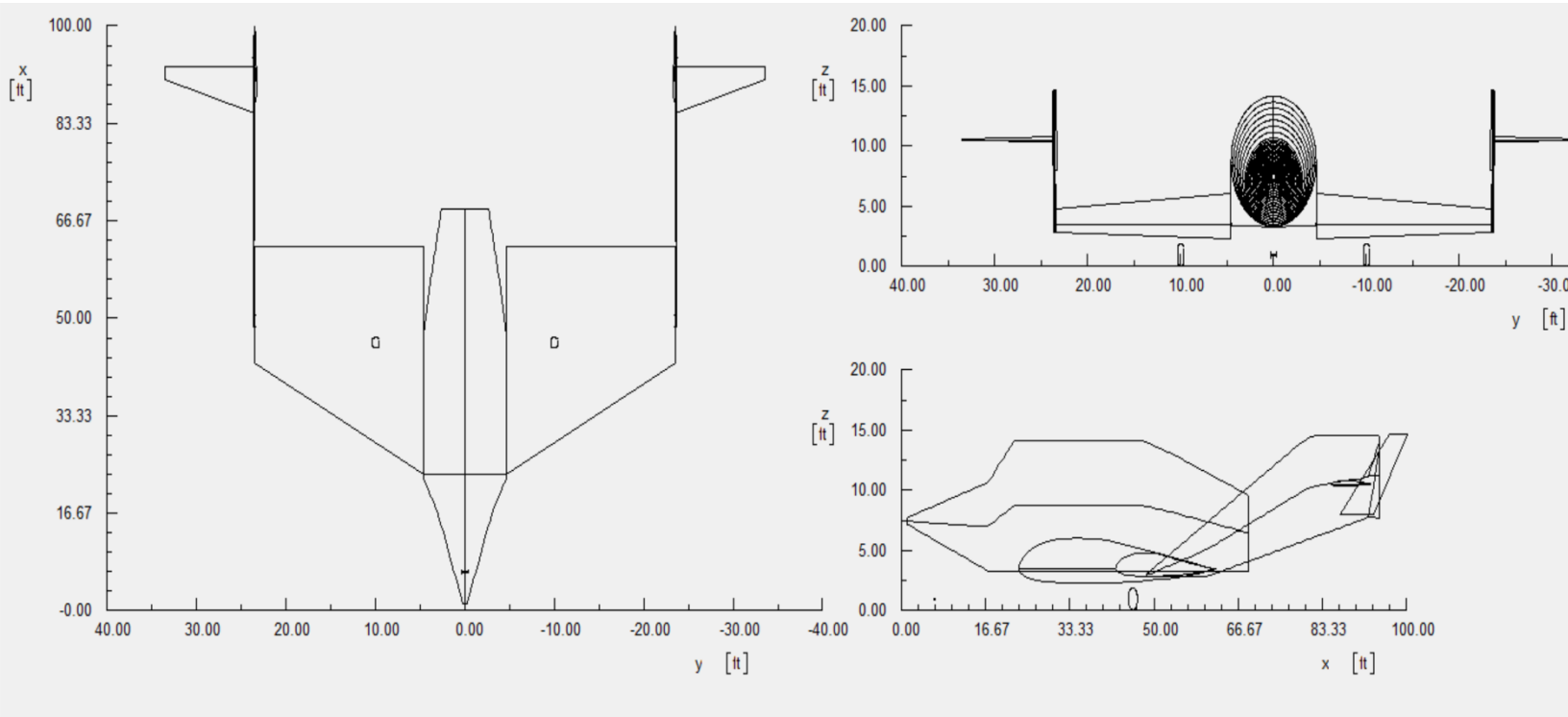

Figure 13.5. AAA output design of X-69 CargoSat

References

Roskam, J. (1997). *Airplane Design Part I - Preliminary Sizing of Airplanes* (Vol. I). Ottawa, Kan.: Roskam Aviation and Engineering Corp.

Roskam, J. (1997). *Airplane Design Part II - Preliminary Configuration Design and Integration of Propulsion System* (Vol. II). Ottawa, Kan.: Roskam Aviation and Engineering Corp.

Roskam, J. (1997). *Airplane Design Part III - Layout Design of Cockpit, Fuselage, Wing, Empennage - Cutaways and Inboard profiles* (Vol. III). Ottawa, Kan.: Roskam Aviation and Engineering Corp.

Roskam, J. (1997). *Airplane Design Part IV - Layout Design of Landing Gears and Systems* (Vol. IV). Ottawa, Kan.: Roskam Aviation and Engineering Corp.

Roskam, J. (1997). *Airplane Design Part V – Component Weight Estimation* (Vol. V). Ottawa, Kan.: Roskam Aviation and Engineering Corp.

Roskam, J. (1997). *Airplane Design Part VI - Preliminary Calculation of Aerodynamic, Thrust and Power Characteristics* (Vol. VI). Ottawa, Kan.: Roskam Aviation and Engineering Corp.

Roskam, J. (1997). *Airplane Design Part VII - Determination of Stability, Control and Performance Characteristics - FAR & Military Requirements* (Vol. VII). Ottawa, Kan.: Roskam Aviation and Engineering Corp.

Roskam, J. (1997). *Airplane Design Part VIII – Airplane Cost Estimation: Design, Development, Manufacturing and Operating* (Vol. VIII). Ottawa, Kan.: Roskam Aviation and Engineering Corp.

Raymer, D. (2019). *Aircraft Design: A Conceptual Approach* (Second). S.l.: AIAA - Education Series.

Anderson, J. D. (2007). *Fundamentals of Aerodynamics*. London: Mcgraw-hill Publishing Co.

Griffin, M. D., & French, J. R. (2004). *Space vehicle design*. Reston, VA: American Institute of Aeronautics and Astronautics.

Sutton, G. P., & Biblarz, O. (2000). *Rocket propulsion elements: an Introduction to the Engineering of Rockets* (VIII). New York: John Wiley & Sons.

Mattingly, J. D. (1996). *Elements of Gas Turbine Propulsion and Rockets* (II). New York: McGraw-Hill.

Anderson, J. D. (2000). *Introduction to flight* (III). Boston: McGraw-Hill.

Sidi, M. J. (1997). *Spacecraft Dynamics and Control: A Practical Engineering Approach*. Cambridge: Cambridge University Press.

Bate, R. R., Mueller, D. D., White, J. E., & Saylor, W. W. (1971). *Fundamentals of Astrodynamics*. Mineola, NY: Dover Publications, Inc.

Cook, M. A. (2007). *Flight Dynamics Principles* (II). Butterworth Heinemann.

Larson, W. J. (1997). *Space Mission Analysis and Design* (III). Torrance, CA: Microcosm.

Curtis, H. D. (2016). *Orbital Mechanics for Engineering students* (III). Amsterdam: Butterworth-Heinemann.

Aldheeb, M. A., Omar, H. M., Idres, M., & Abido, M. A. (2012). Design Optimization of Micro Air Launch Vehicle Using Differential Evolution. *Design Optimization of Micro Air Launch Vehicle Using Differential Evolution*, *4*(2), 1–12.

Bhattacharjya, R. K. (2007). *Introduction to Differential Evolution*.

Azami, M. H. (2014). Enhancement of Regression Rate in Hybrid Rocket Motor using various techniques. *Enhancement of Regression Rate in Hybrid Rocket Motor Using Various Techniques*, 1–24.

Piggott, D. (2002). *Gliding: a handbook on soaring flight*. London: A. & C. Black.

JetWhiz, & Charles. (2013). *Global Aircraft -- X-15*. Retrieved from https://www.globalaircraft.org/planes/x-15_hyper.pl

North American X-15. (2020, May 10). Retrieved from https://en.wikipedia.org/wiki/North_American_X-15

Evans, M. (2013). *X15FlightLog.pdf*. Retrieved from http://www.mach25media.com/Resources/X15FlightLog.pdf

Storm, R., Skor, M., & Koch, L. D. (2007, April 13). *Pushing the Envelope: A NASA Guide to Engines*. Retrieved 2016, from https://er.jsc.nasa.gov/seh/ANASAGUIDETOENGINES[1].pdf

David, L. (2015, August 13). *US Military's Top-Secret X-37B Space Plane Mission Nears 3-Month Mark*. Retrieved from https://www.space.com/30245-x37b-military-space-plane-100-days.html
X-37B Orbital Test Vehicle. (2018, September 1). Retrieved 2016, from https://www.af.mil/About-Us/Fact-Sheets/Display/Article/104539/x-37b-orbital-test-vehicle/
X-37B OTV – Spacecraft & Satellites. (n.d.). Retrieved 2016, from http://spaceflight101.com/spacecraft/x-37b-otv
Dunbar, B. (2015, August 13). *NASA Dryden Fact Sheets - X-15 Hypersonic Research Program*. Retrieved December 2016, from https://www.nasa.gov/centers/armstrong/news/FactSheets/FS-052-DFRC.html
Martinez-Val, R., & Perez, E. (1997). *Teaching Airplane Design: A Multi-Level Approach*. Retrieved 2016, from https://www.ijee.ie/articles/Vol13-4/ijee950.pdf
Siegmann, H. (2001, September 3). *Airfoil Database for Tailless and Flying Wings.* Retrieved 2016, from http://www.aerodesign.de/english/profile/profile_s.htm
3 Airfoils and Airflow. (1996). Retrieved 2016, from http://www.av8n.com/how/htm/airfoils.html
Greer, D., Hamory, P., Krake, K., & Drela, M. (2000). Design and Predictions for High-Altitude (Low Reynolds Number) Aerodynamic Flight Experiment. *Journal of Aircraft*, *37*(4), 684–689. doi: 10.2514/2.2652
Glider flying handbook. (2003). Retrieved from https://www.faa.gov/regulations_policies/handbooks_manuals/aircraft/glider_handbook/
Products & Services: XPOD Separation System. (2014, January 25). Retrieved 2017, from http://utias-sfl.net/?page_id=87
Mission. (n.d.). Retrieved from https://www.virgingalactic.com/mission/
Badgujar , R., Aguilar, D., Gogula, M., Mendez, C., & Mirador, R. (n.d.). *Space-Based Laser Power Station for In-Space Propulsion.*
Borchardt, M. (n.d.). *The Lagrange points in the Earth-Moon system.*
eoPortal directory. (n.d.). Retrieved from https://directory.eoportal.org/web/eoportal/satellite- missions/c-missions/cubesat-concept
Naisbitt, J. (1978). *Satellite Power System (SPS) Centralization/Decentralization.* Washington, D.C.: DOE/NASA.
Narang, S., Ventura, S., Lorents, D. C., Mill, T., & Mooney, J. L. (n.d.). *High-Flux Solar Photon Processes.*
Safe Hybrid Rocket. (n.d.). Retrieved 2019, from https://openspace.fandom.com/wiki/Safe_Hybrid_Rocket
EASA. (2016). Certification Specifications and Acceptable Means of Compliance for Large Aeroplanes CS-25, *CS*(25), 1–1036. Retrieved from https://www.easa.europa.eu/sites/default/files/dfu/CS-25 Amendment 18.pdf
Barnes, C. S. (1966). A Developed Theory of Spoilers on Aerofoils. *Ministry of Aviation ARC*, *C.P.No*, 887. Retrieved from http://naca.central.cranfield.ac.uk/reports/arc/cp/0887.pdf

Appendix. A

Following is the MATLAB code to iterate for Take-off weight.

```
clc; clear all; close all;
%%
Wpl = 3310; % input your payload weight
A = -0.423; % regression coefficient, A for your aircraft
B = 1.163; % regression coefficient, B for your aircraft
fprintf('Wto w1 w2 w3 w4 w5 We comparison');
for Wto = 14000:10:14300 % create a for loop around the guessed take-off
%weight
w1 = Wto*0.99;
%% Phase II - takeoff/Air launch, w2
w2 = w1*0.995;
%% Phase III - Climb, w323
w3 = w2*0.9;
%% Phase IV - Descent, w4 (glide)
w4 = w3*0.993;
%% Phase V - Landing, w5 (glide)
w5 = w4*0.995;
mff = w5/Wto;
Wf = (1-mff)*Wto;
r = ((log10(Wto))-A)/B;
We = 10^r;
Woe_tent = Wto-Wf-Wpl;
We_tent = Woe_tent-0.005*Wto-350;
comparison = (abs(We-We_tent)/((We_tent+We)/2))*100;
fprintf('\n');
fprintf('%f %f %f %f %f %f %f %f %f %f',Wto,w1,w2,w3,w4,w5,We,comparison,Wf);
end
```

And a solver mention section 3.3 where the obtained take-off weight can be re-verified used given equation

```
clc; close all; clear all;
%%
A=-0.423;
B=1.163;
C=0.872;
D=3660;
syms x
vpasolve(log10(x) == A+ B*log10(C*x-D),x)
```

Table A.1. Payload sensitivity for climb

Climb											
Type of CubeSat	**Weight per Unit**	**Total Number**	**Weight Reduced**	**Total no. of CubeSats reduced**	**Payload remaining**	**Current $\frac{\partial W_{TO}}{\partial W_{c_j}}$**	**Change in $\frac{\partial W_{TO}}{\partial W_{c_j}}$**	**Current $\frac{\partial W_{TO}}{\partial (L/D)}$**	**Change in $\frac{\partial W_{TO}}{\partial (L/D)}$**	**Current $\frac{\partial W_{TO}}{\partial E}$**	**Change in $\frac{\partial W_{TO}}{\partial E}$**
6U	26.45	125	0	0	3310	295.2	0	-421.7	0	50076.5	0
		120	132.25	5	3177.75	304	8.8	-434.3	-12.6	51571.2	1494.7
		115	264.5	10	3045.5	313.3	18.1	-447.6	-25.9	53157.8	3081.3
		110	396.75	15	2913.25	323.3	28.1	-461.8	-40.1	54848.2	4771.7
		105	529	20	2781	333.9	38.7	-477	-55.3	56643.2	6566.7
		100	661.25	25	2648.75	345.2	50	-493.1	-71.4	58563	8486.5
		95	793.5	30	2516.5	357.3	62.1	-510.4	-88.7	60617.6	10541.1
		90	925.75	35	2384.25	370.3	75.1	-529	-107.3	62821.6	12745.1
12U	52.91	62	0	0	3310	295.2	0	-421.7	0	50076.5	0
		60	105.82	2	3204.18	302.2	7	-431.7	-10	51265.4	1188.9
		58	211.64	4	3098.36	309.5	14.3	-442.2	-20.5	52512.1	2435.6
		56	317.46	6	2992.54	317.2	22	-453.2	-31.5	53820.9	3744.4
		54	423.28	8	2886.72	325.3	30.1	-464.8	-43.1	55196.6	5120.1
		52	529.1	10	2780.9	333.9	38.7	-477	-55.3	56644.6	6568.1
		50	634.92	12	2675.08	342.9	47.7	-489.8	-68.1	58170.5	8094
		48	740.74	14	2569.26	352.4	57.2	-503.4	-81.7	59780.9	9704.4
		46	846.56	16	2463.44	362.4	67.2	-517.7	-96	61483	11406.5
		44	952.38	18	2357.62	373	77.8	-532.9	-111.2	63284.9	13208.4
									421.7		
27U	119.05	27	0	0	3310	295.2	0	-421.7	0	50076.5	0
		25	238.1	2	3071.9	311.4	16.2	-444.9	-23.2	52833.3	2756.8
		23	476.2	4	2833.8	329.6	34.4	-470.8	-49.1	55911.4	5834.9
		21	714.3	6	2595.7	349.9	54.7	-499.9	-78.2	59370.2	9293.7
		19	952.4	8	2357.6	373	77.8	-532.9	-111.2	63285.3	13208.8

Table A.2. Payload sensitivity for loiter

Loiter											
Type of CubeSat	**Weight per Unit**	**Total Number**	**Weight Reduced**	**Total no. of CubeSats reduced**	**Payload remaining**	**Current $\frac{\partial W_{TO}}{\partial W_{c_j}}$**	**Change in $\frac{\partial W_{TO}}{\partial W_{c_j}}$**	**Current $\frac{\partial W_{TO}}{\partial (L/D)}$**	**Change in $\frac{\partial W_{TO}}{\partial (L/D)}$**	**Current $\frac{\partial W_{TO}}{\partial E}$**	**Change in $\frac{\partial W_{TO}}{\partial E}$**
6U	26.45	125	0	0	3310	1669.2	0	-1.2	0	25	0
		120	132.25	5	3177.75	1719	49.8	-1.2	0	25.8	0.8
		115	264.5	10	3045.5	1771.9	102.7	-1.3	-0.1	26.6	1.6
		110	396.75	15	2913.25	1828.2	159	-1.3	-0.1	27.4	2.4
		105	529	20	2781	1888.1	218.9	-1.3	-0.1	28.3	3.3
		100	661.25	25	2648.75	1952	282.8	-1.4	-0.2	29.3	4.3
		95	793.5	30	2516.5	2020.6	351.4	-1.4	-0.2	30.3	5.3
		90	925.75	35	2384.25	2094.1	424.9	-1.5	-0.3	31.4	6.4
12U	52.91	62	0	0	3310	1669.2	0	-1.2	0	25	0
		60	105.82	2	3204.18	1708.8	39.6	-1.2	0	25.6	0.6
		58	211.64	4	3098.36	1750.4	81.2	-1.3	-0.1	26.3	1.3
		56	317.46	6	2992.54	1794	124.8	-1.3	-0.1	26.9	1.9
		54	423.28	8	2886.72	1839.9	170.7	-1.3	-0.1	27.6	2.6
		52	529.1	10	2780.9	1888.2	219	-1.3	-0.1	28.3	3.3
		50	634.92	12	2675.08	1939	269.8	-1.4	-0.2	29.1	4.1
		48	740.74	14	2569.26	1990.7	321.5	-1.4	-0.2	29.9	4.9
		46	846.56	16	2463.44	2049.4	380.2	-1.5	-0.3	30.7	5.7
		44	952.38	18	2357.62	2109.5	440.3	-1.5	-0.3	31.6	6.6
27U	119.05	27	0	0	3310	1669.2	0	-1.2	0	25	0
		25	238.1	2	3071.9	1761.1	91.9	-1.3	-0.1	26.4	1.4
		23	476.2	4	2833.8	1863.7	194.5	-1.3	-0.1	28	3
		21	714.3	6	2595.7	1979	309.8	-1.4	-0.2	29.7	4.7
		19	952.4	8	2357.6	2109.5	440.3	-1.5	-0.3	31.6	6.6

Appendix. B

Table B.1. Fuselage cross section co-ordinates from AAA

Station	X	Y1	Z1	Y2	Z2	Y3	Z3	Y12	Z12	Rho_12	Y23	Z23	Rho_23
1	1.2588	0	0.230531	0.228333	-0.03828	0	-0.30709	0.228031	0.230531	0.7077	0.228031	-0.30709	0.7077
2	2.014279	0	0.367894	0.36562	-0.06324	0	-0.49438	0.365394	0.367894	0.7077	0.365394	-0.49438	0.7077
3	2.772725	0	0.505257	0.502907	-0.08821	0	-0.68168	0.502757	0.505257	0.7077	0.502757	-0.68168	0.7077
4	3.53117	0	0.64262	0.640193	-0.11317	0	-0.86897	0.64012	0.64262	0.7077	0.64012	-0.86897	0.7077
5	4.289616	0	0.779948	0.777488	-0.13817	0	-1.0563	0.777488	0.779948	0.7077	0.777488	-1.0563	0.7077
6	5.048062	0	0.916468	0.914956	-0.16393	0	-1.24433	0.914956	0.916468	0.7077	0.914956	-1.24433	0.7077
7	5.806507	0	1.052988	1.052424	-0.18969	0	-1.43236	1.052424	1.052988	0.7077	1.052424	-1.43236	0.7077
8	6.564953	0	1.191573	1.189991	-0.21348	0	-1.61853	1.189991	1.191573	0.7077	1.189991	-1.61853	0.7077
9	7.323399	0	1.333185	1.327703	-0.23439	0	-1.80196	1.327703	1.333185	0.7077	1.327703	-1.80196	0.7077
10	8.081845	0	1.474798	1.465416	-0.2553	0	-1.9854	1.465416	1.474798	0.7077	1.465416	-1.9854	0.7077
11	8.84029	0	1.616411	1.603128	-0.27621	0	-2.16883	1.603128	1.616411	0.7077	1.603128	-2.16883	0.7077
12	9.598736	0	1.758023	1.74084	-0.29712	0	-2.35227	1.74084	1.758023	0.7077	1.74084	-2.35227	0.7077
13	10.35718	0	1.899636	1.878552	-0.31803	0	-2.5357	1.878552	1.899636	0.7077	1.878552	-2.5357	0.7077
14	11.11563	0	2.041248	2.016264	-0.33895	0	-2.71914	2.016264	2.041248	0.7077	2.016264	-2.71914	0.7077
15	11.87407	0	2.182861	2.153976	-0.35986	0	-2.90257	2.153976	2.182861	0.7077	2.153976	-2.90257	0.7077
16	12.63252	0	2.321017	2.290295	-0.38263	0	-3.08627	2.290295	2.321017	0.7077	2.290295	-3.08627	0.7077
17	13.39096	0	2.45779	2.426057	-0.40614	0	-3.27007	2.426057	2.45779	0.7077	2.426057	-3.27007	0.7077
18	14.14941	0	2.594563	2.561819	-0.42965	0	-3.45386	2.561819	2.594563	0.7077	2.561819	-3.45386	0.7077
19	14.90786	0	2.731336	2.69758	-0.45316	0	-3.63766	2.69758	2.731336	0.7077	2.69758	-3.63766	0.7077
20	15.6663	0	2.868109	2.833342	-0.47667	0	-3.82146	2.833342	2.868109	0.7077	2.833342	-3.82146	0.7077
21	16.42475	0	3.004882	2.969104	-0.50018	0	-4.00525	2.969104	3.004882	0.7077	2.969104	-4.00525	0.7077
22	17.18319	0	3.185473	3.11386	-0.4906	0	-4.16667	3.11386	3.185473	0.7077	3.11386	-4.16667	0.7077
23	17.94164	0	3.682067	3.323481	-0.2423	0	-4.16667	3.323481	3.682067	0.7077	3.323481	-4.16667	0.7077
24	18.70008	0	4.178661	3.533102	0.005997	0	-4.16667	3.533102	4.178661	0.7077	3.533102	-4.16667	0.7077
25	19.45853	0	4.675256	3.742724	0.254295	0	-4.16667	3.742724	4.675256	0.7077	3.742724	-4.16667	0.7077
26	20.21698	0	5.17185	3.952345	0.502592	0	-4.16667	3.952345	5.17185	0.7077	3.952345	-4.16667	0.7077
27	20.97542	0	5.668445	4.161966	0.750889	0	-4.16667	4.161966	5.668445	0.7077	4.161966	-4.16667	0.7077
28	21.73387	0	6.165039	4.371587	0.999186	0	-4.16667	4.371587	6.165039	0.7077	4.371587	-4.16667	0.7077
29	22.49231	0	6.661633	4.581209	1.247483	0	-4.16667	4.581209	6.661633	0.7077	4.581209	-4.16667	0.7077
30	23.25076	0	6.666667	4.583333	1.25	0	-4.16667	4.583333	6.666667	0.7077	4.583333	-4.16667	0.9919
31	24.0092	0	6.666667	4.583333	1.25	0	-4.16667	4.583333	6.666667	0.7077	4.583333	-4.16667	0.9919
32	24.76765	0	6.666667	4.583333	1.25	0	-4.16667	4.583333	6.666667	0.7077	4.583333	-4.16667	0.9919
33	25.5261	0	6.666667	4.583333	1.25	0	-4.16667	4.583333	6.666667	0.7077	4.583333	-4.16667	0.9919
34	26.28454	0	6.666667	4.583333	1.25	0	-4.16667	4.583333	6.666667	0.7077	4.583333	-4.16667	0.9919
35	27.04299	0	6.666667	4.583333	1.25	0	-4.16667	4.583333	6.666667	0.7077	4.583333	-4.16667	0.9919
36	27.80143	0	6.666667	4.583333	1.25	0	-4.16667	4.583333	6.666667	0.7077	4.583333	-4.16667	0.9919
37	28.55988	0	6.666667	4.583333	1.25	0	-4.16667	4.583333	6.666667	0.7077	4.583333	-4.16667	0.9919
38	29.31832	0	6.666667	4.583333	1.25	0	-4.16667	4.583333	6.666667	0.7077	4.583333	-4.16667	0.9919
39	30.07677	0	6.666667	4.583333	1.25	0	-4.16667	4.583333	6.666667	0.7077	4.583333	-4.16667	0.9919
40	30.83522	0	6.666667	4.583333	1.25	0	-4.16667	4.583333	6.666667	0.7077	4.583333	-4.16667	0.9919
41	31.59366	0	6.666667	4.583333	1.25	0	-4.16667	4.583333	6.666667	0.7077	4.583333	-4.16667	0.9919
42	32.35211	0	6.666667	4.583333	1.25	0	-4.16667	4.583333	6.666667	0.7077	4.583333	-4.16667	0.9919
43	33.11055	0	6.666667	4.583333	1.25	0	-4.16667	4.583333	6.666667	0.7077	4.583333	-4.16667	0.9919
44	33.869	0	6.666667	4.583333	1.25	0	-4.16667	4.583333	6.666667	0.7077	4.583333	-4.16667	0.9919
45	34.62744	0	6.666667	4.583333	1.25	0	-4.16667	4.583333	6.666667	0.7077	4.583333	-4.16667	0.9919
46	35.38589	0	6.666667	4.583333	1.25	0	-4.16667	4.583333	6.666667	0.7077	4.583333	-4.16667	0.9919
47	36.14434	0	6.666667	4.583333	1.25	0	-4.16667	4.583333	6.666667	0.7077	4.583333	-4.16667	0.9919
48	36.90278	0	6.666667	4.583333	1.25	0	-4.16667	4.583333	6.666667	0.7077	4.583333	-4.16667	0.9919
49	37.66123	0	6.666667	4.583333	1.25	0	-4.16667	4.583333	6.666667	0.7077	4.583333	-4.16667	0.9919
50	38.41967	0	6.666667	4.583333	1.25	0	-4.16667	4.583333	6.666667	0.7077	4.583333	-4.16667	0.9919
51	39.17812	0	6.666667	4.583333	1.25	0	-4.16667	4.583333	6.666667	0.7077	4.583333	-4.16667	0.9919
52	39.93656	0	6.666667	4.583333	1.25	0	-4.16667	4.583333	6.666667	0.7077	4.583333	-4.16667	0.9919
53	40.69501	0	6.666667	4.583333	1.25	0	-4.16667	4.583333	6.666667	0.7077	4.583333	-4.16667	0.9919
54	41.45346	0	6.666667	4.583333	1.25	0	-4.16667	4.583333	6.666667	0.7077	4.583333	-4.16667	0.9919
55	42.2119	0	6.666667	4.583333	1.25	0	-4.16667	4.583333	6.666667	0.7077	4.583333	-4.16667	0.9919
56	42.97035	0	6.666667	4.583333	1.25	0	-4.16667	4.583333	6.666667	0.7077	4.583333	-4.16667	0.9919
57	43.72879	0	6.666667	4.583333	1.25	0	-4.16667	4.583333	6.666667	0.7077	4.583333	-4.16667	0.9919
58	44.48724	0	6.666667	4.583333	1.25	0	-4.16667	4.583333	6.666667	0.7077	4.583333	-4.16667	0.9919
59	45.24568	0	6.666667	4.583333	1.25	0	-4.16667	4.583333	6.666667	0.7077	4.583333	-4.16667	0.9919
60	46.00413	0	6.666667	4.583333	1.25	0	-4.16667	4.583333	6.666667	0.7077	4.583333	-4.16667	0.9919
61	46.76257	0	6.666667	4.583333	1.25	0	-4.16667	4.583333	6.666667	0.7077	4.583333	-4.16667	0.9919
62	47.52102	0	6.662815	4.581718	1.248074	0	-4.16667	4.581718	6.662815	0.7077	4.581718	-4.16667	0.7077
63	48.27947	0	6.523832	4.523438	1.178583	0	-4.16667	4.523438	6.523832	0.7077	4.523438	-4.16667	0.7077
64	49.03791	0	6.384849	4.465158	1.109091	0	-4.16667	4.465158	6.384849	0.7077	4.465158	-4.16667	0.7077
65	49.79636	0	6.245867	4.406879	1.0396	0	-4.16667	4.406879	6.245867	0.7077	4.406879	-4.16667	0.7077
66	50.5548	0	6.106884	4.348599	0.970109	0	-4.16667	4.348599	6.106884	0.7077	4.348599	-4.16667	0.7077
67	51.31325	0	5.967901	4.290319	0.900617	0	-4.16667	4.290319	5.967901	0.7077	4.290319	-4.16667	0.7077
68	52.07169	0	5.828918	4.232039	0.831126	0	-4.16667	4.232039	5.828918	0.7077	4.232039	-4.16667	0.7077
69	52.83014	0	5.689936	4.173759	0.761634	0	-4.16667	4.173759	5.689936	0.7077	4.173759	-4.16667	0.7077
70	53.58859	0	5.550953	4.11548	0.692143	0	-4.16667	4.11548	5.550953	0.7077	4.11548	-4.16667	0.7077
71	54.34703	0	5.381558	4.045315	0.607446	0	-4.16667	4.045315	5.381558	0.7077	4.045315	-4.16667	0.7077
72	55.10548	0	5.20345	3.971746	0.518392	0	-4.16667	3.971746	5.20345	0.7077	3.971746	-4.16667	0.7077
73	55.86392	0	5.025342	3.898177	0.429337	0	-4.16667	3.898177	5.025342	0.7077	3.898177	-4.16667	0.7077
74	56.62237	0	4.847233	3.824608	0.340283	0	-4.16667	3.824608	4.847233	0.7077	3.824608	-4.16667	0.7077
75	57.38081	0	4.669125	3.751038	0.251229	0	-4.16667	3.751038	4.669125	0.7077	3.751038	-4.16667	0.7077
76	58.13926	0	4.491017	3.677469	0.162175	0	-4.16667	3.677469	4.491017	0.7077	3.677469	-4.16667	0.7077
77	58.89771	0	4.314521	3.6039	0.073927	0	-4.16667	3.6039	4.314521	0.7077	3.6039	-4.16667	0.7077
78	59.65615	0	4.145134	3.530331	-0.01077	0	-4.16667	3.530331	4.145134	0.7077	3.530331	-4.16667	0.7077
79	60.4146	0	3.975748	3.456762	-0.09546	0	-4.16667	3.456762	3.975748	0.7077	3.456762	-4.16667	0.7077
80	61.17304	0	3.806362	3.383192	-0.18015	0	-4.16667	3.383192	3.806362	0.7077	3.383192	-4.16667	0.7077
81	61.93149	0	3.636976	3.309623	-0.26485	0	-4.16667	3.309623	3.636976	0.7077	3.309623	-4.16667	0.7077
82	62.68993	0	3.46759	3.236054	-0.34954	0	-4.16667	3.236054	3.46759	0.7077	3.236054	-4.16667	0.7077
83	63.44838	0	3.298203	3.162485	-0.43423	0	-4.16667	3.162485	3.298203	0.7077	3.162485	-4.16667	0.7077
84	64.20683	0	3.126196	3.088841	-0.52024	0	-4.16667	3.088841	3.126196	0.7077	3.088841	-4.16667	0.7077
85	64.96527	0	2.952386	3.015145	-0.60714	0	-4.16667	3.015145	2.952386	0.7077	3.015145	-4.16667	0.7077
86	65.72372	0	2.778575	2.941449	-0.69405	0	-4.16667	2.941449	2.778575	0.7077	2.941449	-4.16667	0.7077
87	66.48216	0	2.604765	2.867754	-0.78095	0	-4.16667	2.867754	2.604765	0.7077	2.867754	-4.16667	0.7077
88	67.24061	0	2.430954	2.794058	-0.86786	0	-4.16667	2.794058	2.430954	0.7077	2.794058	-4.16667	0.7077
89	67.99905	0	2.257144	2.720362	-0.95476	0	-4.16667	2.720362	2.257144	0.7077	2.720362	-4.16667	0.7077
90	68.7575	0	2.083333	2.646667	-1.04167	0	-4.16667	2.646667	2.083333	0.7077	2.646667	-4.16667	0.7077

Appendix. C

Table C.1. Left tail boom station-wise coordinates for AAA

Station	X	Y1	Z1	Y2	Z2	Y3	Z3	Y12	Z12	Rho_12	Y23	Z23	Rho_23	A	s
1	48.47083	23.53	3.034167	23.66167	2.93	23.53	2.825833	23.66167	3.034167	0.935	23.66167	2.825833	0.935	0.053848	0.893063
2	48.98769	23.53	3.218436	23.66346	3.022135	23.53337	2.825833	23.66167	3.218436	0.935	23.66526	2.825833	0.935	0.101562	1.243457
3	49.50454	23.53	3.402706	23.66526	3.11427	23.53674	2.825833	23.66167	3.402706	0.935	23.66886	2.825833	0.935	0.149358	1.59861
4	50.0214	23.53	3.586976	23.66706	3.206404	23.54011	2.825833	23.66167	3.586976	0.935	23.67245	2.825833	0.935	0.197235	1.956298
5	50.53825	23.53039	3.771442	23.66794	3.29867	23.54152	2.825833	23.66088	3.771442	0.935	23.675	2.825833	0.935	0.245001	2.315523
6	51.0551	23.53174	3.956386	23.66659	3.391255	23.53815	2.825833	23.65818	3.956386	0.935	23.675	2.825833	0.935	0.292171	2.675717
7	51.57196	23.53309	4.14133	23.66524	3.483839	23.53478	2.825833	23.65549	4.14133	0.935	23.675	2.825833	0.935	0.339099	3.036853
8	52.08881	23.53444	4.326273	23.6639	3.576423	23.5314	2.825833	23.65279	4.326273	0.935	23.675	2.825833	0.935	0.376846	3.388266
9	52.60566	23.53579	4.511086	23.66255	3.668876	23.53105	2.825833	23.64996	4.511086	0.935	23.675	2.825833	0.935	0.411416	3.739435
10	53.12252	23.53713	4.695805	23.6612	3.761236	23.53285	2.825833	23.64704	4.695805	0.935	23.675	2.825833	0.935	0.447236	4.094639
11	53.63937	23.53848	4.880524	23.65985	3.853596	23.53464	2.825833	23.64412	4.880524	0.935	23.675	2.825833	0.935	0.481222	4.450419
12	54.15623	23.53983	5.065243	23.6585	3.945955	23.53644	2.825833	23.6412	5.065243	0.935	23.675	2.825833	0.935	0.513376	4.806715
13	54.67308	23.54118	5.249963	23.65715	4.038118	23.53804	2.825833	23.63847	5.249963	0.935	23.675	2.825833	0.935	0.543454	5.163453
14	55.18993	23.54253	5.434682	23.65581	4.130253	23.53962	2.825833	23.63578	5.434682	0.935	23.675	2.825833	0.935	0.571623	5.520614
15	55.70679	23.54388	5.619401	23.65446	4.222388	23.54119	2.825833	23.63308	5.619401	0.935	23.675	2.825833	0.935	0.597917	5.878169
16	56.22364	23.54433	5.80412	23.65307	4.31456	23.54224	2.825833	23.63038	5.80412	0.935	23.675	2.825833	0.935	0.628575	6.239499
17	56.7405	23.54028	5.988839	23.6515	4.406919	23.54066	2.825833	23.62769	5.988839	0.935	23.675	2.825833	0.935	0.688883	6.616809
18	57.25735	23.53624	6.173558	23.64993	4.499279	23.53909	2.825833	23.62499	6.173558	0.935	23.675	2.825833	0.935	0.737962	6.987521
19	57.7742	23.53219	6.358277	23.64835	4.591639	23.53752	2.825833	23.62229	6.358277	0.935	23.675	2.825833	0.935	0.788018	7.358318
20	58.29106	23.53319	6.542275	23.64688	4.683689	23.53667	2.825833	23.61949	6.542275	0.935	23.675	2.825833	0.935	0.818045	7.718977
21	58.80791	23.54016	6.725421	23.64553	4.775375	23.53667	2.825833	23.61657	6.725421	0.935	23.675	2.825833	0.935	0.794221	8.057175
22	59.32477	23.54713	6.908567	23.64419	4.86706	23.53667	2.825833	23.61365	6.908567	0.935	23.675	2.825833	0.935	0.736533	8.385668
23	59.84162	23.55409	7.091713	23.64284	4.958745	23.53667	2.825833	23.61073	7.091713	0.935	23.675	2.825833	0.935	0.67032	8.71551
24	60.35847	23.57724	7.277051	23.64115	5.073521	23.56195	2.869991	23.60798	7.277219	0.935	23.67433	2.869991	0.935	0.486807	8.932849
25	60.87533	23.60578	7.463118	23.63935	5.195993	23.59566	2.928867	23.60528	7.463511	0.935	23.67343	2.928867	0.935	0.255999	9.127208
26	61.39218	23.63432	7.649185	23.63756	5.318464	23.62936	2.987743	23.60258	7.649803	0.935	23.67253	2.987743	0.935	0.149437	9.37752
27	61.90904	23.66167	7.835197	23.63575	5.441348	23.66167	3.047491	23.59989	7.836021	0.935	23.67162	3.047491	0.935	0.289478	9.644098
28	62.42589	23.66167	8.019916	23.63373	5.573708	23.66167	3.127266	23.59719	8.020515	0.935	23.6705	3.127266	0.935	0.309413	9.856106
29	62.94274	23.66167	8.204635	23.6317	5.706067	23.66167	3.207041	23.59449	8.205009	0.935	23.66937	3.207041	0.935	0.329931	10.06818
30	63.4596	23.66167	8.389354	23.62968	5.838427	23.66167	3.286816	23.5918	8.389504	0.935	23.66825	3.286816	0.935	0.35103	10.28033
31	63.97645	23.66167	8.574148	23.62766	5.970712	23.66167	3.366592	23.58903	8.574073	0.935	23.66705	3.366592	0.935	0.372723	10.49276
32	64.49331	23.66167	8.759092	23.62564	6.102846	23.66167	3.446367	23.5861	8.758792	0.935	23.6657	3.446367	0.935	0.395026	10.70571
33	65.01016	23.66167	8.944036	23.62361	6.234981	23.66167	3.526142	23.58318	8.943511	0.935	23.66435	3.526142	0.935	0.417914	10.9188
34	65.52701	23.66167	9.128979	23.62159	6.367116	23.66167	3.605918	23.58026	9.12823	0.935	23.66301	3.605918	0.935	0.441389	11.13204
35	66.04387	23.66167	9.313502	23.61971	6.499251	23.66167	3.685693	23.57748	9.312809	0.935	23.6618	3.685693	0.935	0.464618	11.34475
36	66.56072	23.66167	9.497772	23.61791	6.631386	23.66167	3.765468	23.57478	9.497303	0.935	23.66067	3.765468	0.935	0.493371	11.55729
37	67.07757	23.66167	9.682041	23.61611	6.763521	23.66167	3.845243	23.57209	9.681798	0.935	23.65955	3.845243	0.935	0.523594	11.76999
38	67.59443	23.66167	9.866311	23.61432	6.895655	23.66167	3.925019	23.56939	9.866292	0.935	23.65843	3.925019	0.935	0.554579	11.98281
39	68.11128	23.66167	10.05099	23.61231	7.02779	23.66167	4.004588	23.56669	10.05099	0.935	23.6573	4.004588	0.935	0.587628	12.19675
40	68.62814	23.66167	10.23571	23.61029	7.159925	23.66167	4.084139	23.564	10.23571	0.935	23.65618	4.084139	0.935	0.621607	12.41085
41	69.14499	23.66167	10.42043	23.60827	7.29206	23.66167	4.163689	23.5613	10.42043	0.935	23.65506	4.163689	0.935	0.656397	12.625
42	69.66184	23.66167	10.60515	23.60625	7.424242	23.66167	4.243287	23.55856	10.60515	0.935	23.65389	4.243287	0.935	0.69228	12.8392
43	70.1787	23.66167	10.78987	23.60422	7.556601	23.66167	4.323062	23.55564	10.78987	0.935	23.65254	4.323062	0.935	0.730063	13.05343
44	70.69555	23.66167	10.97459	23.6022	7.688961	23.66167	4.402837	23.55272	10.97459	0.935	23.65119	4.402837	0.935	0.768703	13.26772
45	71.21241	23.66167	11.15931	23.60018	7.82132	23.66167	4.482612	23.54979	11.15931	0.935	23.64984	4.482612	0.935	0.808198	13.48205
46	71.72926	23.66167	11.34403	23.59816	7.953567	23.66167	4.562388	23.54699	11.34403	0.935	23.6486	4.562388	0.935	0.847825	13.69618
47	72.24611	23.66167	11.52875	23.59613	8.085702	23.66167	4.642163	23.54429	11.52875	0.935	23.64748	4.642163	0.935	0.887552	13.9101
48	72.76297	23.66167	11.71346	23.59411	8.217837	23.66167	4.721938	23.54159	11.71346	0.935	23.64636	4.721938	0.935	0.92809	14.12404
49	73.27982	23.66167	11.89818	23.59209	8.349972	23.66167	4.801713	23.5389	11.89818	0.935	23.64523	4.801713	0.935	0.969439	14.338
50	73.79668	23.66167	12.08272	23.59007	8.482107	23.66167	4.881489	23.53691	12.08272	0.935	23.64411	4.881489	0.935	1.009097	14.55064
51	74.31353	23.66167	12.26722	23.58804	8.614242	23.66167	4.961264	23.53511	12.26722	0.935	23.64299	4.961264	0.935	1.049064	14.76298
52	74.83038	23.66167	12.45171	23.58602	8.746376	23.66167	5.041039	23.53331	12.45171	0.935	23.64186	5.041039	0.935	1.089271	14.97524
53	75.34724	23.66167	12.63623	23.584	8.878511	23.66167	5.12089	23.53191	12.63623	0.935	23.64074	5.120815	0.935	1.129014	15.18694
54	75.86409	23.66167	12.82095	23.58198	9.010646	23.66167	5.201564	23.53483	12.82095	0.935	23.63962	5.20059	0.935	1.153578	15.3918
55	76.38095	23.66167	13.00566	23.57995	9.142781	23.66167	5.282238	23.53775	13.00566	0.935	23.63849	5.280365	0.935	1.178392	15.59685
56	76.8978	23.66167	13.19038	23.57793	9.274916	23.66167	5.362912	23.54067	13.19038	0.935	23.63737	5.36014	0.935	1.203443	15.80196
57	77.41465	23.66167	13.37451	23.57599	9.406798	23.66167	5.442912	23.54351	13.37451	0.935	23.63616	5.439916	0.935	1.228632	16.00712
58	77.93151	23.66167	13.55766	23.57419	9.538258	23.66167	5.521788	23.54621	13.55766	0.935	23.63481	5.519691	0.935	1.253891	16.21231
59	78.44836	23.66167	13.74081	23.5724	9.669719	23.66167	5.600665	23.5489	13.74081	0.935	23.63346	5.599466	0.935	1.27939	16.41755
60	78.96522	23.66167	13.92395	23.5706	9.80118	23.66167	5.679541	23.5516	13.92395	0.935	23.63212	5.679242	0.935	1.305129	16.62285
61	79.48207	23.66167	14.06755	23.56895	9.912865	23.66167	5.758867	23.5537	14.06755	0.935	23.63092	5.758867	0.935	1.325353	16.74936
62	79.99892	23.66167	14.19137	23.56738	10.01466	23.66167	5.838418	23.5555	14.19137	0.935	23.62979	5.838418	0.935	1.342834	16.83647
63	80.51578	23.66167	14.31519	23.56581	10.11646	23.66167	5.917968	23.55729	14.31519	0.935	23.62867	5.917968	0.935	1.360425	16.92361
64	81.03263	23.66167	14.43901	23.56423	10.21826	23.66167	5.997519	23.55909	14.43901	0.935	23.62755	5.997519	0.935	1.378128	17.01077
65	81.54949	23.66167	14.48358	23.56331	10.28043	23.66167	6.077285	23.55981	14.48358	0.935	23.62642	6.077285	0.935	1.381804	16.94076
66	82.06634	23.66167	14.5247	23.56241	10.34088	23.66167	6.15706	23.56049	14.5247	0.935	23.6253	6.15706	0.935	1.384783	16.86392
67	82.58319	23.66167	14.56582	23.56151	10.40133	23.66167	6.236835	23.56116	14.56582	0.935	23.62418	6.236835	0.935	1.387675	16.7871
68	83.10005	23.66167	14.59667	23.56066	10.45661	23.66167	6.31661	23.56167	14.59667	0.935	23.623	6.31661	0.935	1.38919	16.69005
69	83.6169	23.66167	14.59667	23.55999	10.49639	23.66167	6.396386	23.56167	14.59667	0.935	23.62165	6.396386	0.935	1.386665	16.5323
70	84.13375	23.66167	14.59667	23.55932	10.53616	23.66167	6.476161	23.56167	14.59667	0.935	23.6203	6.476161	0.935	1.383928	16.37458
71	84.65061	23.66167	14.59667	23.55864	10.57594	23.66167	6.555936	23.56167	14.59667	0.935	23.61895	6.555936	0.935	1.380979	16.21688
72	85.16746	23.66167	14.59667	23.55809	10.61583	23.66167	6.635712	23.56167	14.59667	0.935	23.61772	6.635712	0.935	1.376377	16.05908
73	85.68432	23.66167	14.59667	23.55764	10.65583	23.66167	6.715487	23.56167	14.59667	0.935	23.6166	6.715487	0.935	1.370385	15.90118
74	86.20117	23.66167	14.59667	23.55719	10.69583	23.66167	6.795262	23.56167	14.59667	0.935	23.61548	6.795262	0.935	1.364234	15.7433
75	86.71802	23.66167	14.59667	23.55674	10.73583	23.66167	6.875037	23.56167	14.59667	0.935	23.61435	6.875037	0.935	1.357926	15.58545
76	87.23488	23.66167	14.59667	23.5561	10.77565	23.66167	6.954813	23.56167	14.59667	0.935	23.61323	6.954813	0.935	1.352901	15.42763
77	87.75173	23.66167	14.59667	23.55543	10.81542	23.66167	7.034588	23.56167	14.59667	0.935	23.61211	7.034588	0.935	1.347972	15.26983
78	88.26859	23.66167	14.59667	23.55476	10.8552	23.66167	7.114363	23.56167	14.59667	0.935	23.61098	7.114363	0.935	1.34285	15.11205
79	88.78544	23.66167	14.59667	23.55417	10.89	23.66167	7.19411	23.56167	14.59667	0.935	23.60848	7.19411	0.935	1.342044	14.95586
80	89.30229	23.66167	14.59667	23.55417	10.89	23.66167	7.273661	23.56167	14.59667	0.935	23.59635	7.273661	0.935	1.37168	14.81113
81	89.81915	23.66167	14.59667	23.55417	10.89	23.66167	7.353212	23.56167	14.59667	0.935	23.58421	7.353212	0.935	1.399456	14.66725
82	90.336	23.66167	14.59667	23.55417	10.89	23.66167	7.432762	23.56167	14.59667	0.935	23.57208	7.432762	0.935	1.425374	14.52408
83	90.85286	23.66167	14.59667	23.55726	10.92324	23.66167	7.512406	23.56185	14.59667	0.935	23.56884	7.512406	0.935	1.397697	14.36917
84	91.36971	23.66167	14.59667	23.56467	11.00301	23.66167	7.592182	23.5623	14.59667	0.935	23.57805	7.592182	0.935	1.297936	14.19732
85	91.88656	23.66167	14.59667	23.57209	11.08279	23.66167	7.671957	23.56275	14.59667	0.935	23.58727	7.671957	0.935	1.199427	14.02578
86	92.40342	23.66167	14.59667	23.5795	11.16257	23.66167	7.751732	23.5632	14.59667	0.935	23.59648	7.751732	0.935	1.102171	13.85459
87	92.92027	23.66167	14.59667	23.58167	11.18583	23.66326	7.763699	23.5662	14.59667	0.935	23.59519	7.76338	0.935	1.068659	13.82656
88	93.43713	23.66167	14.59667	23.58167	11.18583	23.66551	7.747743	23.57024	14.59667	0.935	23.58957	7.746976	0.935	1.061087	13.85746
89	93.95398	23.66167	14.59667	23.58167	11.18583	23.66775	7.731788	23.57429	14.59667	0.935	23.58395	7.730571	0.935	1.053545	13.88848
90	94.47083	23.66167	14.59667	23.58167	11.18583	23.67	7.715833	23.57833	14.59667	0.935	23.57833	7.714167	0.935	1.046033	13.91962

Table C.2. Right tail boom station-wise coordinates for AAA

Station	X	Y1	Z1	Y2	Z2	Y3	Z3	Y12	Z12	Rho_12	Y23	Z23	Rho_23	A	s
1	48.47083	23.53	3.034167	23.66167	2.93	23.53	2.825833	23.66167	3.034167	0.935	23.66167	2.825833	0.935	0.053848	0.893063
2	48.98769	23.53	3.218436	23.66346	3.022135	23.53337	2.825833	23.66167	3.218436	0.935	23.66526	2.825833	0.935	0.101562	1.243457
3	49.50454	23.53	3.402706	23.66526	3.11427	23.53674	2.825833	23.66167	3.402706	0.935	23.66886	2.825833	0.935	0.149358	1.59861
4	50.0214	23.53	3.586976	23.66706	3.206404	23.54011	2.825833	23.66167	3.586976	0.935	23.67245	2.825833	0.935	0.197235	1.956298
5	50.53825	23.53039	3.771442	23.66794	3.29867	23.54152	2.825833	23.66088	3.771442	0.935	23.675	2.825833	0.935	0.245001	2.315523
6	51.0551	23.53174	3.956386	23.66659	3.391255	23.53815	2.825833	23.65818	3.956386	0.935	23.675	2.825833	0.935	0.292171	2.675717
7	51.57196	23.53309	4.14133	23.66524	3.483839	23.53478	2.825833	23.65549	4.14133	0.935	23.675	2.825833	0.935	0.339099	3.036853
8	52.08881	23.53444	4.326273	23.6639	3.576423	23.5314	2.825833	23.65279	4.326273	0.935	23.675	2.825833	0.935	0.376846	3.388266
9	52.60566	23.53579	4.511086	23.66255	3.668876	23.53105	2.825833	23.64996	4.511086	0.935	23.675	2.825833	0.935	0.411416	3.739435
10	53.12252	23.53713	4.695805	23.6612	3.761236	23.53285	2.825833	23.64704	4.695805	0.935	23.675	2.825833	0.935	0.447236	4.094639
11	53.63937	23.53848	4.880524	23.65985	3.853596	23.53464	2.825833	23.64412	4.880524	0.935	23.675	2.825833	0.935	0.481222	4.450419
12	54.15623	23.53983	5.065243	23.6585	3.945955	23.53644	2.825833	23.6412	5.065243	0.935	23.675	2.825833	0.935	0.513376	4.806715
13	54.67308	23.54118	5.249963	23.65715	4.038118	23.53804	2.825833	23.63847	5.249963	0.935	23.675	2.825833	0.935	0.543454	5.163453
14	55.18993	23.54253	5.434682	23.65581	4.130253	23.53962	2.825833	23.63578	5.434682	0.935	23.675	2.825833	0.935	0.571623	5.520614
15	55.70679	23.54388	5.619401	23.65446	4.222388	23.54119	2.825833	23.63308	5.619401	0.935	23.675	2.825833	0.935	0.597917	5.878169
16	56.22364	23.54433	5.80412	23.65307	4.31456	23.54224	2.825833	23.63038	5.80412	0.935	23.675	2.825833	0.935	0.628575	6.239499
17	56.7405	23.54028	5.988839	23.6515	4.406919	23.54066	2.825833	23.62769	5.988839	0.935	23.675	2.825833	0.935	0.688883	6.616809
18	57.25735	23.53624	6.173558	23.64993	4.499279	23.53909	2.825833	23.62499	6.173558	0.935	23.675	2.825833	0.935	0.737962	6.987521
19	57.7742	23.53219	6.358277	23.64835	4.591639	23.53752	2.825833	23.62229	6.358277	0.935	23.675	2.825833	0.935	0.788018	7.358318
20	58.29106	23.53319	6.542275	23.64688	4.683689	23.53667	2.825833	23.61949	6.542275	0.935	23.675	2.825833	0.935	0.818045	7.718977
21	58.80791	23.54016	6.725421	23.64553	4.775375	23.53667	2.825833	23.61657	6.725421	0.935	23.675	2.825833	0.935	0.794221	8.057175
22	59.32477	23.54713	6.908567	23.64419	4.86706	23.53667	2.825833	23.61365	6.908567	0.935	23.675	2.825833	0.935	0.736533	8.385668
23	59.84162	23.55409	7.091713	23.64284	4.958745	23.53667	2.825833	23.61073	7.091713	0.935	23.675	2.825833	0.935	0.67032	8.71551
24	60.35847	23.57724	7.277051	23.64115	5.073521	23.56195	2.869991	23.60798	7.277219	0.935	23.67433	2.869991	0.935	0.486807	8.932849
25	60.87533	23.60578	7.463118	23.63935	5.195993	23.59566	2.928867	23.60528	7.463511	0.935	23.67343	2.928867	0.935	0.255999	9.127208
26	61.39218	23.63432	7.649185	23.63756	5.318464	23.62936	2.987743	23.60258	7.649803	0.935	23.67253	2.987743	0.935	0.149437	9.37752
27	61.90904	23.66167	7.835197	23.63575	5.441348	23.66167	3.047491	23.59989	7.836021	0.935	23.67162	3.047491	0.935	0.289478	9.644098
28	62.42589	23.66167	8.019916	23.63373	5.573708	23.66167	3.127266	23.59719	8.020515	0.935	23.6705	3.127266	0.935	0.309413	9.856106
29	62.94274	23.66167	8.204635	23.6317	5.706067	23.66167	3.207041	23.59449	8.205009	0.935	23.66937	3.207041	0.935	0.329931	10.06818
30	63.4596	23.66167	8.389354	23.62968	5.838427	23.66167	3.286816	23.5918	8.389504	0.935	23.66825	3.286816	0.935	0.35103	10.28033
31	63.97645	23.66167	8.574148	23.62766	5.970712	23.66167	3.366592	23.58903	8.574073	0.935	23.66705	3.366592	0.935	0.372723	10.49276
32	64.49331	23.66167	8.759092	23.62564	6.102846	23.66167	3.446367	23.5861	8.758792	0.935	23.6657	3.446367	0.935	0.395026	10.70571
33	65.01016	23.66167	8.944036	23.62361	6.234981	23.66167	3.526142	23.58318	8.943511	0.935	23.66435	3.526142	0.935	0.417914	10.9188
34	65.52701	23.66167	9.128979	23.62159	6.367116	23.66167	3.605918	23.58026	9.12823	0.935	23.66301	3.605918	0.935	0.441389	11.13204
35	66.04387	23.66167	9.313502	23.61971	6.499251	23.66167	3.685693	23.57748	9.312809	0.935	23.6618	3.685693	0.935	0.464618	11.34475
36	66.56072	23.66167	9.497772	23.61791	6.631386	23.66167	3.765468	23.57478	9.497303	0.935	23.66067	3.765468	0.935	0.493371	11.55729
37	67.07757	23.66167	9.682041	23.61611	6.763521	23.66167	3.845243	23.57209	9.681798	0.935	23.65955	3.845243	0.935	0.523594	11.76999
38	67.59443	23.66167	9.866311	23.61432	6.895655	23.66167	3.925019	23.56939	9.866292	0.935	23.65843	3.925019	0.935	0.554579	11.98281
39	68.11128	23.66167	10.05099	23.61231	7.02779	23.66167	4.004588	23.56669	10.05099	0.935	23.6573	4.004588	0.935	0.587628	12.19675
40	68.62814	23.66167	10.23571	23.61029	7.159925	23.66167	4.084139	23.564	10.23571	0.935	23.65618	4.084139	0.935	0.621607	12.41085
41	69.14499	23.66167	10.42043	23.60827	7.29206	23.66167	4.163689	23.5613	10.42043	0.935	23.65506	4.163689	0.935	0.656397	12.625
42	69.66184	23.66167	10.60515	23.60625	7.424242	23.66167	4.243287	23.55856	10.60515	0.935	23.65389	4.243287	0.935	0.69228	12.8392
43	70.1787	23.66167	10.78987	23.60422	7.556601	23.66167	4.323062	23.55564	10.78987	0.935	23.65254	4.323062	0.935	0.730063	13.05343
44	70.69555	23.66167	10.97459	23.6022	7.688961	23.66167	4.402837	23.55272	10.97459	0.935	23.65119	4.402837	0.935	0.768703	13.26772
45	71.21241	23.66167	11.15931	23.60018	7.82132	23.66167	4.482612	23.54979	11.15931	0.935	23.64984	4.482612	0.935	0.808198	13.48205
46	71.72926	23.66167	11.34403	23.59816	7.953567	23.66167	4.562388	23.54699	11.34403	0.935	23.6486	4.562388	0.935	0.847825	13.69618
47	72.24611	23.66167	11.52875	23.59613	8.085702	23.66167	4.642163	23.54429	11.52875	0.935	23.64748	4.642163	0.935	0.887552	13.9101
48	72.76297	23.66167	11.71346	23.59411	8.217837	23.66167	4.721938	23.54159	11.71346	0.935	23.64636	4.721938	0.935	0.92809	14.12404
49	73.27982	23.66167	11.89818	23.59209	8.349972	23.66167	4.801713	23.5389	11.89818	0.935	23.64523	4.801713	0.935	0.969439	14.338
50	73.79668	23.66167	12.08272	23.59007	8.482107	23.66167	4.881489	23.53691	12.08272	0.935	23.64411	4.881489	0.935	1.009097	14.55064
51	74.31353	23.66167	12.26722	23.58804	8.614242	23.66167	4.961264	23.53511	12.26722	0.935	23.64299	4.961264	0.935	1.049064	14.76298
52	74.83038	23.66167	12.45171	23.58602	8.746376	23.66167	5.041039	23.53331	12.45171	0.935	23.64186	5.041039	0.935	1.089271	14.97524
53	75.34724	23.66167	12.63623	23.584	8.878511	23.66167	5.12089	23.53191	12.63623	0.935	23.64074	5.120815	0.935	1.129014	15.18694
54	75.86409	23.66167	12.82095	23.58198	9.010646	23.66167	5.201564	23.53483	12.82095	0.935	23.63962	5.20059	0.935	1.153578	15.3918
55	76.38095	23.66167	13.00566	23.57995	9.142781	23.66167	5.282238	23.53775	13.00566	0.935	23.63849	5.280365	0.935	1.178392	15.59685
56	76.8978	23.66167	13.19038	23.57793	9.274916	23.66167	5.362912	23.54067	13.19038	0.935	23.63737	5.36014	0.935	1.203443	15.80196
57	77.41465	23.66167	13.37451	23.57599	9.406798	23.66167	5.442912	23.54351	13.37451	0.935	23.63616	5.439916	0.935	1.228632	16.00712
58	77.93151	23.66167	13.55766	23.57419	9.538258	23.66167	5.521788	23.54621	13.55766	0.935	23.63481	5.519691	0.935	1.253891	16.21231
59	78.44836	23.66167	13.74081	23.5724	9.669719	23.66167	5.600665	23.5489	13.74081	0.935	23.63346	5.599466	0.935	1.27939	16.41755
60	78.96522	23.66167	13.92395	23.5706	9.80118	23.66167	5.679541	23.5516	13.92395	0.935	23.63212	5.679242	0.935	1.305129	16.62285
61	79.48207	23.66167	14.06755	23.56895	9.912865	23.66167	5.758867	23.5537	14.06755	0.935	23.63092	5.758867	0.935	1.325353	16.74936
62	79.99892	23.66167	14.19137	23.56738	10.01466	23.66167	5.838418	23.5555	14.19137	0.935	23.62979	5.838418	0.935	1.342834	16.83647
63	80.51578	23.66167	14.31519	23.56581	10.11646	23.66167	5.917968	23.55729	14.31519	0.935	23.62867	5.917968	0.935	1.360425	16.92361
64	81.03263	23.66167	14.43901	23.56423	10.21826	23.66167	5.997519	23.55909	14.43901	0.935	23.62755	5.997519	0.935	1.378128	17.01077
65	81.54949	23.66167	14.48358	23.56331	10.28043	23.66167	6.077285	23.55981	14.48358	0.935	23.62642	6.077285	0.935	1.381804	16.94076
66	82.06634	23.66167	14.5247	23.56241	10.34088	23.66167	6.15706	23.56049	14.5247	0.935	23.6253	6.15706	0.935	1.384783	16.86392
67	82.58319	23.66167	14.56582	23.56151	10.40133	23.66167	6.236835	23.56116	14.56582	0.935	23.62418	6.236835	0.935	1.387675	16.7871
68	83.10005	23.66167	14.59667	23.56066	10.45661	23.66167	6.31661	23.56167	14.59667	0.935	23.623	6.31661	0.935	1.38919	16.69005
69	83.6169	23.66167	14.59667	23.55999	10.49639	23.66167	6.396386	23.56167	14.59667	0.935	23.62165	6.396386	0.935	1.386665	16.5323
70	84.13375	23.66167	14.59667	23.55932	10.53616	23.66167	6.476161	23.56167	14.59667	0.935	23.6203	6.476161	0.935	1.383928	16.37458
71	84.65061	23.66167	14.59667	23.55864	10.57594	23.66167	6.555936	23.56167	14.59667	0.935	23.61895	6.555936	0.935	1.380979	16.21688
72	85.16746	23.66167	14.59667	23.55809	10.61583	23.66167	6.635712	23.56167	14.59667	0.935	23.61772	6.635712	0.935	1.376377	16.05908
73	85.68432	23.66167	14.59667	23.55764	10.65583	23.66167	6.715487	23.56167	14.59667	0.935	23.6166	6.715487	0.935	1.370385	15.90118
74	86.20117	23.66167	14.59667	23.55719	10.69583	23.66167	6.795262	23.56167	14.59667	0.935	23.61548	6.795262	0.935	1.364234	15.7433
75	86.71802	23.66167	14.59667	23.55674	10.73583	23.66167	6.875037	23.56167	14.59667	0.935	23.61435	6.875037	0.935	1.357926	15.58545
76	87.23488	23.66167	14.59667	23.5561	10.77565	23.66167	6.954813	23.56167	14.59667	0.935	23.61323	6.954813	0.935	1.352901	15.42763
77	87.75173	23.66167	14.59667	23.55543	10.81542	23.66167	7.034588	23.56167	14.59667	0.935	23.61211	7.034588	0.935	1.347972	15.26983
78	88.26859	23.66167	14.59667	23.55476	10.8552	23.66167	7.114363	23.56167	14.59667	0.935	23.61098	7.114363	0.935	1.34285	15.11205
79	88.78544	23.66167	14.59667	23.55417	10.89	23.66167	7.19411	23.56167	14.59667	0.935	23.60848	7.19411	0.935	1.342044	14.95586
80	89.30229	23.66167	14.59667	23.55417	10.89	23.66167	7.273661	23.56167	14.59667	0.935	23.59635	7.273661	0.935	1.37168	14.81113
81	89.81915	23.66167	14.59667	23.55417	10.89	23.66167	7.353212	23.56167	14.59667	0.935	23.58421	7.353212	0.935	1.399456	14.66725
82	90.336	23.66167	14.59667	23.55417	10.89	23.66167	7.432762	23.56167	14.59667	0.935	23.57208	7.432762	0.935	1.425374	14.52408
83	90.85286	23.66167	14.59667	23.55726	10.92324	23.66167	7.512406	23.56185	14.59667	0.935	23.56884	7.512406	0.935	1.397697	14.36917
84	91.36971	23.66167	14.59667	23.56467	11.00301	23.66167	7.592182	23.5623	14.59667	0.935	23.57805	7.592182	0.935	1.297936	14.19732
85	91.88656	23.66167	14.59667	23.57209	11.08279	23.66167	7.671957	23.56275	14.59667	0.935	23.58727	7.671957	0.935	1.199427	14.02578
86	92.40342	23.66167	14.59667	23.5795	11.16257	23.66167	7.751732	23.5632	14.59667	0.935	23.59648	7.751732	0.935	1.102171	13.85459
87	92.92027	23.66167	14.59667	23.58167	11.18583	23.66326	7.763699	23.5662	14.59667	0.935	23.59519	7.76338	0.935	1.068659	13.82656
88	93.43713	23.66167	14.59667	23.58167	11.18583	23.66551	7.747743	23.57024	14.59667	0.935	23.58957	7.746976	0.935	1.061087	13.85746
89	93.95398	23.66167	14.59667	23.58167	11.18583	23.66775	7.731788	23.57429	14.59667	0.935	23.58395	7.730571	0.935	1.053545	13.88848
90	94.47083	23.66167	14.59667	23.58167	11.18583	23.67	7.715833	23.57833	14.59667	0.935	23.57833	7.714167	0.935	1.046033	13.91962

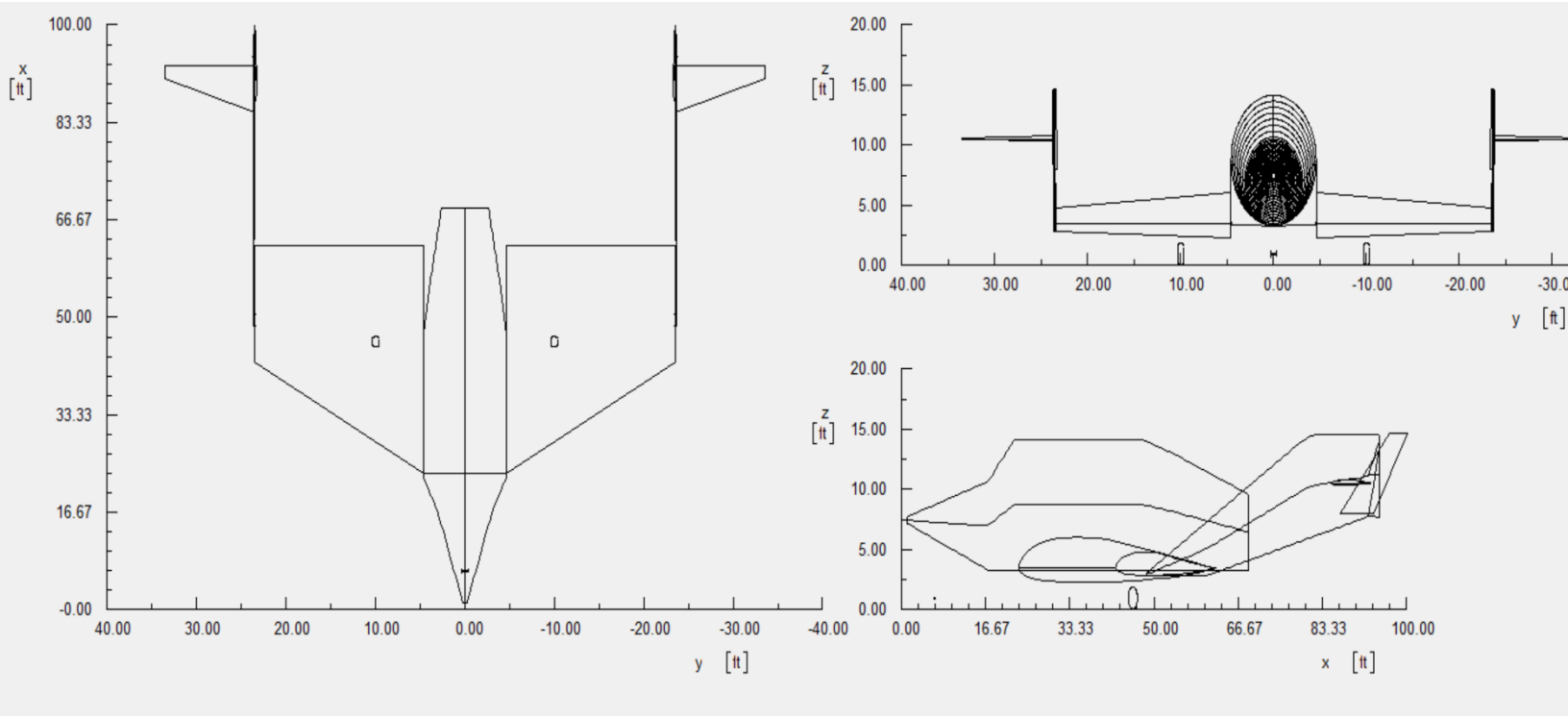

Figure C. 1 Completed X-69 from AAA